Evaluating the Biogeochemical and Geotechnical Behavior of Oil Sands Tailings in Pit Lakes and Mitigating Pit Lake Turbidity with Biofilms

by

Heidi Lynn Cossey

A thesis submitted in partial fulfillment of the requirements for the degree of

Doctor of Philosophy

in

Geoenvironmental Engineering

Department of Civil and Environmental Engineering

University of Alberta

ABSTRACT

Permanent storage and reclamation of oil sands mine waste (fluid fine tailings, FFT) in pit lakes has been proposed by industry. Pit lakes are considered best practice in terms of geotechnical stability, however, there are numerous challenges and knowledge gaps surrounding this proposed oil sands tailings reclamation practice, including water cap quality and biogeochemical cycling processes which can generate greenhouse gases and $H_2S_{(g)}$. This research included three laboratory studies, the first of which was designed to improve pit lake water chemistry by mitigating turbidity generation. Two column studies were also designed to evaluate the biogeochemical and geotechnical behavior of untreated and treated FFT in pit lakes and to investigate the effects of pressure on these behaviors. Collectively, these studies provide valuable information regarding a promising biological turbidity mitigation mechanism, as well as key biogeochemical and geotechnical behaviors of untreated and treated FFT that will be important to mitigate, monitor, and/or manage as part of ensuring successful reclamation of oil sands tailings in pit lakes.

The first laboratory study investigated turbidity mitigation in oil sands pit lakes using mudline biofilms that were made up of diverse microbial communities indigenous to oil sands tailings. Mudline biofilms were grown on FFT that was capped with water in 1 L jars. Biofilms reduced turbidity generation by up to 99% during physical mixing experiments, depending on the biofilm age and mixing speed. This study demonstrated that biostabilization of FFT with mudline biofilms is a promising mechanism of turbidity mitigation in pit lakes.

The second laboratory study involved 64 columns (1 L or 19 L), each containing FFT and a water cap and stored under anaerobic conditions. FFT was either left untreated or treated with a coagulant

(alum) and flocculant (polyacrylamide, PAM). Over the 540 d study, the tailings in all columns underwent self-weight consolidation, though FFT had a higher net water release (NWR) in 19 L columns than 1 L columns and, surprisingly, treated FFT had a lower NWR than untreated FFT. Water cap concentrations of pore water constituents generally increased over time due to consolidation-driven advection, diffusion (particularly in 1 L columns), and biogeochemical reactions in the FFT. The dominant microbial process in all columns was sulfate reduction, which subsequently influenced alkalinity, $CO_{2(g)}$, and pore water concentrations of divalent cations. Treated FFT and/or FFT amended with hydrocarbons had the most extensive sulfate reduction, which resulted in the generation of aqueous sulfide species throughout the pore water and water caps.

The third laboratory study involved 12 columns (5 L), each containing (alum and PAM) treated FFT and a water cap. All columns were stored under anaerobic conditions for 360 d. Pressure (0.3 to 5.1 kPa) was applied to the tailings in six columns using dead loads and a multi-step loading scheme. This study revealed that pressure (0.3 to 5.1 kPa) significantly influences microbial activity and biogeochemical cycling in treated FFT, presumably by increasing the solubility of microbial substrates and metabolites. Pressure enhanced methanogenesis, leading to increased generation of $CH_{4(g)}$ and $CO_{2(g)}$, and shifted the predominant methanogenic pathway from hydrogenotrophic to acetoclastic methanogenesis. Further, pressure led to increased ammonium concentrations, likely through PAM degradation and/or N_2 fixation. Both sulfate reduction (which generated gaseous and aqueous H_2S) and methanogenesis (which generated $CH_{4(g)}$ and $CO_{2(g)}$) occurred in the treated FFT and, similar to the previous column study, hydrocarbon amendments enhanced sulfate reduction in the tailings.

PREFACE

This thesis is an original work by Heidi Cossey under the supervision of Dr. Ania Ulrich and Dr. Heather Kaminsky, though some of the research for this thesis was completed through collaboration with others. Several chapters of this thesis were reproduced from existing or future publications (with modifications). The publications and author contributions for each applicable chapter are summarized below:

Portions of Chapter 2 have been published in:

Cossey, H.L.; Batycky, A.E.; Kaminsky, H.; Ulrich, A.C. Geochemical stability of oil sands tailings in mine closure landforms. *Minerals* **2021**, *11*, 830.

I compiled the literature and was responsible for writing the majority of the manuscript. Ms. Batycky primarily assisted in writing the Polymer Degradation subsection of the manuscript, though she contributed information to other subsections as well. Dr. Ulrich and Dr. Kaminsky contributed to review and editing of the manuscript.

A version of Chapter 3 has been published as:

Cossey, H.L.; Anwar, M.N.; Kuznetsov, P.V.; Ulrich, A.C. Biofilms for turbidity mitigation in oil sands end pit lakes. *Microorganisms* **2021**, *9*, 1443.

I developed and conducted the experiment and was responsible for manuscript preparation. Dr. Kuznetsov assisted in experimental design. Dr. Anwar assisted with the following experimental analyses: SEM, LIVE/DEAD staining, and 16S sequencing. Dr. Ulrich contributed to review and editing of the manuscript.

Chapter 4 represents the results of a journal article, which will be submitted to *Science of the Total Environment*.

Chapter 5 represents the results of a journal article, which will be submitted to *Science of the Total Environment*.

ACKNOWLEDGEMENTS

First, I would like to thank my supervisors, Dr. Ania Ulrich and Dr. Heather Kaminsky. Ania, your support and guidance over the years has had an immense impact on both my professional and personal life. I would not be where I am today without your mentorship and leadership. Heather, I am so thankful for your expertise, mentorship, and enthusiasm. Your passion for research has been an important source of inspiration for me these last couple of years. I am also grateful to have had Dr. Nicholas Beier on my supervisory committee – thank you for providing thoughtful feedback, advice, and support throughout my program.

Thank you to all of my colleagues/lab mates in the Ulrich lab for your assistance, encouragement, and friendship over the last four years. I would especially like to thank my wonderful friend and travel buddy Amy-lynne Balaberda, as well as Dr. Petr Kuznetsov, Anya Batycky, Dr. Korris Lee, Dr. Nesma Allam, Dr. Nabeel Anwar, and Dr. Sarah Miles for their support. I would also like to thank the team at NAIT's Centre for Oil Sands Sustainability, especially Niamh Donoghue and Mohammed Ghuzi, for providing technical support and assistance during my column studies.

I am immensely grateful for the financial support I received through scholarships which allowed me to focus full-time on my studies. These scholarships include the Vanier Canada Graduate Scholarship, University of Alberta President's Doctoral Prize of Distinction, Canadian Foundation for Geotechnique Michael Bozozuk National Graduate Scholarship, Westmoreland Coal Company Graduate Scholarship in Environmental Engineering, Earle Klohn Graduate Scholarship in Geotechnical Engineering, Petro-Canada Graduate Scholarship in Petroleum Engineering, Golder Associates Mine Closure Scholarship, Canadian Federation of University Women National Dr. Margaret McWilliams Pre-Doctoral Fellowship, Canadian Federation of University Women Edmonton Margaret Brine Graduate Scholarship for Women, Alberta Graduate Excellence Scholarship, and the University of Alberta Doctoral Recruitment Scholarship. I am also grateful to have received financial support for my research through the NSERC/COSIA Industrial Research Chair in Oil Sands Tailings Geotechnique, the NSERC/COSIA Industrial Research Chair for Colleges in Oil Sands Tailings Management, an NSERC TERRE-NET (Toward Environmental Responsible Resource Extraction Network) Grant, and the NSERC Discovery Grants Program.

Lastly, I am forever grateful for my family. Mom, dad, Amber, and Nicole - thank you for your continuous support, and endless laughter and love. Kurt, I am so fortunate to have had you by my side through all of this. Thank you for your love and encouragement, and for taking such good care of Lucas, Monkey, and I.

TABLE OF CONTENTS

LIST OF TABLES

LIST OF FIGURES

LIST OF ACRONYMS

AER	Alberta Energy Regulator
ANOVA	Analysis of variance
BCR	Beaver Creek Reservoir
BDL	Below detection limit
BML	Base Mine Lake
BTEX	Benzene, toluene, ethylbenzene, and xylene
Ca^{2+}	Calcium
$CaCO_{3(s)}$	Calcite
$CaMg(CO_3)_{2(s)}$	Dolomite
CH_4	Methane
Chl *a*	Chlorophyll a
CNRL	Canadian Natural Resources Limited
CNUL	Canadian Natural Upgrading Limited
CO_2	Carbon dioxide
COD	Chemical oxygen demand
CT	Composite tailings
D_{50}	Median particle diameter
DDA	Dedicated Disposal Area
DO	Dissolved oxygen
DOC	Dissolved organic carbon
EC	Electrical conductivity
EPS	Extracellular polymeric substances
FFT	Fluid fine tailings
FTT	Froth treatment tailings
GC-FID	Gas chromatography – flame ionization detector
GC-MS	Gas chromatography – mass spectrometry
GC-SCD	Gas chromatography – sulfur chemiluminescence detector
GC-TCD	Gas chromatography – thermal conductivity detector
HCO_3^-	Bicarbonate

HPAM	Partially hydrolyzed polyacrylamide
HS^-	Bisulfide
H_2S	Hydrogen sulfide
ICP-OES	Inductively coupled plasma – optical emission spectrometry
MBI	Methylene Blue Index
MFT	Mature fine tailings
Mg^{2+}	Magnesium
Na^+	Sodium
NAFC	Naphthenic acid fraction compound
NAIT	Northern Alberta Institute of Technology
NH_4^+	Ammonium
NRAL	Natural Resources Analytical Laboratory
NTU	Nephelometric turbidity units
OD	Optical density
PAM	Polyacrylamide
PASS	Permanent Aquatic Storage Structure
pCH_4	Partial pressure of CH_4
pCO_2	Partial pressure of CO_2
PCR	Polymerase chain reaction
PSD	Particle size distribution
RSC	Reduced sulfur compound
SEC-HPLC	Size exclusion – high performance liquid chromatography
SEM	Scanning electron microscopy
SFR	Sand to fines ratio
SO_4^{2-}	Sulfate
SRB	Sulfate-reducing bacteria
TOC	Total organic carbon
XRF	X-ray fluorescence

1 INTRODUCTION

The purpose of this research is to evaluate and improve upon a proposed oil sands tailings reclamation strategy called pit lakes (synonymous with end pit lakes). In terms of geotechnical stability, storing tailings in pit lakes is considered best practice because it reduces the amount of mine waste stored in above-ground facilities (Golder Associates Ltd. 2017). However, there are other concerns and knowledge gaps surrounding the permanent storage and reclamation of oil sands tailings in pit lakes, including water cap quality and biogeochemical cycling processes in untreated and treated tailings. This thesis presents three laboratory studies that were designed to evaluate the biogeochemical and geotechnical behavior of untreated and treated tailings in oil sands pit lakes and improve pit lake water chemistry by mitigating turbidity generation. These laboratory studies provide valuable information regarding key biogeochemical processes and geotechnical behaviors of untreated and treated tailings that will be important to mitigate, manage, and/or monitor as additional pit lakes are developed by oil sands operators.

1.1 Background

Alberta has the fourth largest oil reserve in the world, with a deposit area of 142,200 km^2 (Government of Alberta 2023). Approximately 3.4% of Alberta's oil sands ore deposit is within 75 m of the ground surface and thus can be extracted through surface mining (Government of Alberta 2023). There are currently eight oil sands surface mines in operation in northern Alberta: Suncor Energy Inc. (Suncor) Base Plant, Syncrude Canada Ltd. (Syncrude) Mildred Lake (operated by Suncor), Syncrude Aurora North (operated by Suncor), Canadian Natural Upgrading Limited (CNUL) Muskeg River mine, CNUL Jackpine mine, Canadian Natural Resources Limited (CNRL) Horizon, Imperial Oil Resources Limited (Imperial) Kearl, and Fort Hills (operated by Suncor) (AER 2022).

Bitumen extraction from surface mined oil sands ore generates large amounts of waste, known as tailings, which is stored in aboveground or in-pit containment structures, called tailings ponds. Oil sands tailings consist of solids (sand, silt, and clay), water, various ions (namely chloride, sodium, and sulfate), residual bitumen, and other organic compounds (Cossey et al. 2021a). Tailings sand quickly settles out, leaving behind a stable clay-water slurry that is typically referred to as fluid

fine tailings (FFT) (though FFT may also be referred to as fluid tailings, fine tailings, or mature fine tailings (MFT)). Prior to 2015, approximately 1.25 m^3 of FFT was produced per barrel of bitumen, but according to 2015 to 2021 data, FFT generation has decreased to roughly 0.44 m^3 of FFT per barrel of bitumen produced (AER 2022).

Initially, FFT has a solids content of 6-10 wt% and after several years it will plateau at a solids content of roughly 30 wt% (Chalaturnyk et al. 2002). In addition to having a very slow consolidation rate (Chalaturnyk et al. 2002), FFT has a high clay content, with a Methylene Blue Index (MBI) ranging from 1.4 to 14 meq/100 g (Kaminsky and Omotoso 2016), and a peak undrained shear strength ranging from 0.01 to 1 kPa (McKenna 2009; Sawatsky et al. 2018). As such, water capping is often the only capping and reclamation option for FFT. To improve some of the problematic geotechnical characteristics of FFT, oil sands operators will often treat FFT with physical and/or chemical amendments, such as centrifugation, coagulation, and/or flocculation. In 2015, the Government of Alberta released a framework for managing the accumulation of fluid tailings in tailings ponds, called the *Lower Athabasca Region: Tailings Management Framework for Mineable Athabasca Oil Sands* (commonly referred to as the TMF). The goal of this framework is to ensure operators are progressively treating and reclaiming FFT throughout the life of mine. It states that legacy tailings and new FFT must be ready to reclaim by end of mine life and 10 years after end of mine life, respectively (Government of Alberta 2015). Ready to reclaim criteria varies depending on the operator, tailings treatment, and type of deposit. As of December 2021, there were over 1345 Mm^3 of FFT that did not meet ready to reclaim criteria (AER 2022).

Pit lakes are a major FFT reclamation strategy that has been proposed by oil sands operators. Pit lakes are decommissioned open pits that have been filled with fresh water, process-affected water, lean ore, overburden, waste rock, tailings, and/or other mine wastes (Golder Associates Ltd. 2017). Thousands of pit lakes already exist across the globe, as these landforms are commonly incorporated into surface mines during closure (Blanchette and Lund 2016; Vandenberg et al. 2022). Many pit lakes are successful, having met the intended purpose of their reclamation design (such as fish habitat, recreation, irrigation, etc.), while others are notorious for their poor water

quality (Golder Associates 2017). Because of the complex nature of oil sands tailings, there are unique challenges and uncertainties associated with permanently storing these tailings in pit lakes.

Alberta Energy Regulator (AER) has not yet approved pit lakes as an oil sands reclamation strategy, as the technology is still in the demonstration and experimental phase (AER 2022). An alternative to pit lakes would be terrestrial reclamation of oil sands tailings, in which tailings are capped with a solid material such as sand or overburden, prior to being integrated into the surrounding landscape. However, pit lakes are a more economical option for oil sands tailings reclamation as it can be difficult to achieve the strength required for trafficable FFT deposits (McKenna 2009). Oil sands operators plan to integrate 20 pit lakes into their mine closure landscapes. These pit lakes will contain various volumes of water (ranging from 6 to 937 Mm^3, some of which may be process-affected water) and 11 of the pit lakes will also contain untreated or treated FFT (>0 to 439 Mm^3) (COSIA 2021). All of the eight operating oil sands mines plan to reclaim at least some of their FFT in a pit lake, though this technology has not been approved by regulators nor has it been accepted by rights holders in the area.

Currently, there are two commercial scale demonstration pit lakes, Base Mine Lake (BML) and Dedicated Disposal Area 3 (DDA3), and several pilot scale demonstration pit lakes in Alberta's oil sands. BML is located on Syncrude's Mildred Lake mine and was commissioned in 2012. Roughly 186 Mm^3 of untreated FFT was deposited in an 800 ha open pit between 1995 and 2012 and capped with a mixture of fresh water and process-affected water (Dompierre et al. 2016; Syncrude 2021). This deposit was commissioned as BML in 2012 and currently consists of a 45 m thick layer of untreated FFT and a 9 to 12 m water cap which is diluted with fresh water from Beaver Creek Reservoir (BCR) (Syncrude 2021). Syncrude also has a pilot scale demonstration pit lake that contains untreated FFT.

Other oil sands operations have proposed depositing treated FFT in pit lakes. Suncor has developed a treatment technology called Permanent Aquatic Storage Structure (PASS), in which FFT is treated in-line with a coagulant, alum ($Al_2(SO_4)_3 \cdot 14H_2O$), and a polymer flocculant, polyacrylamide (PAM), prior to being deposited in an open pit. AER has approved the PASS treatment process (i.e. treating the FFT with alum and PAM) but has not approved any capping

options for PASS-treated FFT, though Suncor is planning to create water-capped PASS deposits (i.e. pit lakes) (AER 2022). Suncor Base Plant has two demonstration PASS deposits, the first of which is DDA3 which will eventually become Upper Pit Lake. As of December 2021, DDA3 contained 66 Mm^3 of PASS-treated FFT, though the volume of PASS-treated FFT in DDA3 is increasing over time (Suncor 2022a). Suncor Base Plant also has Lake Miwasin, which is a smaller version of DDA3 and contains 40,000 m^3 of PASS-treated FFT (COSIA 2021; Suncor 2022a). As of 2021, most of the PASS-treated FFT deposited in Suncor's DDA3 is considered to be ready to reclaim as the ready to reclaim criteria for DDA3 was recently changed from a clay to water ratio of > 0.5 to > 0.3 (AER 2022). The ready to reclaim criteria for total suspended solids released from DDA3's PASS-treated FFT pore water remains unchanged at ≤ 500 ppm. Fort Hills (operated by Suncor) also plans to reclaim FFT in water-capped PASS deposits, though Fort Hills does not currently have an approved tailings treatment technology (Suncor 2022b). The goal of the PASS treatment process is to i) improve pore water quality by reducing the mobility of organic compounds in the FFT with alum addition and ii) increase FFT dewatering (consolidation) with PAM addition (Suncor 2022b).

1.1.1 Research Problem

The reclamation of FFT in pit lakes has made substantial progress over the years and research and monitoring are ongoing at the commercial and pilot scale pit lakes, though there are still a number of ongoing challenges and knowledge gaps surrounding the biogeochemical and geotechnical behavior of oil sands tailings in pit lakes. Turbidity due to erosion of FFT at the FFT-water interface (mudline) has been an ongoing challenge in BML. Water cap turbidity in BML reached 308 NTU (nephelometric turbidity units) at shallow depths (1-3 m) in fall 2015 after lake turnover (Tedford et al. 2019). As such, Syncrude dosed the BML water cap with alum in 2016, which successfully reduced turbidity that year (Syncrude 2021). Syncrude continues to track water cap turbidity, though turbidity is expected to fluctuate seasonally and has reached over 50 NTU for multiple days each year since the alum addition (Syncrude 2021). Even small increases in turbidity, from 10 to 50 NTU, can have negative effects on aquatic life (Birtwell et al. 2008; Shen et al. 2019). Previous research showed that the effect of alum addition may disappear once aluminum ions return to background concentrations (Wei et al. 2021), and thus the longevity of the coagulant effect on turbidity reduction in BML is unclear. Further, a recent study of BML found that the

alum addition led to increased production of easily degradable carbon in the water cap and increased sulfide species generation, which ultimately led to increased oxygen consumption and expansion of the water cap's anoxic layer (Jessen et al. 2022). Thus, reducing turbidity generation using biological mechanisms may be the best strategy. As such, a natural, biological mechanism of turbidity reduction is proposed in which microorganisms indigenous to oil sands tailings form mudline biofilms, effectively stabilizing the mudline and mitigating turbidity generation. Previous biostabilization research has shown promising results in turbidity mitigation in marine (Amos et al. 2004; Friend et al. 2003; Widdows et al. 2007; Wotton 2004) and fresh water (Droppo et al. 2007; Droppo 2009) sediments, however, no studies have been conducted to investigate turbidity mitigation in oil sands pit lakes using biostabilization.

In addition to some ongoing challenges with existing demonstration pit lakes, there are a number of knowledge gaps surrounding the biogeochemical and geotechnical behavior of FFT in pit lakes. In particular, the biogeochemical and geotechnical implications of Suncor's new PASS treatment process remain largely unknown and there is limited publicly available research on this new treatment technology. Some of the knowledge gaps surrounding pit lakes include chemical mass loading into the water cap, the effects of PASS treatment on sulfur cycling, and the environmental fate of PAM in PASS-treated FFT. Self-weight consolidation of untreated FFT is expected to take decades to centuries (McKenna et al. 2016) and as such, consolidation-driven advective pore water fluxes and subsequent chemical mass loading of ions and organic compounds into a pit lake water cap will also occur over many years, as has been observed thus far in BML (Dompierre et al. 2017). Advection-dispersion is driving chemical mass loading in BML while the FFT undergoes self-weight consolidation, but eventually chemical transport will likely be governed by diffusion (Dompierre and Barbour 2016; Dompierre et al. 2017). Chemical mass loading from PASS-treated FFT is expected to differ from that of untreated FFT as PASS treatment should increase consolidation rates and reduce the mobility of organic compounds. Chemical mass loading and the rate at which it occurs will have important implications for water cap quality, water management, and the development of freshwater aquatic ecosystems.

Though sulfur cycling occurs in numerous tailings deposits, including tailings ponds (Stasik et al. 2014) and BML (Dompierre et al. 2016), sulfur cycling in PASS-treated FFT is of particular

interest because of the increase in pore water sulfate (SO_4^{2-}) concentrations associated with alum addition. Reduction of SO_4^{2-} can lead to the generation of aqueous and gaseous hydrogen sulfide (H_2S) and carbon dioxide (CO_2), as well as the precipitation of metal sulfides. Previous research has shown that oil sands tailings amended with gypsum ($CaSO_4 \cdot 2H_2O$) undergo extensive sulfate reduction (Ramos-Padrón et al. 2011; Reid and Warren 2016; Warren et al. 2016), and as such, similar microbial processes may dominate in PASS-treated FFT. This could potentially hinder methanogenesis and subsequent methane (CH_4) emissions in PASS-treated FFT if sulfate-reducing bacteria (SRB) have a competitive advantage over methanogens (Bordenave et al. 2009; Holowenko et al. 2000; Ramos-Padrón et al. 2011), and/or it could lead to emissions of toxic H_2S gas from PASS-treated deposits. Thus, it is important to investigate the biogeochemical implications of any new oil sands tailings treatment processes.

Given the relatively high doses of PAM used in the oil sands, compared to that of water and wastewater treatment applications, the potential biodegradation of PAM in PASS-treated FFT is of particular interest (Cossey et al. 2021a). The most likely biodegradation pathway for PAM in anaerobic pit lake tailings is through hydrolysis of the amide nitrogen (Cossey et al. 2021a; Grula et al. 1994; Guezennec et al. 2015; Haveroen et al. 2005; Hu et al. 2018). PAM degradation has the potential to further stimulate microbial activity in FFT, including methanogenesis and sulfate reduction, as ammonia/ammonium generated from PAM biodegradation could be used as a nitrogen source (Grula et al. 1994; Haveroen et al. 2005).

Further, the effect of pressure on microbial activity and biogeochemical cycling in oil sands tailings is unknown. High pressures (several dozen MPa) can have a widespread impact on microbial physiology, affecting their shape (Fichtel et al. 2015), macromolecular structures, and/or cellular processes such as metabolism, cell growth, viability, and motility (Abe 2007; Fichtel et al. 2015). While it is well established that high pressures negatively impact cell growth and microbial metabolic processes (though the mechanisms by which pressure impacts cellular functions are not well understood) (Abe 2007; Pope and Berger 1973), there has been little research into the effects of lower pressures (in the kPa range) on microbial activity. As such, this research incorporates low dead load pressures (0.3 to 5.1 kPa) into a pit lake column study to elucidate the impact of pressure on microbial activity and subsequent biogeochemical cycling in FFT. Ultimately, these research

projects will aid in addressing some of the ongoing challenges and knowledge gaps surrounding oil sands pit lakes, which is critical in order to evaluate the potential for aquatic reclamation of oil sands tailings in pit lakes.

1.2 Research Objectives

Alberta's oil sands demonstration pit lakes have been the subject of various research and monitoring programs since their inception. However, because of the complex nature of oil sands tailings, there are a number of ongoing challenges as well as uncertainties related to the biogeochemical and geotechnical behavior of oil sands pit lakes. These challenges and knowledge gaps should be addressed as part of ensuring successful reclamation of oil sands tailings. As such, the purpose of this research is to evaluate and improve the biogeochemical and geotechnical behavior of oil sands tailings in pit lakes. In order to achieve this purpose, three objectives were formulated, along with accompanying research question(s) and hypotheses, which correspond to the three laboratory studies that were conducted as part of this research.

Objective 1. Mitigate turbidity in oil sands pit lakes using biofilms

Research Question: Can mudline biofilms made up of microbial communities indigenous to oil sands tailings reduce turbidity in the overlying water cap in a pit lake?

Hypothesis: Biofilms have been found to have a stabilization effect (called biostabilization) in marine (Amos et al. 2004; Friend et al. 2003; Widdows et al. 2007; Wotton 2004) and fresh water (Droppo et al. 2007; Droppo 2009) sediments wherein they significantly increase the energy required to erode underlying sediments (Droppo et al. 2001; Droppo et al. 2007). Reid et al. (2016) investigated biostabilization in oil sands tailings ponds and found that aged tailings had greater microbial diversity and more extensive biofilms, both of which contributed to enhanced biostabilization of aged versus fresh tailings. Thus, mudline biofilms made up of microorganisms indigenous to oil sands tailings are expected to substantially reduce turbidity in the overlying water.

This laboratory study is novel as it is the first to demonstrate turbidity mitigation and biostabilization of oil sands pit lake mudlines using microbial communities indigenous to oil sands tailings.

Objective 2. Evaluate the biogeochemical and geotechnical behavior of untreated and PASS-treated oil sands tailings in pit lakes

Research Questions: How do the biogeochemical and geotechnical properties of pit lake tailings (untreated and PASS-treated) and cap water evolve over time? How is the evolution of biogeochemical and geotechnical properties impacted by accelerating microbial activity and/or microbially-derived processes (through elevated temperature, hydrocarbon amendments, and/or CO_2 addition)? Does column size influence geotechnical and biogeochemical behaviour?

Hypotheses:

As tailings in laboratory scale columns (which contain FFT and a water cap to mimic pit lakes) undergo self-weight consolidation, the solids content of the FFT should increase. Water cap concentrations of cations, anions, and organic compounds should also increase because of advective chemical fluxes associated with consolidation. In untreated FFT, degradation of organic compounds is expected to occur primarily through methanogenesis, leading to biogenic gas emissions of CO_2 and CH_4 (Foght et al. 2017). pH is anticipated to decrease as a result of biogenic CO_2 generation and dissolution, resulting in carbonate mineral dissolution and increased alkalinity and bicarbonate concentrations in the FFT (Dompierre et al. 2016; Siddique et al. 2014a). Water cap alkalinity will likely also increase due to advection of bicarbonate ions.

PASS-treated FFT is expected to undergo self-weight consolidation at a faster rate than untreated FFT, which should result in larger advective fluxes (and higher concentrations) of ions and organics in(to) the water caps. Because of the higher sulfate concentrations in the pore water of PASS-treated FFT, it is anticipated that sulfate reduction will be the dominant microbial process in these tailings (Holowenko et al. 2000; Ramos-Padrón et al. 2011). As such, it is expected that total sulfide concentrations in the pore water will increase. H_2S may be released and detectable in

the headspace, or it may precipitate under anaerobic conditions. DNA extraction and sequencing of microbial communities in PASS-treated FFT is expected to reveal more extensive SRB.

Columns under elevated temperature and/or with hydrocarbon amendments are expected to undergo more extensive biogeochemical cycling, including generating higher amounts of biogenic gases, increased degradation of organic compounds, and reduced concentrations of electron acceptors (Pavlostathis and Zhuang 1991; Siddique et al. 2006, 2007, 2011, 2015, 2020; Stasik and Wendt-Potthoff 2014; Wong et al. 2015). CO_2 addition is intended to mimic the bioconsolidation pathway proposed by Siddique et al. (2014a). As such, tailings amended with CO_2 should have a lower initial pH which is expected to increase carbonate mineral dissolution and ionic strength, and thereby improve clay flocculation and tailings consolidation. Column shape and size are expected to primarily impact tailings consolidation as there is a general consensus that interface settlement in cohesive sediment and slurries is hindered by smaller cross-sectional areas (Baotian et al. 2013; Gao et al. 2016). As such, tailings in the 19 L columns (which have a larger cross-sectional area than the 1 L columns) should consolidate more and thereby have a higher net water release (NWR) and higher water cap concentrations of ions and organic compounds.

This laboratory column study is the first to investigate the behavior of untreated versus PASS-treated tailings and the impact of column size on biogeochemical and geotechnical behavior of oil sands tailings.

Objective 3. Evaluate the effects of pressure on the biogeochemical and geotechnical behavior of PASS-treated oil sands tailings in pit lakes

Research Question: How does pressure impact the biogeochemical and geotechnical behavior of oil sands tailings in a pit lake?

Hypothesis: Pressure will increase tailings consolidation, thereby increasing pore water release from the tailings. Because of the enhanced dewatering associated with applying additional pressure to tailings, water cap concentrations of ions and organic compounds should be higher. The relatively low pressures that are incrementally applied to FFT in this work (0.3 to 5.1 kPa) could

potentially impact the composition of microbial communities in the tailings (Cassarini et al. 2019; Barbato and Scoma 2020), though the primary effect of these lower pressures is expected to be on solubility. For example, the solubility of biogenic CO_2 will be increased under pressure, which could enhance bioconsolidation processes. Extensive PAM biodegradation is not expected in the columns (Collins et al. 2016).

This laboratory column study is the first to investigate the effects of low pressures (in the kPa range) on the biogeochemical behavior of oil sands tailings.

1.3 Thesis Organization

Chapter 1 introduces the research problem, and highlights key background information, research objectives, and hypotheses. Chapter 2 reviews literature relevant to the research objectives. Portions of Chapter 2 were published in *Minerals*. Chapter 3 summarizes the results of a study that was conducted to evaluate turbidity mitigation in oil sands pit lakes using biofilms (Objective 1). A modified version of Chapter 3 was published in *Microorganisms*. Chapter 4 summarizes a column study that was conducted to evaluate the biogeochemical and geotechnical behavior of untreated and PASS-treated oil sands tailings in pit lakes (Objective 2). A modified version of Chapter 4 will be submitted to *Science of the Total Environment*. Chapter 5 summarizes the results of a second column study which evaluated the effects of pressure on the biogeochemical and geotechnical behavior of PASS-treated oil sands tailings in pit lakes (Objective 3). A modified version of Chapter 5 will be submitted to *Science of the Total Environment*. Chapter 6 provides a summary of key findings and recommendations for future research.

1.4 References

Abe, F. Exploration of the effects of high hydrostatic pressure on microbial growth, physiology and survival: perspectives from piezophysiology. *Biosci. Biotechnol. Biochem.* **2007**, *71*, 2347-2357.

Alberta Energy Regulator (AER). State of Fluid Tailings Management for Mineable Oil Sands, 2021; Alberta Energy Regulator: Calgary, CA, 2022; Available online: https://static.aer.ca/prd/documents/reports/State-Fluid-Tailings-Management-Mineable-OilSands.pdf

Amos, C.L.; Bergamasco, A.; Umgiesser, G.; Cappucci, S.; Cloutier, D.; DeNat, L.; Flindt, M.; Bonardi, G.; Cristante, S. The stability of tidal flats in Venice Lagoon—The results of in-situ measurements using two benthic annular flumes. *J. Mar. Syst.* **2004***, 51*, 211–241.

Baotian, W.; Shuaijie, G.; Funhai, Z. Research on deposition and consolidation behavior of cohesive sediment with settlement column experiment. *Eur. J. Environ. Civ. Eng.* **2013***, 17*, s144-s157.

Barbato, M.; Scoma, A. Mild hydrostatic-pressure (15 Mpa) affects the assembly, but not the growth, of oil-degrading coastal microbial communities tested under limiting conditions (5°C, no added nutrients). *FEMS Microbiol. Ecol.* **2020**, *96*, fiaa160.

Birtwell, I.K.; Farrell, M.; Jonsson, A. The Validity of Including Turbidity Criteria for Aquatic Resource Protection in Land Development Guideline (Pacific and Yukon Region); Fisheries and Oceans Canada: Vancouver, CA, 2008. Available online: https://publications.gc.ca/collections/collection_2014/mpo-dfo/Fs97-4-2852-eng.pdf

Blanchette, M.L.; Lund, M.A. Pit lakes are a global legacy of mining: an integrated approach to achieving sustainable ecosystems and value for communities. *Curr. Opin. Environ. Sustain.* **2016**, *23,* 28-34.

Bordenave, S.; Ramos, E.; Lin, S.; Voordouw, G.; Gieg, L.; Guo, C.; Wells, S. Use of calcium sulfate to accelerate densification while reducing greenhouse gas emissions from oil sands tailings ponds. In Proceedings of the Canadian International Petroleum Conference, Calgary, CA, 16–18 June 2009.

Canada's Oil Sands Innovation Alliance (COSIA). Pit Lakes: A Surface Mining Perspective; Canada's Oil Sands Innovation Alliance: Calgary, CA, 2021; Available online: https://cosia.ca/sites/default/files/attachments/Park%20-%20COSIA%20-%20Pit%20Lakes%20- %20Final.pdf

Cassarini, C.; Zhang, Y.; Lens, P.N.L. Pressure selects dominant anaerobic methanotrophic phylotype and sulfate reducing bacteria in coastal marine Lake Grevelingen sediment. *Front. Environ. Sci.* **2019**, *6*, 162.

Chalaturnyk, R.J.; Scott, J.D.; Özüm, B. Management of oil sands tailings. *Pet. Sci. Technol.* **2002**, *20*, 1025–1046.

Collins, C.E.V.; Foght, J.M.; Siddique, T. Co-occurrence of methanogenesis and N_2 fixation in oil sands tailings. *Sci. Total Environ.* **2016**, *565*, 306–312.

Cossey, H.L.; Batycky, A.E.; Kaminsky, H.; Ulrich, A.C. Geochemical stability of oil sands tailings in mine closure landforms. *Minerals* **2021a**, *11*, 830.

Dompierre, K.A.; Barbour, S.L. Characterization of physical mass transport through oil sands fluid fine tailings in an end pit lake: A multi-tracer study. *J. Contam. Hydrol.* **2016**, *189*, 12–26.

Dompierre, K.A.; Barbour, S.L.; North, R.L.; Carey, S.K.; Lindsay, M.B.J. Chemical mass transport between fluid fine tailings and the overlying water cover of an oil sands end pit lake. *Water Resour. Res.* **2017**, *53*, 4725–4740.

Dompierre, K.A.; Lindsay, M.B.J.; Cruz-Hernández, P.; Halferdahl, G.M. Initial geochemical characteristics of fluid fine tailings in an oil sands end pit lake. *Sci. Total Environ.* **2016**, *556*, 196–206.

Droppo, I. Biofilm structure and bed stability of five contrasting freshwater sediments. *Mar. Freshw. Res.* **2009***, 60*, 690–699.

Droppo, I.G.; Lau, Y.L.; Mitchell, C. The effect of depositional history on contaminated bed sediment stability. *Sci. Total Environ.* **2001***, 266*, 7–13.

Droppo, I.G.; Ross, N.; Skafel, M.; Liss, S.N. Biostabilization of cohesive sediment beds in a freshwater wave-dominated environment. *Limnol. Oceanogr.* **2007**, *52*, 577–589.

Fichtel, K.; Logemann, J.; Fichtel, J.; Rullkötter, Cypionka, H.; Engelen, B. Temperature and pressure adaptation of sulfate reducer from the deep subsurface. *Front. Microbiol.* **2015**, *6*, 1078.

Foght, J.M.; Gieg, L.M.; Siddique, T. The microbiology of oil sands tailings: Past, present, future. *FEMS Microbiol. Ecol.* **2017**, *93*, fix034.

Friend, P.L.; Ciavola, P.; Cappucci, S.; Santos, R. Bio-dependent bed parameters as a proxy tool for sediment stability in mixed habitat intertidal areas. *Cont. Shelf Res.* **2003***, 23*, 1899–1917.

Gao, Y.F.; Zhang, Y.; Zhou, Y.; Li, D. Effects of column diameter on settling behavior of dredged slurry in sedimentation experiments. *Mar. Georesources Geotechnol.* **2016**, *34*, 431-439.

Golder Associates Ltd. Literature Review of Global Pit Lakes: Pit Lake – Case Studies; Report 1777450, Golder Associate Ltd: Calgary, CA, 2017; Available online: https://cosia.ca/sites/default/files/attachments/Literature%20Review%20of%20Global%20Pit%20Lakes_0.pdf

Government of Alberta. Lower Athabasca Region: Tailings Management Framework for the Mineable Athabasca Oil Sands. Government of Alberta: Edmonton, CA, 2015; Available online: https://open.alberta.ca/publications/9781460121740

Government of Alberta. Oil sands facts and statistics. 2023. Available online: https://www.alberta.ca/oil-sands-facts-and-statistics.aspx#:~:text=Alberta's%20oil%20sands%20has%20the,165.4%20billion%20barrels%20(bbl) (accessed 6 February 2023).

Grula, M.M.; Huang, M.; Sewell, G. Interactions of certain polyacrylamides with soil bacteria. *Soil Sci.* **1994**, *158*, 291–300.

Guezennec, A.G.; Michel, C.; Bru, K.; Touze, S.; Desroche, N.; Mnif, I.; Motelica-Heino, M. Transfer and degradation of polyacrylamide-based flocculants in hydrosystems: a review. *Environ. Sci. Pollut. Res.* **2015**, *22*, 6390–6406.

Haveroen, M.E.; MacKinnon, M.D.; Fedorak, P.M. Polyacrylamide added as a nitrogen source stimulates methanogenesis in consortia from various wastewaters. *Water Res.* **2005**, *29*, 3333–3341.

Holowenko, F.M.; MacKinnon, M.D.; Fedorak, P.M. Methanogens and sulfate-reducing bacteria in oil sands fine tailings waste. *Can. J. Microbiol.* **2000**, *46*, 927–937.

Hu, H.; Liu, J.F.; Li, C.Y.; Yang, S.Z.; Gu, J.D.; Mu, B.Z. Anaerobic biodegradation of partially hydrolyzed polyacrylamide in long-term methanogenic enrichment cultures from production water of oil reservoirs. *Biodegradation*, **2018**, *29*, 233-243.

Jessen, G.L.; Chen, L.-X.; Mori, J.F.; Nelson, Nelson, T.E.C.; Slater, G.F.; Lindsay, M.B.J.; Banfield, J.F.; Warren, L.A. Alum addition triggers hypoxia in an engineered pit lake. *Microorganisms* **2022**, *10*, 510.

Kaminsky, H.; Omotoso, O. Variability in fluid fine tailings. In Proceedings of the 5th International Oil Sands Tailings Conference, Lake Louise, CA, 4–7 December 2016.

McKenna, G. Landscape design for mine reclamation. In Proceedings of the Tailings and Mine Waste '09, Banff, CA, 1–4 November 2009.

McKenna, G.; Mooder, B.; Burton, B.; Jamieson, A. Shear strength and density of oil sands fine tailings for reclamation of a boreal forest landscape. In Proceedings of the 5th International Oil Sands Tailings Conference, Lake Louise, CA, 4–7 December 2016.

Pavlostathis, S.G.; Zhuang, P. Effect of temperature on the development of anaerobic cultures from a contaminated subsurface soil. *Environ.Technol.* **1991**, *12*, 679-687.

Pope, D.H.; Berger, L.R. Inhibition of metabolism by hydrostatic pressure: what limits microbial growth? *Arch. Mikrobiol.* **1973**, *93*, 367-370.

Ramos-Padrón, E.; Bordenave, S.; Lin, S.; Bhaskar, I.M.; Dong, X.; Sensen, C.W.; Fournier, J.; Vourdouw, G.; Gieg, L.M. Carbon and sulfur cycling by microbial communities in a gypsum-treated oil sands tailings pond. *Environ. Sci. Technol.* **2011**, *45*, 439–446.

Reid, M.L.; Warren, L.A. S reactivity of an oil sands composite tailings deposit undergoing reclamation wetland construction. *J. Environ. Manag.* **2016**, *166*, 321–329.

Reid, T.; VanMansel, D.; Droppo, I.G.; Weisener, C.G. The symbiotic relationship of sediment and biofilm dynamics at the sediment water interface of oil sands industrial tailings ponds. *Water Res.* **2016**, *100*, 337–347.

Sawatsky, L.; Hyndman, A.; McKenna, G.; Vandenberg, J. Fluid fine tailings processes: disposal, capping, and closure alternatives. In Proceedings of the 6th International Oil Sands Tailings Conference, Edmonton, CA, 9–12 December 2018.

Shen, X.; Sun, T.; Su, M.; Dang, Z.; Yang, Z. Short-term response of aquatic ecosystem metabolism to turbidity disturbance in experimental estuarine wetlands. *Ecol. Eng*. **2019**, *136*, 55–61.

Siddique, T.; Fedorak, P.M.; Foght, J.M. Biodegradation of short-chain n-alkanes in oil sands tailings under methanogenic conditions. *Environ. Sci. Technol.* **2006**, *40*, 5459-5464.

Siddique, T.; Fedorak, P.M.; Mackinnon, M.D.; Foght, J.M. Metabolism of BTEX and naphtha compounds to methane in oil sands tailings. *Environ. Sci. Technol.* **2007**, *41*, 2350–2356.

Siddique, T.; Kuznetsov, P.; Kuznetsova, A.; Arkell, N.; Young, R.; Li, C.; Guigard, S.; Underwood, E.; Foght, J.M. Microbially-accelerated consolidation of oil sands tailings. Pathway I: changes in porewater chemistry. *Front. Microbiol.* **2014a**, *5*, Article 106.

Siddique, T.; Mohamad Shahimin, M.F.; Zamir, S.; Semple, K.; Li, C.; Foght, J.M. 2015. Long-term incubation reveals methanogenic biodegradation of C_5 and C_6 iso-alkanes in oil sands tailings. *Environ. Sci. Technol.* **2015,** *49*, 14732-14739.

Siddique, T.; Penner, T.; Semple, K.; Foght, J.M. Anaerobic biodegradation of longer-chain n-alkanes coupled to methane production in oil sands tailings. *Environ. Sci. Technol.* **2011**, *45*, 5892–5899.

Siddique, T.; Semple, K.; Li, C.; Foght, J.M. Methanogenic biodegradation of *iso*-alkanes and cycloalkanes during long-term incubation with oil sands tailings. *Environ. Pollut.* **2020,** *258*, 113768.

Stasik, S.; Loick, N.; Knöller, K.; Weisener, C.; Wendt-Potthoff, K. Understanding biogeochemical gradients of sulfur, iron and carbon in an oil sands tailings pond. *Chem. Geol.* **2014**, *382*, 44–53.

Stasik, S.; Wendt-Potthoff, K. Interaction of microbial sulphate reduction and methanogenesis in oil sands tailings ponds. *Chemosphere* **2014**, *103*, 59–66.

Suncor Energy Inc. (Suncor). 2021 Base Plant Fluid Tailings Management Report; Suncor Energy Inc: Calgary, CA, 2022a.

Suncor Energy Operating Inc. (Suncor) 2021 Fort Hills Fluid Tailings Management Report; Suncor Energy Operating Inc. on behalf of Fort Hills Energy Corporation; Calgary, CA, 2022b.

Syncrude Canada Ltd. (Syncrude). 2021 Pit Lake Monitoring and Research Report (Base Mine Lake Demonstration Summary: 2021-2020); Syncrude Canada Ltd: Fort McMurray, CA, 2021.

Tedford, E.; Halferdahl, G.; Pieters, R.; Lawrence, G.A. Temporal variations in turbidity in an oil sands pit lake. *Environ. Fluid Mech.* **2019**, *19*, 457–473.

Vandenberg, J.; Schultze, M.; McCullough, C.D.; Castendyk, D. The future direction of pit lakes: part 2, corporate and regulatory closure needs to improve management. *Mine Water Environ.* **2022**, *41,* 544-556.

Warren, L.A.; Kendra, K.E.; Brady, A.L.; Slater, G.F. Sulfur biogeochemistry of an oil sands composite tailings deposit. *Front. Microbiol.* **2016**, *6*, 1–14.

Wei, K.; Cossey, H.L.; Ulrich, A.C. Effects of calcium and aluminum on particle settling in an oil sands end pit lake. *Mine Water Environ.* **2021**, *40*, 1025-1036.

Widdows, J.; Friend, P.L.; Bale, A.J.; Brinsley, M.D.; Pope, N.D.; Thompson, C.E.L. Inter-comparison between five devices for determining erodibility of intertidal sediments. *Cont. Shelf Res.* **2007***, 27*, 1174–1189.

Wong, M.; An, D.; Caffrey, S.M.; Soh, J.; Dong, X.; Sensen, C.W.; Oldenburg, T.B.P.; Larter, S.R.; Voordouw, G. 2015. Roles of thermophiles and fungi in bitumen degradation in mostly cold oil sands outcrops. *Appl. Environ. Microbiol.* **2015**, *81*, 6825-6838.

Wotton, R.S. The essential role of exopolymers (EPS) in aquatic systems. *Oceanogr. Mar. Biol.* **2004**, *42*, 57–94.

2 LITERATURE REVIEW

2.1 Oil Sands Tailings Generation

All of Canada's oil sands surface mining takes places in the Athabasca region in northern Alberta (Government of Alberta 2023). Surface mining is advantageous where possible because it results in significantly greater bitumen recovery than in situ extraction methods (Kasperski and Mikula 2011). However, surface mining also requires more land disturbance and results in large volumes of tailings.

Bitumen is extracted from surface mined oil sands ore using a technique called the Clark Hot Water Process, patented by Dr. Karl Clark in 1929 (Chalaturnyk et al. 2002). The process has since been improved to achieve a recovery of greater than 90% from high grade ore containing > 10 wt% bitumen (Chow et al. 2008). In the Hot Water Process, caustic soda (sodium hydroxide, NaOH) and hot water are mixed with crushed oil sands ore, allowing bitumen to froth and float to the surface of primary and secondary separation vessels while solids settle to the bottom (Clark and Pasternack 1932). Sodium hydroxide addition promotes bitumen recovery by increasing the pH of the crushed ore mixture and causing organic acids that are naturally present in bitumen to become water-soluble surfactants (Bakhtiari 2015; Chalaturnyk et al. 2002). This effectively reduces surface and interfacial tensions in the mixture and causes the ore structure to disintegrate, releasing a water-in-bitumen emulsion called froth. The froth must undergo further treatment (froth treatment) to separate the bitumen. Sodium hydroxide addition is beneficial for bitumen recovery, but it also causes dispersion of clays which makes the tailings difficult to process (Chalaturnyk et al. 2002). The organic acids released from bitumen during the Hot Water Process are called naphthenic acid fraction compounds (NAFCs), which are a broad family of polar organic carboxylic acids, some of which are acutely and chronically toxic to aquatic organisms (Brown and Ulrich 2015; Headley et al. 2016; Kavanagh et al. 2011; Morandi et al. 2015; Quinlan and Tam 2015; Scott et al. 2005).

While the bitumen froth undergoes froth treatment with a hydrocarbon diluent to reduce bitumen viscosity and enhance separation, the remainder of the tailings slurry is treated in separation vessels to further separate the solids and recover residual bitumen (Chalaturnyk et al. 2002; Chow et al. 2008). This results in three main tailings streams: coarse tailings (approximately 55 wt% solids),

FFT (6–10 wt% solids), and froth treatment tailings (FTT) (Chalaturnyk et al. 2002; Kasperski and Mikula 2011). Coarse tailings are collected from the bottom of the primary separation cell and as such coarse tailings solids consist largely of sand (>44 μm). Conversely, FFT consists mostly of fines (<44 μm) and has a sand to fines ratio (SFR) of <1. The fines fraction of tailings is made up of silt and clay minerals, predominately kaolinite, illite, and quartz (Kasperski and Mikula 2011). FTT contains diluent, either naphtha, which is comprised mainly of aliphatic C_5 to C_{16} hydrocarbons and monoaromatic hydrocarbons (BTEX, benzene, toluene, ethylbenzene, and xylenes), or light paraffinic diluents which consist mainly of C_5 to C_6 alkanes (Foght et al. 2017; Kasperski and Mikula 2011; Rao et al. 2013). Naphtha is used at Suncor Base Plant, Syncrude Mildred Lake, and CNRL Horizon and paraffinic solvents are used at CNUL's Muskeg River mine, Imperial's Kearl mine, and Fort Hills operated by Suncor (Imperial 2020; Small et al. 2015; Suncor 2023a). Bitumen froth from Syncrude Aurora North is processed at Mildred Lake and similarly, froth from CNUL's Jackpine mine is processed at the Muskeg River mine. The produced streams (coarse tailings, FFT, and FTT) may or may not be combined, depending on the operator.

After being deposited in tailings ponds, tailings sand is quick to settle and segregate from the rest of the tailings (Chalaturnyk et al. 2002; Kasperski and Mikula 2011). The sand forms a beach that can be used to build containment dykes to retain the remainder of the tailings (collectively referred to as FFT). After a few years of settling, FFT develops a loose card-house structure of clay particles surrounded by water with a solids content of roughly 30 wt% and will remain in this state for decades as they slowly dewater and consolidate. This stable slurry structure is due to the low flocculation and consolidation characteristics of the clay water slurry and the high clay content of the tailings. These geotechnical characteristics make reclamation of FFT challenging. As such, many operators are treating tailings with physical and/or chemical amendments to enhance dewatering and consolidation and increase the bearing capacity and shear strength of the tailings. Figure 2-1 provides a visual comparison of untreated versus polymer treated FFT. Treated tailings may be deposited (back) in tailings ponds or in dedicated disposal areas (DDAs) to undergo further dewatering. Eventually all the tailings generated from oil sands surface mining must be reclaimed in one of two landforms: a pit lake or terrestrial landform.

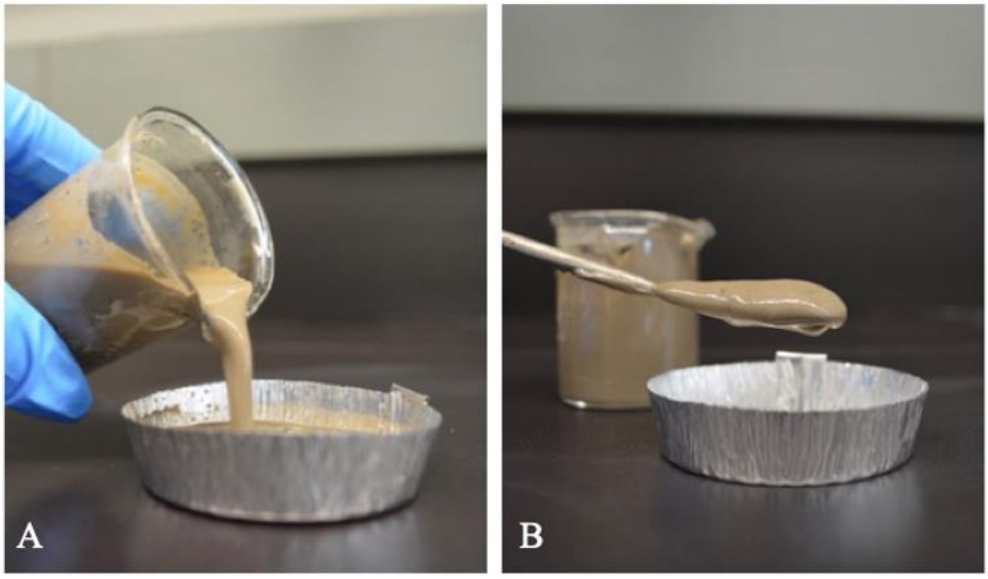

Figure 2-1. (A) Untreated FFT and (B) thickened tailings (FFT with PAM flocculant). Taken from Cossey et al. (2021a).

2.2 Oil Sands Tailings Reclamation

2.2.1 Pit Lakes

Oil sands pit lakes are engineered water bodies that contain oil sands by-product materials stored below grade in decommissioned open pits (Westcott and Watson 2007). In general, there are expected to be two main types of pit lakes in oil sands mine closure landscapes: (i) pit lakes with tailings storage; and (ii) pit lakes without tailings storage (Charette et al. 2010). Pit lakes with tailings storage will generally be comprised of thick deposits (10–80 m) of untreated or treated tailings capped with water (3–10 m). Because of the low strength (0.01 to 1 kPa) and low wet density (1250 kg/m^3) of untreated FFT, water capping is the only possible capping and closure option for these tailings (McKenna 2009; Sawatsky et al. 2018). However, water capping untreated FFT is more challenging than capping denser, treated tailings and increases the potential for particle resuspension in the water cap (Sawatsky et al. 2018). Pit lakes without tailings storage are simpler, especially from a design and management point of view, as they will consist of decommissioned open pits that have been allowed to fill with surface runoff and groundwater. The end goal is for pit lakes to develop into self-sustaining boreal lake ecosystems that will receive surface and groundwater inputs from the surrounding land and discharge water to downstream environments (Westcott and Watson 2007; Suncor 2023b). Ideally, the water cap will serve as

habitat for a freshwater aquatic ecosystem while the tailings can naturally dewater over time (in the case of pit lakes with tailings storage). The remainder of this thesis will focus on pit lakes that contain tailings.

Syncrude's commercial scale demonstration pit lake, BML, is located at the Mildred Lake mine and contains roughly a 45 m thick deposit of untreated FFT (Syncrude 2023). The FFT in BML was impacted by residual naphtha diluent (i.e. the FFT was previously combined with FTT in a tailings pond), which may have influenced biogeochemical cycling processes in BML because diluent acts as a carbon source for microorganisms. Suncor's commercial and pilot scale PASS deposits (DDA3 and Lake Miwasin) are located at their Base Plant mine and contain PASS-treated tailings (FFT treated with alum and PAM) that have not been impacted by residual diluent. Fort Hills (operated by Suncor) plans to implement PASS as well, though they will use ferric sulfate as the coagulant instead of alum (Suncor 2023c). The tailings that will undergo PASS treatment at Fort Hills will be impacted by residual paraffinic diluent, though Suncor indicates that the ferric sulfate addition will enhance the biodegradation of residual diluent (pentane) (Suncor 2023c), presumably through sulfate reduction. Suncor (2023c) proposes that this will reduce CH_4 generation (via pentane degradation) from PASS-treated deposits.

The reclamation of FFT in pit lakes has not been approved yet by AER and there are a number of ongoing challenges and uncertainties surrounding the biogeochemical and geotechnical behavior of FFT in pit lakes that are currently being evaluated. The biogeochemical and geotechnical challenges and knowledge gaps relevant to this thesis are discussed in the following subsections.

2.2.1.1 Turbidity

Water cap turbidity in a pit lake can occur due to i) particle settling and ii) resuspension of underlying FFT through processes such as wind waves, wind-driven circulation, penetrative convection, inflows and outflows, gas ebullition, and pore water fluxes (Lawrence et al. 2016; Zhao et al. 2021). Turbidity was an ongoing challenge in BML and as such, the water cap was dosed with alum in the fall of 2016 which reduced turbidity that year (Syncrude 2022). However, turbidity in BML still fluctuates seasonally and is typically highest during spring/early summer and fall each year. Post alum addition, turbidity as high as 100 NTU has been reported in the BML

water cap during fall mixing events (Syncrude 2022). Interestingly, alum addition unintentionally triggered hypoxia in BML (Jessen et al. 2022). This occurred because alum increased the production of easily degradable biomass and aqueous sulfide species, leading to increased oxygen consumption. Further, CH_4 oxidation, which reduces $CH_{4(g)}$ release from BML, decreased by an order of magnitude following alum addition, possibly a result of methanotrophs being stripped out of the water cap by alum (Slater et al. 2021). As such, alternative adaptive management strategies should be explored to mitigate turbidity in BML and other pit lakes in the future.

Turbidity may limit the ability of pit lakes to develop into self-sustaining aquatic ecosystems as turbidity can limit light penetration, thereby hindering the development of a littoral zone (Charette et al. 2010). Littoral zones are important for habitat, protection, and food for organisms, as well as dissolved oxygen, erosion control, and water quality. Alberta's surface water quality guidelines for the protection of freshwater aquatic life indicate that for turbid waters, turbidity should not increase more than 8 NTU (where background turbidity is between 8 and 80 NTU) or more than 10% of background turbidity (where background turbidity is >80 NTU) (Government of Alberta 2018). Based on 2014 to 2021 turbidity data presented in Syncrude (2022), turbidity in BML is above Alberta's surface water quality guidelines for extended periods of time (30 to 60 d) each year, even post alum addition. Further, the duration of exposure is important, as long-term (greater than 10 months) exposure to a relatively low turbidity of 3 NTU can have significant effects on fish growth and habitat (Birtwell et al. 2008). As such, turbidity in pit lake water caps could have negative impacts on aquatic organisms and ecosystems. However, if the processes that contribute to physical water mixing, and thereby turbidity, are limited, then dissolved oxygen will be consumed and potentially lead to hypoxia in pit lake water caps. Given the negative effects of turbidity on aquatic ecosystems, as well as the unintended outcomes of alum addition in BML, there are opportunities to develop new adaptive management strategies which can reduce the resuspension of FFT particles from the mudline, thereby mitigating turbidity generation.

2.2.1.2 Consolidation

Consolidation of FFT refers to the decrease in pore pressure that occurs as water escapes the tailings matrix and the corresponding increase in effective stress. During consolidation, the volume of tailings decreases in accordance with the volume of water expressed. Thus, tailings

consolidation also corresponds with an increase in density and solids content. BML is currently undergoing self-weight consolidation which has increased the FFT density, along with the average fines solids content which increased by 4.1% (from 41.7% to 45.8%) between 2013 and 2017 (Dunmola et al. 2023). Tailings consolidation is closely tied to geochemistry as tailings dewatering contributes to chemical mass loading in overlying surface water and contaminant transport to nearby surface water and groundwater.

Self-weight consolidation has been used to naturally dewater oil sands tailings for over 50 years, however this process can be slow depending on the properties of the tailings and requires large areas to contain the tailings and expressed pore water (BGC Engineering Inc. 2010). Because of the unique properties of oil sands tailings, their consolidation behavior is described using Gibson's finite strain theory which can account for the large strain (volume change) and non-linear permeability and compressibility that are characteristic of FFT undergoing consolidation (Gibson et al. 1967; Jeeravipoolvarn et al. 2008b; Suthaker and Scott 1994). Gibson's finite strain theory is provided in Equation 2-1, where ρ_s is solids density, ρ_w is fluid density, k is hydraulic conductivity, e is void ratio, σ' is effective stress, z is depth, and t is time. The change in hydraulic conductivity, as a function of void ratio, can be represented by the power law function in Equation 2-2, where C and D are fitted parameters. The change in effective stress with void ratio (i.e. compressibility) can be represented by the Weibull function in Equation 2-3, where A, B, E, and F are fitted parameters (Jeeravipoolvarn et al. 2009), though a power law function is also widely used for compressibility (Rourke and Hockley 2018) or a modified power law function may also be used.

$$\pm\left(\frac{\rho_s}{\rho_w}-1\right)\frac{d}{de}\left[\frac{k(e)}{1+e}\right]\frac{\partial e}{\partial z}+\frac{\partial}{\partial z}\left[\frac{k(e)}{\rho_w(1+e)}\frac{d\sigma'}{de}\frac{\partial e}{\partial z}\right]+\frac{\partial e}{\partial t}=0 \tag{2-1}$$

$$k = Ce^D \tag{2-2}$$

$$e = A - Bexp(-E{\sigma'}^F) \tag{2-3}$$

Untreated FFT has low hydraulic conductivity, typically between 1 x 10^{-6} and 1 x 10^{-9} m/s, and high compressibility and as such self-weight consolidation of this material can take decades (BGC Engineering Inc. 2010). Consolidation behavior is different for untreated versus treated tailings and will vary depending on material properties of the tailings including solids content, fines content, and SFR. Generally, tailings with a higher initial solids content consolidate at a faster rate (Jeeravipoolvarn et al. 2009). SFR is also indicative of consolidation behavior as sand can act as an internal surcharge on FFT. Therefore, mixing sand and FFT will result in a mixture that undergoes self-weight consolidation faster and to a greater extent than FFT alone (Jeeravipoolvarn et al. 2009; Sorta et al. 2015). Composite tailings (CT), which typically have a solids content of 60 wt% and an SFR of 4, have a higher hydraulic conductivity and lower compressibility than untreated FFT and will therefore consolidate at a faster rate. Jeeravipoolvarn et al. (2009) analyzed self-weight consolidation in three 10 m standpipes filled with tailings and found that a standpipe with a mixture of FFT and sand (74.8 wt% solids, 18.0 dry wt% fines, ~5 dry wt% clays, 4.56 SFR) had a 6.4% increase in solids content and generated significant effective stress over a 25-year period. Conversely, untreated FFT typically has a low solids content (~30 wt%) and low SFR (~0.1) and is very slow to consolidate (Beier 2015; Jeeravipoolvarn et al. 2008a, 2009). Jeeravipoolvarn et al. (2009) found that untreated FFT (30.6 wt% solids, 89.0 dry wt% fines, ~45 dry wt% clays, 0.12 SFR) in a 10 m standpipe strained more than 30% over 25 years and the solids content increased to 41.8 wt%, but there was little to no effective stress generation in the tailings. The lack of strength generation in untreated FFT even after large volume changes has implications for closure of these tailings, as trafficability (bearing capacity) and capping options are limited (Jeeravipoolvarn et al. 2009). As such, most operators are using physical and/or chemical amendments to improve the geotechnical properties of their tailings for closure.

Several studies have reported that treating FFT with sand or flocculants improved consolidation behavior (Jeeravipoolvarn et al. 2009; Sorta et al. 2016; Wilson et al. 2018). Wilson et al. (2018) used large strain consolidation tests to compare consolidation behavior in six tailings samples: five thickened tailings samples (49.0–55.0 wt% solids; 51–67 dry wt% fines) and one untreated FFT sample (46.1 wt% solids; 96 dry wt% fines). In all cases, the treatment (flocculant addition and thickening) of the tailings increased hydraulic conductivity of the tailings by at least half an order of magnitude, which in turn results in faster consolidation. Further, Sorta et al. (2016) reported

that an FFT-sand mixture (20 dry wt% fines, 10 dry wt% clay) had an order of magnitude higher hydraulic conductivity and a lower compressibility than thickened tailings (50–60 dry wt% fines, 26–31 dry wt% clay) during large strain consolidation tests, indicating improved consolidation behavior for sand-treated tailings over thickened tailings. There are currently no publicly available studies comparing the consolidation behavior of PASS-treated FFT to that of other untreated or treated FFT, though PASS-treated FFT is expected to have improved consolidation behavior relative to untreated FFT (Suncor 2022b).

2.2.1.3 Pore Water Fluxes

BML studies by Dompierre and Barbour (2016) and Dompierre et al. (2017) identified two key processes by which chemical constituents in tailings pore water may move from FFT into the overlying water cap shortly after a pit lake is commissioned: (i) advection and dispersion driven by upward pore water flow as tailings dewater and consolidate; and (ii) FFT disturbance due to fluid movement in the water cover (for example, internal waves), which would cause rapid, but intermittent mass loading to the water cap. Dompierre and Barbour (2016) and Dompierre et al. (2017) determined that, at the time of the studies, an advection-dispersion mass transport regime (from FFT dewatering) was dominant in BML, with intermittent disturbance near the mudline causing additional mass transport of pore water constituents. Using a mass balance of BML water, Dompierre et al. (2017) estimated the advective vertical pore water flux to be 0.002 $m^3/m^2/d$, equivalent to 0.73 m of FFT settlement per year. In an earlier study conducted one year after BML was commissioned, advective vertical mass transport was estimated to be 0.004 $m^3/m^2/d$ (Dompierre and Barbour 2016), suggesting that consolidation rates have decreased over time and/or that disturbances at the mudline have decreased due to the greater depth of the water cap, thus reducing chemical mass loading (Dompierre et al. 2017). Data presented in Dunmola et al. (2023) (2012 to 2019 inclusive) shows that settlement of the BML mudline has slowed since 2012, which is consistent with self-weight consolidation decreasing over time. Initially, chemical mass loading into BML water cap was primarily due to advection. However, over time as consolidation rates decrease, chemical mass loading into the water cap is expected to be predominantly due to diffusion (Dompierre et al. 2017; Francis et al. 2022). Francis et al. (2022) and Slater et al. (2021) also suggest that gas ebullition from FFT enhances chemical mass transport into the BML water cap. Compared to untreated FFT, treated FFT is generally expected to have higher hydraulic

conductivity and improved consolidation behavior, which would theoretically increase the initial advective pore water fluxes from treated tailings deposits.

Chemical pore water constituents in BML FFT include high concentrations of sodium (Na^+, 977 mg/L), chloride (Cl^-, 633 mg/L), and bicarbonate (HCO_3^-, 1885 mg/L) as well as lesser amounts of calcium, magnesium, and potassium (Syncrude 2020). The presence and concentrations of these constituents in BML pore water indicates that pore water release (advective transport) and diffusion will likely contribute these constituents to the water cap for many years, thus influencing BML water quality in the long term (Dompierre et al. 2016). White and Liber (2018) identified Na^+, Cl^-, and HCO_3^- as the ions making up the majority of BML's surface water salinity, comprising 92% of the total osmolarity, which is consistent with the dominant ions in BML FFT (Dompierre et al. 2016; Syncrude 2020). Additionally, BML FFT contains various metals and organic constituents such as residual bitumen, NAFCs (65 mg/L), and polycyclic aromatic hydrocarbons which are also being released into BML surface water (Syncrude 2020, 2022). Though freshwater dilutions have helped to improve BML water cap quality, more than 70% of samples collected from the BML water cap in 2020 exceeded Alberta's chronic surface water quality guidelines for the protection of freshwater aquatic life for chloride, boron, chromium, sulfide, and F2 hydrocarbons (which also exceeded acute guidelines) (Syncrude 2023). As such, chemical mass loading into pit lake water caps has implications for the types of aquatic organisms that the lakes can support as well as water management requirements, and ultimately may influence the timeline within which a pit lake becomes a self-sustaining aquatic ecosystem.

2.2.1.4 Biogeochemical Cycling

Oil sands tailings, especially sand-dominated tailings such as CT and coarse sand tailings, are nutrient limited, with generally low amounts of phosphorous and nitrogen available for microbial metabolism (Boldt-Burisch et al. 2018; Foght et al. 2017). Carbon sources in tailings include residual bitumen, hydrocarbon diluents, and carboxylic acids, whereas possible nitrogen sources may include PAM, recalcitrant organic nitrogen, and/or nitrogen cycling (Collins et al. 2016; Small et al. 2015). Despite nutrient limitations, diverse and active microbial communities in FFT contribute to the cycling of nitrogen, iron, sulfur, and carbon in tailings (Foght et al. 2017; Penner and Foght 2010; Warren et al. 2016). Redox conditions and the availability of terminal electron

acceptors (e.g. O_2, NO_3^-, Fe(III), SO_4^{2-}, CO_2) within tailings will dictate the biogeochemical cycling that occurs within a particular redox zone, as shown in Figure 2-2. Redox potentials measured by Dompierre et al. (2016) in BML indicated anoxic conditions throughout the FFT with Eh values ranging from < -250 to -100 mV. Though the redox potential of the BML water cap was not measured in that study, oxic conditions near the water surface have been reported in other studies (Arriaga et al. 2019; Risacher at al. 2018). Anoxic conditions below the mudline have also been observed in oil sands tailings ponds (Penner and Foght 2010; Stasik and Wendt-Potthoff 2016; Stasik et al. 2014) and terrestrial deposits (Reid and Warren 2016; Warren et al. 2016).

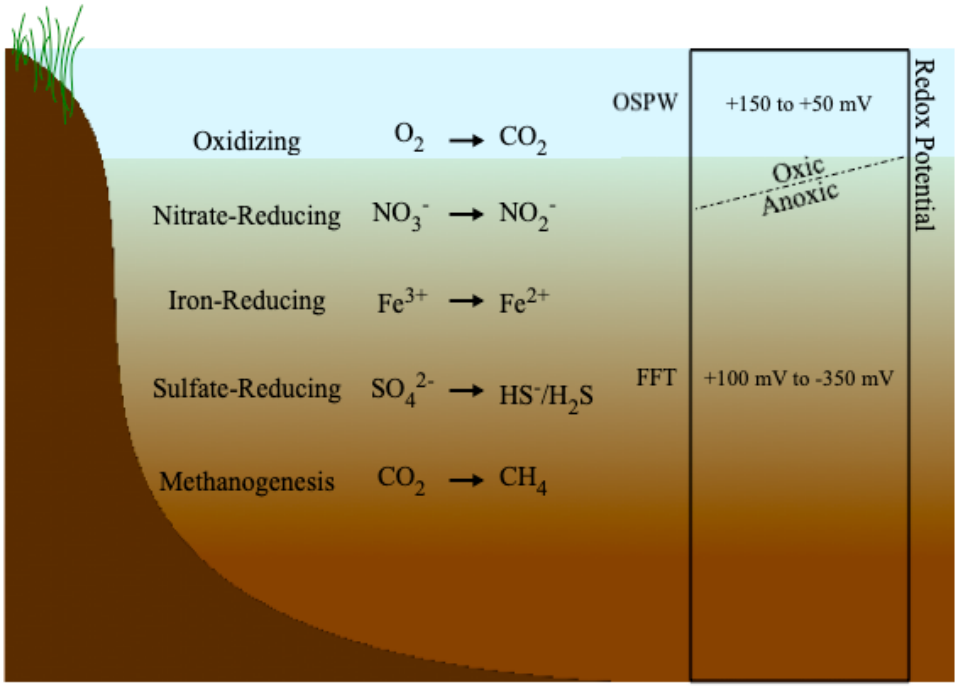

Figure 2-2. Redox profile for tailings landforms (tailings ponds, pit lakes, etc.) and redox potential ranges for cap water and tailings. Note that the oxic/anoxic boundary does not necessarily start at the mudline as suggested in this figure and instead, may start above the mudline. Taken from Cossey et al. (2021a).

Oxic conditions in tailings ponds, pit lakes, and terrestrial deposits exist when there is free molecular oxygen (O_2) present. Risacher et al. (2018) found that BML had oxygen throughout the 10 m water cap during the summer season (prior to alum addition), reaching as high as 85% saturation near the surface, although oxygen concentrations decreased with depth and were at low

levels near the mudline (<5% saturation). During ice cover, oxygen levels in BML have been found to decrease steadily, and Lawrence et al. (2016) reported oxygen levels reaching 0% saturation near the BML surface right before ice-off in 2013/2014. However, physical mixing processes, such as seasonal lake turnovers in the spring and fall, can help to increase oxygen levels in the BML water cap (Arriaga et al. 2019).

Oxygen levels within the BML water cap are also impacted by carbon, sulfur, and nitrogen cycling (Arriaga et al. 2019; Risacher et al. 2018). CH_4, ammonium (NH_4^+), and hydrogen sulfide species (ΣH_2S) have been identified as important oxygen consuming constituents in the BML water cap and/or near the mudline (Albakistani et al. 2022; Arriaga et al. 2019; Mori et al. 2019; Risacher et al. 2018; Yan et al. 2022). Several studies of BML have found that aqueous CH_4 and NH_4^+ concentrations decrease moving upwards from the mudline to the surface due to aerobic methanotrophy and nitrification, respectively (Chen et al. 2020; Mori et al. 2019; Risacher et al. 2018). Alum addition further increased oxygen consumption and the extent of the anoxic zone in the BML water cap through increased production of easily biodegradable carbon and aqueous sulfide species (Jessen et al. 2022; Yan et al. 2022), though alum addition also reduced CH_4 oxidation, possibly due to stripping out of methanotrophs (Slater et al. 2021). The various biogeochemical cycling processes occurring in the BML water cap will likely impact BML oxygen concentrations for decades.

Bioremediation can occur in oil sands tailings deposits through aerobic and anaerobic biodegradation of hydrocarbons and NAFCs. Biodegradation of hydrocarbons and NAFCs in tailings ponds has been studied extensively (Herman et al. 1994; Holowenko et al. 2000; Mohamad Shahimin and Siddique 2017a,b; Penner and Foght 2010; Rochman et al. 2017; Saidi-Mehrabad et al. 2013; Scott et al. 2005; Mohamad Shahimin et al. 2016, 2021; Siddique et al. 2006, 2007, 2011, 2015; Stasik and Wendt-Potthoff 2014, 2016; Stasik et al. 2015; Yu et al. 2018). Several studies have demonstrated aerobic biodegradation of hydrocarbons (Rochman et al. 2017; Saidi-Mehrabad et al. 2013; Yu et al. 2018) and NAFCs (Herman et al. 1994; Scott et al. 2005; Clemente et al. 2004) in oil sands tailings by bacteria. Additional studies have found algae (Quesnel et al. 2011; Yu et al. 2019) and fungi (Miles et al. 2020) capable of biodegrading NAFCs. Aerobic biodegradation may occur in tailings landforms, particularly in the uppermost layer of pit lake

water caps and in wetlands, and in aerated tailings deposits, which would improve water and seepage quality over time. However, anaerobic biodegradation is more likely to occur in tailings because the saturated, fine grained nature of tailings makes it difficult for oxygen to penetrate (Bornstein et al. 1980; Keiluweit and Fendorf 2016; Neira et al. 2015).

Information on nitrogen cycling in FFT is limited. While facultative nitrate (NO_3^-) reducing bacteria are abundant in tailings (Foght et al. 2017), nitrate and nitrite (NO_2^-) concentrations are generally below detection (Stasik and Wendt-Potthoff 2014; Stasik et al. 2014). This finding may suggest that nitrate reduction is not an important microbial process in FFT. However, NH_4^+ is known to be important oxygen consuming constituent in the BML water cap through nitrification (Risacher et al. 2018). It is thus important to note the potential for nitrogen cycling and nitrate-reducing conditions within the tailings redox profile (Figure 2-2).

Iron-reducing bacteria can influence solid phase chemistry of clay minerals containing insoluble ferric (Fe^{III}) oxides and can potentially impact water quality by allowing ferrous (Fe^{II}) cations, Fe^{2+}, generated through iron reduction to react with reduced sulfur species and precipitate $FeS_{(s)}$ (Penner and Foght 2010; Rudderham 2019). Dompierre et al. (2016) reported slightly elevated concentrations of dissolved Fe directly below the mudline in BML, which was attributed to Fe^{2+} (because Fe^{3+} is relatively insoluble at a pH > 5) and therefore iron reduction. Sulfate reduction was also evident in this same zone below the mudline in BML. Similarly, Stasik et al. (2014) reported that synchronous iron and sulfur cycling was occurring 1 to 4 m below the mudline of an active tailings pond and that reduced sulfide species (primarily HS^-) were precipitating to form $FeS_{(s)}$. Iron reduction and subsequent secondary mineral precipitation, specifically $FeS_{(s)}$, have been linked to dewatering in BML (Dompierre et al. 2016).

To date, most of the studies evaluating microbial activity in oil sands FFT have focused on methanogenesis, which is the dominant microbial activity in untreated FFT. However, sulfate reduction may dominate in sulfate-amended FFT which includes centrifuged tailings, CT, and PASS-treated tailings. The addition of sulfate, which acts as an electron acceptor in sulfate reduction, to tailings may create conditions that encourage the growth and activity of SRB. For example, Bordenave et al. (2009) reported an average sulfate reduction rate of 10 mmol sulfate

reduced/m^3 tailings/day (roughly 960 mg/m^3 tailings/day) in Suncor Pond 6, which contains CT, and Ramos-Padrón et al. (2011) reported active sulfate reducing zones 2 to 15 m below the mudline in Pond 6. Further, sulfur cycling has been reported in terrestrial deposits of sulfate-amended tailings. Warren et al. (2016) conducted a biogeochemical study of Syncrude's 34 m thick Kingfisher CT deposit and found an extensive SRB zone (22–34 m) characterized by higher total organic carbon concentrations and highly reducing environments. An average of 70% of the SO_4^{2-} originally present in the CT (due to gypsum amendments) was lost and ΣH_2S (>300 μM or 10 mg/L) was detected in pore water throughout the deposit (except in the shallow zone). While the shallow zone (2–4 m) of the CT deposit was primarily an iron reducing zone, an abundance of *Clostridium*, which can reduce thiosulfate and S^0, was found within the iron reducing zone and the transition zone (6–8 m), suggesting that sulfur cycling was also occurring in the surface layers of the deposit. Interestingly, DNA sequencing of microbial communities in the deposit revealed that known sulfate/sulfur reducing bacteria (such as *Desulfovibrio, Desulfuromonas, Desulfocapsa,* and *Clostridium)* made up only 2% of the total bacterial community, though up to 90% of the Operational Taxonomic Units were considered to be capable of sulfur metabolism and the microbial communities present in the CT were highly sulfur active (Warren et al. 2016).

Another example of sulfur cycling in a sulfate-amended terrestrial deposit was presented in Reid and Warren (2016) who evaluated the biogeochemistry of three zones within Syncrude's Sandhill Fen: the 40 m of CT deposit, the 10 m intermediary layer of sand tailings, and the wetland. Oxygen was present only in the ponded water in the wetland, while anoxic conditions existed at the wetland-sand interface and continued down through the sand cap and CT. Extensive sulfate reduction due to the presence of gypsum in the CT generated ΣH_2S in all three zones, however, the highest concentrations of aqueous and gaseous H_2S were found in the sand cap. The sand layer acted as a mixing zone wherein sulfur rich porewater from the dewatering CT mixed with labile organic carbon from the developing wetland and stimulated microbial generation of H_2S (Reid and Warren 2016). Because Suncor's PASS treatment process is still relatively new, there is no data available on biogeochemical cycling in PASS, though like in CT deposits, sulfate reduction is expected to be an important microbial process in PASS. Sulfate is also present in untreated FFT (though to a lesser extent) and both Dompierre et al. (2016) and Syncrude (2020) have reported zones of low SO_4^{2-} below the mudline in BML, consistent with sulfate reduction. Alum addition

enhanced sulfur cycling and the extent of anoxic zone in the BML water cap and as a result, SRB activity has now also been observed above the mudline (Yan et al. 2022).

Sulfate reduction can lead to the generation of toxic hydrogen sulfide (H_2S) gas and other reduced sulfur compounds (RSCs) through the degradation of a variety of organic compounds in FFT (Gee et al. 2017). Aqueous hydrogen sulfide species (ΣH_2S) may also persist after sulfate reduction. Unionized aqueous hydrogen sulfide (H_2S) has been found to be toxic to aquatic organisms, with freshwater fish showing the greatest sensitivity and experiencing adverse effects at concentrations < 5 µg S/L (based on chronic and acute data) (ANZECC & ARMCANZ 2000; USEPA 1986). Under anoxic conditions, ΣH_2S may precipitate as metal sulfides resulting in heavy metal immobilization and sedimentation within FFT. Oxidation of ΣH_2S to sulfate or sulfur oxidation intermediates (such as S^0, SO_3^{2-}, $S_2O_3^{2-}$) under oxic conditions has been found to remove ΣH_2S in the BML water cap (Risacher et al. 2018; Yan et al. 2022). Various products and substrates of sulfur cycling reactions (ΣH_2S, SO_4^{2-}, S^0, SO_3^{2-}, $S_2O_3^{2-}$) are present in the BML water cap, suggesting that sulfate reduction and subsequent sulfur cycling reactions will be important biogeochemical processes in both the FFT and cap water in oil sands pit lakes (Yan et al. 2022).

Methanogenesis is the dominant microbial process occurring in FFT and is a major mechanism of hydrocarbon degradation (Fedorak et al. 2003; Siddique et al. 2006, 2007, 2011; Stasik and Wendt-Potthoff 2014). Residual diluent, commonly naphtha, in the tailings is the main substrate that sustains methanogenesis in FFT (Siddique et al. 2007). Hydrogenotrophic and acetoclastic methanogens, as well as other methanogenic archaea and a consortium of syntrophic bacteria are primarily responsible for methanogenic activity in tailings (Penner and Foght 2010; Siddique et al. 2011; Small et al. 2015). Siddique et al. (2006, 2007, 2011) and Mohamad Shahimin et al. (2016) found that under methanogenic conditions in the laboratory, n-alkanes (short and long chain) and monoaromatics can be degraded, both of which are present in naphtha diluent. It was later found that iso- and cyclo-alkanes can also be metabolized in tailings under methanogenic conditions following the depletion of n-alkanes, and that both naphtha and paraffinic diluents can be degraded (Mohamad Shahimin and Siddique 2017a,b; Mohamad Shahimin et al. 2021; Siddique et al. 2015, 2020; Tan et al. 2015). While hydrocarbon degradation is beneficial in tailings deposits

in that it reduces acute diluent toxicity, methanogenic biodegradation also contributes substantially to greenhouse gas emissions of CO_2 and CH_4 (Small et al. 2015).

Methanogenic degradation of hydrocarbons has also been observed in the field. The concentration of light hydrocarbons, such as BTEX and naphtha, typically decreases with tailings depth (age) within a deposit as these light compounds are preferentially degraded over more recalcitrant compounds (Penner and Foght 2010; Stasik et al. 2015). Tailings can take years to develop competent communities of methanogens, with 15-year lag periods reported for Suncor's Pond 1 and Syncrude's Mildred Lake Settling Basin (Holowenko et al. 2000; Fedorak et al. 2002). As such, the microbial activity and hydrocarbon degradation in tailings deposits will vary for deposits that consist of legacy tailings (tailings that are currently in tailings ponds) versus fresh tailings (Foght et al. 2017). Microbial activity will also vary for different types of tailings and different treatment methods. For example, FTT is more likely to trigger methanogenesis because it contains diluent. Syncrude's Mildred Lake Settling Basin and Suncor's Pond 2/3 both contain FTT and are responsible for the highest CH_4 production, 26.3 t/ha/year and 9.5 t/ha/year, respectively, of all tailings deposits based on 2011 and 2012 data compiled by Burkus et al. (2014) (though measurements of gases emitted per hectare do not account for the depth of the tailings deposit which will also influence emissions). Methanogenic microbial activity has also generated greenhouse gas emissions of CO_2 and CH_4 from BML. Clark et al. (2021) used eddy covariance to measure CH_4 and CO_2 fluxes from BML and found that fluxes were highest in 2014, the year following the fresh water capping, with median fluxes of 2.0 t/ha/year and 20.2 t/ha/year for CH_4 and CO_2, respectively. Carbon fluxes from BML have since decreased, with mean fluxes of 0.9 t/ha/year and 3.2 t/ha/year for CH_4 and CO_2, respectively, during the last three years of the Clark et al. (2021) study (2017 to 2019). $CH_{4(aq)}$ consumption by aerobic methanotrophy has been noted in BML water cap which may contribute to lower CH_4 emissions, though it also contributes to oxygen depletion (Risacher et al. 2018). The greenhouse gas potential of each pit lake will be different and will relate to the amount of unrecovered hydrocarbons remaining in the tailings at the time of deposition (Charette et al. 2010).

2.2.1.5 Bioconsolidation

The biogenic production of CO_2 and CH_4 in tailings has been found to contribute to tailings dewatering through a process referred to as bioconsolidation (Fedorak et al. 2003; Siddique et al. 2014a,b). Siddique et al. (2014a) proposed a bioconsolidation pathway in which methanogenesis in FFT contributes to dewatering. Firstly, the ebullition of biogenic gases can create transient physical channels through which pore water can escape (Siddique et al. 2014a). Ebullition may be dominated by CH_4 (rather than CO_2) because of its poor solubility in water. Research has also shown that CH_4 bubbles moving across the mudline can increase fluxes of salts moving into the water cap (COSIA 2020). Second, biogenic gases promote tailings dewatering by altering the pore water chemistry. Siddique et al. (2014a) found that under methanogenic conditions, the dissolution of biogenic CO_2 lowered the pH of MFT which resulted in the dissolution of carbonate minerals and increased the concentrations of divalent cations (Ca^{2+} and Mg^{2+}) and HCO_3^-. These higher ion concentrations increased the ionic strength of the pore water, decreasing the thickness of the diffuse double layer surrounding the clay particles thereby promoting clay flocculation. Siddique et al. (2014a) further suggested that cation exchange did not play a significant role in this bioconsolidation pathway. SRB also contributes to biogenic CO_2 production and could therefore, theoretically, contribute to bioconsolidation.

In a companion paper, Siddique et al. (2014b) suggested an additional pathway by which microbial metabolism can accelerate tailings dewatering. They found that an anaerobic microbial community comprised of bacteria and archaea reduced Fe^{III} minerals in MFT (ferrihydrite and goethite) to amorphous Fe^{II} minerals (such as $FeS_{(s)}$ and possibly green rust (mixed-valence Fe^{II}-Fe^{III} hydroxides, carbonates and/or sulfates)). Siddique et al. (2014b) proposed a pathway in which *Clostridiales* and *Synergistaceae* bacteria ferment organic carbon in FFT to produce fatty acids, alcohols, CO_2, and H_2 as substrates for SRB and methanogens. Subsequent electron flows/transfers (possibly from SRB, methanogens, etc.) reduce Fe^{III} to Fe^{II}. The resulting amorphous Fe^{II} minerals entrap, coat, and mask negative clay surfaces, reducing the repulsive forces between the clay particles and increasing consolidation (Siddique et al. 2014b).

Bioconsolidation may contribute to tailings consolidation, particularly in fines dominated deposits that have active anaerobic microbial communities and slow rates of self-weight consolidation.

Dompierre et al. (2016) found that FFT in BML likely underwent microbially enhanced dewatering through carbonate mineral dissolution, as suggested by Siddique et al. (2014a). The pH of BML FFT decreased by approximately 0.5 pH units from the mudline to a depth of 10 m below the mudline, consistent with biogenic CO_2 dissolution, while concentrations of Ca and Mg increased (Dompierre et al. 2016) The authors suggested that these geochemical changes contributed to bioconsolidation of the FFT. Pore water in BML was near saturation for calcite, dolomite, and siderite but X-ray diffraction indicated that the dissolution of carbonate minerals had largely depleted calcite and dolomite minerals in the tailings at the time of sampling in 2013 (Dompierre et al. 2016). This suggests that the role of carbonate mineral dissolution in bioconsolidation will decrease over time as these minerals are depleted (Dompierre et al. 2016).

2.2.1.6 Polyacrylamide

PAM is a high molecular weight, water-soluble polymer and the most commonly used flocculant in oil sands mining, though it also has a number of water and wastewater treatment applications (Vedoy and Soares 2015). PAM is available in a variety of forms with varying charges (anionic, cationic, or non-ionic), charge densities, and molecular weights, though the primary monomer of all these different types of PAM is acrylamide (Haveroen et al. 2005; Lipp and Kozakiewicz 1991). The most frequently used form of PAM in tailings treatment is partially hydrolyzed PAM (HPAM), where a portion of the acrylamide monomers are replaced with acrylate, making the polymer slightly anionic. Studies often do not distinguish between PAM and HPAM, and thus the term PAM will be used to collectively refer to PAM in all its various forms, unless it is important to differentiate between the degradation of PAM and HPAM.

In comparison to water and wastewater treatment applications of PAM, biodegradation of PAM in oil sands tailings is more likely, given the higher doses used (often 10 times higher) and the lack of other available nutrients in tailings. Studies have demonstrated the microbial degradation of PAM in both aerobic (Bao et al. 2010; Berdugo-Clavijo et al. 2019; Kay-Shoemake et al. 1998; Li et al. 2023; Liu et al. 2012; Song et al. 2017, 2018; Wen et al. 2010) and anaerobic (Dai et al. 2014, 2015; Haveroen et al. 2005; Hu et al. 2018; Song et al. 2017) environments. PAM biodegradation is thought to occur as a result of microbial degradation of the main carbon chain backbone or hydrolysis of the amide nitrogen (Joshi and Abed 2017; Kay-Shoemake et al. 1998; Nakamiya et

al. 1995; Wen et al. 2010). Kay-Shoemake et al. (1998) found that aerobic microorganisms can produce extracellular amidases that remove the amide group from PAM, which generates NH_4^+ that can be used as a nitrogen source (see also Figure 2-3). Further, Haveroen et al. (2005) found that nitrogen derived from PAM stimulated methanogenesis in Syncrude thickened tailings, Syncrude FFT, and domestic sewage sludge. In addition to methanogenesis, PAM may also serve as a nitrogen source and stimulate SRB (Grula et al. 1994).

In contrast to the findings of Haveroen et al. (2005), Collins et al. (2016) found that PAM did not serve as a nitrogen source for methanogenesis in Shell Albian Sands (now CNUL) FFT. Instead, methanogenic activity was determined to be a result of nitrogen fixation. The contradictory findings of Haveroen et al. (2005) and Collins et al. (2016) may be due to: (i) differences in tailings microbial communities because each study used tailings from different operators; (ii) different carbon amendments; (iii) different PAM concentrations (CNUL's PAM doses are much lower than that of other operators); and (iv) the fact that Haveroen et al. (2005) performed serial transfers to dilute fixed nitrogen (2016). The discrepancy in the results of Havereon et al. (2005) and Collins et al. (2016) suggest that the extent to which PAM may biodegrade will vary among tailings deposits and operators and will be at least partially dependent on the availability of other sources of nitrogen and/or carbon.

The large size of the polymer (molecular weight > 10^6 Da) and a lack of enzymes capable of depolymerizing the polymer make it is much more difficult for microorganisms to use PAM as the sole carbon source (Collins et al. 2016; Haveroen et al. 2005; Kay-Shoemake et al. 1998). Conditions where PAM was the only available carbon source resulted in a decrease in higher molecular weight compounds, suggesting cleavage of the polymer backbone (Hu et al. 2018; Song et al. 2017). However, if biodegradation of PAM were to occur in PAM-amended tailings, it would be most likely due to PAM serving as a nitrogen source.

Little is known about the extent of PAM biodegradation in tailings and therefore, the generation of PAM biodegradation products and their fate in tailings deposits. Potential PAM biodegradation products and intermediates may include polyacrylate (Haveroen et al. 2005; Kay-Shoemake et al. 1998) or polyacrylic acid (Bao et al. 2010; Liu et al. 2012; Song et al. 2018) following hydrolysis

of the amide group, as well as pyruvic acid (Dai et al. 2015), acetyl-coenzyme A (CoA) (Dai et al. 2015; Song et al. 2018), and acrylamide monomer, a neurotoxin (Dai et al. 2014), though to date there is limited research that shows PAM biodegradation to acrylamide monomer. These products may be further deaminated or metabolized to carboxylic acids and lower molecular weight organic compounds (Bao et al. 2010; Song et al. 2018; Dai et al. 2014, 2015). Based on previous biodegradation studies of PAM and HPAM, possible mechanisms of HPAM biodegradation are presented in Figure 2-3. The predicted biodegradation products for HPAM and PAM are similar, though the negatively charged carboxylic group of HPAM may inhibit interactions of the polymer backbone with the negatively charged bacteria cell wall, shifting priority to hydrolysis of the amide group (Bao et al. 2010; Song et al. 2018).

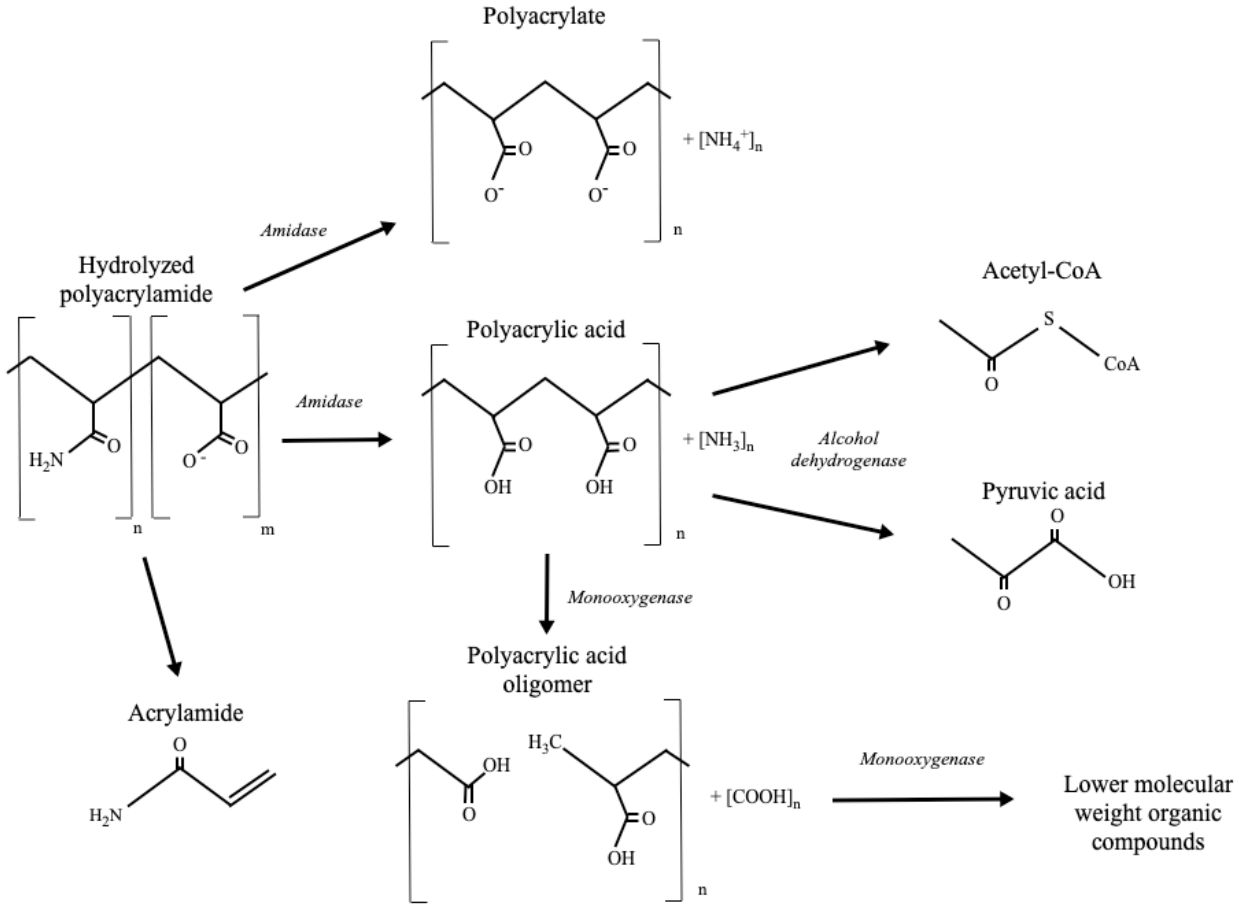

Figure 2-3. Potential biodegradation pathways of partially hydrolyzed polyacrylamide in oil sands tailings. Taken from Cossey et al. (2021a).

Other mechanisms of PAM degradation are possible as well, such as mechanical, photolytic, thermal, and/or chemical degradation. Mechanical degradation of PAM through shear flow and/or direct mechanical loads has been reported in several studies (Caulfield et al. 2002; Neelakantan et al. 2018; Xiong et al. 2020) and likely occurs in oil sands mining operations during transport of tailings in pumps and pipelines and deposition of tailings in a pond or DDA. Mechanical degradation of PAM can decrease the molecular weight of the parent compound, though mechanically degraded PAM should remain chemically similar to the undegraded parent compound (Xiong et al. 2020). It is unknown how mechanical degradation of PAM during tailings transport and deposition may impact its biodegradation. Photolytic degradation of PAM is also possible (Woodrow et al. 2002; Xiong et al. 2018a) and may occur in tailings depending on terrestrial deposition conditions or light penetration in pit lakes. While thermal and chemical degradation of PAM have been reported in studies (Caulfield et al. 2002; Gröllmann et al. 1982; Pei et al. 2016; Uranta et al. 2018; Xiong et al. 2018b), these mechanisms of degradation are less likely to occur in oil sands tailings unless tailings are stored at high temperatures (50°C) and/or under acidic conditions.

2.2.1.7 Pressure

The effects of total and effective stresses and hydrostatic pressure on microbial activity and biogeochemical cycling in oil sands tailings deposits are largely unknown. Microbial activity in marine sediments and seawater has been found to be impacted by hydrostatic pressures (Abe 2007; Barbato and Scoma 2020; Fichtel et al. 2015; Scoma et al. 2019; Tholosan et al. 1999). Barbato and Scoma (2020) noted a shift in the composition of microbial communities at a hydrostatic pressure of 15 MPa. High hydrostatic pressures can negatively impact microbial physiology, including cell shape, macromolecular structures, and processes such as metabolism (especially protein synthesis), cell growth, viability, and motility, though the mechanisms by which hydrostatic pressure impacts these cellular functions are not well understood (Abe 2007; Fichtel et al. 2015; Pope and Berger 1973). Most mesophilic microorganisms will experience a reduction in cell growth at hydrostatic pressures of several dozen MPa and cell growth will be completely inhibited at hydrostatic pressures of roughly 50 MPa (Abe 2007). However, the hydrostatic pressures in these studies are much greater than that of an oil sands pit lake. Even a 100 m deep

pit lake would have a hydrostatic pressure of < 1 MPa at the bottom. To date no studies have explicitly investigated the effects of total/effective stress on microbial communities.

Various laboratory studies have used microcosms or high pressure bioreactors to investigate the effects of partial pressure on microbial activity. Researchers have reported both positive and inhibitory effects, depending on the microbially-mediated reaction, gas, and partial pressure. Positive effects were generally associated with more thermodynamically favorable reaction conditions. Deusner et al. (2010), Meulepas et al. (2010), and Timmers et al. (2015) evaluated the effects of CH_4 partial pressures (pCH_4) ranging from 0.1 up to 10 MPa on (trace) anaerobic methane oxidation and sulfate reduction in sediments and sludge and found that higher pCH_4 generally increased CH_4 oxidation and sulfate reduction and reduced methanogenesis. However, in one instance, Timmers et al. (2015) found that long-term (160 d) incubation of a sludge at 10 MPa pCH_4 did not improve CH_4 oxidation or sulfate reduction. Cassarini et al. (2019) conducted a similar microcosm study on lake sediment with pCH_4 up to 40 MPa and found that CH_4 oxidation and sulfate reduction increased up to 0.45 MPa and 10 MPa, respectively. Cassarini et al. (2019) and Timmers et al. (2015) also noted distinct shifts in microbial communities under elevated pCH_4. Mayumi et al. (2013) evaluated the effect of CO_2 partial pressure (pCO_2, 200 kPa) on methanogenic pathways in oil reservoir samples and noted increased CH_4 production and a shift in dominant microbial communities and methanogenic pathways when the pCO_2 was increased relative to control microcosms. Hao et al. (2017) evaluated the effects of H_2 partial pressure on anaerobic digestion in batch reactors and found that a H_2 partial pressure of 33 kPa enhanced methanogenesis without inhibiting acidogenesis or acetogenesis. However, another anaerobic digestion study found that under higher H_2 partial pressures (80 kPa), CH_4 production decreased sharply (Cazier et al. 2015). The findings from the studies presented in this subsection may differ for numerous reasons including differences in research methodology (especially the method of applying pressure), magnitude of pressure, microbial communities and the pressures and temperatures they are accustomed to, microbial reactions, and available substrates. Regardless of these differences it is evident that partial pressure can influence and even enhance microbial activity in sediments and sludges.

There is limited information on the effects of pressure on microbial activity in oil sands tailings. One study by Penner and Foght (2010) found that deeper tailings deposits (up to 30 m) in tailings ponds generally had lower numbers of viable microorganisms (based on most probable number values) than shallower deposits (6 to 10 m), though microbial diversity was similar across all depths. Pore water sulfate concentrations increased with depth within the tailings ponds, which was attributed to a decrease in the number of viable SRB with depth (Penner and Foght 2010). Penner and Foght (2010) attributed the decrease in most probable number values with depth to the depletion and diffusion-limited replenishment of substrates and nutrients in deeper tailings deposits. To date there are no laboratory studies that have explicitly investigated the effects of pressure (hydrostatic pressure or total/effective stress) on microbial activity and biogeochemical cycling in oil sands tailings.

2.2.2 Terrestrial Reclamation

Terrestrial reclamation of oil sands tailings involves additional geotechnical challenges because the tailings are capped with a solid material, and as such tailings destined for terrestrial reclamation require a higher strength and bearing capacity than tailings deposited in pit lakes. Tailings suitable for capping with solids materials may include both fines-dominated tailings (thickened tailings and centrifuged tailings) and fines-enriched sand tailings (CT and non-segregating tailings) (OSTC and COSIA 2012). The closure landform targeted for these fines-dominated or fines-enriched sand tailings is a terrestrial deposit with a wetland (AER 2020). Some amount of residual subsidence is anticipated for solid-capped tailings deposits, especially for fines-dominated deposits, however if the subsidence is substantial, a water capped deposit may be more appropriate to reduce the requirement for long-term management and maintenance of the solid capping layers and expressed pore water (OSTC and COSIA 2012).

The biogeochemical challenges and knowledge gaps associated with terrestrial reclamation of oil sands tailings are similar to that of pit lakes (with the exception of turbidity). For example, pore water fluxes from underlying CT are impacting water quality in Syncrude's Sandhill Fen, which is a pilot wetland constructed on top of 40 m CT deposit with a 10 m intermediary layer of sand tailings (Biagi et al. 2019; Reid and Warren 2016). The major ions in near-surface water in Syncrude's Sandhill Wetland are HCO_3^-, SO_4^{2-}, Cl^-, Na^+, Ca^{2+}, and Mg^{2+} (Hartsock et al. 2021),

which is consistent with the chemicals elevated in FFT. Biagi et al. (2019) found that during the first years of operation (2013–2015), concentrations of SO_4^{2-}, Cl^-, Na^+, Ca^{2+}, and Mg^{2+} increased annually in the wetland. Using stable isotopes, Biagi et al. (2019) were able to show that these ions primarily stemmed from upward fluxes of pore water from the underlying CT deposit. Salt fluxes from terrestrial tailings deposits will have implications for water quality and vegetation growth in overlying wetlands and may impact the type of wetland that develops (fen, marsh, etc.) (Biagi and Carey 2022; Biagi et al. 2021; Hartsock et al. 2021; Vitt et al. 2016).

Microbial activity and biogeochemical cycling processes in terrestrial landforms containing FFT will likely be similar to that of tailings ponds and pit lakes, though these processes will also depend on oxic versus anoxic conditions in terrestrial landforms, as well as the type of tailings deposited (FTT, chemically amended tailings, etc.). Reid and Warren (2016) have shown that sulfate reduction has occurred extensively throughout the Sandhill Fen, as discussed previously in subsection 2.2.1.4. CH_4 fluxes from the Sandhill Fen were low for the years 2013 to 2015, with a median flux of 0.04 t/ha/year, possibly a result of SRB outcompeting methanogens given the abundance of electron acceptors for SRB (Clark et al. 2020). It is not known yet how the greenhouse gas emissions from pit lakes will compare to those of terrestrial reclamation methods. Over time, terrestrial landforms that incorporate peat may develop into carbon sinks, as is the case for the lowland within Syncrude's Sandhill Fen, though the midland and upland areas are still carbon sources (Clark et al. 2019).

2.3 References

Abe, F. Exploration of the effects of high hydrostatic pressure on microbial growth, physiology and survival: perspectives from piezophysiology. *Biosci. Biotechnol. Biochem.* **2007**, *71*, 2347-2357.

Albakistani, E.A.; Nwosu, F.C.; Furgason, C.; Haupt, E.S.; Smirnova, A.V.; Verbeke, T.J.; Lee, E.S.; Kim, J.J.; Chan, A.; Ruhl, I.A.; et al. Seasonal dynamics of methanotrophic bacteria in a boreal oil sands end pit lake. *Appl. Environ. Microbiol.* **2022**, *88*, e01455-21.

Alberta Energy Regulator (AER). State of Fluid Tailings Management for Mineable Oil Sands, 2019; Alberta Energy Regulator: Calgary, CA, 2020.

Arriaga, D.; Colenbrander Nelson, T.; Risacher, F.F.; Morris, P.K.; Goad, C.; Slater, G.F.; Warren, L.A. The co-importance of physical mixing and biogeochemical consumption in controlling water cap oxygen levels in Base Mine Lake. *Appl. Geochem.* **2019**, *111*, 104442.

Australian and New Zealand Environment and Conservation Council & Agriculture and Resource Management Council of Australia and New Zealand (ANZECC & ARMCANZ). Australian and New Zealand Guidelines for Fresh and Marine Water Quality; ANZECC & ARMCANZ: Canberra, AU, 2000.

Bakhtiari, M.T. Role of Sodium Hydroxide in Bitumen Extraction: Production of Natural Surfactants and Slime Coating. Ph.D. Thesis, University of Alberta, Edmonton, CA, 2015.

Bao, M.; Chen, Q.; Li, Y.; Jiang, G. Biodegradation of partially hydrolyzed polyacrylamide by bacteria isolated from production water after polymer flooding in an oil field. *J. Hazard. Mater.* **2010**, *184*, 105–110.

Barbato, M.; Scoma, A. Mild hydrostatic-pressure (15 Mpa) affects the assembly, but not the growth, of oil-degrading coastal microbial communities tested under limiting conditions (5°C, no added nutrients). *FEMS Microbiol. Ecol.* **2020**, *96*, fiaa160.

Beier, N.A. Development of a Tailings Management Simulation and Technology Evaluation Tool. Ph.D. Thesis, University of Alberta, Edmonton, CA, 2015.

Berdugo-Clavijo, C.; Sen, A.; Seyyedi, M.; Quintero, H.; O'Neil, B.; Gieg, L.M. High temperature utilization of PAM and HPAM by microbial communities enriched from oilfield produced water and activated sludge. *AMB Express* **2019**, *9*, 1–10.

BGC Engineering Inc. Oil Sands Tailings Technology Review; Oil Sands Research and Information Network, University of Alberta: Edmonton, CA, 2010.

Biagi, K.M.; Carey, S.K. The hydrochemical evolution of a constructed peatland in a post-mining landscape six years after construction. *J. Hydrol. Reg. Stud.* **2022**, *39*, 100978.

Biagi, K.M.; Clark, M.G.; Carey, S.K. Hydrological functioning of a constructed peatland watershed in the Athabasca oil sands region: Potential trajectories and lessons learned. *Ecol. Eng.* **2021**, *166*, 106236.

Biagi, K.M.; Oswald, C.J.; Nicholls, E.M.; Carey, S.K. Increases in salinity following a shift in hydrologic regime in a constructed wetland watershed in a post-mining oil sands landscape. *Sci. Total Environ.* **2019**, *653*, 1445–1457.

Birtwell, I.K.; Farrell, M.; Jonsson, A. The Validity of Including Turbidity Criteria for Aquatic Resource Protection in Land Development Guideline (Pacific and Yukon Region); Fisheries and Oceans Canada: Vancouver, CA, 2008. Available online: https://publications.gc.ca/collections/collection_2014/mpo-dfo/Fs97-4-2852-eng.pdf

Boldt-Burisch, K.; Naeth, M.A.; Schneider, U.; Schenider, B.; Hüttl, R.F. Plant growth and arbuscular mycorrhizae development in oil sands processing by-products. *Sci. Total Environ.* **2018**, *621*, 30–39.

Bordenave, S.; Ramos, E.; Lin, S.; Voordouw, G.; Gieg, L.; Guo, C.; Wells, S. Use of calcium sulfate to accelerate densification while reducing greenhouse gas emissions from oil sands tailings ponds. In Proceedings of the Canadian International Petroleum Conference, Calgary, CA, 16–18 June 2009.

Bornstein, J.; Hedstrom, W.E.; Scott, F.R. Oxygen Diffusion Rate Relationships under Three Soil Conditions; Life Sciences and Agriculture Experiment Station, University of Maine: Orono, US, 1980; Volume 98, pp. 1–14.

Brown, L.D.; Ulrich, A.C. Oil sands naphthenic acids: A review of properties, measurement, and treatment. *Chemosphere* **2015**, *127*, 276–290.

Burkus, Z.; Wheler, J.; Pletcher, S. GHG Emissions from oil sands tailings ponds: Overview and modelling based on fermentable substrates. In Part I: Review of Tailings Pond Facts and Practices; Alberta Environment and Sustainable Resource Development: Edmonton, CA, 2014.

Canada's Oil Sands Innovation Alliance (COSIA). 2019 Water Mining Research Report; Canada's Oil Sands Innovation Alliance: Calgary, CA, 2020.

Cassarini, C.; Zhang, Y.; Lens, P.N.L. Pressure selects dominant anaerobic methanotrophic phylotype and sulfate reducing bacteria in coastal marine Lake Grevelingen sediment. *Front. Environ. Sci.* **2019**, *6*, 162.

Caulfield, M.J.; Qiao, G.G.; Solomon, D.H. Some aspects of the properties and degradation of polyacrylamides. *Chem. Rev.* **2002**, *102*, 3067–3083.

Cazier, E.A.; Trably, E.; Steyer, J.P.; Escudie, R. Biomass hydrolysis inhibition at high hydrogen partial pressures in solid-state anaerobic digestion. *Bioresour. Technol.* **2015**, *190*, 106-113.

Chalaturnyk, R.J.; Scott, J.D.; Özüm, B. Management of oil sands tailings. *Pet. Sci. Technol.* **2002**, *20,* 1025–1046.

Charette, T.; Castendyk, D.; Hrynyshyn, J.; Küpper, A.; McKenna, G.; Mooder, B. End Pit Lakes Guidance Document 2012; Cumulative Effects Management Association: Fort McMurray, CA, 2010.

Chen, L.X.; Méheust, R.; Crits-Christoph, A.; McMahon, K.D.; Colenbrander Nelson, T.; Slater, G.F.; Warren, L.A.; Banfield, J.F. Large freshwater phages with the potential to augment aerobic methane oxidation. *Nat. Microbiol.* **2020**, *5*, 1504–1515.

Chow, D.L.; Nasr, T.N.; Chow, R.S.; Sawatzky, R.P. Recovery techniques for Canada's heavy oil and bitumen resources. *J. Can. Petrol. Technol.* **2008**, *47*, 12–17.

Clark, K.A.; Pasternack, D.S. Hot water separation of bitumen from Alberta bituminous sand. *Ind. Eng. Chem.* **1932**, *24*, 1410–1416.

Clark, M.G.; Drewitt, G.B.; Carey, S.K. Energy and carbon fluxes from an oil sands pit lake. *Sci. Total Environ.* **2021**, *752*, 141966.

Clark, M.G.; Humphreys, E.R.; Carey, S.K. The initial three years of carbon dioxide exchange between the atmosphere and a reclaimed oil sands wetland. *Ecol. Eng.* **2019**, *17*, 667–682.

Clark, M.G.; Humphreys, E.R.; Carey, S.K. Low methane emissions from a boreal wetland constructed on oil sands mine tailings. *Biogeosciences* **2020**, *135*, 116–126.

Clemente, J.S.; MacKinnon, M.D.; Fedorak, P.M. Aerobic biodegradation of two commercial naphthenic acids preparations. *Environ. Sci. Technol.* **2004**, *38*, 1009–1016.

Collins, C.E.V.; Foght, J.M.; Siddique, T. Co-occurrence of methanogenesis and N2 fixation in oil sands tailings. *Sci. Total Environ.* **2016**, *565*, 306–312.

Cossey, H.L.; Batycky, A.E.; Kaminsky, H.; Ulrich, A.C. Geochemical stability of oil sands tailings in mine closure landforms. *Minerals* **2021a**, *11*, 830.

Dai, X.; Luo, F.; Yi, J.; He, Q.; Dong, B. Biodegradation of polyacrylamide by anaerobic digestion under mesophilic condition and its performance in actual dewatered sludge system. *Bioresour. Technol*. **2014**, *153*, 55–61.

Dai, X.; Luo, F.; Zhang, D.; Dai, L.; Chen, Y.; Dong, B. Waste-activated sludge fermentation for polyacrylamide biodegradation improved by anaerobic hydrolysis and key microorganisms involved in biological polyacrylamide removal. *Sci. Rep.* **2015**, *5*, 11675.

Deusner, C.; Meyer, V.; Ferdelman, T.G. High-pressure systems for gas-phase free continuous incubation of enriched marine microbial communities performing anaerobic oxidation of methane. *Biotechnol. Bioeng.* **2010***, 105,* 524-533.

Dompierre, K.A.; Barbour, S.L. Characterization of physical mass transport through oil sands fluid fine tailings in an end pit lake: A multi-tracer study. *J. Contam. Hydrol.* **2016**, *189*, 12–26.

Dompierre, K.A.; Barbour, S.L.; North, R.L.; Carey, S.K.; Lindsay, M.B.J. Chemical mass transport between fluid fine tailings and the overlying water cover of an oil sands end pit lake. *Water Resour. Res.* **2017**, *53*, 4725–4740.

Dompierre, K.A.; Lindsay, M.B.J.; Cruz-Hernández, P.; Halferdahl, G.M. Initial geochemical characteristics of fluid fine tailings in an oil sands end pit lake. *Sci. Total Environ.* **2016**, *556*, 196–206.

Dunmola, A.; Werneiwski, R.A.; McGowan, D.; Shaw, B.; Carrier. D. Geotechnical performance of fine tailings in an oil sands pit lake. *Can. Geotech. J.* **2023***, 60*, 595-610.

Fedorak, P.M.; Coy, D.L.; Dudas, M.J.; Simpson, M.J.; Renneberg, A.J.; MacKinnon, M.D. Microbially-mediated fugitive gas production from oil sands tailings and increased tailings densification rates. *J. Environ. Eng. Sci.* **2003**, *2*, 199–211.

Fedorak, P.M.; Coy, D.L.; Salloum, M.J.; Dudas, M.J. Methanogenic potential of tailings samples from oil sands extraction plants. *Can. J. Microbiol.* **2002**, *48*, 21–33.

Fichtel, K.; Logemann, J.; Fichtel, J.; Rullkötter, Cypionka, H.; Engelen, B. Temperature and pressure adaptation of sulfate reducer from the deep subsurface. *Front. Microbiol.* **2015**, *6*, 1078.

Foght, J.M.; Gieg, L.M.; Siddique, T. The microbiology of oil sands tailings: Past, present, future. *FEMS Microbiol. Ecol.* **2017**, *93*, fix034.

Francis, D.J.; Barbour, S.L.; Lindsay, M.B.J. Ebullition enhances chemical mass transport across the tailings-water interface of oil sands pit lakes. *J. Contam. Hydrol.* **2022**, *245*, 103938.

Gee, K.; Poon, H.Y.; Hashisho, Z.; Ulrich, A.C. Effect of naphtha diluent on greenhouse gases and reduced sulfur compounds emissions from oil sands tailings. *Sci. Total Environ.* **2017**, *598*, 916-924.

Gibson, R.E.; England, G.L.; Hussey, M.J.L. The theory of one-dimensional consolidation of saturated clays. I. Finite non-linear consolidation of thin homogeneous layers. *Géotechnique* **1967**, *17*, 261–273.

Government of Alberta. Environmental Quality Guidelines for Alberta Surface Waters; Water Policy Branch, Alberta Environment and Parks: Edmonton, CA, 2018.

Government of Alberta. Oil sands facts and statistics. 2023. Available online: https://www.alberta.ca/oil-sands-facts-and-statistics.aspx#:~:text=Alberta's%20oil%20sands%20has%20the,165.4%20billion%20barrels%20(bbl) (accessed 31 May 2023).

Gröllmann, U.; Schnabel, W. Free radical-induced oxidative degradation of polyacrylamide in aqueous solution. *Polym. Degrad. Stab.* **1982**, 4, 203–212.

Grula, M.M.; Huang, M.; Sewell, G. Interactions of certain polyacrylamides with soil bacteria. *Soil Sci.* **1994**, *158*, 291–300.

Hao, X.; Liu, R.; van Loosdrecht, M.C.M.; Cao, D. Batch influences of exogenous hydrogen on both acidogenesis and methanogenesis of excess sludge. *Chem. Eng. J.* **2017**, *317*, 544-550.

Hartsock, J.A.; Piercey, J.; House, M.K.; Vitt, D.H. An evaluation of water quality at Sandhills Wetland: Implications for reclaiming wetlands above soft tailings deposits in northern Alberta, Canada. *Wetl. Ecol. Manag.* **2021**, *29*, 111–127.

Haveroen, M.E.; MacKinnon, M.D.; Fedorak, P.M. Polyacrylamide added as a nitrogen source stimulates methanogenesis in consortia from various wastewaters. *Water Res.* **2005**, *29*, 3333–3341.

Headley, J.V.; Peru, K.M.; Barrow, M.P. Advances in mass spectrometric characterization of naphthenic acids fraction compounds in oil sands environmental samples and crude oil—A review. *Mass Spectrom. Rev.* **2016**, *35*, 311–328.

Herman, D.C.; Fedorak, P.M.; Mackinnon, M.D.; Costerton, J.W. Biodegradation of naphthenic acids by microbial populations indigenous to oil sands tailings. *Can. J. Microbiol.* **1994**, *40*, 467–477.

Holowenko, F.M.; MacKinnon, M.D.; Fedorak, P.M. Methanogens and sulfate-reducing bacteria in oil sands fine tailings waste. *Can. J. Microbiol.* **2000**, *46,* 927–937.

Hu, H.; Liu, J.F.; Li, C.Y.; Yang, S.Z.; Gu, J.D.; Mu, B.Z. Anaerobic biodegradation of partially hydrolyzed polyacrylamide in long-term methanogenic enrichment cultures from production water of oil reservoirs. *Biodegradation* **2018**, *29*, 233–243.

Imperial Oil Resources Ltd. (Imperial). Kearl Oil Sands Mine: Fluid Tailings Management Report; Imperial Oil Resources Ltd.: Calgary, CA, 2020.

Jeeravipoolvarn, S.; Chalaturnyk, R.J.; Scott, J.D. Consolidation modeling of oil sands fine tailings: history matching. In Proceedings of the 61st Canadian Geotechnical Conference, Edmonton, CA, 22–24 September 2008a,

Jeeravipoolvarn, S.; Scott, J.D.; Chalaturnyk, R.J. Multi-dimensional finite strain consolidation theory: modeling study. In Proceedings of the 61st Canadian Geotechnical Conference, Edmonton, CA, 22–24 September 2008b.

Jeeravipoolvarn, S.; Scott, J.D.; Chalaturnyk, R.J. 10 m standpipe tests on oil sands tailings: long-term experimental results and prediction. *Can. Geotech. J*. **2009**, *46*, 875-888.

Jessen, G.L.; Chen, L.-X.; Mori, J.F.; Nelson, Nelson, T.E.C.; Slater, G.F.; Lindsay, M.B.J.; Banfield, J.F.; Warren, L.A. Alum addition triggers hypoxia in an engineered pit lake. *Microorganisms* **2022**, *10*, 510.

Joshi, S.; Abed, A. Biodegradation of polyacrylamide and its derivatives. *Environ. Process.* **2017**, *4*, 463–476.

Kasperski, K.L.; Mikula, R.J. Waste streams of mined oil sands: Characteristics and remediation. *Elements* **2011**, *7*, 387–392.

Kavanagh, R.J.; Frank, R.A.; Oakes, K.D.; Servos, M.R.; Young, R.F.; Fedorak, P.M.; MacKinnon, M.D.; Solomon, K.R.; Dixon, D.G.; Van Der Kraak, G. Fathead minnow (*Pimephales promelas*) reproduction is impaired in aged oil sands process-affected waters. *Aquat. Toxicol.* **2011**, *101*, 214–220.

Kay-Shoemake, J.L.; Watwood, M.E.; Lentz, R.D.; Sojka, E.R. Polyacrylamide as an organic nitrogen source for soil microorganisms with potential effects on inorganic soil nitrogen in agricultural soil. *Soil Biol. Biochem*. **1998**, *30*, 1045–1052.

Keiluweit, M.; Fendorf, S. Texture-dependent anaerobic microsites constrain soil carbon oxidation rates. In Proceedings of the EGA General Assembly, Vienna, AT, 17–22 April 2016.

Lawrence, G.A.; Tedford, E.W. Pieters, R. Suspended solids in an end pit lake: Potential mixing mechanisms. *Can. J. Civ. Eng.* **2016**, *43*, 211–217.

Li, J.; How, Z.T.; El-Din, M.G. Aerobic degradation of anionic polyacrylamide in oil sands tailings: impact factor, degradation effect, and mechanism. *Sci. Total Environ.* **2023***, 856*, 159079.

Lipp, D.; Kozakiewicz, J. Acrylamide polymers. In Kirk-Othmer Encyclopedia of Chemical Technology; Kroschwitz, J.I., Ed.; Wiley: Toronto, CA, 1991; pp. 266–287.

Liu, L.; Wang, Z.; Lin, K.; Cai, W. Microbial degradation of polyacrylamide by aerobic granules. *Environ. Technol.* **2012**, *33*, 1049–1054.

Mayumi, D.; Dolfing, J.; Sakata, S.; Maeda, H.: Miyagawa, Y.; Ikarashi, M.; Tamaki, H.; Takeuchi, M.; Nakatsu, C.H.; Kamagata, Y. Carbon dioxide concentration dictates alternative methanogenic pathways in oil reservoirs. *Nat. Commun.* **2013**, *4*, 1998.

McKenna, G. Landscape design for mine reclamation. In Proceedings of the Tailings and Mine Waste ’09, Banff, CA, 1–4 November 2009.

Meulepas, R.J.W.; Jagersma, C.G.; Zhang, Y.; Petrillo, M.; Cai, H.; Buisman, C.J.N.; Stams, A.J.M.; Lens, P.N.L. Trace methane oxidation and the methane dependency of sulfate reduction in anaerobic granular sludge. *FEMS Microbiol. Ecol.* **2010**, *72*, 261-271.

Miles, S.M.; Asiedu, E.; Balaberda, A.; Ulrich, A.U. Oil sands process affected water sourced *Trichoderma harzianum* demonstrates capacity for mycoremediation of naphthenic acid fraction compounds. *Chemosphere* **2020**, *258*, 127281.

Mohamad Shahimin, M.F.; Foght, J.M.; Siddique, T. Preferential methanogenic biodegradation of short-chain *n*-alkanes by microbial communities from two different oil sands tailings ponds. *Sci. Total Environ.* **2016**, *553*, 250-257.

Mohamad Shahimin, M.F.; Foght, J.M.; Siddique, T. Methanogenic biodegradation of *iso*- alkanes by indigenous microbes from two different oil sands tailings ponds. *Microorganisms* **2021**, *9*, 1569.

Mohamad Shahimin, M.F.; Siddique, T. Sequential biodegradation of complex naphtha hydrocarbons under methanogenic conditions in two different oil sands tailings. *Environ. Pollut.* **2017a**, *221*, 398–406.

Mohamad Shahimin, M.F.; Siddique, T. Methanogenic biodegradation of paraffinic solvent hydrocarbons in two different oil sands tailings. *Sci. Total Environ.* **2017b**, *583*, 115–122.

Morandi, G.D.; Wiseman, S.B.; Pereira, A.; Mankidy, R.; Gault, I.G.M.; Martin, J.W.; Giesy, J.P. Effects-directed analysis of dissolved organic compounds in oil sands process-affected water. *Environ. Sci. Technol.* **2015**, *49*, 12395–12404.

Mori, J.F.; Chen, L.X.; Jessen, G.L.; Rudderham, S.G.; McBeth, J.M.; Lindsay, M.B.J.; Slater, G.F.; Banfield, J.F.; Warren, L.A. Putative mixotrophic nitrifying-denitrifying gammaproteobacterial implicated in nitrogen cycling within the ammonia/oxygen transition zone of an oil sands pit lake. *Front. Microbiol.* **2019**, *10*, 2435.

Nakamiya, K.; Kinoshita, S. Isolation of polyacrylamide-degrading bacteria. *J. Ferment. Bioeng.* **1995**, *80*, 418–420.

Neelakantan, R.; Vaezi, G.F.; Sanders, R.S. Effects of shear on the yield stress and aggregate structure of flocculant-dosed, concentrated kaolinite suspensions. *Miner. Eng.* **2018**, *123*, 95–103.

Neira, J.; Ortiz, M.; Morales, L.; Acevedo, E. Oxygen diffusion in soils: Understanding the factors and processes needed for modeling. *Chil. J. Agric. Res.* **2015**, *75*, 35–44.

Oil Sands Tailings Consortium (OSTC) and Canada's Oil Sands Innovation Alliance (COSIA). Technical Guide for Fluid Fine Tailings Management; OSTC and COSIA: Calgary, CA, 2012.

Pei, Y.; Zhao, L.; Du, G.; Li, N.; Xu, K.; Yang, H. Investigation of the degradation and stability of acrylamide-based polymers in acid solution: Functional monomer modified polyacrylamide. *Petroleum* **2016**, *2*, 399–407.

Penner, T.J.; Foght, J.M. Mature fine tailings from oil sands processing harbour diverse methanogenic communities. *Can. J. Microbiol.* **2010***, 56*, 459-470.

Pope, D.H.; Berger, L.R. Inhibition of metabolism by hydrostatic pressure: what limits microbial growth? *Arch. Mikrobiol.* **1973**, *93*, 367-370.

Quesnel, D.M.; Bhaskar, I.M.; Gieg, L.M.; Chua, G. Naphthenic acid biodegradation by the unicellular alga *Dunaliella tertiolecta*. *Chemosphere* **2011**, *84*, 504–511.

Quinlan, P.J.; Tam, K.C. Water treatment technologies for the remediation of naphthenic acids in oil sands process-affected water. *Chem. Eng. J.* **2015**, *279*, 696–714.

Ramos-Padrón, E.; Bordenave, S.; Lin, S.; Bhaskar, I.M.; Dong, X.; Sensen, C.W.; Fournier, J.; Vourdouw, G.; Gieg, L.M. Carbon and sulfur cycling by microbial communities in a gypsum-treated oil sands tailings pond. *Environ. Sci. Technol.* **2011**, *45*, 439–446.

Rao, F.; Liu, Q. Froth treatment in Athabasca oil sands bitumen recovery process: A review. *Energy Fuels* **2013**, *27*, 7199–7207.

Reid, M.L.; Warren, L.A. S reactivity of an oil sands composite tailings deposit undergoing reclamation wetland construction. *J. Environ. Manag.* **2016**, *166*, 321–329.

Risacher, F.F.; Morris, P.K.; Arriaga, D.; Goad, C.; Colenbrander Nelson, T.; Slater, G.F.; Warren, L.A. The interplay of methane and ammonia as key oxygen consuming constituents in early

stage development of Base Mine Lake, the first demonstration oil sands pit lake. *Appl. Geochem.* **2018**, *93*, 49–59.

Rochman, F.F.; Sheremet, A.; Tamas, I.; Saidi-Mehrabad, A.; Kim, J.J.; Dong, X.; Sensen, C.W.; Gieg, L.M.; Dunfield, P.F. Benzene and naphthalene degrading bacterial communities in an oil sands tailings pond. *Front. Microbiol.* **2017**, *8*, 1–12.

Rourke, H.; Hockley, D. Assessing oil sands tailings consolidation parameters relative to long-term reclamation. In Proceedings of the 22nd International Conference on Tailings and Mine Waste, Keystone, USA, 30 September – 2 October 2018.

Rudderham, S.B. Geomicrobiology and Geochemistry of Fluid Fine Tailings in an Oil Sands End Pit Lake. Master's Thesis, Department of Geological Sciences, University of Saskatchewan, Saskatoon, CA, 2019.

Saidi-Mehrabad, A.; He, Z.; Tamas, I.; Sharp, C.E.; Brady, A.L.; Rochman, F.F.; Bodrossy, L.; Abell, G.C.J.; Penner, T.; Dong, X.; et al. Methanotrophic bacteria in oil sands tailings ponds of northern Alberta. *ISME J.* **2013**, *7*, 908–921.

Sawatsky, L.; Hyndman, A.; McKenna, G.; Vandenberg, J. Fluid fine tailings processes: disposal, capping, and closure alternatives. In Proceedings of the 6th International Oil Sands Tailings Conference, Edmonton, CA, 9–12 December 2018.

Scoma, A.; Heyer, R.; Rifal, R.; Dandyk, C.; Marshall, I.; Kerckhof, F.M.; Marietou, A.; Boshker, H.T.S.; Meysman, F.J.R.; Malmos, K.G.; et al. Reduced TCA cycle rates at high hydrostatic pressure hinder hydrocarbon degradation and obligate oil degraders in natural, deep-sea microbial communities. *ISME J.* **2019**, *13*, 1005-1018.

Scott, A.C.; Mackinnon, M.D.; Fedorak, P.M. Naphthenic acids in Athabasca oil sands tailings waters are less biodegradable than commercial naphthenic acids. *Environ. Sci. Technol.* **2005**, *39*, 8388–8394.

Siddique, T.; Fedorak, P.M.; Foght, J.M. Biodegradation of short-chain n-alkanes in oil sands tailings under methanogenic conditions. *Environ. Sci. Technol.* **2006**, *40*, 5459–5464.

Siddique, T.; Fedorak, P.M.; Mackinnon, M.D.; Foght, J.M. Metabolism of BTEX and naphtha compounds to methane in oil sands tailings. *Environ. Sci. Technol.* **2007**, *41*, 2350–2356.

Siddique, T.; Kuznetsov, P.; Kuznetsova, A.; Arkell, N.; Young, R.; Li, C.; Guigard, S.; Underwood, E.; Foght, J.M. Microbially-accelerated consolidation of oil sands tailings. Pathway I: Changes in porewater chemistry. *Front. Microbiol*. **2014a**, *5*, 106.

Siddique, T.; Kuznetsov, P.; Kuznetsova, A.; Li, C.; Young, R.; Arocena, J.M.; Foght, J.M. Microbially-accelerated consolidation of oil sands tailings. Pathway II: Solid phase biogeochemistry. *Front. Microbiol.* **2014b**, *5*, 107.

Siddique, T.; Mohamad Shahimin, M.F.; Zamir, S.; Semple, K.; Li, C.; Foght, J.M. Long-term incubation reveals methanogenic biodegradation of C5 and C6 iso-alkanes in oil sands tailings. *Environ. Sci. Technol.* **2015**, *49*, 14732–14739.

Siddique, T.; Penner, T.; Semple, K.; Foght, J.M. Anaerobic biodegradation of longer-chain n-alkanes coupled to methane production in oil sands tailings. *Environ. Sci. Technol.* **2011**, *45*, 5892–5899.

Siddique, T.; Semple, K.; Li, C.; Foght, J.M. Methanogenic biodegradation of iso-alkanes and cycloalkanes during long-term incubation with oil sands tailings. *Environ. Pollut.* **2020**, *258*, 113768.

Slater, G.F.; Goad, C.A.; Lindsay, M.B.J.; Mumford, K.G.; Colenbrander Nelson, T.E.; Brady, A.L.; Jessen, G.L.; Warren, L.A. Isotopic and chemical assessment of the dynamics of methane sources and microbial cycling during early development on an oil sands pit lake. *Microorganisms* **2021***, 9*, 2509.

Small, C.C.; Cho, S.; Hashisho, Z.; Ulrich, A.C. Emissions from oil sands tailings ponds: Review of tailings pond parameters and emission estimates. *J. Petrol. Sci. Eng.* **2015**, *127*, 490–501.

Song, T.; Li, S.; Ding, W.; Li, H.; Bao, M.; Li, Y. Biodegradation of hydrolyzed polyacrylamide by the combined expanded granular sludge bed reactor-aerobic biofilm reactor biosystem and key microorganisms involved in this bioprocess. *Bioresour. Technol.* **2018**, *263*, 153–162.

Song, W.; Zhang, Y.; Gao, Y.; Chen, D.; Yang, M. Cleavage of the main carbon chain backbone of high molecular weight polyacrylamide by aerobic and anaerobic biological treatment. *Chemosphere* **2017**, *189*, 277–283.

Sorta, A.; Beier, N.; Kabwe, L.K.; Scott, J.D.; Wilson, G.W. The case for using fines void ratio. In Proceedings of the 68th Canadian Geotechnical Conference, Quebec City, CA, 21–23 September 2015.

Sorta, A.R.; Sego, D.C.; Wilson, W. Physical modelling of oil sands tailings consolidation. *Int. J. Phys. Model. Geotech.* **2016**, *16*, 47–64.

Stasik, S.; Loick, N.; Knöller, K.; Weisener, C.; Wendt-Potthoff, K. Understanding biogeochemical gradients of sulfur, iron and carbon in an oil sands tailings pond. *Chem. Geol.* **2014**, *382*, 44–53.

Stasik, S.; Wendt-Potthoff, K. Interaction of microbial sulphate reduction and methanogenesis in oil sands tailings ponds. *Chemosphere* **2014**, *103*, 59–66.

Stasik, S.; Wendt-Potthoff, K. Vertical gradients in carbon flow and methane production in a sulfate-rich oil sands tailings pond. *Water Res.* **2016**, *106*, 223–231.

Stasik, S.; Wick, L.Y.; Wendt-Potthoff, K. Anaerobic BTEX degradation in oil sands tailings ponds: Impact of labile organic carbon and sulfate-reducing bacteria. *Chemosphere* **2015**, *138*, 133–139.

Suncor Energy Operating Inc. (Suncor). 2021 Fort Hills Fluid Tailings Management Report; Suncor Energy Operating Inc. on behalf of Fort Hills Energy Corporation; Calgary, CA, 2022b.

Suncor Energy Inc. (Suncor). Fort Hills. 2023a. Available online: https://www.suncor.com/en-ca/what-we-do/oil-sands/fort-hills (accessed on 31 May 2023).

Suncor Energy Inc. (Suncor). 2022 Base Plant Fluid Tailings Management Report; Suncor Energy Inc.: Calgary, CA, 2023b.

Suncor Energy Operating Inc. (Suncor). 2022 Fort Hills Fluid Tailings Management Report; Suncor Energy Operating Inc.; Calgary, CA, 2023c.

Suncor Energy (Syncrude) Operating Inc. (Syncrude). 2022 Pit Lake Monitoring and Research Report (Base Mine Lake Demonstration Summary: 2012-2021); Suncor Energy (Syncrude) Operating Inc.: Fort McMurray, CA, 2022.

Suncor Energy (Syncrude) Operating Inc. (Syncrude). 2022 Mildred Lake Tailings Management Report; Suncor Energy (Syncrude) Operating Inc.: Fort McMurray, CA, 2023.

Suthaker, N.N.; Scott, J.D. Large scale consolidation testing of oil sand fine tails. In Proceedings of the 1st International Congress on Environmental Geotechnics, Edmonton, CA, 10–15 July 1994.

Syncrude Canada Ltd. (Syncrude). 2019 Mildred Lake Tailings Management Report; Syncrude Canada Ltd.: Fort McMurray, CA, 2020.

Tan, B.F.; Semple, K.; Foght, J. Anaerobic alkane biodegradation by cultures enriched from oil sands tailings ponds involves multiple species capable of fumarate addition. *FEMS Microbiol. Ecol.* **2015**, *91*, fiv042.

Tholosan, O.; Garcin, J.; Bianchi, A. Effects of hydrostatic pressure on microbial activity through a 2000 m deep water column in the NW Mediterranean Sea. *Mar. Ecol. Prog. Ser.* **1999**, *183*, 49-57.

Timmers, P.H.A.; Gieteling, J.; Widjaja-Greefkes, H.C.A.; Plugge, C.M.; Stams, A.J.M.; Lens, P.N.L.; Meulepas, R.J.W. Growth of anaerobic methane-oxidizing archaea and sulfate-reducing bacteria in a high-pressure membrane capsule bioreactor. *Appl. Environ. Microbiol.* **2015**, *81*, 1286-1296.

United States Environmental Protection Agency (USEPA). Quality Criteria for Water; United States Department of Commerce, National Technical Information Service, USEPA: Springfield, US, 1986.

Uranta, K.G.; Rezaei-Gomari, S.; Russell, P.; Hamad, F. Studying the effectiveness of polyacrylamide (PAM) application in hydrocarbon reservoirs at different operational conditions. *Energies* **2018**, *11*, 2201.

Vedoy, D.R.J.; Soares, J.B.P. Water-soluble polymers for oil sands tailing treatment: A review. *Can. J. Chem. Eng.* **2015**, *93*, 888–904.

Vitt, D.H.; House, M.; Hartsock, J.A. Sandhill Fen, an initial trial for wetland species assembly on in-pit substrates: Lessons after three years. *Botany* **2016**, *94*, 1015–1025.

Warren, L.A.; Kendra, K.E.; Brady, A.L.; Slater, G.F. Sulfur biogeochemistry of an oil sands composite tailings deposit. *Front. Microbiol.* **2016**, *6*, 1–14.

Wen, Q.; Chen, Z.; Zhao, Y.; Zhang, H.; Feng, Y. Biodegradation of polyacrylamide by bacteria isolated from activated sludge and oil-contaminated soil. *J. Hazard. Mater.* **2010**, *175*, 955–959.

Westcott, F.; Watson, L. End pit Lakes Technical Guidance Document; Clearwater Environmental Consultants for Cumulative Effects; Project 2005-61; Management Association End Pit Lakes Subgroup: Calgary, CA, 2007.

White, K.B.; Liber, K. Early chemical and toxicological risk characterization of inorganic constituents in surface water from the Canadian oil sands first large-scale end pit lake. *Chemosphere* **2018**, *211*, 745–757.

Wilson, G.W.; Kabwe, L.K.; Beier, N.A.; Scott, J.D. Effect of various treatments on consolidation of oil sands fluid fine tailing. *Can. Geotech. J.* **2018**, *55*, 1059–1066.

Woodrow, J.E.; Seiber, J.N.; Miller, G.C. Acrylamide release resulting from sunlight irradiation of aqueous polyacrylamide/iron mixtures. *J. Agric. Food Chem.* **2008**, *56*, 2773–2779.

Xiong, B.; Dettam Loss, R.; Shields, D.; Pawlik, R.; Hochreiter, R.; Zydney, A.L.; Kumar, M. Polyacrylamide degradation and its implications in environmental systems. *NPJ Clean Water* **2018a**, *1*, 17.

Xiong, B.; Miller, Z.; Roman-White, S.; Tasker, T.; Farina, B.; Piechowicz, B.; Burgos, W.D.; Joshi, P.; Zhu, L.; Gorski, C.A.; et al. Chemical Degradation of Polyacrylamide during Hydraulic Fracturing. *Environ. Sci. Technol.* **2018b**, *52*, 327–336.

Xiong, B.; Purswani, P.; Pawlik, T.; Samineni, L.; Karpyn, Z.T.; Zydney, A.L.; Kumar, M. Mechanical degradation of polyacrylamide at ultra high deformation rates during hydraulic fracturing. *Environ. Sci. Water Res. Technol*. **2020**, *6*, 166–172.

Yan, Y.; Colenbrander Nelson, T.E.; Twible, L.; Whaley-Martin, K.; Jarolimek, C.V.; King, J.J.; Apte, S.C.; Arrey, J.; Warren, L.A. Sulfur mass balance and speciation in the water cap during early-stage development in the first pilot pit lake in the Alberta oil sands. *Environ. Chem.* **2022**, *19*, 236-253.

Yu, X.; Lee, K.; Ma, B.; Asiedu, E.; Ulrich, A.C. Indigenous microorganisms residing in oil sands tailings biodegrade residual bitumen. *Chemosphere* **2018**, *209*, 551–559.

Yu, X.; Lee, K.; Ulrich, A.C. Model naphthenic acids removals by microalgae and Base Mine Lake cap water microbial inoculum. *Chemosphere* **2019**, *234*, 796–805.

Zhao, K.; Tedford, E.W.; Zare, M.; Lawrence, G.A. Impact of atmospheric pressure variations on methane ebullition and lake turbidity during ice-cover. *L&O Letters* **2021**, *6*, 253-261.

3 BIOFILMS FOR TURBIDITY MITIGATION IN OIL SANDS END PIT LAKES

3.1 Introduction

Reclamation of FFT in oil sands pit lakes allows for the FFT to naturally dewater (consolidate) over time, while the water cap (hereinafter referred to as surface water) provides habitat for an aquatic ecosystem (Charette et al. 2010). However, settlement and resuspension of FFT particles (especially clay particles) in the surface water generates turbidity, which may limit light penetration and thereby be detrimental to the development of a healthy aquatic ecosystem in a pit lake (Charette et al. 2010). Furthermore, turbidity can result in lower dissolved oxygen concentrations in pit lake surface water, which would negatively impact the biodegradation of acutely toxic NAFCs that are present in oil sands process-affected water (Garcia-Garcia et al. 2011; Mahdavi et al. 2015; Morandi et al. 2015).

Turbidity generation in BML has been an ongoing challenge. Tedford et al. (2019) measured seasonal turbidity changes in BML's surface water over a period of three years and reported turbidity as high as 308 NTU at a depth of 2.5 m after lake turnover in fall 2015. Turbidity in BML is thought to be due to the settling of fine particles suspended in the surface water and the resuspension of fine particles from the mudline (FFT–water interface) (Lawrence et al. 2016). There are a number of processes that could conceivably contribute to particle suspension and turbidity in BML, including, but not limited to, wind waves and other wind-driven processes, convection, gas ebullition, and pore water expression (Lawrence et al. 2016). In 2016, BML was dosed with a chemical coagulant, alum, which substantially reduced the surface water turbidity that year (Syncrude 2019). However, once the aluminum ions are consumed down to background levels, this coagulation effect may disappear (Wei et al. 2021). As such, biological mechanisms have been proposed as a new approach to turbidity reduction in BML.

Biofilms formed on the mudline of oil sands pit lakes have been proposed as a novel solution for mitigating turbidity in the long term. Biofilms have been found to have a stabilization effect, referred to as biostabilization, whereby they reduce the ability of sediments to resuspend and of contaminants to re-mobilize from a sediment–water interface in comparison to purely mineral

sediments (Droppo et al. 2001; Reid et al. 2016). Biostabilization has been shown to significantly increase the energy required to erode sediments, thereby reducing turbidity in the overlying water (Droppo et al. 2001; 2007). These effects are thought to be due to the secretion of gel-like extracellular polymeric substances (EPS), made up of lipids, polysaccharides, proteins, and nucleic acids, which attach microbial cells to particle surfaces (de Brouwer et al. 2000; Droppo et al. 2007; Droppo 2009; Flemming and Wingender 2010; Gerbersdorf and Wieprecht 2015; Reid et al. 2016). EPS are hydrated, which causes them to swell on exudation and fill pore spaces (Droppo 2009; Wotton 2004). This facilitates stabilization and results in EPS making up a large volume of the biofilm matrix. Stabilizing biofilms often consist of multiple layers of multispecies communities, which may include diatoms, green algae, photoautotrophic cyanobacteria, and other phototrophic and heterotrophic bacteria (de Brouwer et al. 2000; Droppo 2009; Gerbersdorf and Wieprecht 2015; van Gemerden 1993). Though consolidation and electrochemical interactions are thought to also affect the stabilization of bed sediments (Droppo and Amos 2001; Tolhurst et al. 2000), there is a consensus that the secretion of EPS by microorganisms is the primary reason for the stabilization effects (Amos et al. 2004; Droppo 2009; Gerbersdorf et al. 2008; Lundkvist et al. 2007; Reid et al. 2016).

Previous work has largely focused on biofilm formation and stabilization of marine (Amos et al. 2004; Friend et al. 2003; Widdows et al. 2007; Wotton 2004) and fresh water (Droppo et al. 2007; Droppo 2009) sediments. However, the high surface area to volume ratio and the charged nature of clay particles in FFT should be advantageous for microbial growth and biostabilization (Gerbersdorf and Wieprecht 2015). Bordenave et al. (2010) observed increased clay aggregation and sedimentation in Albian sands tailings under nitrate-reducing and methanogenic conditions and attributed this to the development of microbial biofilms on fine particles. Furthermore, Reid et al. (2016) compared biostabilization in fresh and aged FFT in tailings ponds and found that aged tailings had greater microbial diversity and biofilms extending past the FFT–water interface, both of which led to higher biostabilization in aged tailings. Conversely, fresh tailings had lower microbial diversity, and only a shallow biofilm formed at the FFT–water interface (Reid et al. 2016). This current study used laboratory mixing tests to evaluate biostabilization as a possible mechanism for turbidity mitigation in BML. This work is the first to investigate pit lake turbidity mitigation using mudline biofilms made up of microbial communities indigenous to FFT. The

results of this study will help mitigate turbidity issues that may be detrimental to the long-term success of oil sands pit lakes.

3.2 Materials and Methods

3.2.1 Sample Collection and Characterization

3.2.1.1 BML Surface Water and FFT Collection

Grab samples of BML FFT and BML surface water were collected in 20 L pails by Syncrude in August 2017 and stored at the University of Alberta at 4°C until use. BML FFT was collected at a depth of 10.2 m below the lake surface (approximately 1.0 m below the FFT–water interface). This depth was chosen because particles near the FFT–water interface are fine-grained and are most likely to be resuspended in the surface water. As such, the fines content and water content of the FFT used in this experiment are considered to be generally representative of the FFT that may contribute to turbidity in BML. BML surface water was collected from the top 2 m of BML.

3.2.1.2 Water Chemistry

Prior to biofilm growth and mixing experiments, the BML surface water and FFT pore water were characterized by measuring pH, electrical conductivity (EC), dissolved oxygen (DO), major cations and anions, NAFCs, and turbidity (in surface water only). pH and EC were measured using a Fisher Scientific Accumet AR50 Dual Channel pH/Ion/Conductivity Meter. DO was evaluated using a YSI 52 Dissolved Oxygen Meter (YSI Incorporated, Yellowsprings, US). Major cation analysis was conducted at the Natural Resources Analytical Laboratory (NRAL) at the University of Alberta. Samples were filtered with 0.45 μm nylon filters and analyzed for Na^+, K^+, Ca^{2+}, and Mg^{2+} via inductively coupled plasma optical emission spectrometry (ICP-OES) (Thermo iCAP 600 series, Thermo Fisher Scientific, Cambridge, UK). Filtered samples (using 0.45 μm nylon filters) were analyzed for major anions (Cl^-, SO_4-S, NH_4-N, NO_2-N, NO_3-N, and PO_4-P) at NRAL with a Thermo Gallery Plus Beermaster Colorimetric Autoanalyzer (Thermo Fisher Scientific, Vantaa, FI). NAFCs were determined using Fourier-transform infrared spectrometry (Spectrum 100 FT-IR Spectrometer, PerkinElmer, Shelton, USA) following the procedure described in Ripmeester and Duford (2019). Turbidity was measured using a HACH 2100Q Portable Turbidimeter (Loveland, US).

3.2.1.3 FFT Characterization

Initial characterization of BML FFT (prior to biofilm growth and mixing tests) included measurements of solids and water content, bulk density, and particle size distribution (PSD). Solids and water content were measured using oven analysis and following the procedure in ASTM D2216-19: Standard Test Methods for Laboratory Determination of Water (Moisture) Content of Soil and Rock by Mass (2019). Sedimentation analysis was used to measure the PSD and was conducted in accordance with ASTM D79828-17: Standard Test Method for Particle-size Distribution (Gradation) of Fine-grained Soils Using the Sedimentation (Hydrometer) Analysis (2017) using a 152H hydrometer (Fisherbrand, Buena, US).

3.2.2 Biofilm Growth and Characterization

3.2.2.1 Biofilm Growth

Mixing experiments were conducted in triplicate in 1 L pre-autoclaved glass jars, each containing 200 ± 1 g of FFT capped with 450 mL of BML surface water. BML surface water was carefully added to the jars to minimize the disturbance and suspension of FFT in the surface water. A total of 30 1 L jars were set up, and biofilms were grown in 18 of these jars. Prior to this experiment, naturally occurring biofilms were observed growing in two 1 L jars, each containing approximately 200 g of FFT and 450 mL BML water that had been stored at room temperature in natural light conditions for upwards of two years. Small samples (<0.5 mL) of these biofilms made up of microbial communities indigenous to FFT were pipetted into 18 of the jars containing FFT and BML surface water to enhance and accelerate biofilm growth for this experiment. Any FFT that was suspended as a result of the experimental setup was allowed to settle prior to the jar being inoculated with the biofilm. The remaining 12 control jars of FFT and BML surface water were sterilized by autoclaving (121°C, 100 kPa) them three times. All 30 jars were then covered with a clear acrylic sheet to prevent evaporation of the surface water. The jars were stored at room temperature under a light intensity of approximately 60 μmol/m^2/s, as suggested by Anderson and Kawachi (2005), with a 16-h light: 8-h dark cycle to promote biofilm growth and to mimic the conditions under which the biofilms were initially grown. All jars were left under quiescent conditions for a 10-week or 20-week growth period before the mixing tests.

3.2.2.2 Biofilm Age

Previous research by Droppo et al. (2007) noted the importance of the age of biofilms in their ability to stabilize underlying sediment and observed that lifting due to gas release and decay in older biofilms resulted in weaker attachment of the biofilm to the sediment. Thus, it was hypothesized that the age of biofilms may influence their ability to mitigate turbidity. To test this hypothesis, two different biofilm ages were examined: biofilms were grown for 20 weeks in 12 of the jars (hereinafter referred to as Biofilm20) and for 10 weeks in six of the jars (hereinafter referred to as Biofilm10) before conducting mixing tests. Control jars were placed under the same 20-week growth conditions as the Biofilm20 jars before conducting mixing tests. Based on laboratory observations, the 10-week and 20-week growth periods were selected because both periods were sufficient to grow biofilms that coated the surface of the FFT in the jars, but gas bubble release and subsequent lifting and layering of the biofilms were only evident under the 20-week growth period.

3.2.2.3 Biofilm Characterization

Following biofilm development but before mixing tests, the BML surface water and FFT in the control jars and biofilm jars were characterized. The surface water was once again characterized by measuring pH, EC, DO, major cations and anions, initial turbidity, as well as total organic carbon (TOC) and chemical oxygen demand (COD). TOC was measured using a Shimadzu TOC-LCPH analyzer (Kyoto, JP) (sparging time: 6 min; injection volume: 50 µL; injection number: 3 out of 4; acid added: 2.3%). COD was analyzed using HACH COD Digestion Vials (HR 20-1500 mg/L) in conjunction with a HACH Digital Reactor Box (DRB) 200 and a HACH DR 900 Multiparameter Portable Colorimeter (Loveland, US). FFT was characterized by measuring solids and water content and bulk density.

Prior to the mixing tests, the biofilms were characterized by measuring chlorophyll a (Chl *a*) and conducting LIVE/DEAD staining, scanning electron microscopy (SEM), and DNA extractions and 16S and 18S sequencing. Chl *a* was extracted using a method adapted from Thompson et al. (1999). Briefly, a sterile scalpel was used to cut approximately 1 cm^2 biofilm samples, which were then placed in 2 mL of > 99.9% methanol in the dark for 24 h at room temperature. The optical density (OD) of the chlorophyll/methanol mixture was measured at 665 and 652 nm using a

Thermo Scientific NanoDrop 2000c Spectrophotometer (Wilmington, US). The Chl *a* content of the biofilms was then determined using Equation 3-1, taken from Lichtenthaler (1987).

$$\text{Chl } a \left(\frac{mg}{mL\ methanol}\right) = 16.73 * OD_{665} - 9.16 * OD_{652} \quad (3\text{-}1)$$

The viability of microorganisms in the biofilms was assessed using a LIVE/DEAD® BacLight™ Bacterial Viability Kit (L7012-Invitrogen, Carlsbad, US). A mixture of SYTO® 9 green fluorescent nucleic acid stain and propidium iodide red fluorescent nucleic acid stain is used in this kit. A sterile scalpel was used to cut a thin section of the biofilm, which was then washed in phosphate-buffered saline to remove any unattached biomass. Immediately after staining with the LIVE/DEAD® BacLight™ Bacterial Viability Kit, biofilm samples were incubated for 30 min in the dark. The stain was formulated from 3 µL of SYTO9 and propidium iodide dye mixture per mL. The distribution of live and dead cells could be observed via fluorescence; the fluorescent dye on live cells produced green fluorescence, while dead cells emitted bright red fluorescence. Prior to examining the biofilm samples under a microscope, the samples were washed with 0.85% sodium chloride (NaCl) to remove dye residues. A Zeiss Axio Imager M2 microscope (Jena, DE) was used to analyze the stained biofilm samples with four FITC (red) and Cy3 (green) tracks. Image quantification was carried out using Fuji Image J software.

SEM was conducted on biofilm samples at the Microscopy Facility at the University of Alberta using a Zeiss EVO 10 Scanning Electron Microscope (Jena, DE). In preparation for SEM analysis, biofilm samples were processed using a hexamethyldisilazane (HMDS) procedure. Briefly, the samples were placed in a fixative (2.5% glutaraldehyde; 2% paraformaldehyde in 0.1 M phosphate buffer), washed with a 0.1 M phosphate buffer, and dehydrated with a series of ethanol washes.

DNA extractions were conducted on biofilm samples and the initial FFT using a FastDNA™ Spin Kit for Soils (MP Biomedical, Solon, US). DNA samples were sent to Microbiome Insights (Vancouver, CA) to perform polymerase chain reaction (PCR) amplification of the V4 region of the 16S rRNA gene in bacteria and archaea using the primers 515F (GTGCCAGCMGCCGCGGTAA) and 806R (GGACTACHVGGGTWTCTAAT) (Caporaso et al. 2011; Yu 2019) and the V4 region of the 18S rRNA gene in eukaryotes using the primers 565F

(CCAGCASCYGCGGTAATTCC) and 948R (ACTTTCGTTCTTGATYRA). Amplicon sequencing was conducted using the Illumina PE250 platform (Illumina, US). 16S sequencing was conducted on both biofilm samples and the initial BML FFT, while 18S sequencing was conducted on only the biofilm samples. The generated raw data were processed using the QIIME 2 (release 2018.8) next-generation microbiome bioinformatics platform (Callahan et al. 2016). The taxonomy was assigned with 99% similarity using the Greengenes 16S rRNA gene database (release gg_13_5) in accordance with McDonald et al. (2012) and Werner et al. (2012). Sequencing reads were pre-processed, quality-filtered, and analyzed using the Divisive Amplicon Denoising Algorithm 2 (DADA2) software package, wrapped in QIIME version 2018.6.0. Statistical comparisons between the abundance values were performed using one-way ANOVA (Tukey's test).

3.2.3 Mixing Tests

3.2.3.1 Mixing Methodology and Procedure

Following the 10-week and 20-week growth periods, mixing tests were conducted on the 1 L jars to understand the influence of biofilms on turbidity mitigation in BML surface water. The mixing tests involved mechanical movement/mixing in the surface water and monitoring of subsequent turbidity generation over a period of 35 d. Lawrence et al. (2016) estimated that the threshold linear velocity of FFT at the BML mudline is approximately 5 cm/s, meaning that the oscillating current at the mudline between the tailings and surface water must be greater than or equal to 5 cm/s to initiate erosion of the tailings. To simulate linear mudline velocities and generate turbidity in the 1 L jars, a 48 mm diameter stainless steel blade impeller with a Caframo Constant Torque Mixer (BDC3030, Georgian Bluffs, CA) was used. The offset distance between the mudline and impeller was set to 35 mm, equivalent to the midway point in the surface water. First, the threshold velocity of approximately 5 cm/s was confirmed in three control jars by mixing the water in the jars for 1 h at either 20, 30, or 40 rpm with the impeller stationary at a distance of 35 mm above the mudline (see Appendix A1, Table A-1). These mixing speeds are equivalent to an average linear velocity of 2.5, 3.8, and 5.0 cm/s, respectively, using Equation 3-2 (Potter et al. 2012):

$$v = \frac{\omega * r}{2} \tag{3-2}$$

where v is the average linear velocity, ω is the angular velocity, and r is the impeller radius. After the threshold velocity was confirmed, the same test was conducted but jars were slowly moved in horizontal and vertical directions throughout the test. The purpose of this test was to confirm that the velocities along the mudline were comparable regardless of whether the impeller was stationary or moving. Because of the relatively small surface area of the mudline (65 cm^2), turbidity was similar for both the stationary and moving impellers (see Appendix A1, Table A-1). This test confirmed that a stationary impeller was not producing intense local velocities at the center of the mudline but was instead producing velocities all across the mudline (similar to that of a moving impeller).

Following these preliminary tests, each mixing test was conducted with a stationary impeller, mixing the BML surface water 35 mm above the mudline for 1 h. An initial mixing speed of 80 rpm was selected (equivalent to an average linear velocity of 10.1 cm/s) to evaluate the effectiveness of biofilms in mitigating turbidity generation. Following this test, higher mixing speeds of 120, 160, and 200 rpm were selected for the remaining jars to determine the mixing speed at which biofilms would 'break', generating turbidity in the jar. A summary of the different mixing speeds tested in triplicate during the mixing tests is provided in Table 3-1. Control jars (hereinafter referred to as No Biofilm jars) and Biofilm20 jars were tested in triplicate at each of the four mixing speeds. The six Biofilm10 jars were only tested at the two higher mixing speeds because it was hypothesized that these jars would perform better than the Biofilm20 jars.

Table 3-1. Summary of mixing speeds and biofilm ages examined in mixing experiments. Each test was conducted in triplicate. Biofilm10 corresponds to 10-week-old biofilms; Biofilm20 corresponds to 20-week-old biofilms.

	Mixing Speed (rpm)			
	80	**120**	**160**	**200**
No Biofilm	✓	✓	✓	✓
Biofilm10			✓	✓
Biofilm20	✓	✓	✓	✓

After the 1 hr mixing period, the FFT in the jars was allowed to settle for 35 d, at which point all turbidity curves had plateaued (see subsection 3.3.2). Turbidity was measured immediately after the 1 hr mixing period and every one to four days thereafter. pH and DO measurements were taken immediately after the 1 hr mixing period and approximately every 10 to 15 d thereafter. The above mixing procedure was repeated after the suspended particles had settled and the jars were again monitored for 35 d. This second mixing test was conducted to see if biofilms continued to show improvement over No Biofilms even after the biofilms were disturbed due to mixing/movement in the surface water.

3.3 Results and Discussion

3.3.1 Surface Water, FFT, and Biofilm Characterization

3.3.1.1 Water Chemistry and FFT Characterization

Table 3-2 presents water chemistry data for the surface water in the No Biofilm, Biofilm10, and Biofilm20 jars. All the measurements in Table 3-2 were taken after 10- or 20-week growth periods but prior to the mixing tests. Biofilms are known to develop in extreme environments. For example, Frederick (2011) transferred established wetland benthic biofilms to slurries containing oil sands process-affected water and noted that the presence of acutely toxic NAFCs in oil sands process-affected water did not have a significant detrimental effect on biofilm growth. Furthermore, Sim et al. (2006) found that high salinities (15, 45, and 70 ppt) did not limit benthic microbial biomass development, and that biofilm development slightly improved at higher salinities, likely a result of reduced competition and predation. In this work, biofilms were able to grow in the presence of NAFCs and elevated salts, with EC ranging from 2.36 to 3.01 mS/cm in the surface water and FFT (see also Appendix A1, Table A-2). pH, EC, and chloride (Cl^-) concentrations were slightly higher in the Biofilm10 and Biofilm20 surface water in comparison to No Biofilm surface water, while cation concentrations were fairly consistent across all jars.

Table 3-2. Surface water chemistry data and Chl *a* biofilm concentrations in No Biofilm, Biofilm10, and Biofilm20 jars prior to mixing tests. Results are presented as average ± one standard deviation of replications. Biofilm10 corresponds to 10-week-old biofilms; Biofilm20 corresponds to 20-week-old biofilms.

Parameter	No Biofilm	Biofilm10	Biofilm20
pH	8.78 ± 0.08	9.08 ± 0.02	9.06 ± 0.04
EC (mS/cm)	2.69 ± 0.05	2.92 ± 0.16	3.01 ± 0.23
DO (mg/L)	5.05 ± 0.96	9.09 ± 0.44	8.18 ± 0.29
TOC (mg/L)	59.3 ± 4.2	70.2 ± 1.9	78.5 ± 3.2
COD (mg/L)	280.7 ± 6.7	281.3 ± 5.8	313.0 ± 10.0
NH_4-N (mg/L)	3.84 ± 0.13	0.030 ± 0.014	0.026 ± 0.007
NO_2-N (µg/L)	7.46 ± 2.42	3.15 ± 1.47	1.22 ± 1.01
NO_3-N (mg/L)	0.045 ± 0.007	0.050 ± 0.007	0.018 ± 0.008
PO_4-P (µg/L)	13.4 ± 2.9	7.46 ± 1.44	7.08 ± 1.61
SO_4-S (mg/L)	99.9 ± 3.6	81.6 ± 12.9	78.3 ± 12.7
Cl^- (mg/L)	381.4 ± 8.7	414.1 ± 18.3	423.8 ± 52.6
Na^+ (mg/L)	608.3 ± 10.9	611.9 ± 18.4	610.6 ± 67.1
K^+ (mg/L)	15.3 ± 0.6	13.7 ± 1.0	14.7 ± 2.0
Ca^{2+} (mg/L)	9.6 ± 0.1	8.8 ± 0.2	8.8 ± 1.4
Mg^{2+} (mg/L)	5.4 ± 0.5	7.4 ± 0.3	6.8 ± 1.2
Turbidity (NTU)	8.93 ± 5.34	2.53 ± 0.75	4.67 ± 3.88
Chl *a* (mg/g biofilm)	0.28 ± 0.23	57.7 ± 6.0	39.4 ± 5.5

Measurements of DO and TOC were also higher in the Biofilm10 and Biofilm20 jars, which is expected given the presence of algal communities in the biofilms that generate DO through photosynthesis and TOC through cell metabolism (further details in subsection 3.3.1.2) (He et al. 2019; Leloup et al. 2006). The higher pH in the Biofilm10 and Biofilm20 surface water in comparison to the No Biofilm surface water is consistent with algae in biofilms consuming CO_2 during photosynthesis. Nutrients in the Biofilm10 and Biofilm20 surface water were largely depleted in comparison to that of the No Biofilm jars, with lower concentrations of nitrogen (as ammonium (NH_4-N), nitrate (NO_3-N), and nitrite (NO_2-N)) and phosphorous (as phosphate (PO_4-P)). It is likely that nutrient concentrations in the FFT in the Biofilm20 and Biofilm10 jars were also lower than that of the No Biofilm jars (Vadeboncoeur et al. 2006); however, the FFT pore water chemistry after biofilm growth was not evaluated, as pore water sampling would have substantially disturbed and damaged the overlying biofilm. In addition to nitrogen and phosphorous, potassium (K^+) may act as a nutrient to support algal growth (Anishchenko et al.

2010), and sulfate (SO_4^{2-}) can also support biofilm development, particularly in the presence of SRB, colorless sulfur bacteria, or purple sulfur bacteria (Tolhurst et al. 2000). Sulfur concentrations (as SO_4-S) were approximately 20% lower in the Biofilm10 and Biofilm20 surface water compared to the surface water in the No Biofilm jars. A similar trend was expected in the FFT pore water of these jars, though, again, this was not sampled to preserve the biofilm for the mixing tests. This trend is consistent with the SRB present in the biofilms, which is further discussed in subsection 3.3.1.2. The initial turbidity was highest in the No Biofilm jars, but all initial turbidity values were less than 9 NTU.

Sedimentation analysis of the FFT revealed that the vast majority (more than 70 wt%) of particles were clay-sized, having a diameter of less than 2 μm. The median diameter (D_{50}) of the FFT particles was 1.08 ± 0.14 μm. Table 3-3 presents further FFT characterization data for the FFT used in this study. All the measurements in Table 3-3 were taken prior to the mixing tests. The original solids content of the FFT was approximately 32.6 ± 0.0 wt%, with a corresponding water content of 67.4 ± 0.0 wt% and a bulk density of 1.13 ± 0.09 g/mL. Even after the 10-week or 20-week growth periods, the solids and water contents and bulk densities of the FFT in the Biofilm10, Biofilm20, and No Biofilm jars did not change substantially, which indicates that over the course of this experiment, self-weight consolidation of the FFT in the jars was minimal.

Table 3-3. FFT characterization data for the initial BML FFT and FFT in No Biofilm, Biofilm10, and Biofilm20 jars prior to mixing tests. Results are presented as average ± one standard deviation of replications. Biofilm10 corresponds to 10-week-old biofilms; Biofilm20 corresponds to 20-week-old biofilms.

Parameter	Initial BML FFT	No Biofilm	Biofilm10	Biofilm20
Solids content (wt%)	32.6 ± 0.0	31.6 ± 0.7	32.5 ± 0.9	31.9 ± 0.6
Water content (wt%)	67.4 ± 0.0	68.4 ± 0.7	67.5 ± 0.9	68.1 ± 0.6
Bulk density (g/mL)	1.13 ± 0.09	1.12 ± 0.05	1.13 ± 0.11	1.13 ± 0.06

3.3.1.2 Biofilm Characterization

The biofilms in all 18 jars were seen to visibly coat the surface of the FFT in the jars, equivalent to a surface area of 65 cm^2 (see also Appendix A1, Figure A-1). The biofilms visibly extended past the FFT surface in all the Biofilm20 jars and some of the Biofilm10 jars, and it was suspected that the biofilms had developed distinct, stratified layers (Frederick 2011). Biofilm20 jars had

noticeable gas bubbles form underneath the top layer of the biofilms, which resulted in lifting and then layering once the gas bubbles were released (see Appendix A1, Figure A-2). In contrast, Biofilm10 jars had no gas bubbles, and the biofilms coating the FFT surface were smooth with no overlapping layers.

Prior to mixing, the Chl *a* concentration of the biofilms was measured as an indication of algal activity, such as green algae, diatoms, and cyanobacteria, and the results are presented in Table 3-2 (Droppo et al. 2007; Sutherland et al. 1998). Biofilm10 jars had a 46% higher Chl *a* concentration of 57.7 ± 6.0 mg/g biofilm compared to the Biofilm20 jars, which had a Chl *a* concentration of 39.4 ± 5.5 mg/g biofilm. Furthermore, there were noticeable color differences between biofilms of different ages. Biofilm10 jars contained biofilms that were strongly green, whereas the Biofilm20 jars had biofilms that were darker in color and were a mixture of brown and green. The differences in pigmentation and Chl *a* concentration in the Biofilm10 and Biofilm20 jars may reflect decaying algal communities or species succession in Biofilm20 jars (Jarvie et al. 2002). Spatial variability in the collected samples due to heterogeneity within each biofilm may also contribute to differences between the Biofilm10 and Biofilm20 Chl *a* concentrations, though this is less likely given the differences in pigmentation between the two types of biofilms. Chl *a* concentration was also measured in the No Biofilm jars as a control, with a concentration of 0.28 ± 0.23 mg/g tailings.

The Chl *a* concentrations are consistent with the DO, COD, and TOC water chemistry results in Table 3-2 and the LIVE/DEAD staining results in Figure 3-1. Prior to mixing, both Biofilm10 and Biofilm20 jars had high DO concentrations of 9.09 ± 0.44 and 8.18 ± 0.29 mg/L, respectively, compared to the No Biofilm jars, which had an average DO concentration of 5.05 ± 0.96 mg/L. The Biofilm20 jars had 11% lower DO on average than the Biofilm10 jars and had COD and TOC concentrations that were 11% and 12% higher on average, respectively, in comparison to that of the Biofilm10 jars. These results are consistent with the trend noted by He et al. (2019), in which COD and TOC concentrations were highest during the stage of algae death and decay, likely due to a rapid release of intracellular organic matter into the surface water. Based on LIVE/DEAD staining of Biofilm10 (Figure 3-1A) and Biofilm20 (Figure 3-1D), it appears that Biofilm20 contained more dead cells than Biofilm10, though the biofilm matrix impacted the quality of these images. Taken together, these results indicate that decaying algal communities were likely more

prevalent in the 20-week-old biofilms. However, only the top layer of biofilm was sampled for LIVE/DEAD staining in order to disturb the biofilms as little as possible. Because biofilm growth and development is a successional process, new layers of biofilm were likely integrating into FFT underneath the older top layer (Droppo et al. 2007).

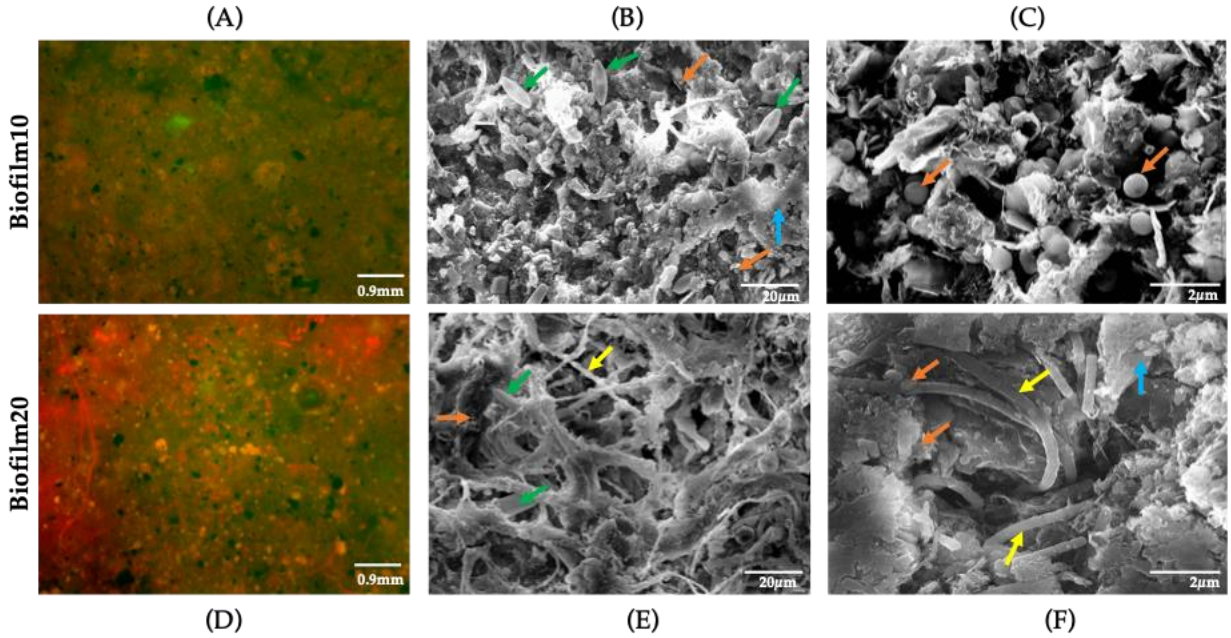

Figure 3-1. Viability of the cells was determined by LIVE/DEAD staining (A and D) at 200x magnification (green, live; red, dead). SEM was utilized to visualize the status of biofilms at week 10 (B and C) and week 20 (E and F). B and C are different SEM images of Biofilm10 taken at different scales, 20 and 2 µm, respectively. Similarly, E and F are different SEM images of Biofilm20 taken at different scales, 20 and 2 µm, respectively. Green arrows represent *Pinnularia* (phylum = Ochrophyta), yellow arrows represent filamentous cyanobacteria, orange arrows represent *Choricystis* (phylum = Chlorophyta), and blue arrows indicate EPS mixed with mineral particles. Biofilm10 corresponds to 10-week-old biofilms; Biofilm20 corresponds to 20-week-old biofilms. Note that only the top layer of biofilms was sampled for LIVE/DEAD staining and SEM imaging.

The biofilm topography under SEM showed a mixed appearance of bacteria and algae in both Biofilm10 and Biofilm20. Note that only the top layers of biofilms were sampled for SEM imaging. In Biofilm10 (Figure 3-1B,C), more species were visible; *Pinnularia* (diatoms) and coccoid *Choricystis* were witnessed profusely at 20 µm (Figure 3-1B), and a large colony of coccoid *Choricystis* appeared in Biofilm10 at a higher magnification of 2 µm (Figure 3-1C). The presence of diatoms (which belong to Ochrophyta) and *Choricystis* (which belong to Chlorophyta)

in Biofilm10 is consistent with the 16S and 18S DNA sequencing results (discussed below). In contrast, observations of Biofilm20 revealed cyanobacteria, primarily of the filamentous type, and diatoms, most of which were coated in EPS at 20 µm (Figure 3-1E). At a higher magnification of 2 µm, clusters of coccoid *Choricystis* and filamentous cyanobacteria were visible coated in EPS (Figure 3-1F). The predominance of cyanobacteria in Biofilm20 and the presence of diatoms (which belong to Ochrophyta) and *Choricystis* (which belong to Chlorophyta) are also consistent with the 16S DNA sequencing results, which will be discussed further below. The higher amount of EPS evident in the SEM images of Biofilm20, in comparison to that of Biofilm10, is consistent with the older age of the biofilm (Leriche et al. 2000).

Samples for DNA extraction and 16S and 18S sequencing were taken from the top layers of the biofilms in Biofilm20 and Biofilm10 before commencing the mixing tests. These top layer samples are referred to as Biofilm20a and Biofilm10a, respectively, in the following discussion. Distinct black and pink microbial communities (see Appendix A1, Figure A-1) were visible below the FFT–water interface in the majority of the biofilm jars, and additional samples were taken from the Biofilm20 and Biofilm10 jars to capture these communities. These communities were especially prominent in the Biofilm20 jars, though they were evident to a lesser extent in many of the Biofilm10 jars. These additional samples are referred to as Biofilm10b and Biofilm10c and Biofilm20b and Biofilm20c in the following discussion (b: samples of pink microbial communities; c: samples of black microbial communities). The 18S sequencing data are only shown for Biofilm20a and Biofilm10a, as eukaryotes in the other biofilm samples were largely negligible.

A predominance of Proteobacteria was observed at the phylum level, covering 33% of the overall microbial community, while other dominating phyla included Cyanobacteria (18.7%), Bacteria_unclassified (18.6%), Chloroflexi (8%), Desulfobacterota (7.2%) Bacteroidota (5.6%), Cloacimonadota (3.3%), and Planctomycetota (1.9%). All biofilm samples showed a complex and diverse microbial community to be more prominent at the class level. Figure 3-2 shows the 10 most abundant genera from each sample, augmented by many unclassified genera at the class level.

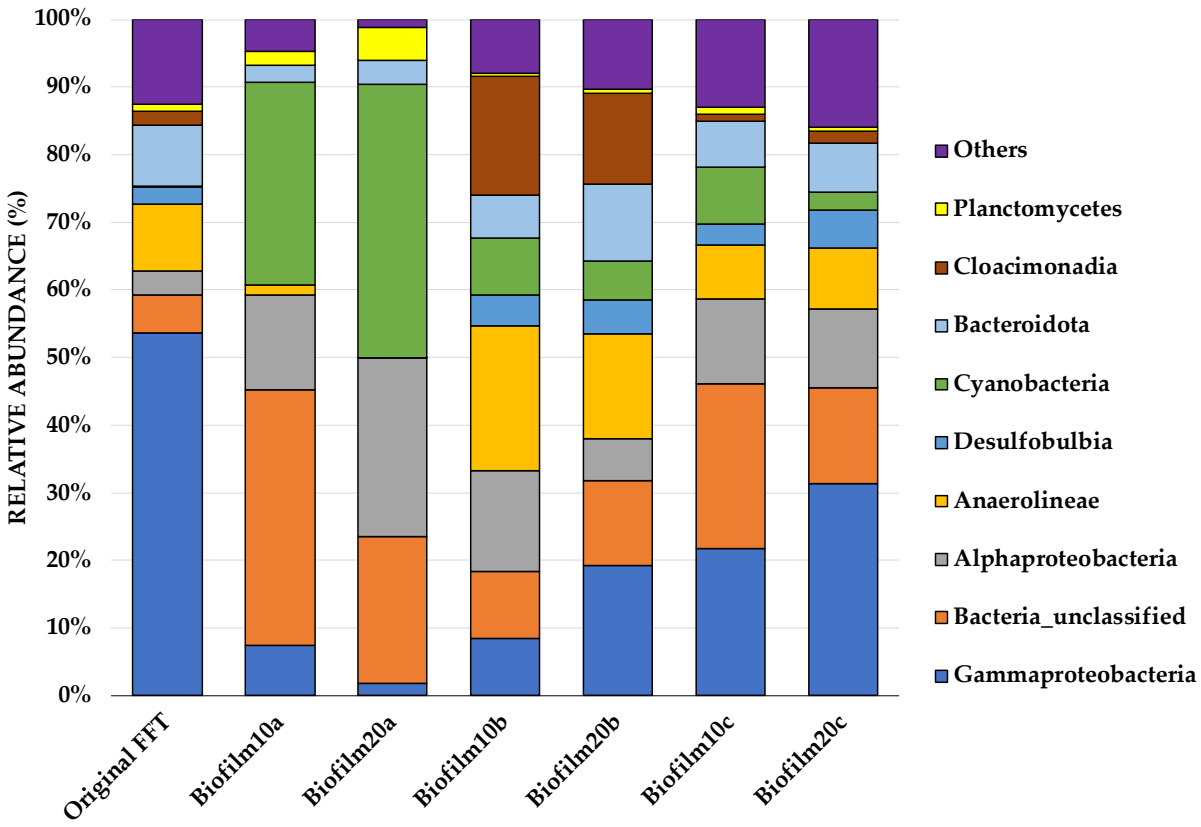

Figure 3-2. Stacking bars illustrating the relative abundances of microorganisms at the class level, represented by the percentage of the 16S rRNA read counts within each group. A relative abundance of less than 1% is assigned to 'Others'. Original FFT refers to the FFT sampled before biofilms were inoculated and grown in jars. Biofilm10 corresponds to 10-week-old biofilms; Biofilm20 corresponds to 20-week-old biofilms. Biofilm10a and Biofilm20a refer to biofilm samples taken from the top layer of the biofilms. Biofilm10b and Biofilm20b refer to distinct pink microbial communities that were seen developing below the FFT–water interface (see Appendix A1, Figure A-1). Biofilm10c and Biofilm20c refer to distinct black microbial communities that were seen developing below the FFT–water interface (see Appendix A1, Figure A-1).

Sequences from the original FFT showed a predominance of *Gammaproteobacteria* at the class level, which represented 54% of the total community on average. Furthermore, *Gammaproteobacteria* were dominant in sample groups such as Biofilm20c (31.4%), Biofilm10c (21.8%), and Biofilm20b (19.3%); however, they were dramatically reduced in the top biofilm layers, Biofilm10a (7.4%) and Biofilm20a (1.8%). Compared to biofilm samples a and c, Biofilm10b had a relatively balanced, mixed community and consisted of only 8.5% *Gammaproteobacteria.* In aerobic primary cultures derived from FTT, *Gammaproteobacteria* and other taxa are key players in degrading hydrocarbons (Foght and Semple 2014). Furthermore,

Alphaproteobacteria and *Gammaproteobacteria* are the two most well-known groups of methanotrophic aerobic bacteria (Op den Camp et al. 2009; Saidi-Mehrabad et al. 2013). In comparison with the original FFT samples (3.6% on average), the *Alphaproteobacteria* population in all biofilms had doubled. Biofilm10a, Biofilm20a, and Biofilm10b contained the highest relative abundances of *Alphaproteobacteria* (14.1%, 26.3%, and 14.9%, respectively).

The phylum Chloroflexi, which contains *Anaerolineae*, is a well-known thermophilic bacterial group that was found in the original FFT samples (10% on average). Despite being absent from Biofilm20a and weakened sharply in Biofilm10a, they constituted 21.5% of the total bacterial count in Biofilm10b and 15.5% in Biofilm20b. The presence of thermophilic bacteria within the microbial community is not surprising given that tailings are exposed to high temperatures (historically up to 60°C) during processing (MacKinnon 1989), and Chloroflexi *(Anaerolineae*) have previously been reported in Syncrude tailings ponds (Collins et al. 2016; Siddique et al. 2015). *Desulfobulbia* is part of Desulfobacterota, which contribute to sulfate reduction, iron oxidation, and aromatic hydrocarbon degradation (Murphy et al. 2021). In nearly all samples, *Desulfobulbia* was present at an abundance of up to 6%, except in Biofilm10a and Biofilm20a. This is consistent with the decreased sulfur concentrations in the surface water in Biofilm10 and Biofilm20 jars presented in Table 3-2. While biofilm samples b and c (pink and black microbial communities, respectively) were fairly similar at the class level, Biofilm10b and Biofilm20b had notably higher proportions of *Anaerolineae* and *Cloacimonadia* relative to Biofilm10c and Biofilm20c. A dominant number of cyanobacteria was observed predominantly in Biofilm10a (30%) and Biofilm20a (40.5%) samples. In all other biofilm samples, cyanobacteria were present at an abundance of less than 10%. A very small percentage of cyanobacteria was also observed in the original FFT (0.12%).

On the phylum-level distribution of whole eukaryotes, Chlorophyta (known as green algae) predominated (50%), followed by Ochrophyta (18%), Cercozoa (12%), Eukaryota_unclassified (8%), and fungi (8%). Figure 3-3 shows the most abundant Eukaryota from each sample, augmented at the phylum level. Interestingly, the most notable differences between biofilms of different ages (Biofilm10 and Biofilm20) occurred amongst the eukaryotes. The most dominant species in Biofilm10a were *Choricystis* sp. (observed in abundance under SEM), which belong to

Chlorophyta, and *Cryptofilida_unclassified* sp., which belonged to Cercozoa. Biofilm20a was dominated by *Pinnularia brebissonii* and *Scenedesmus obliquus*, belonging to the phyla Ochrophyta and Chlorophyta, respectively (see Appendix A1, Figure A-3). There was a notable difference among the Eukaryota phylum Chlorophyta, which accounted for 77% of Biofilm10a, compared to 22% of Biofilm20a. While Biofilm10a had a 55% higher relative abundance of Chlorophyta, Biofilm20a had a 10.5% higher relative abundance of cyanobacteria. Lifting and layering of Biofilm20 and/or algal self-shading may have limited light penetration, contributing to a greater proportion of cyanobacteria, which have higher growth rates than green algae under low light intensities, and a lesser amount of green algae in Biofilm20a (Roeselers et al. 2007).

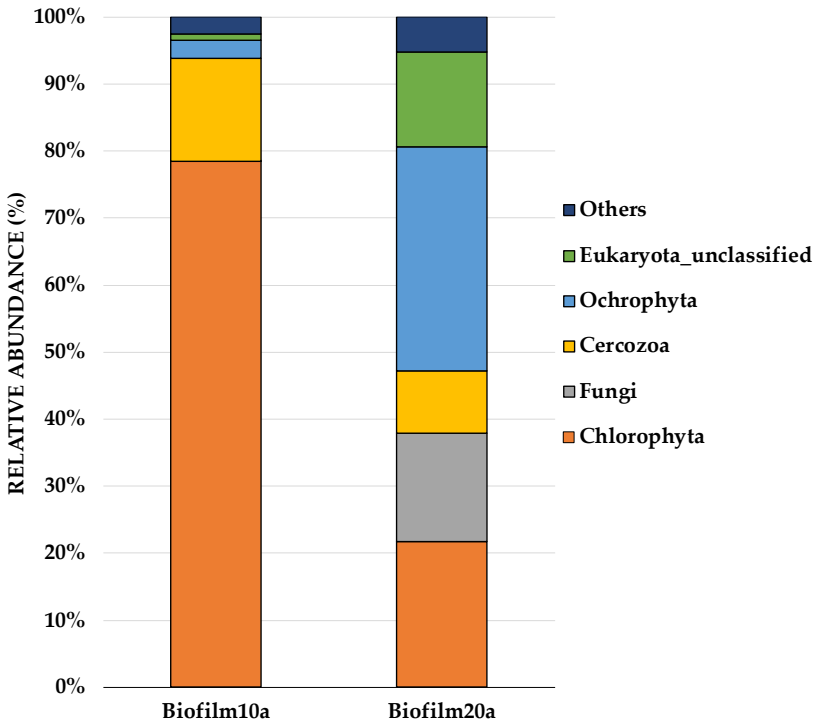

Figure 3-3. Stacking bars illustrating the relative abundances of Eukaryota at the phylum level in Biofilm10a and Biofilm20a, revealed by 18S sequencing. Microbial phyla that composed less than 1% of the dataset were grouped under the 'Other' category. Biofilm10 corresponds to 10-week-old biofilms; Biofilm20 corresponds to 20-week-old biofilms. Biofilm10a and Biofilm20a refer to biofilm samples taken from the top layer of the biofilms.

In general, Biofilm10a and Biofilm20a samples contained higher proportions of aerobic photoautotrophic cyanobacteria and green algae, which is consistent with the top layer of the biofilms being exposed to light (Frederick 2011; Roeselers et al. 2008). Samples taken from

beneath the top layer (Biofilm10b and 10c and Biofilm20b and 20c) included higher proportions of facultative or anaerobic heterotrophs, such as *Gammaproteobacteria, Desulfobulbia,* and *Anaerolineae,* which may use organic carbon produced by the photoautotrophs as a carbon source (Frederick 2011; Roeselers et al. 2008; van Gemerden 1993). The coexistence of heterotrophic bacteria and microalgae in biofilms is believed to result in a mutually beneficial relationship in which both parties rely less on external nutrient sources, EPS yields increase, and biostabilization is further enhanced (Gerbersdorf and Wieprecht 2015). Future research is needed to determine the factors that lead to specific microbial community structure changes within biofilms at different times, which will allow for a clearer understanding of how specific microorganisms play a role in the biostabilization of FFT.

3.3.2 Mixing Tests

Figure 3-4 presents a comparison of the initial turbidity in the BML surface water in the No Biofilm, Biofilm10, and Biofilm20 jars immediately after the first and second 1 hr mixing periods (which occurred 35 days apart). As anticipated, turbidity increased with mixing speed in all jars. However, the presence of a biofilm substantially reduced turbidity at all four mixing speeds during both tests. During the first mixing test, Biofilm20 reduced the initial turbidity in the overlying water by 73% to 95% on average, depending on the mixing speed, while Biofilm10 reduced the initial turbidity by 99% and 96% on average for mixing speeds of 160 and 200 rpm, respectively. The mixing test was conducted a second time to determine if biofilms continued to show improvement over No Biofilms even after the biofilms were ‘disturbed’ due to mixing/movement in the overlying surface water. The effectiveness of biofilms in mitigating turbidity decreased slightly when particles were resuspended during the second mixing test. During the second test, Biofilm20 reduced the initial turbidity by 69% to 93% on average, and Biofilm10 reduced turbidity by 93% to 99% on average compared to No Biofilm.

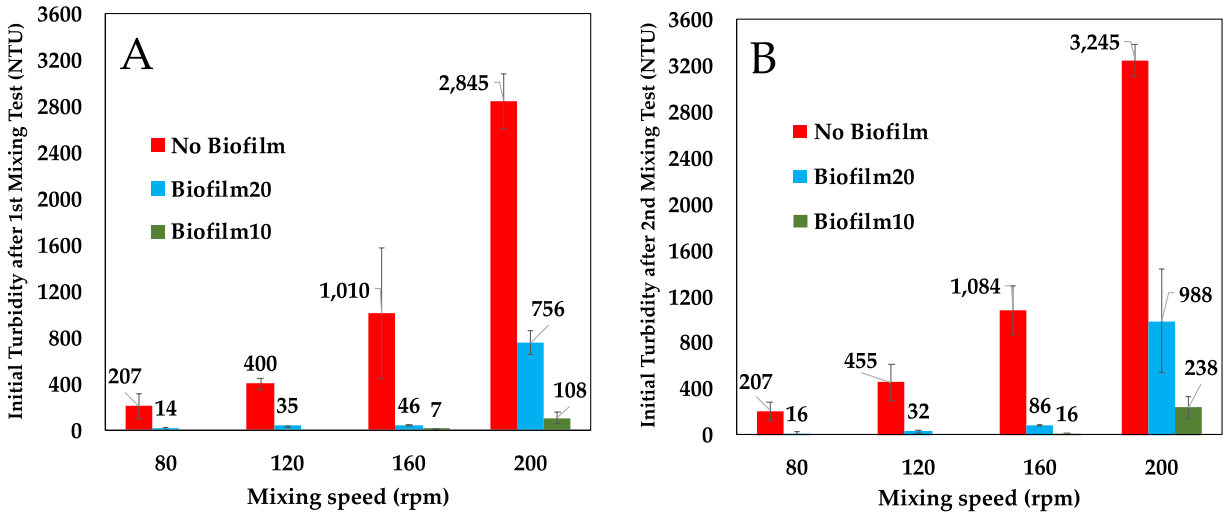

Figure 3-4. Comparison of initial turbidity in No Biofilm, Biofilm10, and Biofilm20 jars from the first and second mixing tests after 1 hr mixing periods. A corresponds to the initial turbidity during the first mixing test, which commenced on Day 0; B corresponds to the initial turbidity during the second mixing test that commenced on Day 35. Results are presented as average ± one standard deviation of triplicates. Biofilm10 corresponds to 10-week-old biofilms; Biofilm20 corresponds to 20-week-old biofilms.

Biofilm10 performed better than Biofilm20 at both the 160 and 200 rpm mixing speeds. Biofilm20 had weaker attachment to the underlying FFT as evidenced by the lifting and layering of the top layers of these biofilms, despite having a higher amount of EPS as indicated by SEM imaging. This is likely a result of gas bubble releases and the higher proportion of decaying microbial communities in Biofilm20. Droppo et al. (2007) found that the release of gas bubbles acted as a focal point for initiating ripping and failure of biofilms. As such, it is not surprising that Biofilm20 generated higher turbidity than Biofilm10 (Droppo et al. 2007; Droppo 2009). Prior to the mixing tests, the top layer of the biofilms acted as sheets covering the FFT surface and isolating the underlying FFT from the surface water. During the first mixing test, at a mixing speed of 200 rpm in the Biofilm10 jars and Biofilm20 jars, the top layers of the biofilms rolled up or folded over onto themselves, exposing the underlying biostabilized FFT and leading to erosion of the FFT and higher turbidity in the surface water. Because of the weaker attachment of Biofilm20 to the underlying FFT, larger portions of these biofilms rolled up or folded over in comparison to Biofilm10. Furthermore, during both the first and second mixing tests, isolated failures (ripping) of Biofilm20 occurred at mixing speeds of 120, 160, and 200 rpm, again leading to higher turbidity. These isolated failures were not evident during the Biofilm10 mixing tests. Biofilm20 essentially

remained intact at a mixing speed of 80 rpm, and Biofilm10 remained intact at a mixing speed of 160 rpm.

The consistently higher turbidity measured in Biofilm20 compared to Biofilm10 was predicted, based on the work of Droppo et al. (2007). Because biofilm growth and development is a successional process, biofilms are likely to experience fluctuations in their ability to stabilize sediment over time (Droppo et al. 2007). Processes such as microbial death and decay, species succession, and changes to EPS production and distribution are thought to have a significant effect on biofilm stability. As such, as biofilms age, there may be periods of increased stability and periods of decreased stability. Regardless, biostabilized sediment is expected to have improved stability over purely mineral sediments (Droppo et al. 2007).

Figure 3-5 presents turbidity in No Biofilm, Biofilm10, and Biofilm 20 jars measured over the course of the first and second mixing tests. The spikes in turbidity at Day 35 correspond to the turbidity immediately after the second 1 hr mixing period. The No Biofilm jars had the highest turbidity for all four mixing speeds during both the first and second mixing tests, and they also showed the most variability in the triplicate turbidity measurements. This is likely a result of the high turbidity generated in these jars as well as variability in the FFT solids content and particle sizes. Biofilm20 jars also showed greater variability in triplicate turbidity measurements during the second 200 rpm mixing test, when turbidity measurements were highest.

At all mixing speeds, the turbidity in the Biofilm20 and Biofilm10 jars dissipated faster than that of the No Biofilm jars. This is a result of both the lower turbidity generated in the biofilm jars and the size of the flocs being suspended. While FFT was suspended in both No Biofilm and biofilm jars, visibly larger flocs were suspended in the biofilm jars. These flocs were presumably biostabilized FFT and pieces of the biofilm that had ripped off from the rest of the biofilm coating the FFT surface (Droppo 2009). This observation is consistent with the results of Droppo et al. (2001), who noted that due to the strong binding nature of biofilms, the erosion of biostabilized sediment generated larger and more stable flocs relative to purely mineral sediment.

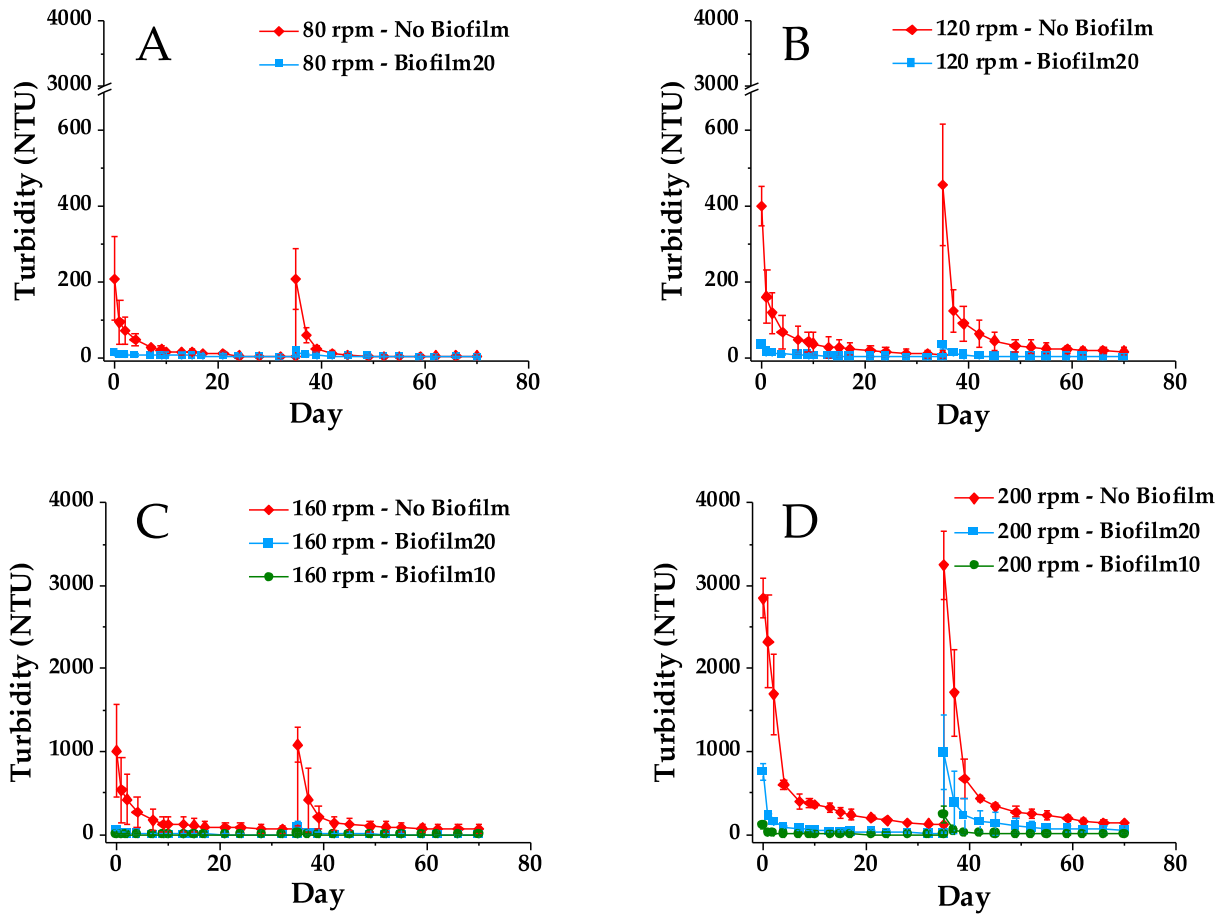

Figure 3-5. Turbidity in No Biofilm, Biofilm10, and Biofilm20 jars during first and second mixing tests. A, B, C, and D correspond to mixing speeds of 80, 120, 160, and 200 rpm, respectively. Results are presented as average ± one standard deviation of triplicates. The spike in turbidity at Day 35 corresponds to the turbidity immediately after the second 1 hr mixing period. Note that A and B have y-axis breaks between 600 and 3000 NTU. Biofilm10 corresponds to 10-week-old biofilms; Biofilm20 corresponds to 20-week-old biofilms.

As illustrated in Figures 3-4 and 3-5, the turbidity was higher during the second mixing test compared to the first mixing test for all jars and all mixing speeds, with the exception of Biofilm20 jars mixed at 120 rpm, which saw an initial turbidity decrease of 3 NTU on average, and No Biofilm jars mixed at 80 rpm, which saw no change in turbidity between the first and second mixing tests. When comparing the percent difference in initial turbidity measured after the first and second 1 hr mixing periods (see Appendix A1, Figure A-4), biofilm jars showed the greatest percent increase in turbidity. For example, during the second 1 hr mixing period, the initial turbidity in Biofilm10 jars mixed at 160 or 200 rpm more than doubled compared to that of the

first mixing period 35 days prior. Despite this increase in turbidity, the presence of biofilms still showed improvement over No Biofilms during the second mixing test, even though most of the biofilms were disturbed to some extent during the first mixing test, either by ripping apart, rolling up, and/or folding over.

The higher turbidity in the biofilm jars during the second mixing test is likely due to a combination of factors, including increasing biofilm age and thereby death and decay of the older uppermost layers of the biofilms, reduced biofilm integrity as a result of mechanical mixing, and decreased photosynthesis and algal growth due to turbidity. The mixing tests appeared to impact algal growth in the biofilms as evidenced by changes in the DO concentrations in the surface water immediately following the 1 hr mixing periods (see Appendix A1, Figure A-5). Immediately after both the first and second 1 hr mixing periods, the DO in the Biofilm20 and Biofilm10 jars decreased, especially in the Biofilm20 jars mixed at higher speeds. Conversely, the No Biofilm jars experienced a spike in DO immediately after the first and second 1 hr mixing periods due to aeration from mechanical mixing. The DO in the biofilm jars continued to decrease for at least 10 days following the two 1 hr mixing periods before gradually recovering. Thus, photosynthesis was likely temporarily hindered by the turbidity in the biofilm jars. This agrees with previous studies, which have found that turbidity and light penetration are dominant factors limiting algal biofilm production (Casco et al. 2009; Frederick 2011; Hart and Lovvorn 2000; Squires et al. 2001). The decrease in DO in the biofilm jars may also have been due to an increase in oxygen demand following the mixing periods, though oxygen demand was not measured during the mixing tests. Turbidity generation in the biofilm jars (due to the suspension of biostabilized FFT and pieces of biofilms) may have increased the amount of TOC and heterotrophs in the surface water, both of which could increase the oxygen demand and thus contribute to the decrease in DO in the biofilm jars. At the end of the two 35-day mixing tests (Day 70), the DO concentrations in all of the No Biofilm jars were greater than or equal to their initial (Day 0) concentration of 5.05 ± 0.96 mg/L. However, the DO concentrations in the Biofilm20 jars on Day 70 were 1.36 to 1.99 mg/L lower than their Day 0 concentration of 8.18 ± 0.29 mg/L, depending on the mixing speed. The higher mixing speeds in the Biofilm20 jars corresponded with lower Day 70 DO concentrations. The DO concentrations in all six Biofilm10 jars on Day 70 were approximately 1.9 mg/L lower than their Day 0 concentration of 9.09 ± 0.44 mg/L, regardless of mixing speed. The decrease in DO in the biofilm jars over the

course of the first and second mixing tests is likely a result of turbidity inhibiting photosynthesis and increasing oxygen demand, as well as microbial death and decay and species succession. The pH of the surface water remained relatively stable in all jars throughout the mixing tests (see Appendix A1, Figure A-6).

The No Biofilm jars mixed at 120, 160, and 200 rpm also had a turbidity increase during the second mixing test. This may be partly because the turbidity in the No Biofilm jars mixed at 160 and 200 rpm was still relatively high, at 62 and 115 NTU, respectively, just prior to commencing the second mixing test compared to that of the Biofilm10 and Biofilm20 jars. Additionally, recently settled FFT particles in the No Biofilm jars could have created an intermediate layer that was less dense and more mobile than the underlying FFT (Lawrence et al. 2016). This material would be more easily and quickly resuspended during the second mixing test, and the resuspension of this intermediate layer would lead to the exposure and subsequent erosion of the underlying FFT. The development of this intermediate layer is most likely to have occurred in the No Biofilm jars mixed at higher speeds (160 and 200 rpm) because of the greater amount of FFT particles that were suspended at these mixing speeds.

Though consolidation has been found to contribute to the stabilization of bed sediments (Droppo and Amos 2001; Tolhurst et al. 2000), this effect is expected to have been minimal in this experiment because of the more significant role of biostabilization (Droppo 2009) and because of the fine-grained nature of the FFT and the small amount of tailings (approximately 200 g) in each jar. After the 10-week or 20-week growth period, the solids and water contents and bulk densities of the FFT in the Biofilm10, Biofilm20, and No Biofilm jars did not change substantially from those of the initial FFT, which indicates that self-weight consolidation of the FFT in the jars was minimal, and therefore, consolidation did not contribute to stabilization. Electrochemical interactions in the FFT may have generated some attraction and stabilizing forces (Droppo 2009). However, because of the substantial turbidity mitigation observed in the biofilm jars compared to the No Biofilm jars, it can be concluded that biostabilization was the dominant factor contributing to reduced FFT turbidity in this work. While microbial communities in the biofilms could have impacted FFT geochemistry, potentially influencing interparticle binding and increasing or decreasing stability (Droppo et al. 2007), the secretion of EPS is still thought to be the primary

mechanism by which biofilms enhance stabilization (Amos et al. 2004; Droppo 2009; Gerbersdorf et al. 2008; Lundkvist et al. 2007; Reid et al. 2016).

In this work, mudline biofilms made up of diverse communities of photoautotrophs and heterotrophs indigenous to oil sands tailings substantially reduced turbidity generated as a result of mixing/movement in the overlying surface water. However, the growth of biofilms on the BML mudline and subsequent biostabilization likely depend on a number of factors, including temporal seasonal changes (Amos et al. 2004; Droppo 2009) and the depth of light penetration in the surface water. Predominately algal biofilms may develop in shallow locations within BML, similar to the algal biofilms that naturally occur in surrounding wetlands (Frederick 2011), while bacterial biofilms may dominate at greater depths or in particularly turbid locations. Additionally, further investigation is necessary to determine how gas ebullition and pore water expression from FFT into overlying surface water may impact the growth and structure of biofilms and turbidity mitigation. The biofilms in this experiment were grown under quiescent conditions, which is also likely to impact biofilm growth and structure, and as such, the impact of surface water mixing/movement during biofilm growth should also be investigated in future studies.

The mixing methodology used in this experiment was not intended to replicate field conditions, but rather to evaluate biofilms as a potential turbidity mitigation mechanism. Turbidity generation in BML due to mixing/movement in the surface water is a result of a number of processes, as previously discussed, including wind waves and other wind-driven processes and convection (Lawrence et al. 2016). These processes may occur in short bursts or intermittently over several days, such as during lake turnover, and the extent to which these processes generate turbidity will depend on several factors, including the depth of the surface water cap. The mixing methodology used in this study involved short (1 h) mixing periods at increasing speeds and linear velocities in order to first evaluate the effectiveness of biofilms in mitigating turbidity generation and second to determine the mixing speed at which biofilms were disturbed, either by ripping, rolling up, and/or folding over, and subsequently generated turbidity in the surface water. The highest mixing speeds tested in this study do not necessarily reflect scenarios under which turbidity will be generated in BML but rather demonstrate the high mixing speed required to disturb otherwise intact biofilms. As such, while the mixing duration and mudline linear velocities used in this work

do not reflect all scenarios under which turbidity may be generated in BML, the results clearly show that the presence of biofilms at the mudline reduced turbidity generation under all mixing conditions evaluated in this work.

3.4 Conclusions

This study is the first to investigate and demonstrate that biostabilization is a promising mechanism for turbidity mitigation in oil sands pit lakes. Mudline biofilms made up of photoautotrophs and heterotrophs indigenous to oil sands tailings reduced surface water turbidity generation by up to 99% during laboratory mixing experiments. Further, turbidity dissipation was faster in biofilm jars because of both the lower turbidity generated in these jars and the visibly larger size of suspended flocs. During the first mixing test, the 10-week-old biofilms reduced initial turbidity by 96% to 99% while the 20-week-old biofilms reduced initial turbidity by 73% to 95% compared to control jars with no biofilm. During the second mixing test, turbidity generation increased in all jars relative to the first mixing test, though biofilms continued to show an improvement over no biofilm jars. During this second test, 10-week-old biofilms reduced the initial turbidity generation by 93% to 99% and 20-week-old biofilms reduced initial turbidity by 69% to 93% compared to no biofilm. The higher turbidity in the biofilm jars during the second mixing test is likely due to a combination of factors including biofilm age (and thereby death and decay of older biofilm layers), reduced biofilm integrity due to mechanical mixing/disturbance, and decreased photosynthesis and algal growth due to turbidity generation.

Biofilm age also impacted turbidity generation. The 20-week-old biofilms were more prone to lifting and layering due to gas release and microbial death and decay in comparison to 10-week-old biofilms, which led to weaker attachment of older biofilms to underlying FFT and higher turbidity measurements. However, regardless of biofilm age, the presence of biofilms substantially reduced surface water turbidity in comparison to sterilized FFT. Biostabilization of FFT in BML is promising, though the development and growth of biofilms in the field would likely be impacted by several factors that could not be accounted for in this study. These factors include temporal seasonal changes, light penetration, and gas ebullition and pore water expression from FFT (which would presumably impact both biofilm development and integrity).

3.5 References

American Society for Testing Materials (ASTM). Standard Test Method for Particle-size Distribution (Gradation) of Fine-grained Soils Using the Sedimentation (Hydrometer) D7928-17; ASTM International: West Conshohocken, US, 2017.

American Standard for Testing Materials (ASTM). Standard Test Methods for Laboratory Determination of Water (Moisture) Content of Soil and Rock by Mass D2216-19; ASTM International: West Conshohocken, US, 2019.

Amos, C.L.; Bergamasco, A.; Umgiesser, G.; Cappucci, S.; Cloutier, D.; DeNat, L.; Flindt, M.; Bonardi, G.; Cristante, S. The stability of tidal flats in Venice Lagoon—The results of in-situ measurements using two benthic annular flumes. *J. Mar. Syst.* **2004**, *51*, 211–241.

Andersen, R.A.; Kawachi, M. Traditional microalgae isolation techniques. In *Algal Culturing Techniques*, 1st ed.; Andersen, R.A., Ed.; Elsevier, Inc.: San Diego, US, 2005; pp. 83–100.

Anishchenko, O.V.; Gladyshev, M.I.; Kravchuk, E.S.; Ivanova, E.A.; Gribovskaya, L.V.; Sushchik, N.N. Seasonal variations of metal concentrations in periphyton and taxonomic composition of the algal community at a Yenisei River littoral site. *Cent. Eur. J. Biol.* **2010**, *5*, 125–134.

Bordenave, S.; Kostenko, V.; Dutkoski, M.; Grigoryanm, A.; Martinuzzi, R.J.; Voordouw, G. Relation between the activity of anaerobic microbial populations in oil sands tailings ponds and the sedimentation of tailings. *Chemosphere* **2010**, *81*, 663–668.

Callahan, B.J.; McMurdie, P.J.; Rosen, M.J.; Han, A.W.; Johnson, A.J.A.; Holmes, S.P. DADA2: High-resolution sample interference from Illumina amplicon data. *Nat. Methods* **2016**, *13*, 581–583.

Caporaso, J.G.; Lauber, C.L.; Walters, W.A.; Berg-Lyons, D.; Lozupone, C.A.; Turnbaugh, P.J.; Fierer, N.; Knight, R. Global patterns of 16S rRNA diversity at a depth of millions of sequences per samples. *PNAS* **2011**, *108 (*Suppl. S1*)*, 4516–4522.

Casco, M.A.; Mac Donagh, M.E.; Cano, M.G.; Solari, L.C.; Claps, M.C.; Gabellone, N.A. Phytoplankton and Epipelon responds to clear and turbid phases in a seepage lake (Buenos Aires, Argentina). *Internat. Rev. Hydrobiol.* **2009**, *94*, 153–168.

Charette, T.; Castendyk, D.; Hrynshyn, J.; Kupper, A.; McKenna, G.; Mooder, B. End Pit Lakes Guidance Document 2012; Cumulative Environmental Management Association: Fort McMurray, CA, 2010.

Collins, V.C.E.; Foght, J.M.; Siddique, T. Co-occurrence of methanogenesis and N_2 fixation in oil sands tailings. *Sci. Total Environ.* **2016**, *565*, 306–312.

de Brouwer, J.F.C.; Bjelic, S., de Deckere, E.M.G.T.; Stal, L.G. Interplace between biology and sedimentology in a mudflat (Biezelingse Ham, Westerschedle, The Netherlands). *Cont. Shelf Res.* **2000**, *20*, 1159–1177.

Droppo, I. Biofilm structure and bed stability of five contrasting freshwater sediments. *Mar. Freshw. Res.* **2009**, *60*, 690–699.

Droppo, I.G.; Amos, C.L. Structure, stability and transformation of contaminated lacustrine surface fine-grained laminae. *J. Sediment. Res.* **2001**, *71*, 717–726.

Droppo, I.G.; Lau, Y.L.; Mitchell, C. The effect of depositional history on contaminated bed sediment stability. *Sci. Total Environ.* **2001**, *266*, 7–13.

Droppo, I.G.; Ross, N.; Skafel, M.; Liss, S.N. Biostabilization of cohesive sediment beds in a freshwater wave-dominated environment. *Limnol. Oceanogr.* **2007**, *52*, 577–589.

Flemming, H.C.; Wingender, J. The biofilm matrix. *Nature Rev. Microbiol.* **2010**, *8*, 623–633.

Foght, J.M.; Semple, K. Microbial Pre-Treatment of Plant 6 Froth Treatment Tailings Before Deposition; Report; Syncrude Canada Ltd.: Calgary, CA, 2014.

Frederick, K.R. Productivity and carbon accumulation potential of transferred biofilms in reclaimed oil sands-affected wetlands. Master Thesis, University of Alberta, Edmonton, CA, 2011.

Friend, P.L.; Ciavola, P.; Cappucci, S.; Santos, R. Bio-dependent bed parameters as a proxy tool for sediment stability in mixed habitat intertidal areas. *Cont. Shelf Res.* **2003**, *23*, 1899–1917.

Garcia-Garcia, E.; Pun, J.; Perez-Estrada, L.A.; Din, M.G.E.; Smith, D.W.; Martin, J.W.; Belosevic, M. Commercial naphthenic acids and organic fraction of oil sands process water downregulate pro-inflammatory gene expression and macrophage antimicrobial responses. *Toxicol. Lett.* **2011**, *203*, 62–73.

Gerbersdorf, S.U.; Jancke, T.; Westrich, B.; Paterson, D.M. Microbial stabilization of riverine sediments by extracellular polymeric substances. *Geobiology* **2008**, *6*, 57–69.

Gerbersdorf, S.U.; Wieprecht, S. Biostabilization of cohesive sediments: Revisiting the role of abiotic conditions, physiology and diversity of microbes, polymeric secretion, and biofilm architecture. *Geobiology* **2015**, *13*, 68–97.

Hart, E.A.; Lovvorn, J.R. Vegetation dynamics and primary production in saline, lacustrine wetlands of a Rocky Mountain basin. *Aquat. Bot.* **2000**, *66*, 21–39.

He, J.; Zhang, Y.; Wu, X.; Yang, Y.; Xu, X.; Zheng, B.; Deng, W.; Shao, Z.; Lu, L.; Wang, L.; et al A study on the relationship between metabolism of Cyanobacteria and chemical oxygen demand in Dianchi Lake, China. *Water Environ. Res.* **2019**, *91*, 1650–1660.

Jarvie, H.P.; Neal, C.; Warwick, Aa.; White, J.; Neal, M.; Wickham, H.D.; Hill, L.K.; Andrews, M.C. Phosphorus uptake into algal blooms in a lowland chalk river. *Sci. Total Environ.* **2002**, *282-283*, 352–373.

Lawrence, G.A.; Tedford, E.W. Pieters, R. Suspended solids in an end pit lake: potential mixing mechanisms. *Can. J. Civ. Eng.* **2016**, *43*, 211–217.

Leloup, M.; Nicolau, R.; Pallier, V.; Yéprémian, C.; Feuillade-Cathalifaud, G. Organic matter produced by algae and cyanobacteria: Quantitative and qualitative characterization. *J. Environ. Sci.* **2013**, *25*, 1089–1097.

Leriche, V.; Sibille, P.; Carpentier, B. Use of an enzyme-linked lectinsorbent assay to monitor the shift in polysaccharide composition in bacterial biofilms. *Appl. Environ. Microbiol.* **2000**, *66*, 1851–1856.

Lichtenthaler, H.K. Chlorophylls and cartenoids: Pigments of photosynthetic biomembranes. *Methods Enzymol.* **1987**, *148*, 350–382.

Lundkvist, M.; Grui, M.; Friend, P.L.; Flindt, M.R. The relative contributions of physical and microbiological factors to cohesive sediment stability. *Cont. Shelf Res.* **2007**, *27*, 1143–1152.

MacKinnon, M.D. Development of the tailings pond at Syncrude's oil sands plant: 1978–1987. *AOSTRA J. Res.* **1989**, *5*, 109–133.

Mahdavi, H.; Prasad, V.; Liu, Y.; Ulrich, A.C. In situ biodegradation of naphthenic acids in oil sands tailings pond water using indigenous algae-bacteria consortium. *Bioresour. Technol.* **2015**, *187*, 97–105.

McDonald, D.; Price, M.N.; Goodrich, J.; Nawrocki, E.P.; DeSantis, T.Z.; Probst, A.' Andersen, G.L.; Knight, R.; Hugenholtz, P. An improved Greengenes taxonomy with explicit ranks for ecological and evolutionary analyses of bacteria and archaea. *ISME J.* **2012**, *6*, 610–618.

Morandi, G.D.; Wiseman, S.B.; Pereira, A.; Mankidy, R.; Gault, I.G.M.; Martin, J.W.; Giesy, J.P. Effects-directed analysis of dissolved organic compounds in oil sands process-affected water. *Environ. Sci. Technol.* **2015**, *49*, 12395–12404.

Murphy, C.L.; Biggerstaff, J.; Eichhorn, A.; Ewing, E.; Shahan, R.; Soriano, D.; Stewart, S.; VanMol, K.; Walker, R.; Walters, P.; et al. Genomic characterization of three novel Desulfobacterota classes expand the metabolic and phylogenetic diversity of the Phylum. *bioRxiv*. **2021**, doi:10.1101/2021.03.22.436540.

Op den Camp, J.J.M.; Islam, T.; Stott, M.B.; Harhangi, H.R.; Hynes, A.; Schouten, S.; Jettens, M.S.M.; Birkeland, N.; Pol, A.; Dunfield, P.F. Environmental, genomic and taxonomic perspectives on methanotrophic *Verrucomicrobia*. *Environ. Microbial. Rep.* **2009**, *1*, 293–306.

Potter, M.C.; Wiggert, D.C.; Ramadan, B.H. Shih, T.I-P. *Mechanics of Fluids*, 4th ed.; Cengage Learning: Stamford, US, 2012.

Reid, T.; VanMansel, D.; Droppo, I.G.; Weisener, C.G. The symbiotic relationship of sediment and biofilm dynamics at the sediment water interface of oil sands industrial tailings ponds. *Water Res.* **2016**, *100*, 337–347.

Ripmeester, M.J.; Duford, D.A. Method for routine "naphthenic acids fraction compounds" determination in oil sands process-affected water by liquid-liquid extraction in dichloromethane and Fourier-Transform Infrared Spectroscopy. *Chemosphere* **2019**, *233*, 687–696.

Roeselers, G.; van Loosdrecht, M.C.M.; Muyzer, G. Heterotrophic pioneers facilitate phototrophic biofilm development. *Microb. Ecol.* **2007**, *54*, 578–585.

Roeselers, G.; van Loosdrecht, M.C.M.; Muyzer, G. Phototrophic biofilms and their potential application. *J. Appl. Phycol.* **2008**, *20*, 227–235.

Saidi-Mehrabad, A.; He, Z.; Tamas, I.; Sharp, C.E.; Brady, A.L.; Rochman, F.F.; Bodrossy, L.; Abell, G.C.J.; Penner, T.; Dong, X.; et al. Methanotrophic bacteria in oilsands tailings ponds of northern Alberta. *ISME J.* **2013**, *7*, 908–921.

Siddique, T.; Mohamad Shahimin, M.F.; Zamir, S.; Semple, K.; Li, C.; Foght, J.M. Long-term incubation reveals methanogenic biodegradation of C_5 and C_6 iso-alkanes in oil sands tailings. *Environ. Sci. Technol.* **2015**, *49*, 14732–14739.

Sim, L.L.; David, J.A.; Chambers, J.M. Ecological regime shifts in salinized wetland systems. II. Factors affecting the dominance of benthic microbial communities. *Hydrobiologia* **2006**, *573*, 109–131.

Squires, M.M.; Lesack, L.E. Benthic algal response to pulsed versus distributed inputs of sediment and nutrients in a Mackenzie Delta Lake. *J. N. Am. Benthol. Soc*. **2001**, *20*, 369–384.

Sutherland, T.F.; Grant, J.; Amos, L.L. The effect of carbohydrate production by diatom *Nitzchia curvilineata* on the erodibility of sediment. *Limnol. Oceanogr.* **1998**, *43*, 65–72.

Syncrude Canada Ltd. (Syncrude). 2019 Base Mine Lake Monitoring and Research Summary Report: Results from 2013-2018; Syncrude: Fort McMurray, CA, 2019.

Tedford, E.; Halferdahl, G.; Pieters, R.; Lawrence, G.A. Temporal variations in turbidity in an oil sands pit lake. *Environ. Fluid Mech*. **2019**, *19*, 457–473.

Thompson, R.C.; Tobin, M.L.; Hawkins, S.J.; Norton, T.A. Problems in extraction and spectrophotometric determination of chlorophyll from epilithic microbial biofilms: Towards a standard method. *J. Mar. Biol. Ass. UK* **1999**, *79*, 551–558.

Tolhurst, T.J.; Reithmueller, P.; Paterson, D.M. In situ versus laboratory analysis of sediment stability from intertidal mudflats. *Cont. Shelf Res.* **2000***, 10/11*, 1317–1334.

Vadeboncoeur, Y.; Kalff, J.; Christoffersen, K.; Jeppesen, E. Substratum as a driver of variation in periphyton chlorophyll and productivity in lakes. *J. N. Am. Benthol. Soc.* **2006**, *25*, 378–392.

van Gemerden, H. Microbial mats: A joint venture. *Mar. Geol.* **1993**, *113*, 3–25.

Wei, K.; Cossey, H.L.; Ulrich, A.C. Effects of calcium and aluminum on particle settling in an oil sands end pit lake. *Mine Water Environ.* **2021**. *40*, 1025-1036.

Werner, J.J.; Koren, O.; Hugenholtz, P.; DeSantis, T.Z.; Walters, W.A.; Caporaso, J.G.; Angenent, L.T.; Knight, R.; Ley, R.E. Impact of training sets on classification of high-throughput bacterial 16s rRNA gene surveys. *ISME J*. **2012**, *6*, 94–103.

Widdows, J.; Friend, P.L.; Bale, A.J.; Brinsley, M.D.; Pope, N.D.; Thompson, C.E.L. Inter-comparison between five devices for determining erodibility of intertidal sediments. *Cont. Shelf Res.* **2007**, *27*, 1174–1189.

Wotton, R.S. The essential role of exopolymers (EPS) in aquatic systems. *Oceanogr. Mar. Biol.* **2004**, *42*, 57–94.

Yu, X. Improving Cap Water Quality in an Oil Sands End Pit Lake with Microbial Applications. PhD Thesis, University of Alberta, Edmonton, CA, 2019.

4 BIOGEOCHEMICAL AND GEOTECHNICAL BEHAVIOR OF UNTREATED AND PASS-TREATED OIL SANDS TAILINGS IN PIT LAKES

4.1 Introduction

All of Alberta's oil sands mines plan to reclaim FFT in pit lakes (COSIA 2021). FFT destined for pit lakes may be untreated or treated, such as Suncor's PASS treatment in which alum and PAM are added to FFT in-line. There are no publicly available comparisons of the behavior of untreated versus treated FFT in pit lakes and further, there is no data available on the geotechnical and biogeochemical behavior of PASS-treated FFT. As such, one of the goals of this column study is to compare the biogeochemical and geotechnical behavior of untreated versus PASS-treated FFT in pit lakes. Previous research has focused heavily on methanogenesis in untreated FFT (Fedorak et al. 2002; Holowenko et al. 2000; Kuznetsov et al. 2023; Mohamad Shahimin and Siddique 2017a,b; Mohamad Shahimin et al. 2016, 2021; Siddique et al. 2006, 2007, 2011, 2014a, 2015, 2020; Stasik and Wendt-Potthoff 2014, 2016; Stasik et al. 2014; Tan et al. 2015), though sulfate reduction in untreated FFT and gypsum-amended tailings has also been reported in some field and laboratory studies (Dompierre et al. 2016; Holowenko et al. 2000; Reid and Warren 2016; Stasik and Wendt-Potthoff 2014; Stasik et al. 2014; Warren et al. 2016). The reduced sulfur that is generated from sulfate reduction can include toxic $H_2S_{(g)}$ and aqueous sulfide species which are known oxygen consuming constituents in BML (Risacher et al. 2018). Because of the alum added during PASS treatment, it is suspected that sulfur cycling will be an important biogeochemical process in PASS-treated FFT.

With regard to geotechnical behavior, PASS-treated FFT should have faster dewatering and consolidation rates than untreated FFT (Suncor 2022b). Consolidation of pit lake tailings produces advective pore water fluxes and increases chemical mass transfer of ions and organics into the water cap, as seen in BML (Dompierre et al. 2017). Dompierre and Barbour (2016) and Dompierre et al. (2017) found that advection-dispersion was driving chemical mass transfer into the BML water cap but predicted that over time, as self-weight consolidation slows, diffusion will govern chemical mass transfer in the pit lake. Chemical mass transfer in pit lakes with PASS-treated FFT may differ from that of BML due to presumably higher advective pore water fluxes and the reduced

mobility of organic compounds in PASS-treated FFT (as suggested by Suncor) (Suncor 2022b). Chemical mass transfer into pit lake water caps will likely occur for decades and will have implications for water cap quality management (through freshwater dilutions, etc.) and the development of lake ecosystems.

In addition to evaluating the impact of PASS treatment on the geotechnical and biogeochemical behavior of FFT in pit lakes, this anaerobic column study also investigates the effects of hydrocarbon amendments, temperature (10 vs. 20 °C), CO_2 addition, and column size (1 vs. 19 L) on the geotechnical and biogeochemical behavior observed in the laboratory. Sixty-four columns, each containing either untreated or PASS-treated FFT and a water cap, were monitored over a period of 540 d as part of the study. This column study is the first to i) compare the geotechnical and biogeochemical behavior of untreated and PASS-treated FFT in pit lake scenarios and ii) evaluate the impact of column size on the biogeochemical and geotechnical behavior of FFT. The findings from this work highlight biogeochemical processes that will be important to monitor in PASS-treated FFT, as well as the impacts of hydrocarbons and column size on geotechnical and biogeochemical behavior of oil sands tailings.

4.2 Materials and Methods

4.2.1 Materials

The oil sands tailings used in this study were collected in 2019 from a tailings pond where FFT and paraffinic FTT are combined (collectively referred to as FFT hereinafter). Approximately 400 L of untreated FFT was collected in 5 L grab samples and transported to the Northern Alberta Institute of Technology (NAIT). The samples were combined and homogenized in two large barrels, and then subsampled into 20 L pails and stored at NAIT until use in 2021. Half of the FFT was left untreated, while the other half was treated at NAIT using a PASS treatment process similar to Suncor's technology. BCR water, which was collected by an oil sands operator in 2015, was used for the column water caps as BCR is the freshwater source used to dilute the BML water cap. The BCR water was transported to the University of Alberta and stored at 4°C until use.

The PASS treatment process involved adding alum ($Al_2(SO_4)_3 \cdot 14H_2O$; dose of 875 mg/L) and partially hydrolyzed anionic PAM (dose of 2.43 g/kg of FFT solids) to the FFT. Prior to conducting

the coagulation/flocculation procedure outlined below, the FFT polymer dosage was optimized using capillary suction time as detailed in Li et al. (2022a). The coagulation/flocculation procedure was conducted in batches in a 6 in. baffled metal cup using an overhead mixer with a torque sensor (Heidolph Hei-TORQUE 100 Precision Base, Schwabach, DE) and a flat impeller blade. The coagulation/flocculation procedure was as follows. First, to pre-shear the FFT, the sample was mixed at 300 rpm for 1 min. While mixing continued at 300 rpm, the required volume of alum was injected into the cup using a 1 mL syringe. Mixing continued for 10 sec after which the mixing speed was reduced to 80 rpm for 13 min. The mixing speed was then increased to 300 rpm and using a peristaltic pump (Cole Parmer Drive/Disp Masterflex 115/230, Vernon Hills, US), the required volume of polymer solution (which consisted of PAM and FFT pore water) was injected at a rate of 1200 mL/min. Once the maximum torque was reached, the mixing speed was reduced to 50 rpm for 15 sec to condition the flocs. A schematic of the flocculation setup is available in Li et al. (2021).

Suncor's PASS-treated FFT is subjected to mechanical shearing, equivalent to a shear energy of 1500 kJ/m^3, during pipeline transport to DDA3. To mimic this shearing in the laboratory, the PASS-treated FFT was over-sheared using a custom-built shearing device. The shearing device consisted of a stationary 25.6 L outer cup and 23.1 L inner cylindrical bob which was rotated within the cup at a speed and duration equivalent to a shear energy of 1500 kJ/m^3. A schematic of the shearing device is available in Li et al. (2022b). Following coagulation/flocculation and shearing of the PASS-treated FFT, all of the untreated and PASS-treated FFT was transported to the University of Alberta and stored at 4°C until use. Prior to placing the FFT in columns, the 20 L pails of untreated FFT were combined and homogenized (mixed) in a 200 L container using a drill with a helical ribbon impeller for roughly 2 min. The 20 L pails of treated FFT were homogenized in the same manner. Transport and homogenization of the tailings were necessary but would have imparted additional shear energy to tailings.

4.2.2 Column Set-up

A total of 64 columns were constructed as part of this study (see Figure 4-1). All columns were set up in June 2021 and monitored until November 2022 (540 d). Sixteen of the columns had a volume of 19 L and were set up in duplicate, while the other 48 columns were roughly 1 L and set up in

triplicate. Table 4-1 presents a summary of the 64 columns, as well as the factors tested as part of this study (size, tailings treatment, temperature, hydrocarbon amendments, and CO_2 addition). Each column contained either untreated or PASS-treated FFT, and a BCR freshwater cap. The initial tailings-to-water ratio in all columns was 2.5:1 (by volume), as previous experiments found that this ratio provided sufficient volumes of both tailings and water for sample collection. On Day 0, the volume of tailings, BCR water, and headspace, respectively, in each column was as follows: 12.5 L, 5 L, and 1.5 L for 19 L columns, and 0.75 L, 0.3 L and 0.13 L for 1 L columns. All columns were kept in the dark and under black tarps, except during sample collection, to mimic pit lake tailings conditions. Anaerobic conditions were maintained in each column for the duration of the study, which mimics the anaerobic conditions of BML FFT (Dompierre et al. 2016).

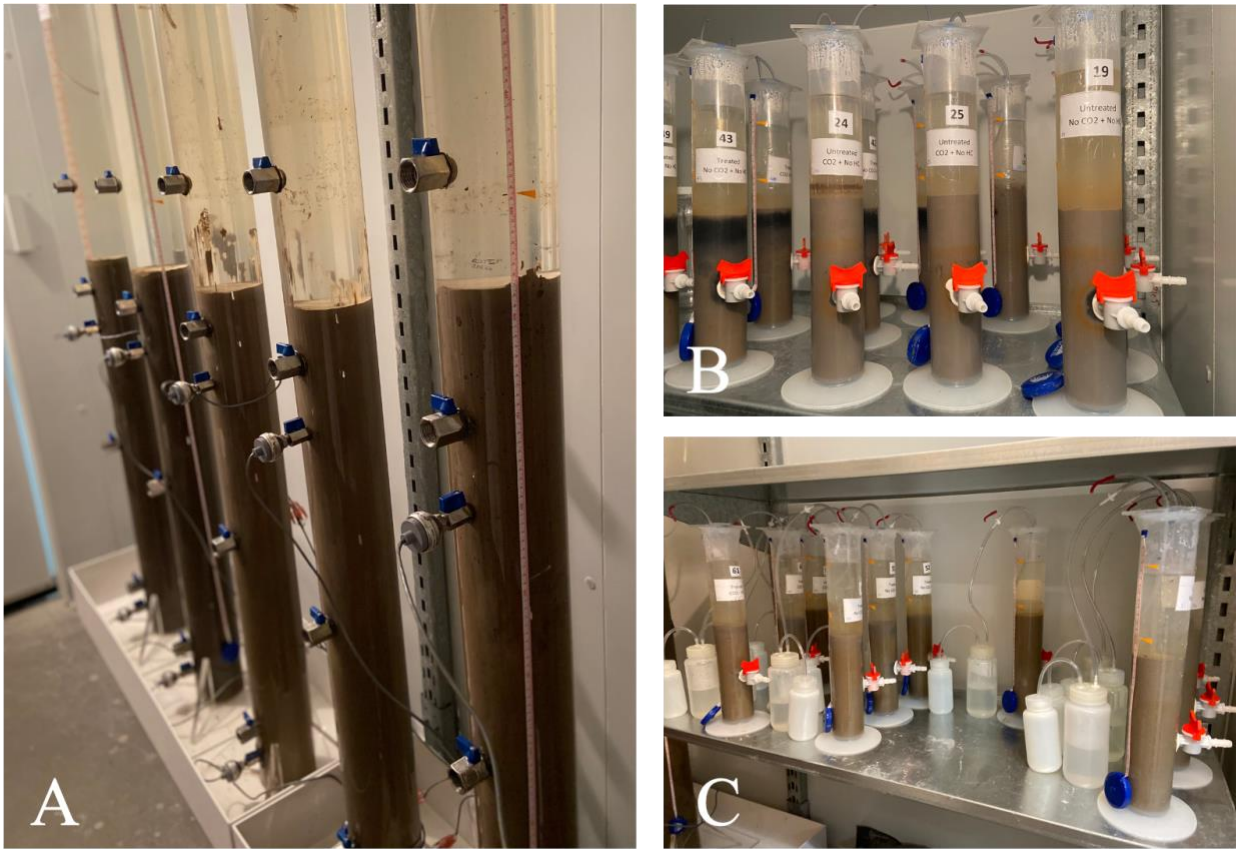

Figure 4-1. Photo of A: 19 L columns stored in 10°C cooler, B: 1 L columns stored in 10°C cooler, and C: 1 L hydrocarbon amended columns with gas collection system stored in 10°C cooler. Photos taken on Day 30. Note in Figure 4-1 B that the black colored tailings in the left columns are PASS-treated tailings.

Table 4-2. Summary of 64 columns set up for pit lake experiments. 19 L columns (Big, B) were set up in duplicate, 1 L columns (Small, S) were set up in triplicate.

Column	Size		Tailings Treatment		Temperature		Amendment	
	1 L	19 L	Untreated	PASS-treated	10°C	20°C	Hydrocarbons (HC)	CO_2
FFT B10		✓	✓		✓			
FFT B20		✓	✓			✓		
FFT B10 + HC		✓	✓		✓		✓	
FFT B20 + HC		✓	✓			✓	✓	
FFT S10	✓		✓		✓			
FFT S20	✓		✓			✓		
FFT S10 + HC	✓		✓		✓		✓	
FFT S20 + HC	✓		✓			✓	✓	
FFT S10 + CO_2	✓		✓		✓			✓
FFT S20 + CO_2	✓		✓			✓		✓
FFT S10 + HC + CO_2	✓		✓		✓		✓	✓
FFT S20 + HC + CO_2	✓		✓			✓	✓	✓
PASS B10		✓		✓	✓			
PASS B20		✓		✓		✓		
PASS B10 + HC		✓		✓	✓		✓	
PASS B20 + HC		✓		✓		✓	✓	
PASS S10	✓			✓	✓			
PASS S20	✓			✓		✓		
PASS S10 + HC	✓			✓	✓		✓	
PASS S20 + HC	✓			✓		✓	✓	
PASS S10 + CO_2	✓			✓	✓			✓
PASS S20 + CO_2	✓			✓		✓		✓
PASS S10 + HC + CO_2	✓			✓	✓		✓	✓
PASS S20 + HC + CO_2	✓			✓		✓	✓	✓

Materials used to construct each 19 L column were as follows: 1.85 m cast acrylic tube with an inner diameter of 11.4 cm and a wall thickness of 0.6 cm (Johnston Industrial Plastics Ltd., Edmonton, CA), 1.3 cm thick cast acrylic sheets for the base and lid (Plastics Plus Ltd., Edmonton, CA), and four sampling ports made up of 1.9 cm stainless steel mini ball valves (316, FxM NPT,

Direct Material, Irving, US). Materials used to construct each 1 L column were as follows: 1 L polypropylene Fisherbrand^{TM} graduated cylinder (3004001000, Mexico) (41.9 cm tall and 6.1 cm inner diameter), 1.3 cm thick cast acrylic sheet for the lid (Plastics Plus Ltd., Edmonton, CA), and one sampling port made up of a 1.3 cm two-way ball valve with a 10 mm hose barb. Each lid had a septum (CLS-4209-14, butyl rubber, Chemglass) for headspace sampling and vinyl tubing (0.3 cm inner diameter, Fisher Scientific, Pittsburgh, US) for water cap sampling. Because it was anticipated that tailings amended with hydrocarbons would generate more biogenic gas than unamended tailings, columns containing hydrocarbon amended tailings had additional tubing connecting the headspace to a series of gas collection bottles. The gas collection system provided additional anaerobic headspace to these columns, ensuring that pressure did not build up in the column headspace. After the columns were filled with tailings and a water cap, the lids were sealed to the columns with silicon and then flushed with nitrogen gas to create anaerobic conditions and to capture biogenic gas emissions. Headspace pressure was measured every 60 to 90 d to ensure columns were not leaking and that anaerobic conditions were maintained.

4.2.2.1 Accelerating Microbial Activity and Microbially-derived Processes

Microbial communities indigenous to oil sands tailings contribute to iron, sulfur, and carbon cycling in tailings deposits, which can lead to biogenic gas emissions (of CO_2, CH_4, and reduced sulfur compounds (RSCs) such as H_2S), mineral transformation and precipitation (such as $FeS_{(s)}$ formation), degradation of diluents and other organic contaminants, and bioconsolidation (Burkus et al. 2014; Clark et al. 2021; Dompierre et al. 2016; Gee et al. 2017; Siddique et al. 2006, 2007, 2011, 2014a, 2015, 2020; Small et al. 2015). However, these microbially-derived processes are often slow as it can take decades for microbial communities to develop (Foght et al. 2017). As such, three methods were used to accelerate microbial activity and/or microbially-derived processes in the laboratory: temperature, hydrocarbon amendments, and CO_2 addition.

Temperature strongly influences microbial activity, including methanogenesis and sulfate reduction, and temperatures above or below an optimum range can slow microbial metabolism (Nozhevnikova et al. 1997; Pavlostathis and Zhuang 1991; Wong et al. 2015). A temperature of 20°C was selected to enhance the microbial activity in FFT based on previous experience and research, including that of Kuznetsov et al. (2023), Siddique et al. (2014a), and Wong et al. (2015).

The selection of a control temperature was based on field measurements of BML FFT which were reported by Tedford et al. (2019) and Dompierre et al. (2016). Tedford et al. (2019) found that temperatures near the mudline range from 3 to 15°C throughout the year, while Dompierre et al. (2016) reported an average temperature of 12.9°C below the mudline during the summer months. As such, a control temperature of 10°C was selected to reflect the average annual temperature of FFT in BML, though this temperature will not necessarily reflect the temperature of the BML water cap, which can vary from 0 to >20°C depending on the season (Tedford et al. 2019). Columns stored at 10°C were placed in a McKinley & Taylor cooler (Edmonton, CA) which was regulated using an electronic temperature controller (Johnson Controls Inc., A419, Milwaukee, US), while the other columns were stored at room temperature (20°C). Temperatures in both the cooler and laboratory fluctuated within ± 2°C of their desired value, though on average the temperatures were 10°C and 20°C in the cooler and laboratory, respectively.

Hydrocarbons were selected as carbon sources to accelerate microbial activity because numerous studies have shown that microorganisms indigenous to oil sands tailings are capable of hydrocarbon degradation (Gee et al. 2017; Mohamad Shahimin and Siddique 2017a,b; Mohamad Shahimin et al. 2021; Siddique et al. 2006, 2007, 2011, 2015, 2020; Stasik and Wendt-Potthoff 2014; Tan et al. 2015). Laboratory studies of oil sands tailings have shown that a broad range of hydrocarbons commonly found in naphtha and paraffinic diluents, including BTEX (benzene, toluene, ethylbenzene, and xylene) compounds, n-alkanes, iso-alkanes, and cycloalkanes, can be degraded through methanogenic pathways (Mohamad Shahimin and Siddique 2017a,b; Mohamad Shahimin et al. 2021; Siddique et al. 2006, 2007, 2011, 2015, 2020; Tan et al. 2015). Fewer studies have been conducted on hydrocarbon degradation by SRB in oil sands tailings, though they are capable of degrading at least some components of naphtha diluent, including n-alkanes (Gee et al. 2017; Tan et al. 2015). The following mixture of BTEX compounds, n-alkanes, and iso-alkanes was selected for this research based on the work of Kuznetsov et al. (2023): 150 ppm of toluene (≥99.9%, Sigma-Aldrich, St. Louis, US), 150 ppm of xylenes (50 ppm of o-xylene (99%, Alfa Aesar, Ottawa, CA), 50 ppm of m-xylene (>99%, TCI AMERICA, Portland, US), and 50 ppm of p-xylene (99%, Alfa Aesar, Ottawa, CA)), 500 ppm of n-octane (99+%, Thermo Fisher Scientific, Fair Lawn, US), 500 ppm of n-decane (99.5%, Fisher Scientific, Fair Lawn, US), 500 ppm of 2-methylpentane (≥99%, Sigma Aldrich, St. Louis, US), and 500 ppm of 3-methylhexane (99%,

ChemSampCo, Dallas, US). The mixture of hydrocarbons was injected into the tailings as a free phase and homogenized (mixed by hand for roughly 1 min), prior to placing the tailings in the columns.

CO_2 gas (Praxair, Edmonton, CA) was added to tailings in select columns on Day 0 to mimic the bioconsolidation processes reported in an FFT column study (Siddique et al. 2014a) and in field investigations of BML (Dompierre et al. 2016). Only 1 L columns were treated with CO_2 as it was hypothesized that of the three factors used to enhance microbial activity and microbially-derived processes (temperature, hydrocarbons, and CO_2), this factor would have the least impact on biogeochemical and geotechnical behavior of tailings. Prior to placing tailings in the columns (and prior to adding hydrocarbon amendments, if applicable), CO_2 gas was bubbled into tailings using an air stone bubble diffuser at a rate of 0.1 L/min. Approximately 0.71 L of CO_2 was bubbled through each of the 24 0.75 L samples of tailings. This CO_2 volume was selected based on the maximum theoretical amount of CO_2 that would be generated from complete degradation of the hydrocarbon amendments.

4.2.3 Column Monitoring and Measurements

4.2.3.1 Geotechnical Parameters

Day 0 samples of the untreated and PASS-treated FFT were measured for solids and water content, bitumen content, yield stress, and elemental composition of the solids. The untreated FFT was also analyzed for PSD to determine the SFR and median particle diameter (D_{50}), as well as MBI which indicates clay content and activity. PSD and MBI were not measured independently in PASS-treated FFT because it was assumed that these parameters were the same as in untreated FFT. Tailings samples that were collected from the 64 columns on Day 540 were analyzed for solids and water content. In addition, tailings collected from the 19 L columns on Day 540 were analyzed for bitumen content and elemental composition of the solids in order to evaluate the precipitation of sulfur species.

Solids and water content were measured using oven analysis, which involves weighing and drying tailings samples in a 105°C oven for 24 hours (see also ASTM 2019). The Dean-Stark procedure was conducted at NAIT to determine bitumen content (Dean and Stark 1920). Briefly, a round-

bottom boiling flask was used to heat toluene, which contacted an FFT sample contained in a thimble. The subsequent toluene/bitumen mixture was separated from the water in the FFT through a reflux condenser, while the solids remained in the thimble. The extraction continued for at least 6 hours, after which the bitumen content was determined by placing 5 mL of the toluene/bitumen mixture on a glass fibre filter paper and allowing it to air dry for 15 min. The bitumen content was calculated from the mass of bitumen left on the filter paper.

Because untreated FFT has a very soft consistency, yield stress was determined using a Brookfield DV3T rheometer (CAN-AM Instruments Ltd., Oakville, CA). Samples were sheared at a rate of 0.1 rpm using V-71 and V-72 spindles (Brookfield Engineering Labs Ltd., Middleboro, US). The elemental composition of the solids was determined using X-ray fluorescence (XRF) which was conducted at NAIT. XRF samples were run as slurries with a cellulose binder, Celleox, using an S8 Tiger Wavelength Dispersive XRF Spectrometer (Bruker AXS, US).

PSD was determined by hydrometer tests, which were performed following the procedure outlined in ASTM D79828 (2017). Briefly, 175 g samples of untreated FFT were mixed with 125 mL of dispersant (4% sodium metaphosphate) before being transferred to a 1 L graduated cylinder. Distilled water was added to the mixture (up to the 1 L mark) and the cylinder was capped and mixed for 1 min. Immediately after mixing, a 152H hydrometer (Fisherbrand, Buena, US) was placed in the cylinder and the meniscus reading was recorded. The temperature of the solution was also recorded at that time. Readings were taken at 15 sec, 30 sec, 1 min, 2 min, 4 min, 8 min, 15 min, 30 min, 1 hr, 2 hr, 4 hr, 8 hr, and 24 hr. Temperature corrections, meniscus corrections, and zero corrections (which account for the effect of the dispersing agent on hydrometer readings) were applied to all hydrometer readings.

MBI was conducted on untreated FFT samples at NAIT following the procedure outlined in Kaminsky (2014). Briefly, the sample was dispersed, acidified, and then titrated with methylene blue. The endpoint was determined using the halo method, wherein a drop of the titrated sample on filter paper has a blue halo, indicating an excess of methylene blue (Kaminsky 2014). Generally, the more titrant that is required to reach the end point, the higher the MBI value.

Settlement of the FFT-water interface was continuously measured throughout the study and used to calculate NWR. NWR indicates consolidation behavior of tailings and can account for the water added to the tailings during chemical treatment processes. NWR was calculated using Equation 4-1 below:

$$NWR\ (\%)\ =\ \frac{Vwr - Vp}{V_w} x\ 100\% \qquad (4\text{-}1)$$

where V_{wr} is the volume of water released from the FFT (which was calculated from interface settlement measurements), V_p is the volume of solution added to FFT during chemical treatment (see subsection 4.2.1), and V_w is the volume of water in the untreated FFT on Day 0.

4.2.3.2 Water Chemistry Parameters

Water cap samples were collected from all 64 columns every 60 d. Water cap samples were analyzed for pH, major cations (Na^+, K^+, Ca^{2+}, Mg^{2+}, Fe, and Al), major anions (Cl^-, SO_4^{2-}, F^-, NO_3^-, NO_2^-, and PO_4^{3-}), aqueous total sulfide species (H_2S, HS^-, S^{2-}), dissolved organic carbon (DOC), total alkalinity (from which bicarbonate (HCO_3^-) concentrations were calculated), and ammonia/ammonium (NH_3/NH_4^+). Tailings samples were collected every 120 d from the 19 L columns only. Due to the small volume of tailings in the 1 L columns, tailings samples were only collected and analyzed on Day 540. Tailings samples were centrifuged at 5000 rpm for 20 min to separate the pore water from the tailings solids. Pore water was analyzed for pH, major cations, major anions, total aqueous sulfide species, DOC, total alkalinity, and ammonia/ammonium. All of these water chemistry parameters were also measured in Day 0 samples of BCR water, FFT pore water, and PASS-treated FFT pore water.

The pH of the water cap and tailings was periodically measured throughout the study through the column sampling ports and/or in the collected samples. pH was measured using an E-135M pH probe (Gain Express) for 19 L columns and a Thomas Scientific micro pH electrode (Swedesboro, US) for 1 L columns, combined with a Thermo Scientific Orion Dual Star pH/ISE Benchtop. Major cations were measured in 0.45 μm nylon filtered samples at the University of Alberta's NRAL. NRAL used a Thermo iCAP6300 Duo ICP-OES (Thermo Fisher Corp., Cambridge, UK) to measure a standard array of elements which included the previously mentioned cations. Initially,

a Dionex 2100 Ion Chromatography System (Thermo Scientific Bannockburn, US) was used to measure major anions (Cl^-, SO_4^{2-}, F^-, NO_3^-, NO_2^-, and PO_4^{3-}) in 0.22 µm filtered samples water samples. However, the instrument had to undergo maintenance for an extended period in 2022. As such, water samples collected on Day 360 and onwards were instead analyzed for Cl and SO_4-S at NRAL using a colormetric autoanalyzer (Thermo Gallery Plus Beermaster AutoAnalyzer, Thermo Scientific, Vantaa, FI). Day 0 samples of BCR water, FFT pore water, and PASS-treated FFT pore water were also measured for Cl and SO_4-S at NRAL using the colormetric autoanalyzer to confirm that the measurements were consistent.

Total sulfide species were measured in water samples following the USEPA Methylene Blue Method (HACH Method 8131) using a HACH DR 900 Multiparameter Portable Colorimeter (Loveland, US) and a HACH sulfide reagent set (Loveland, US). Total sulfide species is time-sensitive measurement because sulfide species may oxidize when exposed to air. Water cap samples from the 1 L columns were only analyzed for total sulfide species on Day 540 because of the large sample volume required for this analysis, while water cap samples from the 19 L columns were analyzed for total sulfide species every 60 d. DOC was measured in 0.45 µm filtered samples water samples using a Shimazdu Model TOC-L_{CPH} (Kyoto, JP) and the non-purgeable organic carbon method, which captures the non-volatile DOC content of the samples. Total alkalinity and bicarbonate were measured using an autotitrator (Metrohm Eco Titrator, Herisau, CH) and 0.02 N H_2SO4 titrant. Total alkalinity was calculated by setting the endpoint to a pH of 4.5 (note that carbonate alkalinity was not applicable to these water samples as its endpoint is a pH of 8.3 which is greater than the pH of the samples). The HACH DR 900 Multiparameter Portable Colorimeter (Loveland, US) was also used to measure ammonia and ammonium (as NH_3-N), following the AmVer™ Salicylate Test 'N Tube™ Method (Hach Method 10031) and using the HACH AmVer™ high range ammonia nitrogen Test 'N Tube™ reactor tubes and reagent set (London, CA).

4.2.3.3 Microbial Activity and Communities

Microbial activity was monitored throughout the study by measuring biogenic gas generation (H_2S, CO_2, and CH_4) and collecting tailings samples for DNA extraction and sequencing. The hydrocarbon content of the tailings was also measured on Day 0 and again on Day 540 (in the 19

L columns only) to confirm that the hydrocarbons added to amended columns on Day 0 were consumed.

Gaseous H_2S was measured in the 19 L columns on Day 180 and Day 360 at AGAT Laboratories (Calgary, CA). AGAT Laboratories used gas chromatography and a sulfur chemiluminescence detector (GC-SCD) to measure headspace H_2S at concentrations greater than 0.1 ppmv. Headspace CO_2 and CH_4 were measured in all columns every 60 to 90 d. CO_2 was measured using an Agilent 7890+ gas chromatograph (Santa Clara, US) and a thermal conductivity detector (GC-TCD) (Agilent HP-PLOT/Q column: 30 m x 320 µm x 0.2 µm). The oven and injection port were kept at 50°C and helium was used as the carrier gas at a flow rate of 4 mL/min. The detector temperature was set to 200°C and the flow rate of the makeup gas (helium) was 5 mL/min. The total run time was 1.65 min. Headspace samples were manually injected at a volume of 0.1 mL. CH_4 was measured using the Agilent 7890+ gas chromatograph and a flame ionization detector (GC-FID) (Agilent HP-5MS column: 30 m x 250 µm x 0.25 µm). The oven and injection port were kept at 80°C and helium was used as the carrier gas at a flow rate of 1.5 mL/min. The detector temperature was set to 300°C. The flow rate of the makeup gas (N_2) was 40 mL/min, air flow was 350 mL/min, and H_2 flow was 35 mL/min. The total run time was 1.40 min. Headspace samples were manually injected at a volume of 0.1 mL.

Tailings samples for DNA extraction and 16S sequencing were collected from 19 L columns on Days 120, 240, 360, and 540. Samples were collected in 1.5 mL microcentrifuge tubes and centrifuged twice at 5000 rpm for 5 min at 4°C (water was removed from the tubes after each round of centrifuging). DNA extractions were conducted using the FastDNA™ Spin Kit for Soil (MP Biomedical, Solon, US) following the protocol suggested by the manufacturer. After DNA extractions, duplicate samples were pooled before being sent to the Molecular Biology Service Unit (MBSU) at the University of Alberta for PCR amplification of the V6 to V8 regions of bacterial and archaeal 16S rRNA genes, using universal primers 926F (AAACTYAAAKGAATWGRCGG) and 1392R (ACGGGCGGTGWGTRC) (An et al. 2013). Amplicon sequencing was performed on the Illumina MiSeq instrument at MBSU using the v3 600 cycle reagent kit (PE300, Cat# MS-102-3003, San Diego, US). The raw data was processed

using the MetaAmp pipeline and SILVA database (Dong et al. 2017). A 97% identity cut-off was assigned to the reads and a 300 bp amplicon length was used.

Hydrocarbon content of the tailings was determined using a liquid extraction and headspace gas chromatography – mass spectrometry (GC-MS) protocol developed by the Soil Chemistry and Environmental Microbiology Laboratory at the University of Alberta. During the liquid extraction, 1 mL of FFT was added to vials containing 5 mL of methanol. The vials were vortexed, shaken for 30 min at a low speed, and centrifuged at 1000 rpm for 20 min (or longer if necessary). The samples were then refrigerated at 4°C for several days, after which 0.5 mL of the methanol extract was added to vials containing 4.5 mL of salt solution. After vortexing, headspace in each vial was analyzed using the Soil Chemistry and Environmental Microbiology Laboratory's GC-MS (Thermo Fisher Scientific, Trace 1300 (GC) and ISQ (MS), TG-5MS capillary column 30 m x 250 μm) equipped with an autosampler (Thermo Fisher Scientific, TriPlus RSH). The vials were heated to 70°C and agitated for 1 min, after which 1 mL of headspace was injected into the GC port. The oven temperature was increased from 30 to 250°C and helium was used as the carrier gas at a flow rate of 1.2 mL/min. The samples' peak areas were compared to that of standards which consisted of varying concentrations of the hydrocarbon mixture detailed in subsection 4.2.2.1.

4.2.4 Statistical Analysis

Multi-factor analysis of variance (ANOVA) tests were performed using XLSTAT software in Microsoft Excel to indicate the statistical significance (at $\alpha = 0.05$) of differences in measurements of various geotechnical and biogeochemical parameters in the columns. ANOVA tests were conducted to evaluate the effects of column size, tailings treatment, temperature, hydrocarbon amendments, and CO_2 addition on geotechnical and biogeochemical behavior. All statistical analyses were performed using the Day 540 value of a measured parameter or the difference between the Day 540 and Day 0 values (if the Day 0 value of a parameter was different for each column). To evaluate the statistical significance of column size, tailings treatment, temperature, and hydrocarbon amendments, ANOVA tests were performed on 40 of the columns (excluding the 24 1 L columns with CO_2 addition). To evaluate the statistical significance of CO_2, ANOVA tests were performed again using only the 48 1 L columns. Any statistical significance noted in the Results section was based on Type III Sum of Squares, as interaction was expected between the

independent variables. All statistically significant factors for each parameter tested, along with F and p values, are available in Appendix B1, Table B-1.

4.2.5 Modeling

Slurry consolidation software FSConsol v3 (GWP Software Inc. 2007) was used to model the consolidation behavior of the FFT. FSConsol uses Gibson's finite strain theory, which accounts for large strain and non-linear properties, to evaluate one dimensional consolidation in slurries (Gibson et al. 1967). In FSConsol, hydraulic conductivity and compressibility are both expressed using the power law. The primary objective of consolidation modeling was to evaluate the effect of column size on NWR. Self-weight consolidation of untreated FFT was modeled using two different FFT deposit thicknesses and water cap heights, which correspond to the different heights of the materials in the 1 L and 19 L columns.

PHREEQC version 3.4.0-12927 (Parkhurst and Appelo 2013) was used to model the geochemistry in untreated and PASS-treated FFT pore water. The primary objective of using PHREEQC was to evaluate the effect of increases in pore water alkalinity and aqueous total sulfide species (generated through sulfate reduction) on water chemistry and precipitation/dissolution reactions. Both the PHREEQC (Parkhurst and Appelo 2013) and WATEQ4F (Ball and Nordstrom 1991) databases were used to confirm the geochemical changes that occurred as a result of sulfate reduction.

4.3 Results and Discussion

4.3.1 Initial Characterization of Materials

Initial characterization data for the tailings and fresh water used in this study is presented in Tables 4-2 and 4-3. Table 4-2 presents geotechnical data for the untreated FFT and PASS-treated FFT. Table 4-3 presents water chemistry data for the pore water in untreated FFT and PASS-treated FFT, as well as the BCR water. The PASS treatment process resulted in a lower initial solids content for the PASS-treated FFT (30.1 ± 0.0%) compared to that of the untreated FFT (33.5 ± 0.7 wt%), as seen in Table 4-2. This is because of the polymer solution added during PASS treatment, which increased the water content of the tailings. The bitumen content of the PASS-treated FFT was also slightly lower than that of the untreated FFT and this bitumen loss is likely a result of bitumen adhering to coagulation/flocculation and conveyance equipment during the PASS

treatment process. Yield stress was low in both untreated and PASS-treated FFT and the difference in measurements for the two types of tailings is expected to be primarily a result of shearing during treatment and/or homogenization of the tailings.

Table 4-2. Geotechnical characterization of untreated FFT and PASS-treated FFT on Day 0. Results are presented as average ± standard deviation of replicates (three or more). Measurements were taken prior to hydrocarbon amendments or CO_2 addition, if applicable. Modified from Cossey et al. (2021b, 2022).

Geotechnical Parameters	Untreated FFT	PASS-treated FFT
Solids content (oven analysis, wt%)	33.5 ± 0.7	30.1 ± 0.0
Water content (oven analysis, wt%)	66.5 ± 0.6	69.9 ± 0.0
Bitumen content (Dean-Stark, wt%)	1.0 ± 0.0	0.8 *
Yield stress (Pa)	10.6 ± 0.8	7.9 ± 0.1
Sand to fines ratio (SFR)	0.07 ± 0.02	**
Median particle diameter (D_{50}) (μm)	1.4 ± 0.1	**
Methylene blue index (MBI) (meq/100 g)	12.2 ± 0.6	**
Sulfur content (solid phase, %)	0.2 ± 0.0	0.2 ± 0.0

** Parameter could not be measured in multiples because of sample volume limitations*

*** Parameter not measured in PASS-treated FFT; assumed to be the same as untreated FFT*

The primary impact of PASS treatment on the initial water chemistry of the FFT was a 314.5 mg/L increase in sulfate and a 106.1 mg $CaCO_3$/L decrease in alkalinity, both of which are a result of alum addition. The decrease in alkalinity and the lack of detectable aluminum in the PASS-treated FFT pore water is consistent with $Al(OH)_{3(s)}$ formation in these tailings. Theoretically, PASS treatment should also decrease the tailings pH, though that did not happen in this instance. This may be partly due to the FFT pore water that was used in the polymer solution during PASS treatment (see subsection 4.2.1), which had a higher pH and higher concentrations of some ions (Na^+, Ca^{2+}, Mg^{2+}, Cl^-) than that of the untreated FFT used in this study. This also explains the higher concentrations of these ions in PASS-treated FFT relative to untreated FFT. BCR water had a higher pH than the untreated and PASS-treated FFT, but lower concentrations for all other parameters listed in Table 4-3. Table 4-3 does not include concentrations of the anions F^-, NO_3^-, NO_2^-, and PO_4^{3-} (which were part of the suite of major anions tested, as per subsection 4.2.3.2)

because their concentrations were low and/or they did not have a substantial impact on the observed biogeochemical and geotechnical behavior of the tailings.

Table 4-3. Water chemistry characterization of untreated FFT, PASS-treated FFT, and BCR water on Day 0. Results are presented as average ± standard deviation of replicates (three or more). Measurements were taken prior to hydrocarbon amendments or CO_2 addition, if applicable. Modified from Cossey et al. (2021b, 2022).

Water Chemistry Parameters	Untreated FFT	PASS-treated FFT	BCR Water
pH	7.3 ± 0.1	7.4 ± 0.2	8.4 ± 0.1
Sodium, Na^+ (mg/L)	230.0 ± 11.0	241.2 ± 2.4	43.0 ± 0.5
Potassium, K^+ (mg/L)	16.9 ± 0.5	17.5 ± 0.2	3.42 ± 0.3
Calcium, Ca^{2+} (mg/L)	60.7 ± 0.5	85.2 ± 2.4	23.6 ± 0.4
Magnesium, Mg^{2+} (mg/L)	29.5 ± 1.9	39.7 ± 0.7	11.7 ± 0.5
Iron, Fe (mg/L)	0.019 ± 0.007	0.017 ± 0.006	0.012 ± 0.004
Aluminum, Al (mg/L)	BDL*	BDL*	BDL*
Chloride, Cl^- (mg/L)	14.8 ± 2.6	35.7 ± 0.6	7.46 ± 0.3
Sulfate, SO_4^{2-} (mg/L)	317.4 ± 9.6	631.9 ± 21.4	21.7 ± 0.9
Sulfide species, H_2S, HS^-, S^{2-} (mg/L)	0.0 ± 0.0	0.0 ± 0.0	0.0 ± 0.0
Dissolved organic carbon (DOC) (mg/L)	54.8 ± 3.1	53.2 ± 0.2	19.2 ± 0.40
Total alkalinity (mg $CaCO_3$/L)	415.8 ± 9.0	309.7 ± 4.2	148.8 ± 10.2
Bicarbonate, HCO_3^- (mg/L)	510.6 ± 10.9	377.8 ± 5.2	181.6 ± 11.6
Ammonia, NH_3-N (mg/L)	0.0 ± 0.0	0.0 ± 0.0	0.0 ± 0.0

**BDL indicates below detection limit*

All values presented in Tables 4-2 and 4-3 were taken prior to any hydrocarbon or CO_2 amendments that were made to the tailings. CO_2 addition, and subsequent dissolution, lowered the initial pH of the untreated and PASS-treated FFT to 7.0 ± 0.0 and 7.0 ± 0.1, respectively. Hydrocarbon amendments had no impact on the initial pH of the tailings, nor did they substantially impact the initial DOC concentration of the pore water because the DOC method only captured non-volatile organic compounds. Further, it is likely that the hydrocarbons mixed with (became soluble in) the bitumen phase and thus could not be separated from solids/bitumen during centrifugation. Additional analysis (such as saturate, aromatic, resin, and asphaltene (SARA) analysis) is necessary to confirm that the hydrocarbons mixed with the bitumen phase.

4.3.2 Geotechnical Parameters

NWR from the tailings in each column over 540 d is shown in Figure 4-2 (19 L columns in Figure 4-2A; 1 L columns in Figure 4-2B). All PASS-treated columns started with a negative NWR which accounts for the water added to the PASS-treated tailings during coagulation/flocculation. A positive NWR indicates the percentage of pore water that was released from the tailings. Of the five factors tested (size, treatment, temperature, hydrocarbon amendments, and CO_2 addition), size had the most influence (highest F-value) on NWR ($p < 0.0001$), followed by treatment ($p < 0.0001$). The 1 L columns had a higher NWR rate between Days 0 and 60 compared to the 19 L columns. However, after Day 60, NWR in all 1 L columns plateaued whereas the 19 L columns continued to undergo self-weight consolidation and release pore water. By Day 540, NWR was higher in all 19 L columns than in comparable 1 L columns. For example, the average NWR in PASS B10 columns on Day 540 was 34.8% whereas NWR in PASS S10 columns on Day 540 was 18.7%.

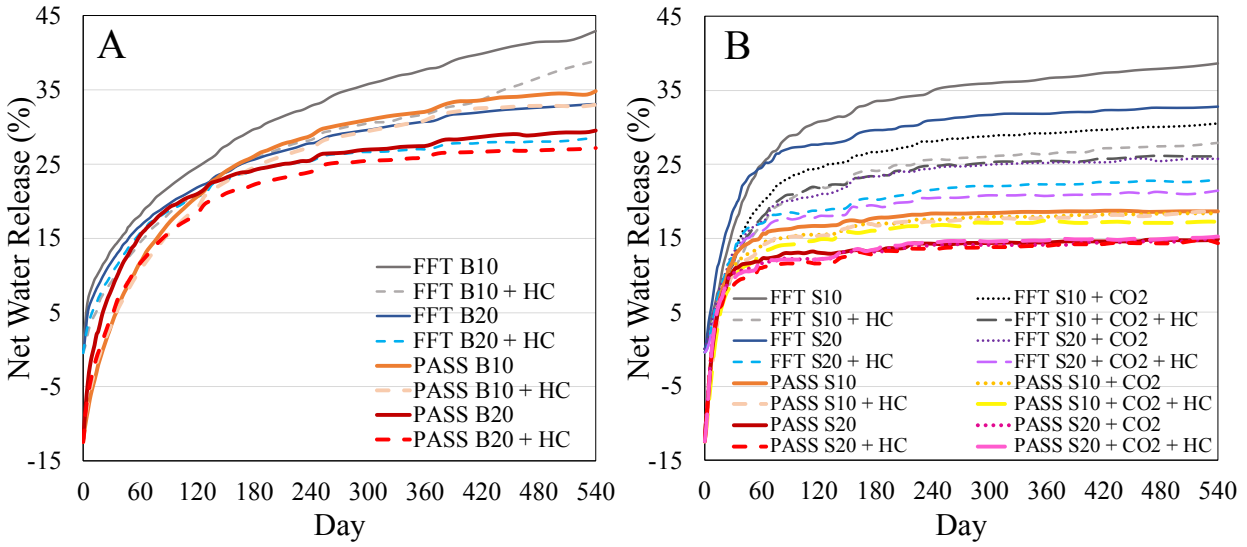

Figure 4-2. Net water release in (A) 19 L columns and (B) 1 L columns over 540 d. Results are averages of duplicate (A) and triplicate (B) columns. Labels B or S refer to Big (19 L) or Small (1 L) columns; 10 or 20 refer to 10°C or 20°C storage temperature; CO2 and HC refer to CO_2 and hydrocarbon amended tailings.

The self-weight consolidation of untreated FFT deposited at two different thicknesses (which correspond to the 19 L and 1 L columns) was modeled in FSConsol. Results of the FSConsol modeling (see Appendix B2) agree with the NWR trends seen in Figure 4-2 as both modeling and

experimental results show that tailings in the 1 L columns undergo rapid self-weight consolidation and water release while tailings in the 19 L columns undergo long-term settlement and self-weight consolidation and continuous water release. Because NWR trends are consistent with the results of FSConsol modeling, the primary reason for the different consolidation behaviors is that the excess pore water pressure (Appendix B2, Figure B-2) and distance for pore water to travel (drainage path) was smaller in the 1 L columns than in the 19 L columns. The 19 L columns had a higher total stress (and excess pore water pressure) and longer drainage pathway, and were therefore slower to consolidate, though tailings in these columns achieved a higher effective stress (Appendix B2, Figure B-3) and solids content (Appendix B2, Figure B-4) overall.

Smooth column walls may have acted as preferential flow paths in all 64 columns because permeability at the column walls was presumably greater than permeability in the center of the columns (Comiti and Renaud 1989; Sentenac et al. 2001). Because the 1 L columns had a larger column surface area per litre of tailings (639 cm^2/L tailings) than the 19 L columns (350 cm^2/L), the 1 L columns may have had more preferential flow paths than the 19 L columns. The FSConsol model does not account for column wall effects or short circuiting and as such, it is possible that preferential flow paths also contributed to the faster NWR seen in the 1 L columns, as suggested previously by Cossey et al. (2022). However, the primary reason for the difference in consolidation behavior is believed to be the deposit thicknesses.

The factor with the second highest influence on NWR was treatment, though rather than improving NWR, PASS treatment lowered NWR in the columns. Previous research found that similarly flocculated tailings had higher hydraulic conductivities than untreated tailings (Wilson et al. 2018; Znidarcic et al. 2016), which should increase the rate of consolidation and NWR in flocculated tailings. However, flocculation performance depends on several factors including slurry properties, type and dosage of flocculant, flocculant injection rate, premixing of the FFT prior to treatment, mixing during treatment, and geometry of the mixer (Li et al. 2021). It is possible that the additional shear energy applied to both the untreated and PASS-treated FFT during homogenization and transport to the University of Alberta contributed to the poor flocculation performance of PASS-treated FFT. The FFT was also purposely underdosed in this study to reduce the mobility of DOC. However, even underdosed flocculated tailings have been shown to have

higher hydraulic conductivities than untreated tailings (Znidarcic et al. 2016). Further, any combination of under, optimal, or over flocculant dosing and under, optimal, or over mixing of FFT has previously been found to improve consolidation and settlement relative to untreated FFT (Znidarcic et al. 2016 as cited in Amoako 2020). The below-optimal flocculation performance of the PASS-treated FFT may be partly due to the high clay content of the tailings (MBI of 12.2 meq/100 g), though there are numerous other slurry properties and treatment conditions that may have contributed to the low NWR (Li et al. 2021). This highlights the challenges in achieving optimal flocculation performance, even in a controlled laboratory setting.

NWR was also impacted by temperature ($p < 0.0001$), hydrocarbon amendments ($p < 0.0001$), and CO_2 addition ($p < 0.0001$), but to a lesser extent than the other two factors (size and treatment) (see also Appendix B1, Table B-1). Temperature had a negative impact on NWR as columns stored at a higher temperature (20°C) had a lower NWR. Similarly, hydrocarbon amendments had a negative effect on NWR. Though hydraulic conductivity (and thereby consolidation) of the tailings should be higher at 20°C than 10°C, this was trumped by the effects of temperature and/or hydrocarbon amendments on microbial activity. Higher temperature and/or hydrocarbon amendments increased the generation of biogenic gases in the columns, some of which remained visibly trapped in the tailings. This created unsaturated pockets in the tailings and resulted in an underestimated NWR (which was calculated using interface settlement measurements rather than measurements of water cap thickness) in these columns. To account for unsaturated conditions in future experiments with microbially active tailings, NWR should be calculated using measurements of the cumulative volume of water (i.e. water cap thickness).

CO_2 addition also resulted in a lower NWR in some columns, which was not anticipated. It may be that the CO_2 treatment was not sufficient to have the desired effect of mimicking bioconsolidation through increases in carbonate mineral dissolution and ionic strength. The bioconsolidation of FFT reported by Siddique et al. (2014a) occurred after a pH drop of approximately 1.3, which was due to the dissolution of biogenic CO_2 over several months. In this study, the pH drop was roughly 0.3 due to a single application of exogenous CO_2. While the application of exogenous CO_2 should still have improved NWR, it was likely insufficient to create the desired effect. Siddique et al. (2014a) found that a single application of exogenous CO_2 slightly

improved consolidation of FFT, but their CO_2 application (in mL CO_2 per L tailings) was 2.5 times greater than that of this study and their pH drop was also greater. In this study, a larger pH drop was likely needed to improve carbonate mineral solubility and dissolution rates (Chou et al. 1989).

The solids content of tailings in each column after 540 d is shown in Figure 4-3 and is generally consistent with the NWR trends in Figure 4-2. The solids content of untreated FFT was consistently higher than comparable PASS-treated FFT on Day 540, and tailings in the 19 L columns generally achieved a higher solids content than tailings in 1 L columns. Column size was the most influential factor ($p < 0.0001$) on the increase in solids content over the 540 d, which agrees with NWR data. However, hydrocarbon amendments had a positive impact on solids content ($p = 0.001$) and hydrocarbon amended tailings achieved a slightly higher solids content (roughly 0.6 wt% on average) than comparable unamended tailings in most cases. This is not consistent with NWR trends but can be explained by the biogenic gases that were visibly trapped in the hydrocarbon amended columns, which led to underestimated NWR but did not impact solids content measurements. Microbial activity likely contributed to the higher solids content in the hydrocarbon amended columns, though the bioconsolidation pathway(s) seen in this study may be different than the pathway proposed by Siddique et al. (2014a) because the dominant microbial processes were different. Further, bioconsolidation had a more substantial impact on dewatering in the Siddique et al. (2014a) study, which may be because this study used tailings with different mineralogy and microbial communities, and Siddique et al. (2014a) used a more labile carbon source (canola meal hydrolysate). Moreover, the tailings used by Siddique et al. (2014a) had a lower clay content and were diluted to a lower solids content (23.4 wt%) than the tailings used in this study, making it easier for biogenic gases to escape the tailings and create transient physical channels for pore water to flow through.

Bitumen content of the tailings in the 19 L columns on Day 540 was most significantly influenced by hydrocarbon amendments ($p=0.031$) (see Appendix B3, Figure B-5), with hydrocarbon amended tailings having a higher bitumen content than comparable unamended tailings on Day 540 and Day 0 in most cases. This is presumably due to the decreased bitumen viscosity associated with hydrocarbon (solvent) addition (Zhang 2012), which may have enhanced the mixing and mobility of bitumen in hydrocarbon amended tailings. It is also possible that bitumen was

biodegraded in the unamended tailings due to lack of other carbon sources, though this would have occurred at very slow rates, if at all (Pannekens et al. 2021).

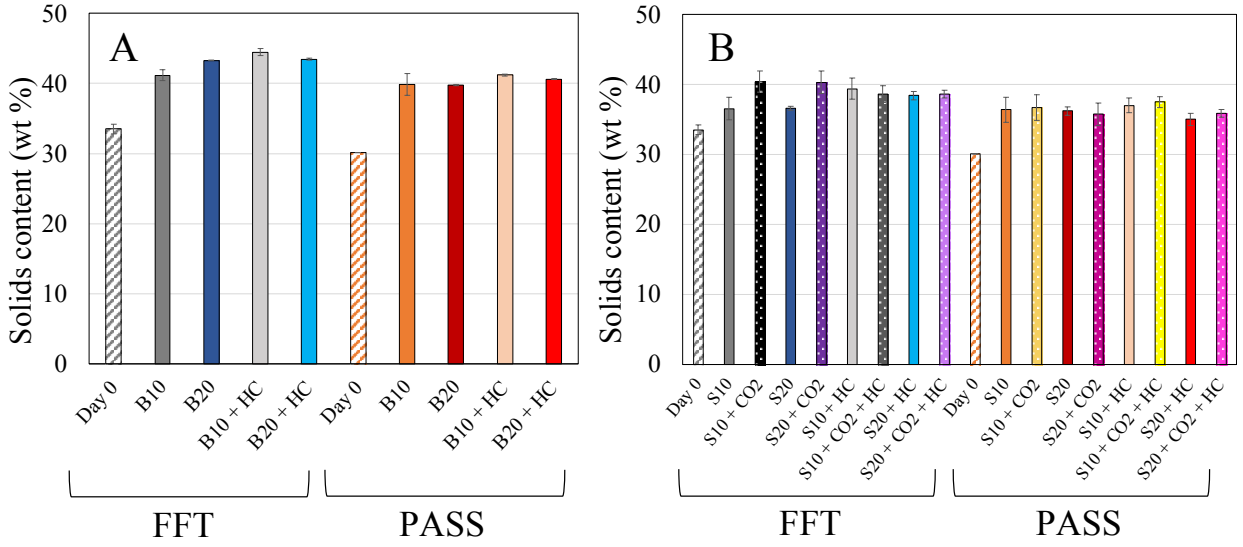

Figure 4-3. Solids content in (A) 19 L columns and (B) 1 L columns on Day 540. The solids content of FFT and PASS-treated FFT on Day 0 are provided for comparison. Results are averages of duplicate (A) and triplicate (B) columns and error bars represent one standard deviation of replicates. Labels B or S refer to Big (19 L) or Small (1 L) columns; 10 or 20 refer to 10°C or 20°C storage temperature; CO2 and HC refer to CO_2 and hydrocarbon amended tailings.

4.3.3 Pore Water Chemistry

Pore water sulfate concentrations decreased in all columns over 540 d, but especially in columns containing PASS-treated FFT and/or hydrocarbon amended tailings, as seen in Figure 4-4. The most influential factor on sulfate reduction in tailings pore water was hydrocarbon amendments ($p < 0.0001$) followed by PASS treatment ($p < 0.0001$). Column size, temperature, and CO_2 addition did not significantly influence sulfate concentrations. Sulfate was quickly reduced in the 19 L columns amended with hydrocarbons, as seen in Figure 4-4A. By Day 120, average pore water sulfate concentrations were reduced by 589 mg/L (over 93%) in PASS + HC columns and by 304 mg/L (96%) in FFT + HC columns. It is likely that the majority of the sulfate reduction in the 1 L columns amended with hydrocarbons (see Figure 4-4B) also occurred in the first 120 d of the study, if not earlier, though pore water sulfate concentrations were only measured on Day 540 in the 1 L columns. In unamended columns, sulfate reduction was slower and thus continued past Day 120. By Day 540, average pore water sulfate concentrations were reduced by 242 mg/L (38%)

in unamended PASS columns and by 71 mg/L (22%) in unamended FFT columns. Thus, PASS treatment increased sulfate reduction in the tailings, regardless of whether or not the tailings were amended with hydrocarbons. This is due to the higher concentration of electron acceptors available for SRB in PASS-treated tailings. Because hydrocarbon amendments led to such rapid and complete sulfate reduction relative to that of unamended tailings, it is suspected that the FFT used in this experiment had limited readily available carbon sources.

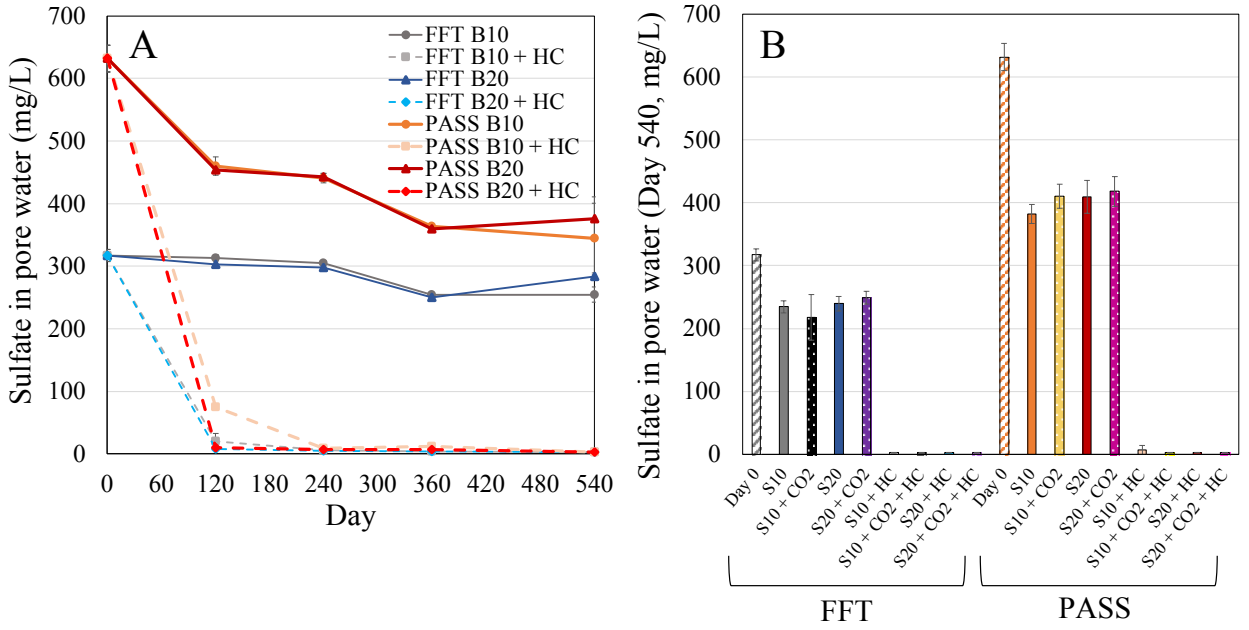

Figure 4-4. Pore water sulfate concentrations in (A) 19 L columns (Day 0 to 540) and (B) 1 L columns (Day 0 and Day 540 only). Results are averages of duplicate (A) and triplicate (B) columns and error bars represent one standard deviation of replicates. Labels B or S refer to Big (19 L) or Small (1 L) columns; 10 or 20 refer to 10°C or 20°C storage temperature; CO2 and HC refer to CO_2 and hydrocarbon amended tailings.

Reduced sulfur should be present in aqueous, gaseous, and/or solid phases throughout the columns as a result of the sulfate reduction seen in Figure 4-4. As such, concentrations of aqueous total sulfide species (H_2S, HS^-, S^{2-}) were measured in the pore water (Figure 4-5) and water cap (Appendix B3, Figure B-6) of each column. Based on the pH of the tailings and water caps (see Appendix B3, Figures B-7 and B-8), aqueous sulfide species in the columns consisted of both dissolved H_2S and HS^-. The highest concentration of total sulfide species was 2.0 mg/L (as S^{2-}) in PASS B20 + HC water caps on Day 540, though in general pore water concentrations of total sulfide species were higher than water cap concentrations. Sulfide species were present in the pore

water of all 19 L columns and all 1 L PASS-treated FFT columns (except PASS S10). Further, 19 L and 1 L columns containing PASS-treated FFT amended with hydrocarbons (PASS + HC) consistently had the highest concentrations of total sulfide species in the pore water ($p < 0.0001$), which agrees with the trends in Figure 4-4 and the high concentration of sulfate reduced in these columns (roughly 630 mg/L). At Suncor's Base Plant Mine, they are currently only applying their PASS treatment process to FFT that has not been impacted by residual diluent (i.e. tailings that do not include FTT). These findings suggests that if PASS treatment is applied to FTT, the additional hydrocarbons in FTT would likely lead to extensive sulfate reduction and the generation of reduced sulfur species and/or RSCs in a short period of time (though the bioavailability of hydrocarbons in the amended FFT in this experiment may be different than that of FTT in the field).

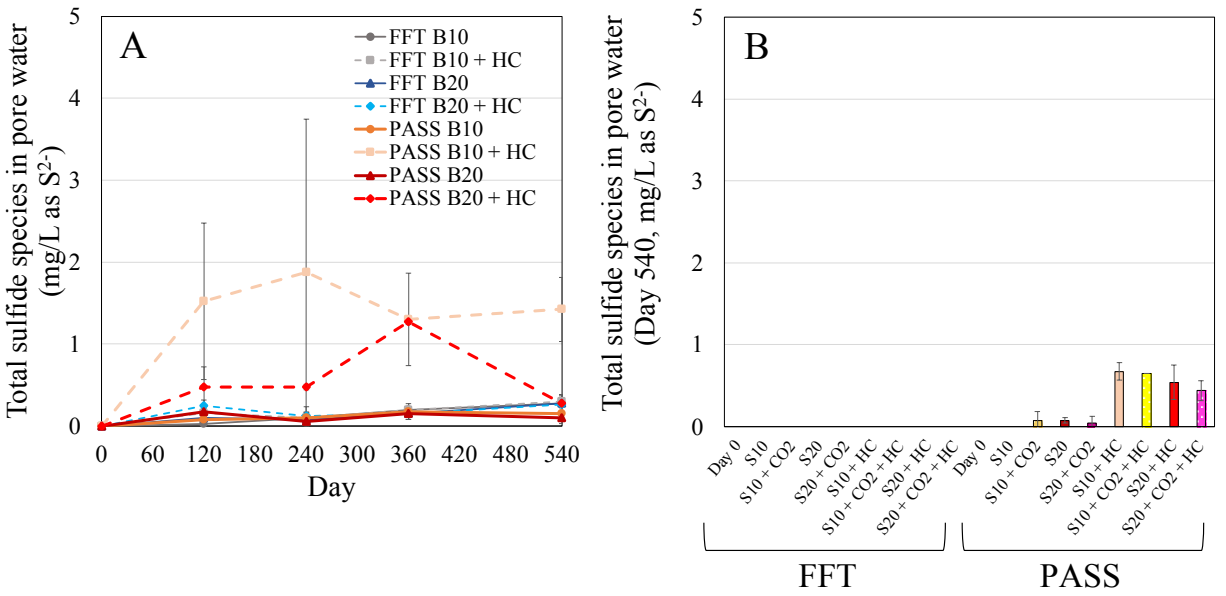

Figure 4-5. Pore water total sulfide species (S^{2-}, HS^-, H_2S) concentrations in (A) 19 L columns (Day 0 to 540) and (B) 1 L columns (Day 0 and Day 540 only). Results are averages of duplicate (A) and triplicate (B) columns and error bars represent one standard deviation of replicates. Labels B or S refer to Big (19 L) or Small (1 L) columns; 10 or 20 refer to 10°C or 20°C storage temperature; CO2 and HC refer to CO_2 and hydrocarbon amended tailings.

As seen in Figure 4-5, standard deviations for the total sulfide species measurements are relatively large. This variability is at least partially due to challenges in measuring pore water sulfide species, as the measurement is time sensitive but pore water must first be separated from the tailings solids via centrifugation. As such, the pore water concentrations of total sulfide species presented in

Figure 4-5 are likely underestimated. Aqueous sulfide species concentrations also fluctuate over the course of the study, as seen in Figure 4-5A. This is presumably a result of both measurement error and metal sulfide precipitation/dissolution reactions. Theoretically, the reduction of 630 mg/L of sulfate (in PASS + HC columns) should generate approximately 210 mg/L (as S^{2-}) of aqueous total sulfide species, assuming all reduced sulfur existed in the aqueous phase as dissolved sulfides. The total sulfide species measured in the pore water and water caps only account for a fraction of this reduced sulfur. This is likely due to the challenges in measuring aqueous sulfide species, as well as the generation of RSCs and the precipitation of metal sulfides. Gaseous H_2S was measured in the headspace of the 19 L columns on Days 180 and 360. While other RSCs may have also been emitted, only H_2S was measured as it was anticipated to be the predominant RSC (Gee et al. 2017). H_2S was below detection (<0.1 ppmv) in all 19 L columns, except in a PASS B10 + HC column on Day 180, which had a headspace H_2S concentration of 2.5 ppmv. It is possible that gaseous reduced sulfur was emitted in the form of other compounds, such as 2-methylthiophene (Gee et al. 2017), or that reduced sulfur primarily existed in the solid phase.

Figure 4-6 presents the solid phase sulfur content of the tailings in the 19 L columns on Day 540. The sulfur content of FFT and PASS on Day 0 is also provided for comparison. By Day 540, the sulfur content of the tailings solids had increased in all columns, which suggests that some of the reduced sulfur that was generated during sulfate reduction precipitated, possibly as metal sulfides (Dompierre et al. 2016; Stasik et al. 2014). This is consistent with the black color that was observed in the tailings over the course of the experiment, especially in PASS-treated FFT (see Figure 4-1B; photo taken on Day 30), which is indicative of $FeS_{(s)}$ formation. Interestingly, PASS-treated FFT amended with hydrocarbons (PASS + HC) had roughly twice as much sulfate reduced as unamended PASS-treated FFT and amended untreated FFT and over eight times as much sulfate reduced as unamended untreated FFT (see Figure 4-4), yet the sulfur content of PASS + HC tailings was less than or similar to that of unamended tailings and there were no statistically significant differences in the sulfur content of tailings in different columns. This, combined with the relatively large standard deviations for some duplicates, highlights the difficulties in capturing reduced sulfur. Depending on the method of analysis and phase, reduced sulfur may volatilize or oxidize, leading to underestimated measurements of reduced sulfur. Nonetheless, these results indicate that reduced sulfur generated from sulfate reduction existed in multiple phases throughout

the columns, particularly in PASS + HC columns. Because the columns in this study were anaerobic, they cannot predict the fate of reduced sulfur under oxic conditions, which may exist in pit lake water caps depending on the depth and season (Lawrence et al. 2016; Risacher et al. 2018).

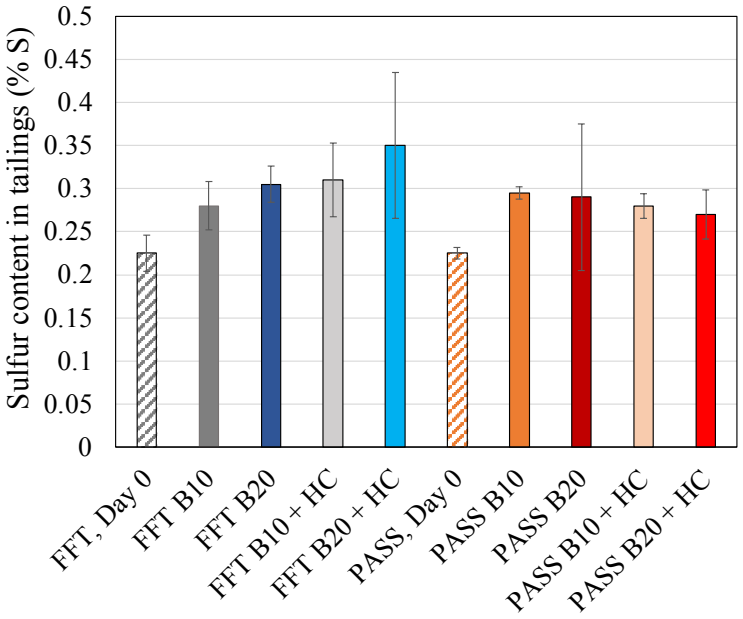

Figure 4-6. Sulfur (S) content in the tailings in 19 L columns on Day 540. Data presented as the percentage of elements in the solid phase that are sulfur. Sulfur contents of the untreated and PASS-treated FFT on Day 0 are provided for comparison. Results are averages of duplicate columns and error bars represent one standard deviation of duplicates. Label B refers to Big (19 L) columns; 10 or 20 refer to 10°C or 20°C storage temperature; HC refers to hydrocarbon amended tailings.

Sulfate reduction can contribute to alkalinity through the production of HCO_3^- and HS^-, such as in Equation 4-2, where C is the organic carbon source (taken from Wersin et al. 2011b):

$$SO_4^{2-} + 2H_2O + 2C \rightarrow HS^- + 2HCO_3^- + H^+ \quad (4\text{-}2)$$

Previous in situ studies of a clay formation found that sulfate reduction was associated with an increase in alkalinity and pCO_2 and a decrease in pH (Wersin et al. 2011a,b). In this study, ≥ 99% of the sulfate in hydrocarbon amended tailings was reduced by Day 540 and consequently, pore water alkalinity in these columns increased substantially, as seen in Figure 4-7. While hydrocarbon amendments had the most influence ($p < 0.0001$) on pore water alkalinity, pore water alkalinity

increased in all columns over 540 d. In the 19 L columns with hydrocarbon amended tailings, the sharp increase in pore water alkalinity between Days 0 and 120 coincides with the dramatic decrease in sulfate in Figure 4-4. The pH of the tailings in all columns had decreased slightly by Day 240 (see Appendix B3, Figure B-7), which is also consistent with the sulfate reduction and CO_2 generation (see subsection 4.3.5) in the columns.

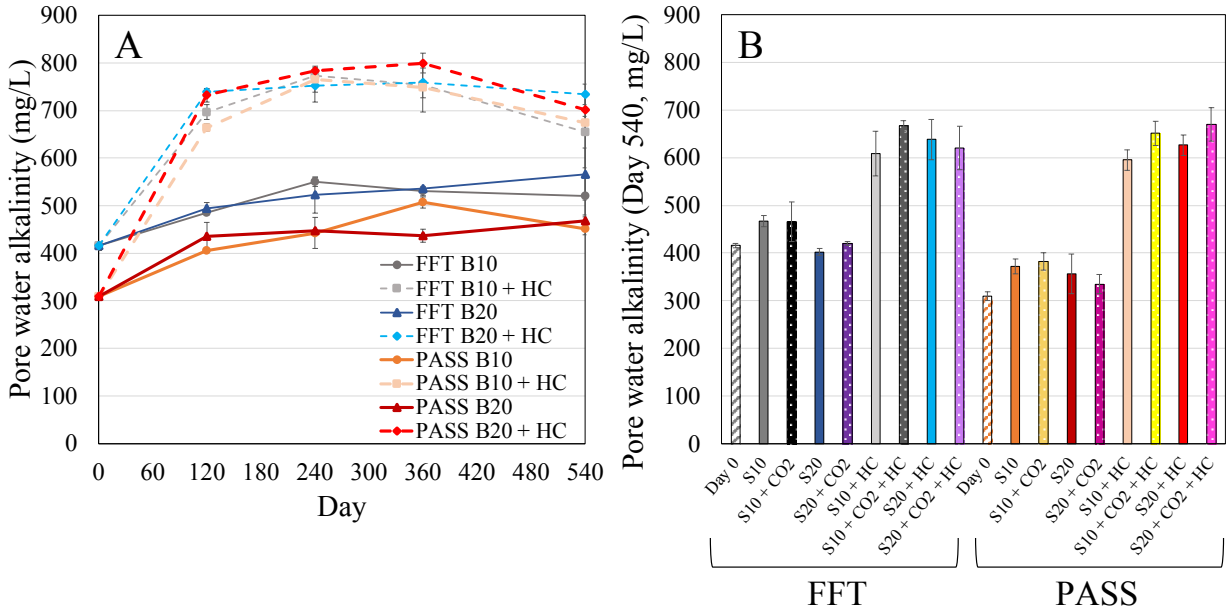

Figure 4-7. Pore water total alkalinity (in mg $CaCO_3$/L) in (A) 19 L columns (Day 0 to 540) and (B) 1 L columns (Day 0 and Day 540 only). Results are averages of duplicate (A) and triplicate (B) columns and error bars represent one standard deviation of replicates. Labels B or S refer to Big (19 L) or Small (1 L) columns; 10 or 20 refer to 10°C or 20°C storage temperature; CO2 and HC refer to CO_2 and hydrocarbon amended tailings.

The simultaneous increase in alkalinity and decrease in pH associated with sulfate reduction can have competing effects on carbonate minerals (Meister 2013; Zhang 2020). While HCO_3^- production can cause the precipitation of carbonate minerals such as calcite and dolomite, as shown in Equations 4-3 (calcite precipitation) and 4-4 (dolomite precipitation), H^+ production favors carbonate mineral dissolution. Calcite (and/or aragonite) and dolomite precipitation would be associated with a decrease in calcium and magnesium concentrations, while dissolution would result in increased concentrations of these ions. In this study, pore water concentrations of calcium (Figure 4-8) and magnesium (Figure 4-9) decreased in almost all of the columns containing

hydrocarbon amended tailings ($p < 0.0001$), which is consistent with carbonate mineral precipitation in these columns.

$$Ca^{2+} + HCO_3^- + OH^- \rightleftharpoons CaCO_{3(s)} + H_2O \quad (4\text{-}3)$$

$$Ca^{2+} + Mg^{2+} + 2HCO_3^- + 2OH^- \rightleftharpoons CaMg(CO_3)_{2(s)} + 2H_2O \quad (4\text{-}4)$$

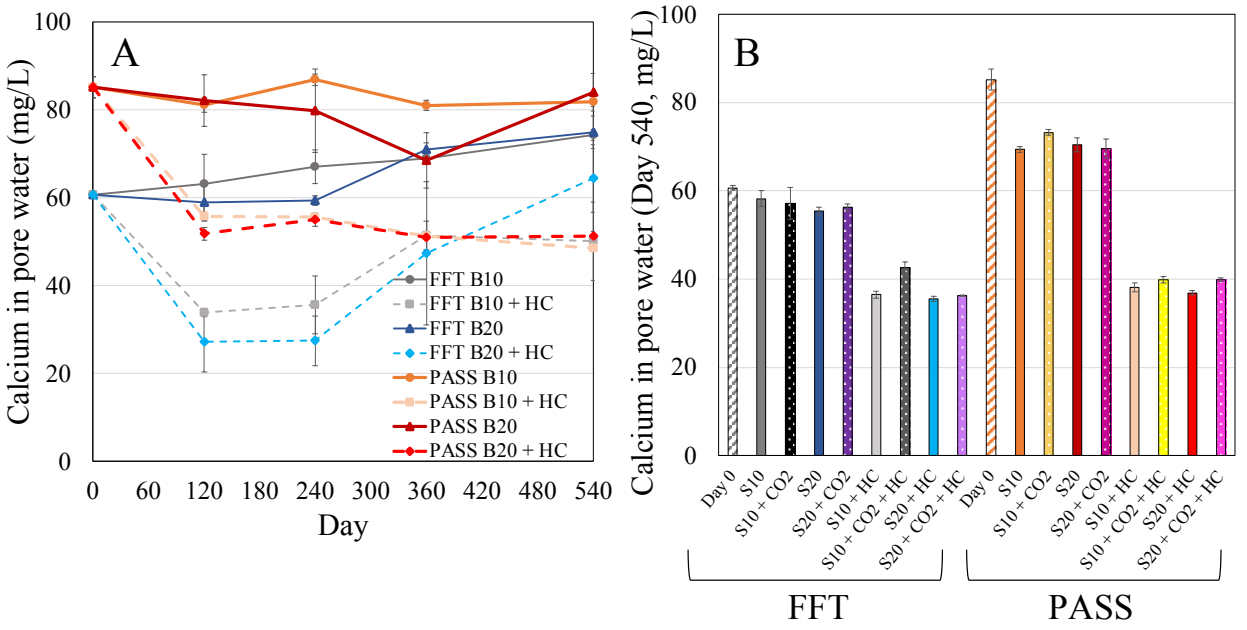

Figure 4-8. Pore water calcium concentrations in (A) 19 L columns (Day 0 to 540) and (B) 1 L columns (Day 0 and Day 540 only). Results are averages of duplicate (A) and triplicate (B) columns and error bars represent one standard deviation of replicates. Labels B or S refer to Big (19 L) or Small (1 L) columns; 10 or 20 refer to 10°C or 20°C storage temperature; CO2 and HC refer to CO_2 and hydrocarbon amended tailings.

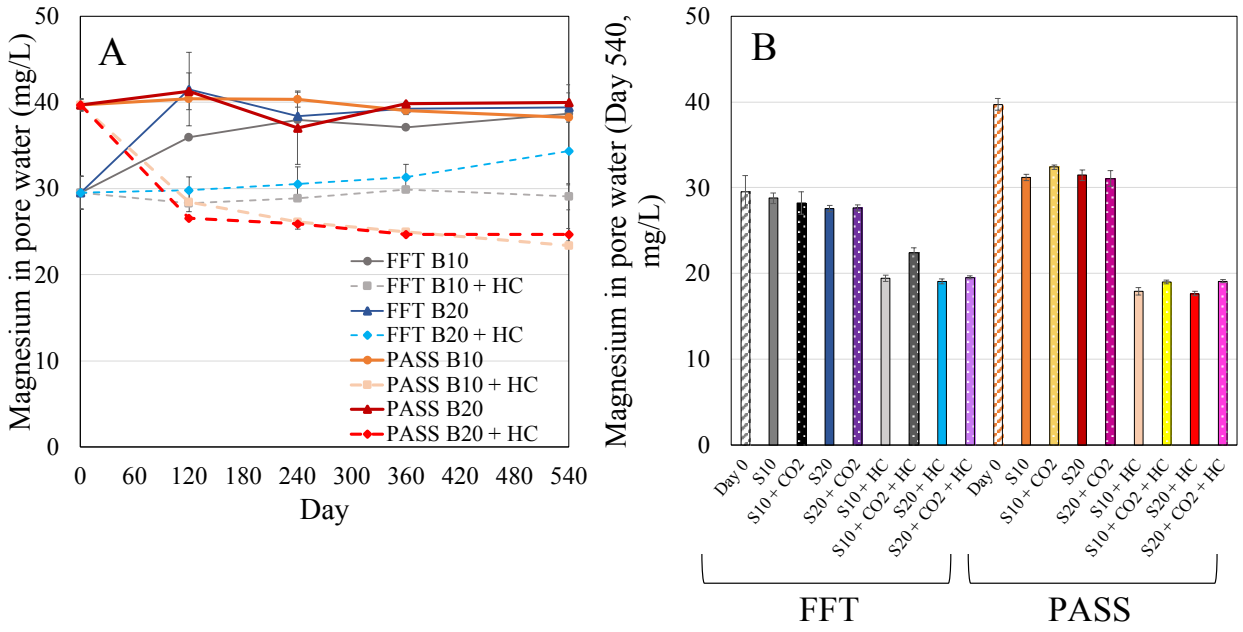

Figure 4-9. Pore water magnesium concentrations in (A) 19 L columns (Day 0 to 540) and (B) 1 L columns (Day 0 and Day 540 only). Results are averages of duplicate (A) and triplicate (B) columns and error bars represent one standard deviation of replicates. Labels B or S refer to Big (19 L) or Small (1 L) columns; 10 or 20 refer to 10°C or 20°C storage temperature; CO2 and HC refer to CO_2 and hydrocarbon amended tailings.

Geochemical modeling was conducted in PHREEQC to confirm that the decrease in sulfate and increase in alkalinity and bisulfide (or hydrogen sulfide) in the tailings was consistent with carbonate mineral precipitation. Numerous analyses were run for both untreated and PASS-treated FFT amended with hydrocarbons, using the initial pore water chemistry data presented in Table 4-3 and the sulfate concentrations on Day 120 (in the 19 L columns). Alkalinity and bisulfide/hydrogen sulfide were calculated based on the theoretical amount produced (according to Equation 4-2) from the sulfate reduction that occurred during the first 120 d. Multiple analyses were run, with and without calcite (assuming calcite was the major carbonate mineral present, calculated based on Poon et al. (2018)). All analyses conducted in PHREEQC showed that carbonate minerals (primarily calcite, aragonite, and dolomite) would precipitate as a result of the pore water chemistry changes (decrease in sulfate and increase in alkalinity and bisulfide/hydrogen sulfide) associated with sulfate reduction. Further, PHREEQC indicated that sulfide species would precipitate, primarily as pyrite (FeS_2), and $CO_{2(g)}$ would increase as a result of the pore water chemistry changes associated with sulfate reduction. The modeling results are consistent with the decrease in pore water concentrations of calcium (Figure 4-8) and magnesium (Figure 4-9) in all

hydrocarbon amended columns during the 540 d. More frequent sampling in the 19 L columns captured the decrease in pore water concentrations of calcium and magnesium in hydrocarbon amended columns during the first 120 d, which coincides with the substantial sulfate reduction that occurred during the same period. Any increases in pore water concentrations of calcium and/or magnesium during the 540 d are presumably due to carbonate mineral dissolution as a result of pH reduction and biogenic CO_2 generation.

The higher average solids content in hydrocarbon amended tailings, relative to unamended tailings, on Day 540 likely indicates that bioconsolidation contributed to tailings consolidation. While bioconsolidation was not substantial in this study, the bioconsolidation pathway is of interest because sulfate reduction was the dominant microbial process. The bioconsolidation pathway suggested by Siddique et al. (2014a), in which the dissolution of biogenic CO_2 decreases the pH of FFT and increases carbonate mineral dissolution, ionic strength, and clay flocculation, was based on methanogenesis. Siddique et al.'s (2014a) bioconsolidation pathway may still be relevant to this column study, mainly because of the generation of CO_2 and H^+ during sulfate reduction. However, because sulfate reduction was the dominant microbial process in this study, it is possible that microbial activity contributed to consolidation through carbonate mineral precipitation (Liang et al. 2014; Liu and Montoya 2020) rather than dissolution. Calcite mineral precipitation on microbes and/or solid surfaces could lead to cohesive bonding within the tailings and thereby improve dewatering (Liang et al. 2014). Further, precipitation of sulfide minerals (such as $FeS_{(s)}$) could have also contributed to bioconsolidation of FFT, as suggested by Siddique et al. (2014b). Figure 4-10 illustrates two possible bioconsolidation pathways for FFT based on the dominant microbial process occurring. The sulfate reduction pathway was developed based on the results of this column study and that of Siddique et al. (2014b); however, additional analysis is necessary to confirm that carbonate (and/or sulfide) mineral precipitation contributed to bioconsolidation of hydrocarbon amended FFT in this study.

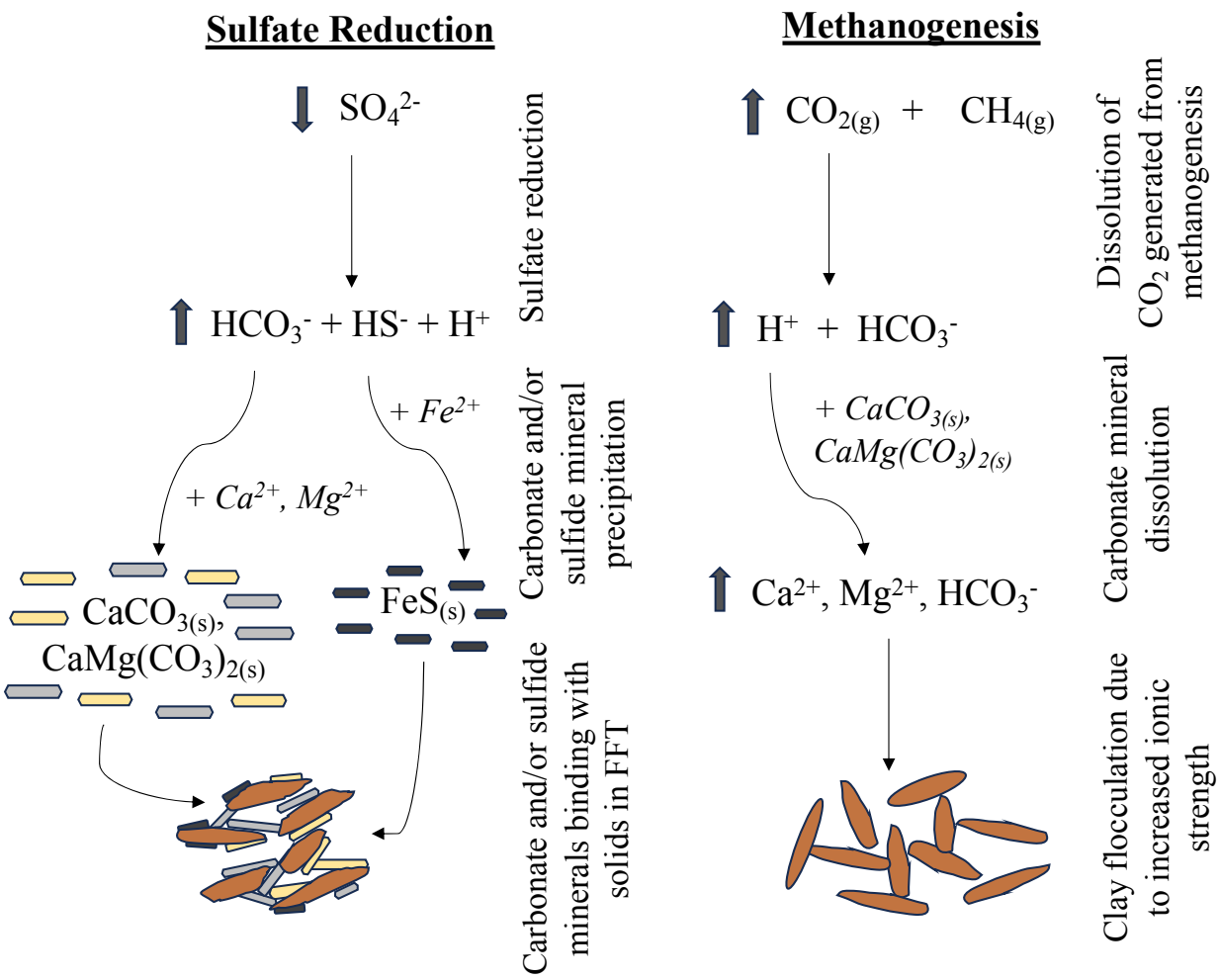

Figure 4-10. Possible bioconsolidation pathways in oil sands fluid fine tailings, influenced by the dominant microbial pathway. Sulfate reduction pathway suggested based on the results of this column study and that of Siddique et al. (2014b). Methanogenesis pathway based on the work of Siddique et al. (2014a). The formation of clay aggregates will vary depending on the type of clay and ionic strength (Stawiński et al. 1990).

Other chemical reactions may also have contributed to the pore water chemistry changes seen in the 64 columns. Cation exchange at clay surfaces could have contributed to the decrease in divalent cations in the pore water of hydrocarbon amended columns, as seen in Figures 4-8 and 4-9. Further, ion exchange would decrease the thickness of the diffuse double layer and increase clay flocculation, resulting in a higher solids content in these columns. However, if ion exchange reactions did occur, pore water concentrations of sodium (Figure 4-11) and potassium (Appendix B3, Figure B-9) were largely unaffected by it. Dompierre et al. (2016) found that pore water

sodium concentrations in BML FFT did not appear to be impacted by in situ reactions (such as ion exchange), though pore water potassium concentrations were affected by in situ reactions.

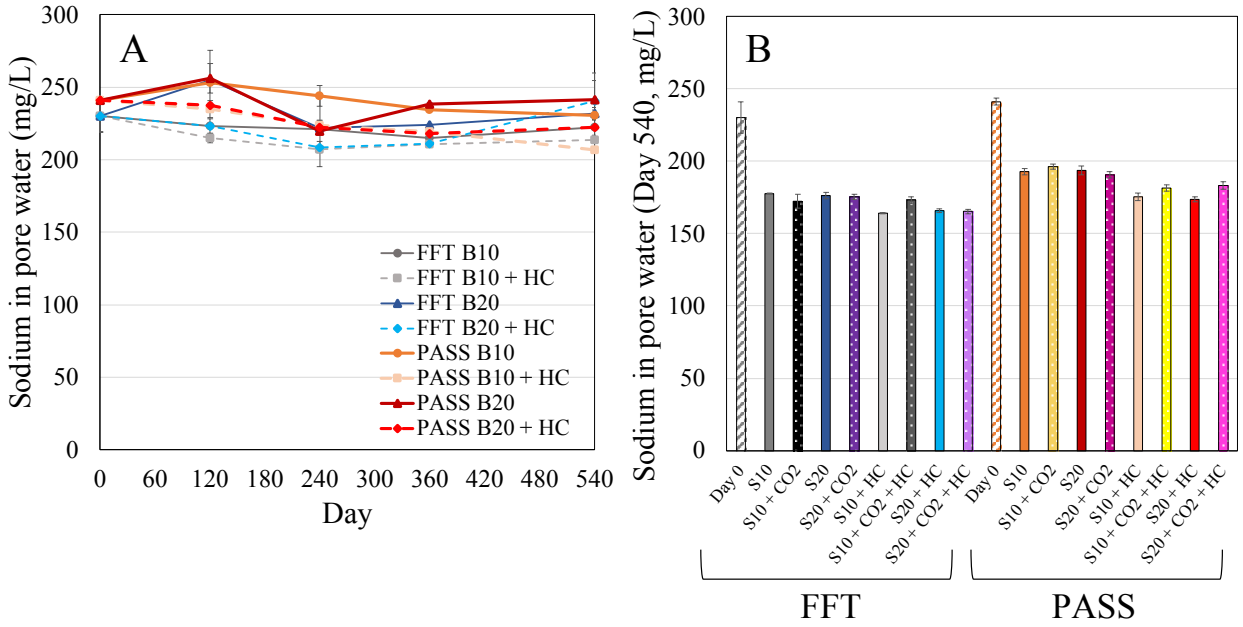

Figure 4-11. Pore water sodium concentrations in (A) 19 L columns (Day 0 to 540) and (B) 1 L columns (Day 0 and Day 540 only). Results are averages of duplicate (A) and triplicate (B) columns and error bars represent one standard deviation of replicates. Labels B or S refer to Big (19 L) or Small (1 L) columns; 10 or 20 refer to 10°C or 20°C storage temperature; CO2 and HC refer to CO_2 and hydrocarbon amended tailings.

Interestingly, pore water sodium concentrations were most strongly influenced by size ($p < 0.0001$). In the 19 L columns, the average change in pore water sodium concentrations between Days 0 and 540 was 3.8%, whereas in the 1 L columns, the average change was a decrease of 24.2%. This difference can likely be attributed to diffusive fluxes. Diffusion of a chemical through porous media can be described by Fick's First Law (Equation 4-5):

$$J = -D^{*}\theta\frac{\partial C}{\partial x} \tag{4-5}$$

where J is the diffusive flux, D^{*} is the effective diffusion coefficient, θ is the volumetric water content, C is the chemical concentration, and x is the distance in the direction of transport. The concentration gradient of sodium was greater than that of some of the other pore water constituents,

such as chloride (Appendix B3, Figure B-10), because sodium had a high initial pore water concentration (relative to both other pore water constituents (chloride) and the BCR cap water). Further, the concentration gradient in the 1 L columns was greater than that of the 19 L columns because of the shorter length over which chemicals had to travel in the 1 L columns. Diffusion likely also contributed to decreased sodium concentrations in the pore water of the 19 L columns, but to a lesser extent than that of the 1 L columns. Trends in the water cap concentrations of sodium (and other chemicals) discussed in the next subsection support this diffusion theory.

Pore water concentrations of DOC are presented in Figure 4-12. Hydrocarbon amendments had the most influence on pore water DOC concentrations ($p < 0.0001$), with hydrocarbon amended tailings having roughly 10 mg/L more DOC than unamended tailings on Day 540. The increase in DOC in hydrocarbon amended tailings, particularly during the first 120 d (in the 19 L columns), is likely a result of microbial activity and may be due to the microbial degradation of high molecular weight hydrocarbons into lower molecular weight organics (Yu 2019) and/or emulsification of hydrocarbons by EPS to form readily available DOC (Gee et al. 2017). In the 19 L columns, the average DOC concentration in PASS-treated FFT pore water was approximately 4 mg/L less than that of untreated FFT pore water on Day 540, but in 1 L columns this difference was roughly 1 mg/L. This suggests that DOC concentrations were not considerably reduced by the PASS treatment in this study. DOC in unamended tailings in the 1 L columns had a roughly 8 mg/L decrease over 540 d but DOC concentrations in most other columns were fairly consistent or increased throughout the study. It is likely that either i) DOC in the tailings was not substantially biodegraded, perhaps because it was recalcitrant or largely consisted of NAFCs (which typically do not degrade under anaerobic conditions), or ii) soluble metabolites produced from degradation processes were quickly consumed, resulting in a seemingly stable level of DOC (Foght et al. 2017; Reid and Warren 2016).

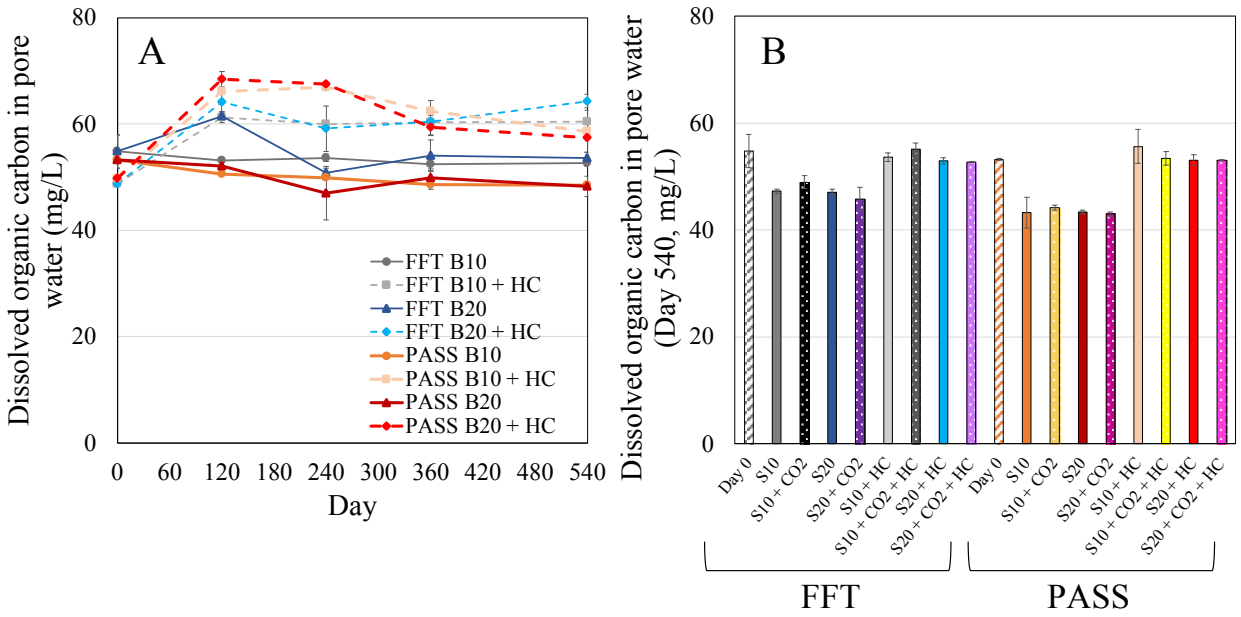

Figure 4-12. Pore water dissolved organic carbon concentrations in (A) 19 L columns (Day 0 to 540) and (B) 1 L columns (Day 0 and Day 540 only). Results are averages of duplicate (A) and triplicate (B) columns and error bars represent one standard deviation of replicates. Labels B or S refer to Big (19 L) or Small (1 L) columns; 10 or 20 refer to 10°C or 20°C storage temperature; CO2 and HC refer to CO_2 and hydrocarbon amended tailings.

PAM concentrations were not measured as part of this study, though ammonia/ammonium was measured in the 19 L columns in the pore water (on Days 360 and 540) and water caps (on Day 540). Ammonia/ammonium was not detected in the majority of the 19 L columns on Days 360 and 540 (see Appendix B3, Table B-2), and when it was detected, average concentrations were low (≤ 1.2 mg/L as NH_3).

4.3.4 Water Cap Chemistry

Water cap chemistry in each column was impacted by numerous factors, including advective and diffusive pore water fluxes, geochemical reactions, microbial activity, and differences in the pore water chemistry of untreated versus PASS-treated FFT on Day 0. Figure 4-13 presents water cap concentrations of sodium, which were most strongly influenced by column size ($p < 0.0001$). The water cap sodium concentrations in the 19 L columns (Figure 4-13A) are fairly consistent with the NWR trends in Figure 4-2, though they were also affected by the higher initial sodium concentration in PASS-treated FFT relative to untreated FFT. Water cap sodium concentrations in the 1 L columns are less consistent with NWR trends, as sodium concentrations continued to

increase in the water caps even though NWR plateaued after Day 60 in most of these columns. Further, by Day 540, all 1 L columns had higher water cap sodium concentrations than the 19 L columns, even though almost all of the 19 L columns had a higher NWR than the 1 L columns. As such, mass flux calculations were performed to compare the theoretical water cap sodium concentration (based on NWR) and the actual (measured) water cap sodium concentration. Figure 4-14 presents the percent difference in the theoretical and actual Day 540 water cap sodium concentrations for all columns. Positive values indicate that the actual concentration was greater than the theoretical concentration. The percent difference for the 1 L columns was substantial, reaching up to 111%. Combined with the decrease in pore water sodium concentrations in the 1 L columns seen in Figure 4-11, this indicates that diffusion contributed to the higher concentrations of sodium in the 1 L column water caps. Further, based on flux calculations and the NWR shown in Figure 4-2B, it appears that diffusion had become dominant in the 1 L columns by at least Day 120.

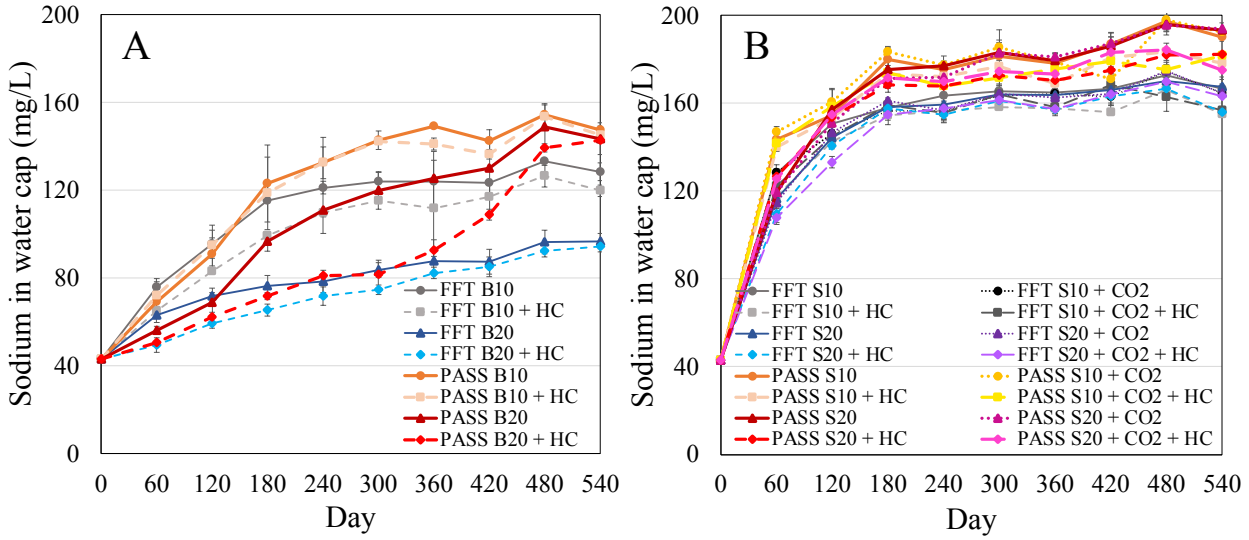

Figure 4-13. Water cap sodium concentrations in (A) 19 L columns and (B) 1 L columns over 540 d. Results are averages of duplicate (A) and triplicate (B) columns and error bars represent one standard deviation of replicates. Labels B or S refer to Big (19 L) or Small (1 L) columns; 10 or 20 refer to 10°C or 20°C storage temperature; CO2 and HC refer to CO_2 and hydrocarbon amended tailings.

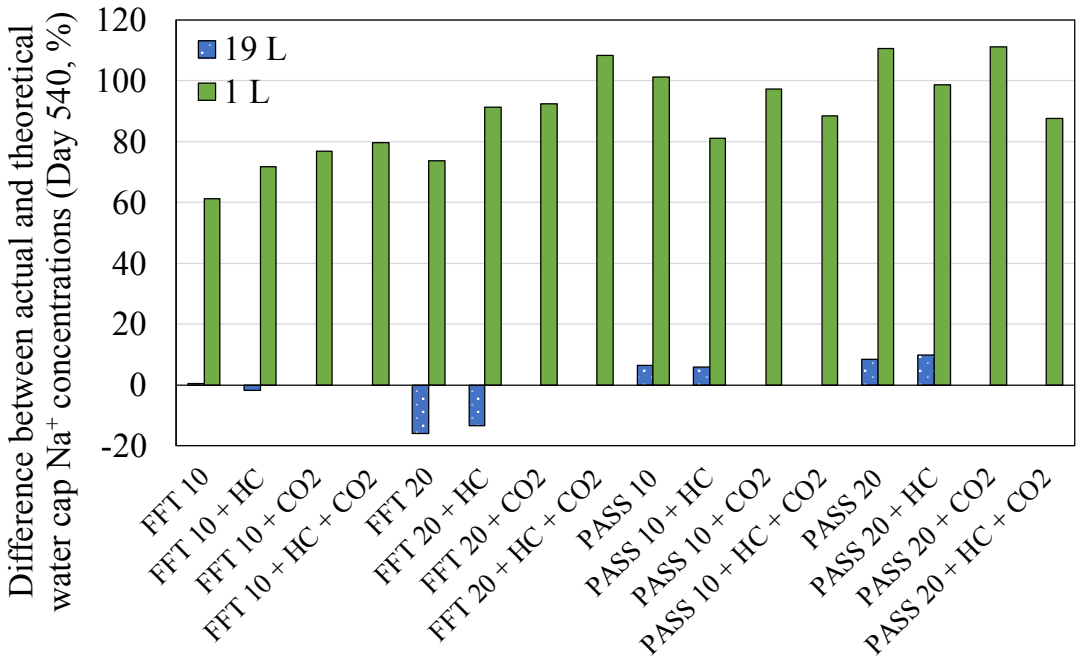

Figure 4-14. Percent difference in Day 540 water cap sodium concentrations (actual versus theoretical (based on NWR)). Labels 10 or 20 refer to 10°C or 20°C storage temperature; CO2 and HC refer to CO_2 and hydrocarbon amended tailings.

Water cap concentrations of chloride are presented in Figure 4-15 and are similar to sodium trends, though diffusion of chloride occurred to a lesser extent because of its smaller concentration gradient. Treatment had the most influence on water cap chloride concentrations ($p < 0.0001$) because the Day 0 pore water chloride concentrations were different for untreated FFT and PASS-treated FFT. Size also influenced water cap chloride concentrations ($p < 0.0001$). Despite almost all of the 19 L columns achieving a higher NWR than the 1 L columns, in columns containing untreated FFT, water cap chloride concentrations were higher in the 1 L columns than in the 19 L columns. Similarly, for columns containing PASS-treated FFT, water cap chloride concentrations were highest in the 1 L columns. This supports the theory that diffusion influenced water cap concentrations in the 1 L columns. Diffusion may have also influenced water cap concentrations in the 19 L columns, particularly in the PASS-treated columns which have a positive percent difference in Figure 4-14, though diffusion occurred to a greater extent in the 1 L columns. Water cap concentrations of calcium, magnesium, and potassium are provided in Appendix B3 and show similar trends to that of sodium and chloride, though water cap concentrations of the divalent cations are more strongly impacted by biogeochemical reactions in the pore water.

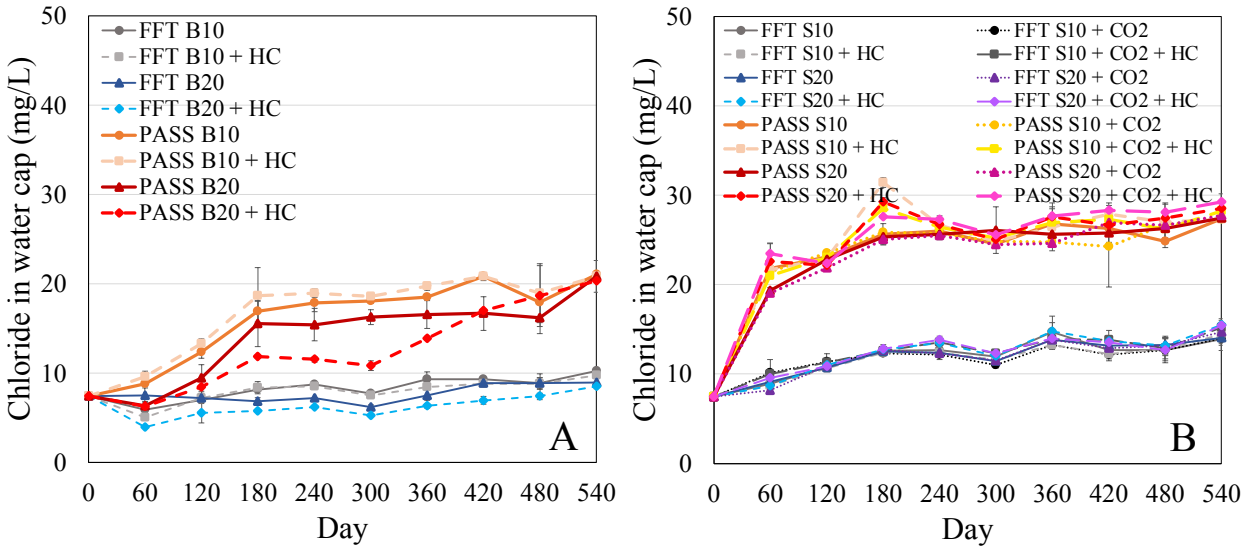

Figure 4-15. Water cap chloride concentrations in (A) 19 L columns and (B) 1 L columns over 540 d. Results are averages of duplicate (A) and triplicate (B) columns and error bars represent one standard deviation of replicates. Labels B or S refer to Big (19 L) or Small (1 L) columns; 10 or 20 refer to 10°C or 20°C storage temperature; CO2 and HC refer to CO_2 and hydrocarbon amended tailings.

Water cap concentrations of sulfate are presented in Figure 4-16. Of the five factors investigated, hydrocarbon amendments had the most influence on water cap sulfate concentrations ($p < 0.0001$), followed by tailings treatment ($p < 0.0001$). In the 19 L columns, water cap sulfate concentrations are fairly consistent with NWR and pore water sulfate concentrations. In the 1 L columns, water cap sulfate concentrations spiked on Day 60 and then decreased in hydrocarbon amended columns and continued to increase in unamended columns. The initial spike may be due to the quick NWR in the 1 L columns, though instrument error is strongly suspected to have contributed to the spike in sulfate. Water cap sulfate concentrations in unamended 1 L columns increased after Day 120, and this can be attributed to the diffusion of sulfate from the pore water into the water cap. In hydrocarbon amended 1 L columns, pore water sulfate was likely depleted by Day 120 (based on trends in the 19 L columns) so diffusion would not have contributed sulfate to the water cap. Instead, water cap sulfate concentrations in these columns decreased after Day 120, likely the result of sulfate reduction in the water cap. Though most of the SRB would have been contained in the tailings, some may have attached to column walls and/or solids suspended in the water cap.

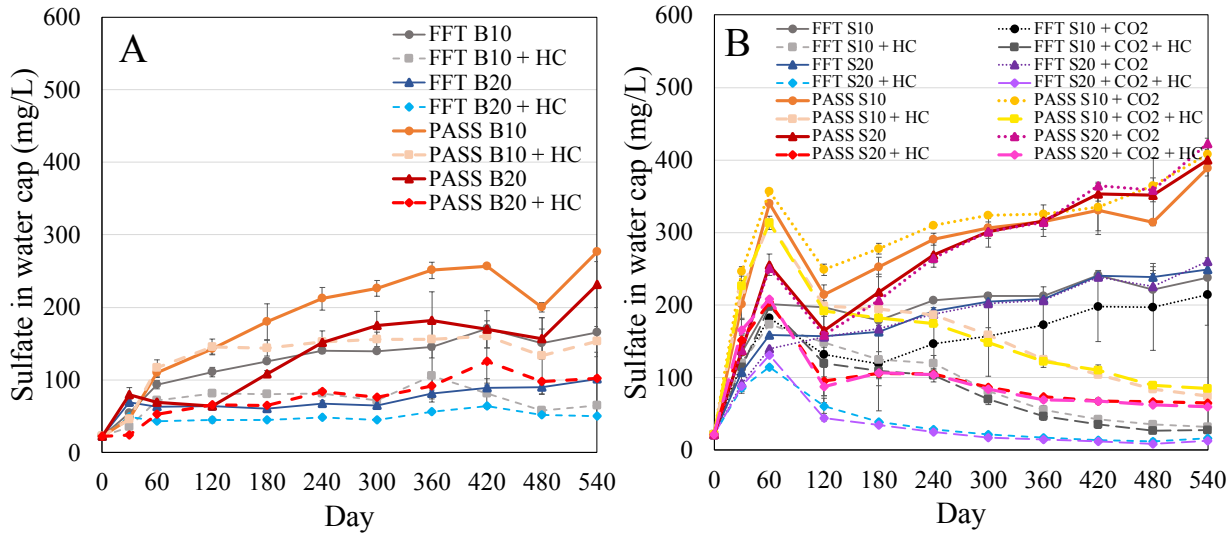

Figure 4-16. Water cap sulfate concentrations in (A) 19 L and (B) 1 L columns over 540 d. Results are averages of duplicate (A) and triplicate (B) columns and error bars represent one standard deviation of replicates. Labels B or S refer to Big (19 L) or Small (1 L) columns; 10 or 20 refer to 10°C or 20°C storage temperature; CO2 and HC refer to CO_2 and hydrocarbon amended tailings.

Water cap alkalinity is presented in Figure 4-17. Similar to pore water alkalinity, water cap alkalinity was most strongly influenced by hydrocarbon amendments ($p < 0.0001$). Alkalinity in the water cap would have also been impacted by NWR, pore water chemistry, biogeochemical reactions, and diffusion (particularly in the 1 L columns). Water cap DOC concentrations are shown in Figure 4-18 and are fairly consistent with NWR trends. Hydrocarbon amendments had the most influence on water cap DOC concentrations ($p < 0.0001$), which is consistent with the pore water DOC trends and microbial activity in general. Size also had a large influence on DOC ($p < 0.0001$), as 1 L columns had higher water cap DOC concentrations than almost all 19 L columns on Day 540. In general, DOC concentrations in the water caps would have been influenced by advection and diffusion, as well as microbial activity (and microbial degradation processes). The Day 60 spike in DOC in the 1 L columns may have been due to the quick initial NWR in these columns, suspension or desorption of organic compounds from tailings particles, and/or an increase in soluble metabolites from biodegradation (Yu 2019). However, instrument error may also be an explanation for the Day 60 spike in water cap DOC concentrations, given the relatively high standard deviations for the columns with high DOC concentrations. Tailings treatment did not have a significant impact on DOC water cap concentrations, which suggests that DOC mobility was not reduced by PASS treatment in this study.

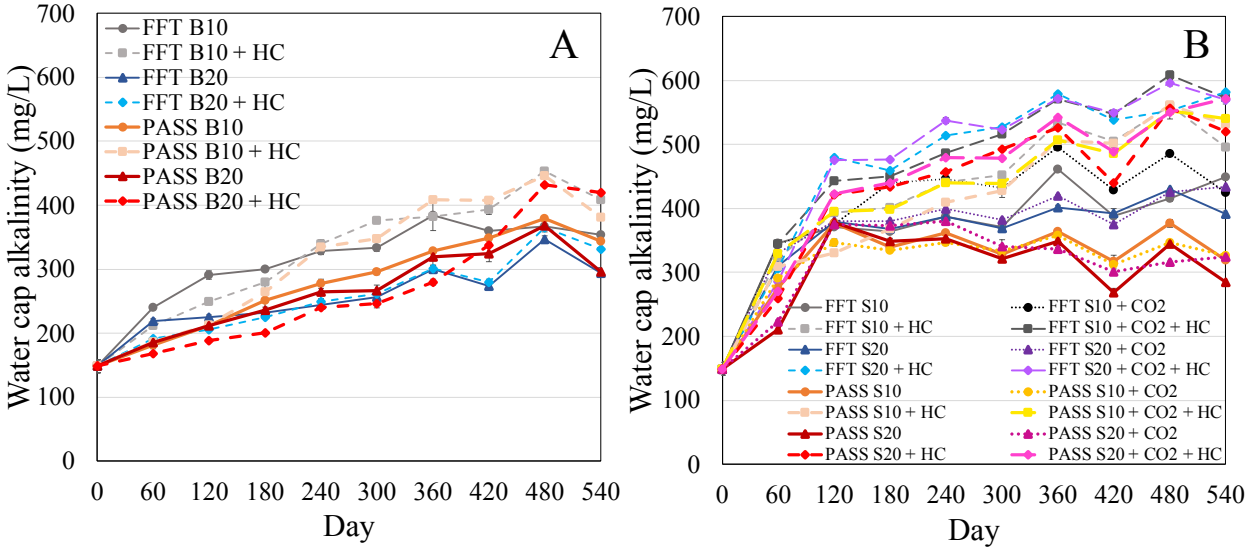

Figure 4-17. Water cap total alkalinity (in mg $CaCO_3$/L) in (A) 19 L columns and (B) 1 L columns over 540 d. Results are averages of duplicate (A) and triplicate (B) columns and error bars represent one standard deviation of replicates. Labels B or S refer to Big (19 L) or Small (1 L) columns; 10 or 20 refer to 10°C or 20°C storage temperature; CO2 and HC refer to CO_2 and hydrocarbon amended tailings.

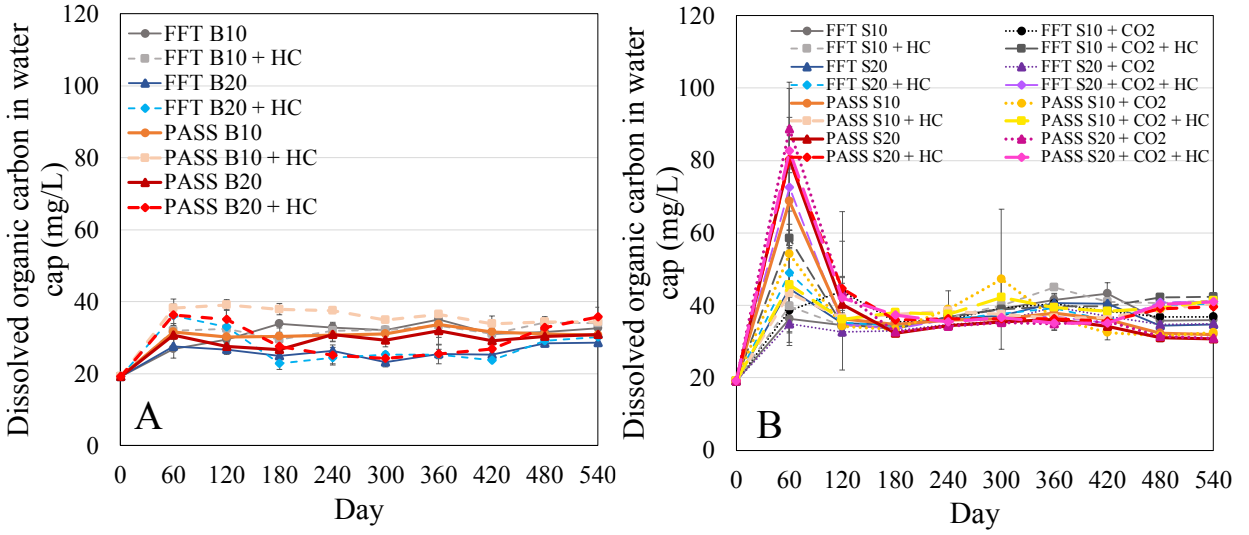

Figure 4-18. Water cap dissolved organic carbon concentrations in (A) 19 L columns and (B) 1 L columns over 540 d. Results are averages of duplicate (A) and triplicate (B) columns and error bars represent one standard deviation of replicates. Labels B or S refer to Big (19 L) or Small (1 L) columns; 10 or 20 refer to 10°C or 20°C storage temperature; CO2 and HC refer to CO_2 and hydrocarbon amended tailings.

4.3.5 Biogenic Gas Emissions and Microbial Communities

Biogenic gas emissions of CO_2 and CH_4 in the column headspaces over 540 d are shown in Figures 4-19 and 4-20, respectively. The range of volumes shown on the y-axis in both figures is larger for the 19 L columns than the 1 L columns. All columns produced CO_2 during the 540 d study, which is indicative of microbial activity in general. Hydrocarbon amendments had the most influence on CO_2 generation in terms of mL of CO_2 generated per L tailings ($p < 0.0001$), which is consistent with the extensive sulfate reduction in hydrocarbon amended columns. Size was not a significant factor in the volume of CO_2 generated per L of tailings. By Day 540 the 19 L unamended columns had produced an average of 10.9 mL CO_2/L tailings and the 1 L unamended columns produced an average of 11.1 mL CO_2/L tailings. The average CO_2 generated in the hydrocarbon amended columns by Day 540 was 18.4 mL CO_2/L tailings for 19 L columns and 17.2 mL CO_2/L tailings for 1 L columns. Figure B-14 in Appendix B3 shows the volume of CO_2 generated per L of tailings in the 19 L and 1 L columns on Day 540.

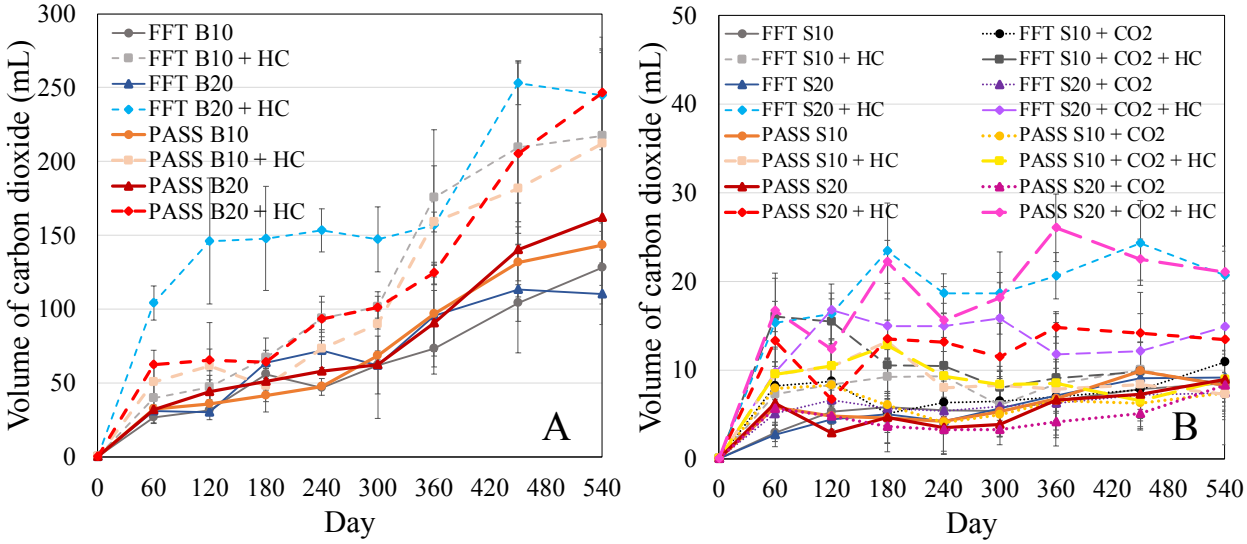

Figure 4-19. Volume of carbon dioxide emitted in (A) 19 L columns and (B) 1 L columns over 540 d. Results are averages of duplicate (A) and triplicate (B) columns and error bars represent one standard deviation of replicates. Labels B or S refer to Big (19 L) or Small (1 L) columns; 10 or 20 refer to 10°C or 20°C storage temperature; CO2 and HC refer to CO_2 and hydrocarbon amended tailings.

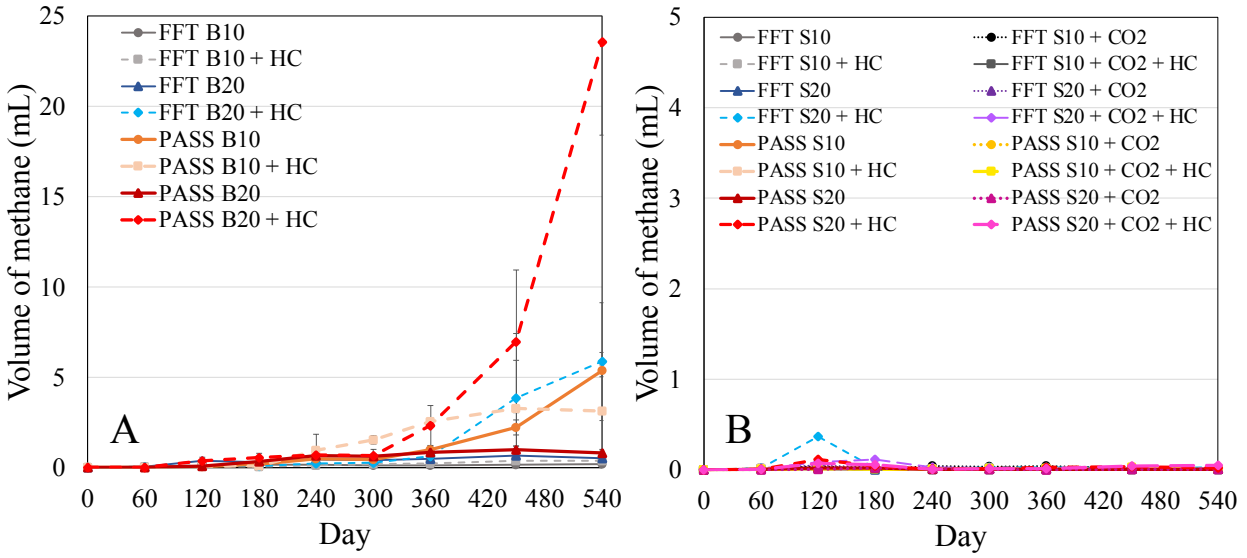

Figure 4-20. Volume of methane emitted in (A) 19 L columns and (B) 1 L columns over 540 d. Results are averages of duplicate (A) and triplicate (B) columns and error bars represent one standard deviation of replicates. Labels B or S refer to Big (19 L) or Small (1 L) columns; 10 or 20 refer to 10°C or 20°C storage temperature; CO2 and HC refer to CO_2 and hydrocarbon amended tailings.

As shown in Figure 4-20, there was only a small amount of CH_4 produced in the 19 L columns, mostly after Day 240, and CH_4 production in the 1 L columns was minimal over the 540 d. CH_4 production in the 19 L columns occurred mostly in the columns containing hydrocarbon amended and/or PASS-treated FFT. By Day 540, PASS B20 + HC columns had produced an average of 1.9 mL CH_4/L tailings but all other columns had produced <1.0 mL CH_4/L tailings. If the study had been extended beyond 540 d, it is likely that most (if not all) of the columns would eventually produce CH_4.

Lag times in methane production have been reported in other FFT studies as well (Mohamad Shahimin and Siddique 2017a,b; Mohamad Shahimin et al. 2016, 2021). Mohamad Shahimin et al. (2021) evaluated CH_4 production from CNUL and CNRL FFT using different iso-alkane mixtures and found a minimum lag time of 200 d, though iso-alkanes are more recalcitrant than some other hydrocarbons such as monoaromatics and n-alkanes. CH_4 production lag times depend on numerous factors including the i) carbon source, ii) source of the tailings, as microbial communities and the carbon sources they are accustomed to will vary for each operator and/or mine, and iii) age of the tailings, as it can take years for methanogenic microbial communities to

develop (Foght et al. 2017; Mohamad Shahimin et al. 2016, 2021). In this study, SRB may have consumed the more readily biodegradable hydrocarbons, leaving more recalcitrant hydrocarbons for methanogens. Further, studies have found that indigenous microbial communities in oil sands tailings need time to shift their community compositions to acclimate to new carbon sources (Mohamad Shahimin et al. 2016, 2021). The hydrocarbon mixture used in this experiment is similar to the naphtha diluent used by some oil sands operators, while the tailings used in this experiment would have been accustomed to paraffinic diluent. It is also possible that the lag time in CH_4 production was partly due to SRB outcompeting methanogens. Previous laboratories studies of FFT have found that if sulfate is abundantly available, it will inhibit methanogenesis because of the competitive (thermodynamic and kinetic) advantage of SRB over methanogens (Fedorak et al. 2002; Holowenko et al. 2000; Ramos-Padrón et al. 2011). Fedorak et al. (2002) found that methanogenesis was inhibited in FFT microcosms until sulfate concentrations were reduced to 20 mg/L. As such, competition with SRB may have inhibited CH_4 production during the first 120 d in hydrocarbon amended tailings and throughout the 540 d experiment in unamended tailings, though PASS B10 columns produced more CH_4 than PASS B10 + HC columns, despite PASS B10 having 345 mg/L of sulfate remaining in the tailings on Day 540. Other studies have found that there is no inhibition of methanogenesis in the presence of sulfate when carbon sources are abundant or used non-competitively (Stasik and Wendt-Potthoff 2014, 2016; Stasik et al. 2014). In this experiment, it is likely that multiple factors contributed to the lag time in CH_4 production.

Figure 4-21 presents the relative abundance of microbial communities (at the class level) on Day 540 in 19 L columns in untreated and PASS-treated FFT. Microbial communities in the untreated and PASS-treated FFT on Day 0 are also provided for comparison. The relative abundance of microbial communities on Day 120 in untreated and PASS-treated FFT is provided in Appendix B4, Figures B-15. There were differences in the microbial communities present on Day 0 in untreated versus PASS-treated FFT, even though both types of tailings were stored in the same manner. PASS treatment occurred over a one month period, which was enough time for microbial communities in the FFT to shift. In both the untreated and PASS-treated FFT, bacteria predominated on Day 0, particularly *Gammaproteobacteria* (21.9% in FFT, 23.9% in PASS) which are often abundant in oil sands tailings (Foght et al. 2017; Saidi-Mehrabad et al. 2013;

Warren et al. 2016), and there were no archaea detected. Compared to PASS-treated FFT, untreated FFT had a greater abundance of *Anaerolineae* (13.8% in FFT, 6.5% in PASS) and *Syntrophia* (16.7% in FFT, 5.7% in PASS). *Anaerolineae* (family *Anaerolineaceae*) and *Syntrophia* (family *Syntrophaceae*) have been found to contribute to anaerobic degradation of hydrocarbon diluents (Foght et al. 2017; Mohamad Shahimin and Siddique 2017a; Mohamad Shahimin et al. 2016). Compared to untreated FFT, PASS-treated FFT had a greater abundance of *Thermodesulfovibrionia* (6.7% in PASS, 3.0% in FFT) and the phylum MBNT15 (2.1% in PASS, 1.3% in FFT). PASS-treated FFT also contained *Clostridia* (2.0%), *Desulfitobacteriia* (7.1%, genus *Desulfosporosinus*), and *Desulfobacteria* (3.4%, order *Desulfobacterales*) which were not present at a relative abundance of >1.0% in the untreated FFT. The class *Thermodesulfovibrionia* contains microorganisms capable of sulfate reduction and sulfur disproportionation (D'Angelo et al. 2023). MBNT15 members are not capable of sulfate reduction but can reduce iron as well as nitrogen and sulfur compounds (Begmatov et al. 2022) and members of the *Clostridia* class are commonly found in oil sands tailings and have been associated with anaerobic hydrocarbon degradation (An et al. 2013; Collins et al. 2016; Foght et al. 2017; Tan et al. 2015). Members of *Desulfobacterales* and *Desulfosporosinus* are known SRB (Burow et al. 2014; Pester et al. 2012; Tan et al. 2015). The differences in the Day 0 microbial communities in untreated and PASS-treated FFT highlights how quickly microbial communities can adapt to chemical amendments, in this case how quickly SRB can accumulate in response to sulfate addition.

On Day 540, *Gammaproteobacteria* (primarily of the order *Burkholderiales*) were still predominant and had increased in all columns, making up 23.9% to 33.0% of the microbial communities in untreated FFT columns and 31.6% to 40.7% of microbial communities in PASS-treated FFT columns. The class *Gammaproteobacteria* contains aerobic hydrocarbon degraders, as well as facultative anaerobes (Foght et al. 2017; Pérez-Pantoja et al. 2011). The SRB-containing class *Thermodesulfovibrionia* was still present in all columns on Day 540, as were MBNT15 and *Anaerolineae*. Two new classes of microorganisms were present on Day 540: *Desulfobulbia* and *Methanomicrobia. Desulfobulbia* contains known SRB associated with the degradation of BTEX compounds (toluene and ethylbenzene) (Ahmar Siddiqui et al. 2022; Wu et al. 2022). *Desulfobulbia* were present in PASS B10 and PASS B20 + HC columns on Day 540 and they were also present in hydrocarbon amended tailings (FFT B10 + HC, PASS B10 + HC, and PASS B20

+ HC) on Day 120 (see Appendix B4, Figure B-15). In general, the relative abundance of known SRB was greater in PASS columns on Day 120 than Day 540, which is consistent with the sulfate reduction trends in Figure 4-4A. On Day 120, *Desulfobacteria* were present in all PASS columns and *Desulfitobacterriia* were present in PASS B10 and PASS B10 + HC columns whereas on Day 540, *Desulfobacteria* were only present in PASS B10 and PASS B10 + HC columns and *Desulfitobacteriia* had decreased below 1.0% in all PASS columns. In addition, the relative abundance of known SRB was greater in PASS-treated FFT than untreated FFT on all days in which microbial communities were analyzed (Days 120, 240, 360, and 540). This is consistent with the higher concentration of electron acceptors for SRB in PASS-treated FFT. Interestingly, microbial communities in FFT B20 + HC did not contain any known SRB on Days 120, 240, 360, or 540. It is possible that the sulfate reduction in FFT B20 + HC tailings occurred earlier than Day 120 and/or other microbial communities capable of sulfur metabolism (other than the identified known SRB) were responsible for the sulfate reduction in FFT B20 + HC columns.

Methanomicrobia were present in FFT B20 + HC and PASS B20 + HC columns on Day 540 at 4.5 and 3.4%, respectively. *Methanomicrobia* (of the genus *Methanosaeta*) produce CH_4 through acetate consumption (Pyzik et al. 2018). This is consistent with the CH_4 production in these columns during the second half of the experiment as seen in Figure 4-20A. Methanogens were present in other columns as well, though their relative abundance was <1.0%. Given the lack of detectable methanogens in the tailings on Day 0, the lag in CH_4 production is at least partly due to the time required for methanogenic communities to establish. Other factors that may have contributed to the lag in CH_4 production include microorganisms involved in methanogenic pathways being left with more recalcitrant hydrocarbons, the need to acclimate to new carbon sources, and/or competition with SRB.

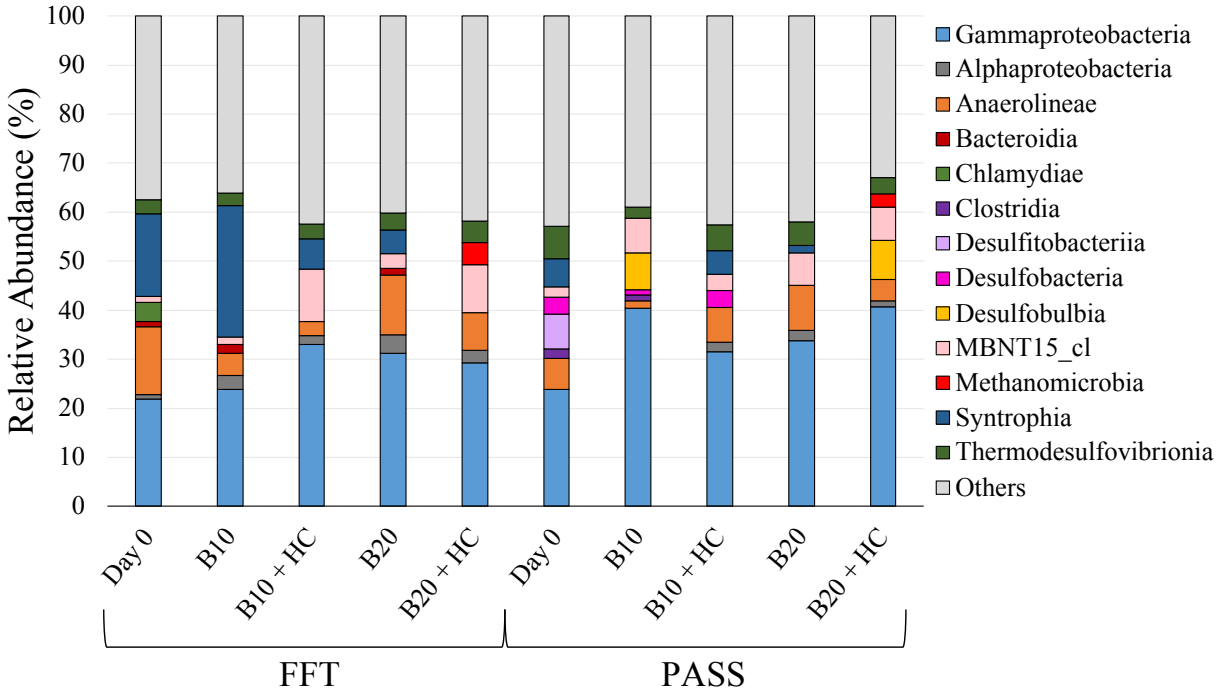

Figure 4-21. Stacked bars illustrating the relative abundances of microorganisms at the class level in FFT and PASS, represented by the percentage of the 16S rRNA read counts within each group. A relative abundance of less than 1% is assigned to 'Others'. All bars (except for FFT, Day 0 and PASS, Day 0) represent tailings samples collected from 19 L columns on Day 540. FFT, Day 0 and PASS, Day 0 are provided for comparison. Stacked bars illustrating the relative abundance of microorganisms at the class level in FFT and PASS samples collected on Day 120 is provided in Appendix B4, Figure B-15. Label B refers to Big (19 L) columns; 10 or 20 refer to 10°C or 20°C storage temperature; HC refers to hydrocarbon amended tailings.

Hydrocarbon concentrations in the tailings of the 19 L columns were measured on Day 540 to confirm that the hydrocarbons added on Day 0 (toluene, o-xylene, m-xylene, p-xylene, octane, decane, 2-methlypentane, and 3-methylhexane) were degraded throughout the study. Greater than 98% of each of the hydrocarbons was biodegraded under anaerobic conditions in the hydrocarbon amended columns. Hydrocarbon amended tailings underwent almost complete sulfate reduction in 120 d, with greater than 96% and 93% of the sulfate reduced in hydrocarbon amended FFT and PASS, respectively. Conversely, during that same period, unamended FFT and PASS saw only 3% and 28% of the sulfate reduced, respectively. As such, the SRB present in the tailings were capable of degrading at least some components of the hydrocarbon mixture of monoaromatics, n-alkanes, and iso-alkanes. Toluene was reduced to an average concentration of $\leq$ 0.2 ppm in all columns and was likely degraded first by SRB (Spormann and Widdel 2000). Concentrations of

xylenes, octane, decane, 2-methlypentane, and 3-methylhexane ranged from 0.6 to 12.7 ppm on Day 540, indicating the hydrocarbons were almost entirely degraded by the microbial communities in the tailings. The average concentration and standard deviation of individual hydrocarbons in the 19 L columns on Day 540 is provided in Appendix B4, Table B-3.

4.4 Conclusions

This column study demonstrates the importance of PASS treatment, hydrocarbon amendments, and column size on the biogeochemical and geotechnical behavior of oil sands tailings. Both column size and PASS treatment impacted NWR from the tailings. The 1 L columns had a rapid initial NWR and quickly achieved self-weight consolidation because of the lower total stress and shorter drainage path in these columns compared to the 19 L columns. However, NWR from 19 L columns ultimately surpassed that of comparable 1 L columns as tailings in the 19 L columns underwent long-term settlement and self-weight consolidation. As a result, tailings in the 19 L columns generally achieved a higher solids content than tailings in the 1 L columns. PASS treatment did not improve dewatering performance and instead resulted in a lower NWR than untreated FFT, possibly due to poor flocculation performance. Further, the solids content of the tailings was not improved by PASS treatment, which is consistent with the lower NWR from PASS-treated FFT. The lower NWR and solids content of PASS-treated FFT in this study highlights challenges in achieving good flocculation conditions and suggests that dewatering performance should be carefully monitored in the field to ensure PASS treatment is reaching its intended targets. Hydrocarbon amendments had a small but positive impact on solids content and this is likely a result of microbially mediated consolidation.

The main impact of PASS treatment on pore water quality was through sulfate reduction; DOC concentrations were largely unaffected by PASS treatment. Further, the dominant microbial process in this study was sulfate reduction, though methanogenic communities had started to develop in some of the columns by Day 540. Sulfate reduction occurred in all 64 columns, though tailings with hydrocarbon amendments and/or PASS treatment had the most extensive sulfate reduction. Hydrocarbon amendments led to almost complete (>99%) reduction of sulfate in untreated and PASS-treated FFT, with average pore water sulfate concentrations reduced by 628 mg/L in PASS + HC columns and 314 mg/L in FFT + HC columns by Day 540. Without

hydrocarbon amendments, average pore water sulfate concentrations were reduced by 242 mg/L in PASS-treated FFT and 71 mg/L in untreated FFT by Day 540. Over the course of the experiment, PASS-treated FFT also had a greater abundance of known SRB than the untreated FFT. Sulfate reduction generated aqueous sulfide species which were present in the tailings and/or water caps in all 19 L columns and in most of the 1 L PASS-treated FFT columns, though the highest concentrations were in PASS + HC columns. $H_2S_{(g)}$ was mostly below detection but the sulfur content of the tailings increased over 540 d, presumably due to the precipitation of reduced sulfur species as metal sulfides. These results suggest that if Suncor Base Plant were to start applying their PASS treatment process to tailings that contain residual diluent, the tailings would undergo almost complete sulfate reduction in a short period time, leading to the generation of reduced sulfur in the aqueous, gaseous, and/or solid phases. The extensive sulfate reduction in hydrocarbon amended tailings also led to significant increases in alkalinity and $CO_{2(g)}$, though alkalinity and $CO_{2(g)}$ increased in all columns over the 540 d. Divalent cations in the hydrocarbon amended tailings were subsequently impacted and presumably precipitated as carbonate minerals, which could have contributed to the higher solids content in these tailings.

The water cap chemistry in the columns was impacted by i) advection, as pore water migrated into the water cap while the tailings underwent self-weight consolidation; ii) diffusion, which was especially apparent after self-weight consolidation was complete; and iii) biogeochemical reactions in the tailings. Column size, which impacts concentration gradient, had a significant impact on diffusion. Diffusion in the 1 L columns resulted in these columns having greater water cap concentrations of various pore water constituents than the 19 L columns, despite the 19 L columns achieving a higher NWR. Further, pore water concentrations of these chemicals decreased in the 1 L columns as a result of diffusion. This indicates that diffusion will continue to drive pore water constituents into a pit lake water cap, even after advective fluxes of these constituents are largely complete.

4.5 References

Ahmar Siddiqui, M.; Biswal, B.K.; Heynderickx, P.M.; Kim, J.; Khanal, S.K.; Chen, G.; Wu, D. Dynamic anaerobic membrane bioreactor coupled with sulfate reduction (SrDMBR) for saline wastewater treatment. *Bioresour. Technol.* **2022**, *346*, 126447.

American Standard for Testing Materials (ASTM). Standard Test Methods for Particle-Size Distribution (Gradation) of Fine-grained Soils Using the Sedimentation (Hydrometer) D7928-17; ASTM International: West Conshohocken, US, 2017.

American Standard for Testing Materials (ASTM). Standard Test Methods for Laboratory Determination of Water (Moisture) Content of Soil and Rock by Mass D2216-19; ASTM International: West Conshohocken, US, 2019.

Amoako, K. Geotechnical Behaviour of Two Novel Polymer Treatments of Oil Sands Fine Tailings. M.Sc. Thesis, University of Alberta, Edmonton, CA, 2020.

An, D.; Caffrey, S.M.; Soh, J.; Agrawal, A.; Brown, D.; Budwill, K.; Dong, X.; Dunfield, P.F.; Foght, J.; Gieg, L.M.; et al. Metagenomics of hydrocarbon resource environments indicates aerobic taxa and genes to be unexpectedly common. *Environ. Sci. Technol.* **2013**, *47*, 10708-10717.

Ball, J. W.; Nordstrom, D. K. User's Manual for WATEQ4F, with Revised Thermodynamic Data Base and Text Cases for Calculating Speciation of Major, Trace, and Redox Elements in Natural Waters, U.S. Geological Survey: Menlo Park, US, 1991.

Begmatov, S.; Beletsky, A.V.; Dedysh, S.N.; Mardanov, A.V.; Ravin, N.V. Genome analysis of the candidate phylum MBNT15 bacterium from a boreal peatland predicted its respiratory versatility and dissimilatory iron metabolism. *Front. Microbiol.* **2022**, *13*, 951761.

Burkus, Z.; Wheler, J.; Pletcher, S. GHG Emissions from oil sands tailings ponds: Overview and modelling based on fermentable substrates. In Part I: Review of Tailings Pond Facts and Practices; Alberta Environment and Sustainable Resource Development: Edmonton, CA, 2014.

Burow, L.C.; Woebken, D.; Marshall, I.P.G.; Singer, S.W.; Pett-Ridge, J.; Prufert-Bebout, L.; Spormann, A.M.; Bebout, B.M.; Weber, P.K.; Hoehler, T.M. Identification of *Desulfobacterales* as primary hydrogenotrophs in a complex microbial mat community. *Geobiology* **2014**, *12*, 221-230.

Canada's Oil Sands Innovation Alliance (COSIA). Pit Lakes: A Surface Mining Perspective; Canada's Oil Sands Innovation Alliance: Calgary, CA, 2021; Available online: https://cosia.ca/sites/default/files/attachments/Park%20-%20COSIA%20-%20Pit%20Lakes%20- %20Final.pdf

Chou, L.; Garrels, R.M.; Wollast, R. Comparative study of the kinetics and mechanics of dissolution of carbonate minerals. *Chem. Geol.* **1989**, *78*, 269-282.

Clark, M.G.; Drewitt, G.B.; Carey, S.K. Energy and carbon fluxes from an oil sands pit lake. *Sci. Total Environ.* **2021**, *752*, 141966.

Collins, C.E.V.; Foght, J.M.; Siddique, T. Co-occurrence of methanogenesis and N_2 fixation in oil sands tailings. *Sci. Total Environ.* **2016**, *565*, 306–312.

Comiti, J.; Renaud, M. A new model for determining mean structure parameters of fixed beds from pressure drop measurements, with application to beds packed with parallelepipedal particles. *Chem. Eng. Sci.* **1989**, *44*, 1539–1545.

Cossey, H.L., Kaminsky, H., Ulrich, A.C. Evaluating the long-term behavior of an oil sands tailings reclamation strategy. In Proceedings of Mine Closure 2022, Brisbane AU, 4-6 October 2022.

Cossey, H.L.; Kuznetsov, P.V.; Ulrich A.C. Evaluating the biogeochemical and consolidation behavior of oil sands end pit lakes with accelerated aging. In Proceedings of the 25th International Conference on Tailings and Mine Waste, Banff, CA, 7-10 November 2021b.

D'Angelo, T.; Goordial, J.; Lindsay, M.R.; McGonigle, J.; Booker, A.; Moser, D.; Stepanauskus, R.; Orcutt, B.N. Replicated life-history patterns and subsurface origins of the bacterial sister phyla *Nitrospirota* and *Nitrospinota*. *ISME J.* **2023**, *17*, 891-902.

Dean, E.W.; Stark, D.D. A convenient method for the determination of water in petroleum and other organic emulsions. *Ind. Eng. Chem.* **1920**, *12(5), 486-490.*

Dompierre, K.A.; Barbour, S.L. Characterization of physical mass transport through oil sands fluid fine tailings in an end pit lake: A multi-tracer study. *J. Contam. Hydrol.* **2016**, *189*, 12–26.

Dompierre, K.A.; Barbour, S.L.; North, R.L.; Carey, S.K.; Lindsay, M.B.J. Chemical mass transport between fluid fine tailings and the overlying water cover of an oil sands end pit lake. *Water Resour. Res.* **2017**, *53*, 4725–4740.

Dompierre, K.A.; Lindsay, M.B.J.; Cruz-Hernández, P.; Halferdahl, G.M. Initial geochemical characteristics of fluid fine tailings in an oil sands end pit lake. *Sci. Total Environ.* **2016**, *556*, 196–206.

Dong, X.; Kleiner, M.; Sharp, C.E.; Thorson, E.; Li, C.; Liu, D.; Strous, M. Fast and simple analysis of MiSeq amplicon sequencing data with MetaAmp. *Front. Microbiol.* **2017**, *8*, 1461.

Fedorak, P.M.; Coy, D.L.; Salloum, M.J.; Dudas, M.J. Methanogenic potential of tailings samples from oil sands extraction plants. *Can. J. Microbiol.* **2002**, *48,* 21-33.

Foght, J.M.; Gieg, L.M.; Siddique, T. The microbiology of oil sands tailings: Past, present, future. *FEMS Microbiol. Ecol.* **2017**, *93*, fix034.

Gee, K.; Poon, H.Y.; Hashisho, Z.; Ulrich, A.C. Effect of naphtha diluent on greenhouse gases and reduced sulfur compounds emissions from oil sands tailings. *Sci. Total Environ.* **2017**, *598*, 916-924.

Gibson, R.E.; England, G.L.; Hussey, M.J.L. The theory of one-dimensional consolidation of saturated clays I, finite non-linear consolidation of thin homogeneous layers. *Géotechnique* **1967**, *17*, 261-273.

GWP Software Inc. FSCONSOL Slurry Consolidation Software User Manual. GWP Software Inc.: Edmonton, CA, 2007.

Holowenko, F.M.; MacKinnon, M.D.; Fedorak, P.M. Methanogens and sulfate-reducing bacteria in oil sands fine tailings waste. *Can. J. Microbiol.* **2000**, *46*, 927–937.

Kaminsky, H. Demystifying the methylene blue index. In Proceedings of the 4th International Oil Sands Tailings Conference, Lake Louise, CA, 7–10 December 2014.

Kuznetsov, P.; Wei, K.; Kuznetsova, A.; Foght, J.; Ulrich, A.; Siddique, T. Anaerobic microbial activity may affect development and sustainability of end-pit lakes: a laboratory study of biogeochemical aspects of oil sands mine tailings. *ACS EST Water*. **2023**, *3*, 1039-1049.

Lawrence, G.A.; Tedford, E.W.; Pieters, R. Suspended solids in an end pit lake: potential mixing mechanisms. *Can. J. Civ. Eng.* **2016**, *43*, 211–217.

Li, Y.; Kaminsky, H.; Gong, X.Y.; Sun, Y.S.; Ghuzi, M.; Sadighian, A. What affects dewatering performance of high density slurry? *Minerals* **2021**, *11*, 761.

Li, Y.; Kaminsky, H.; Revington, A.; Sadighian, A. A protocol to assess and screen new flocculant for Suncor's PASS program planning. In Proceedings of the 7th International Oil Sands Tailings Conference, Edmonton, CA, 4-7 December 2022a.

Li, Y.; Kaminsky, H.; Sadighian, A.; Sun, Y.S.; Murphy, F.; Gong, X.Y.; Ghuzi, M.; Rima, U. Impact of chemical and physical treatments on freeze-thaw dewatering of fluid fine tailings. *Cold Reg. Sci. Technol.* **2022b**, *193*, 103385.

Liang, J.; Guo, Z.; Deng, L.; Liu, Y. Oil Sands Mature Fine Tailings Consolidation Through Microbial Induced Calcite Precipitation, Oil Sands Research and Information Network: Edmonton, CA, 2014.

Liu, Q.; Montoya, B.M. Experimental study of consolidation behavior of mature fine tailings treated with microbial induced calcium carbonate precipitation. In Proceeding of Geo-Congress 2020, Minneapolis, US, 25-28 February 2020.

Meister, P. Two opposing effects of sulfate reduction on carbonate precipitation in normal marine, hypersaline, and alkaline environments. *Geology* **2013**, *41*, 499-502.

Mohamad Shahimin, M.F.; Foght, J.M.; Siddique, T. Preferential methanogenic biodegradation of short-chain *n*-alkanes by microbial communities from two different oil sands tailings ponds. *Sci. Total Environ.* **2016**, *553*, 250-257.

Mohamad Shahimin, M.F.; Foght, J.M.; Siddique, T. Methanogenic biodegradation of *iso*- alkanes by indigenous microbes from two different oil sands tailings ponds. *Microorganisms* **2021**, *9*, 1569.

Mohamad Shahimin, M.F.; Siddique, T. Sequential biodegradation of complex naphtha hydrocarbons under methanogenic conditions in two different oil sands tailings. *Environ. Pollut.* **2017a**, *221*, 398–406.

Mohamad Shahimin, M.F.; Siddique, T. Methanogenic biodegradation of paraffinic solvent hydrocarbons in two different oil sands tailings. *Sci. Total Environ.* **2017b**, *583*, 115–122.

Nozhevnikova, A.N.; Holliger, C.; Ammann, A.; Zehnder, A.J.B. Methanogenesis in sediments from deep lakes at different temperatures (2-70 °C). *Water Sci. Technol.* **1997**, *36*, 57-64.

Pannekens, M.; Voskuhl, L.; Mohammadian, S.; Köster, D.; Meier, A.; Köhne, J.M.; Kulbatzki, M.; Akbari, A.; Haque, S.; Meckenstock, R.U. Microbial degradation rates of natural bitumen. *Environ. Sci. Technol.* **2021**, *55*, 8700-8708.

Parkhurst, D. L., & Appelo, C. A. J. Description of Input and Examples for PHREEQC Version 3 – A Computer Program for Speciation, Batch-reaction, One-Dimensional Transport, and Inverse Geochemical Calculations, U.S. Geological Survey: Denver, US, 2013.

Pavlostathis, S.G.; Zhuang, P. Effect of temperature on the development of anaerobic cultures from a contaminated subsurface soil. *Environ.Technol.* **1991**, *12*, 679-687.

Pérez-Pantoja, D.; Donoso, R.; Agulló, L.; Córdova, M.; Seeger, M.; Pieper, D.H.; González, B. Genomic analysis of the potential for aromatic compounds biodegradation in *Burkholderiales*, *Environ. Microbiol.* **2011**, *14*, 1091-1117.

Pester, M.; Brambilla, E.; Alazard, D.; Rattei, T.; Weinmaier, T.; Han, J.; Lucas, S.; Lapidus, A.; Cheng, J.F.; Goodwin, L.; et al. Complete genome sequences of *Desulfosporosinus orientis* DSM765^T, *Desulfosporosinus youngiae* DSM17734^T, *Desulfosporosinus meridiei* DSM13257^T, and *Desulfosporosinus acidiphilus* DSM22704^T. *J. Bacteriol.* **2012**, *194*, 6300-6301.

Poon, H.Y.; Brandon, J.T.; Yu, X.; Ulrich, A.C. Turbidity mitigation in an oil sands pit lake through pH reduction and fresh water addition. *J. Environ. Eng.* **2018**, *114,* 04018127.

Pyzik, A.; Ciezkowska, M.; Krawczyk, P.S.; Sobczak, A.; Drewniak, L.; Dziembowski, A.; Lipinski, L. Comparative analysis of deep sequenced methanogenic communities: identification of microorganisms responsible for methane production. *Microb. Cell Factories* **2018**, *17*, 197.

Ramos-Padrón, E.; Bordenave, S.; Lin, S.; Bhaskar, I.M.; Dong, X.; Sensen, C.W.; Fournier, J.; Vourdouw, G.; Gieg, L.M. Carbon and sulfur cycling by microbial communities in a gypsum-treated oil sands tailings pond. *Environ. Sci. Technol.* **2011**, *45*, 439–446.

Reid, M.L.; Warren, L.A. S reactivity of an oil sands composite tailings deposit undergoing reclamation wetland construction. *J. Environ. Manag.* **2016**, *166*, 321–329.

Risacher, F.F.; Morris, P.K.; Arriaga, D.; Goad, C.; Colenbrander Nelson, T.; Slater, G.F.; Warren, L.A. The interplay of methane and ammonia as key oxygen consuming constituents in early stage development of Base Mine Lake, the first demonstration oil sands pit lake. *Appl. Geochem.* **2018**, *93*, 49–59.

Saidi-Mehrabad, A.; He, Z.; Tamas, I.; Sharp, C.E.; Brady, A.L.; Rochman, F.F.; Bodrossy, L.; Abell, G.C.J.; Penner, T.; Dong, X.; et al. Methanotrophic bacteria in oilsands tailings ponds of northern Alberta. *ISME J.* **2013**, *7*, 908–921.

Sentenac, P.; Lynch, R.J.; Bolton, M.D. Measurement of a side-wall boundary effect in soil columns using fibre-optics sensing. *Int. J. Phys. Model. Geotech.* **2001**, *4*, 35–41.

Siddique, T.; Fedorak, P.M.; Foght, J.M. Biodegradation of short-chain n-alkanes in oil sands tailings under methanogenic conditions. *Environ. Sci. Technol.* **2006**, *40*, 5459-5464.

Siddique, T.; Fedorak, P.M.; Mackinnon, M.D.; Foght, J.M. Metabolism of BTEX and naphtha compounds to methane in oil sands tailings. *Environ. Sci. Technol.* **2007**, *41*, 2350–2356.

Siddique, T.; Kuznetsov, P.; Kuznetsova, A.; Arkell, N.; Young, R.; Li, C.; Guigard, S.; Underwood, E.; Foght, J.M. Microbially-accelerated consolidation of oil sands tailings. Pathway I: changes in porewater chemistry. *Front. Microbiol.* **2014a**, *5*, Article 106.

Siddique, T.; Kuznetsov, P.; Kuznetsova, A.; Li, C.; Young, R.; Arocena, J.M.; Foght, J.M. Microbially-accelerated consolidation of oil sands tailings. Pathway II: Solid phase biogeochemistry. *Front. Microbiol.* **2014b,** *5*, 107.

Siddique, T.; Mohamad Shahimin, M.F.; Zamir, S.; Semple, K.; Li, C.; Foght, J.M. Long-term incubation reveals methanogenic biodegradation of C_5 and C_6 iso-alkanes in oil sands tailings. *Environ. Sci. Technol.,* **2015**, *49*, 14732–14739.

Siddique, T.; Penner, T.; Semple, K.; Foght, J.M. Anaerobic biodegradation of longer-chain n-alkanes coupled to methane production in oil sands tailings. *Environ. Sci. Technol.* **2011**, *45*, 5892–5899.

Siddique, T.; Semple, K.; Li, C.; Foght, J.M. Methanogenic biodegradation of *iso*-alkanes and cycloalkanes during long-term incubation with oil sands tailings. *Environ. Pollut.* **2020,** *258*, 113768.

Small, C.C.; Cho, S.; Hashisho, Z.; Ulrich, A.C. Emissions from oil sands tailings ponds: Review of tailings pond parameters and emission estimates. *J. Petrol. Sci. Eng.* **2015**, *127*, 490–501.

Spormann, A.M.; Widdel, F. Metabolism of alkylbenzenes, alkanes, and other hydrocarbons in anaerobic bacteria. *Biodegradation* **2000***, 11,* 85 – 105.

Stasik, S.; Loick, N.; Knöller, K.; Weisener, C.; Wendt-Potthoff, K. Understanding biogeochemical gradients of sulfur, iron and carbon in an oil sands tailings pond. *Chem. Geol*. **2014**, *382*, 44–53.

Stasik, S.; Wendt-Potthoff, K. Interaction of microbial sulphate reduction and methanogenesis in oil sands tailings ponds. *Chemosphere* **2014**, *103*, 59–66.

Stasik, S.; Wendt-Potthoff, K. Vertical gradients in carbon flow and methane production in a sulfate-rich oil sands tailings pond. *Water Res*. **2016**, *106*, 223–231.

Stawiński, J.; Wierzchoś, J.; Garoa-Gonzalez, M.T. Influence of calcium and sodium concentration on the microstructure of bentonite and kaolin. *Clays Clay Min.* **1990***, 38*, 617-622.

Suncor Energy Operating Inc. (Suncor). 2021 Fort Hills Fluid Tailings Management Report; Suncor Energy Operating Inc. on behalf of Fort Hills Energy Corporation; Calgary, CA, 2022b.

Tan, B.F.; Semple, K.; Foght, J. Anaerobic alkane biodegradation by cultures enriched from oil sands tailings ponds involves multiple species capable of fumarate addition. *FEMS Microbiol. Ecol.* **2015**, *91*, fiv042.

Tedford, E.; Halferdahl, G.; Pieters, R.; Lawrence, G.A. Temporal variations in turbidity in an oil sands pit lake. *Environ. Fluid Mech.* **2019**, *19*, 457–473.

Warren, L.A.; Kendra, K.E.; Brady, A.L.; Slater, G.F. Sulfur biogeochemistry of an oil sands composite tailings deposit. *Front. Microbiol.* **2016**, *6*, 1–14.

Wersin, P.; Leupin, O.X.; Mettler, S.; Gaucher, E.C.; Mäder, U.; De Cannière, P.; Vinsot, A.; Gäbler, H.E.; Kunimaro, T.; Kiho, K.; et al. Biogeochemical processes in a clay formation in situ experiment: part A – overview, experimental design and water data of an experiment in the Opalinus Clay at the Mont Terri Underground Research Laboratory, Switzerland. *Appl. Geochem.* **2011a**, *26,* 931-953.

Wersin, P.; Stroes-Gascoyne, S.; Pearson, F.J.; Tournassat, C.; Leupin, O.X.; Schwyn, B. Biogeochemical processes in a clay formation in situ experiment: part G – key interpretations and conclusions. Implications for repository safety. *Appl. Geochem.* **2011b**, *26,* 1023-1034.

Wilson, G.W.; Kabwe, L.K.; Beier, N.A.; Scott, J.D. Effect of various treatments on consolidation of oil sands fluid fine tailing. *Can. Geotech. J.* **2018**, *55*, 1059–1066.

Wong, M.; An, D.; Caffrey, S.M.; Soh, J.; Dong, X.; Sensen, C.W.; Oldenburg, T.B.P.; Larter, S.R.; Voordouw, G. 2015. Roles of thermophiles and fungi in bitumen degradation in mostly cold oil sands outcrops. *Appl. Environ. Microbiol.* **2015***, 81*, 6825-6838.

Wu, Z.; Guiping, L.; Ji, Y.; Li, P.; Yu, X.; Qiao, X.; Wang, B.; She, K.; Liu, W.; Liang, B.; et al. Electron acceptors determine the BTEX degradation capacity of anaerobic microbiota via regulating the microbial community. *Environ. Res.* **2022**, *215*, 114420.

Yu, X. Improving Cap Water Quality in an Oil Sands End Pit Lake with Microbial Applications. Ph.D. Thesis, University of Alberta, Edmonton, CA, 2019.

Zhang, M. Role of Bitumen Viscosity in Bitumen Recovery from Athabasca Oil Sands. M.Sc. Thesis, University of Alberta, Edmonton, CA, 2012.

Zhang, S. The relationship between organoclastic sulfate reduction and carbonate precipitation/dissolution in marine sediments. *Mar. Geol.* **2020**, *428,* 106284.

Znidarcic, D.; Van Zyl, D.; Ramirez, M.; Mittal, K.; Kaminsky, H. Consolidation characteristics of flocculated MFT – experimental column and SICT data. In Proceedings of the 5th International Oil Sands Tailings Conference, Lake Louise, CA, 4-7 December 2016.

5 EFFECTS OF PRESSURE ON THE BIOGEOCHEMICAL AND GEOTECHNICAL BEHAVIOR OF PASS-TREATED OIL SANDS TAILINGS IN PIT LAKES

5.1 Introduction

Suncor's PASS treatment process has been approved by AER and although a final capping option has not been approved yet, Suncor plans to cap PASS-treated deposits with water (AER 2022). PASS-treated FFT should have improved consolidation rates and pore water quality relative to untreated FFT (Suncor 2022b) but because this technology is still relatively new, there is no publicly available research on PASS-treated FFT. The environmental fate of two chemicals added during PASS treatment (alum and PAM) is of particular interest to researchers because of their potential to enhance biogeochemical cycling, especially sulfur cycling due to the addition of alum (Reid and Warren 2016; Warren et al. 2016), and the possibility of PAM i) biodegrading under anaerobic conditions (Dai et al. 2014, 2015; Haveroen et al. 2005; Hu et al. 2018; Song et al. 2017, 2020) and/or ii) moving through pit lake tailings and water caps. Further, the effects of pressure (from overlying tailings, for example) on the biogeochemical behavior of tailings have not been investigated to date.

Several studies have evaluated the effects of hydrostatic pressures (10+ MPa) on microbial activity in marine sediments and seawater (Barbato and Scoma 2020; Fichtel et al. 2015; Scoma et al. 2019; Tholosan et al. 1999). There is a general consensus that high pressures negatively impact cell growth and metabolic processes (Abe 2007; Pope and Berger 1973) and alter cell shape (Fichtel et al. 2015). Mesophilic microorganisms and microorganisms that are accustomed to atmospheric pressure are likely to experience negative impacts at hydrostatic pressures of several dozen MPa (Tholosan et al. 1999; Abe 2007) but these hydrostatic pressures are well beyond the hydrostatic pressures and total and effective stresses expected in a pit lake (maximum of roughly 1 MPa). The effects of partial pressures (0.1 to 10 MPa) on microbial activity have been evaluated in microcosm studies and researchers have generally reported enhanced microbial activity and shifts in microbial communities at higher partial pressures (Cassarini et al. 2019; Mayumi et al. 2013; Meulepas et al. 2010). The pressures used in these microcosms studies are more representative of the hydrostatic pressures and total and effective stresses expected in an oil sands pit lake and suggest

that microbial activity and biogeochemical cycling in oil sands tailings will be impacted, and possibly enhanced, by pressure.

This anaerobic column study evaluates i) the biogeochemical and geotechnical behavior of water-capped PASS-treated FFT and ii) the effects of pressures (0.3 to 5.1 kPa) on microbial activity and biogeochemical cycling in PASS-treated FFT. Pressures were applied to the PASS-treated FFT through a series of dead load surcharges, equivalent to increasing the total stress on the tailings, which should enhance consolidation of the PASS-treated FFT similar to the effect of increasing the thickness of an existing tailings deposit (Jeeravipoolvarn et al. 2009). While the effects of pressure on the geotechnical behavior of oil sands tailings are fairly well understood, this study is the first to investigate the effects of pressure on the biogeochemical behavior of oil sands tailings.

5.2 Materials and Methods

5.2.1 Materials

Approximately 1000 L of tailings were collected from an oil sands tailings pond sometime prior to 2021 and stored in a room temperature tote for an unknown period of time. The tailings pond contained untreated FFT, thickened FFT, and paraffinic FTT (collectively referred to as FFT hereinafter). In 2021 the tailings were homogenized and subsampled into 20 L pails, and stored at room temperature at NAIT (Edmonton, CA) until treatment in 2022. Approximately 100 L of FFT was treated at NAIT using a treatment process similar to Suncor's PASS technology. Both alum ($Al_2(SO_4)_3 \cdot 14H_2O$) and partially hydrolyzed anionic PAM were added to FFT as part of the treatment process. Alum was added at a dose of 950 mg/L of FFT pore water and PAM was added at a dose of 1.015 g/kg of FFT solids. The coagulation/flocculation procedure detailed in subsection 4.2.1 was modified for this experiment to allow for a larger treatment volume. Approximately 10.8 L of tailings were treated at a time in 20 L baffled pails. The FFT was pre-mixed at 166 rpm for 1.5 min using a square 8.2 in. impeller, after which alum was injected with a 30 mL syringe and mixing continued for 10 sec. The mixing speed was then reduced to 44 rpm for 13 min to allow the FFT to coagulate. The mixing speed was increased to 166 rpm again while the polymer solution was injected at a rate of 550 mL/min. Mixing continued at 166 rpm until the peak torque was reached, after which the mixing speed was reduced to 50 rpm for 1 min to condition the flocs.

After coagulation/flocculation, the treated FFT was mechanically sheared using an overhead mixer (at a rate and duration equivalent to a shear energy of 1500 kJ/m^3) to mimic the mechanical shearing that Suncor's PASS-treated FFT is subjected to during pipeline transport to DDA3. The PASS-treated FFT was then transported to the University of Alberta in 20 L pails and combined and homogenized in a 200 L container (i.e. mixed for 2 min with a helical ribbon impeller attached to a drill) before being placed in the columns. Transport and homogenization at the University of Alberta would have applied additional shear energy to the PASS-treated FFT.

Freshwater from BCR, which is adjacent to Syncrude's BML, was used for the column water caps. BCR water was collected in 2015 and stored in airtight 20 L pails in the dark in a 4°C cooler at the University of Alberta.

5.2.2 Column Set-up

Twelve cast acrylic columns (30 cm height, 14 cm inner diameter, 5.5 L, Plastics Plus Ltd., Edmonton, CA) were constructed for this experiment (see Figure 5-1). Two sampling ports (1.9 cm stainless steel ball valves, FxM NPT, Direct Material, Irving, US) were installed on each column to sample the tailings and water cap. A 0 to 69 kPa pore pressure transducer (RK-68075-42, Cole Parmer, Montreal, CA) was attached near the base of each column with a stainless steel ball valve (0.6 cm, FxM NPT, Direct Material, Irving, US) to monitor pore pressure dissipation. All columns were equipped with a 0.6 cm thick cast acrylic lid (Plastics Plus Ltd., Edmonton, CA)). The base of each column was made up of either a 0.6 or 1.3 cm thick cast acrylic sheet (Plastics Plus Ltd., Edmonton, CA) and similarly, the column thickness was either 0.6 or 1.3 cm. Thicker (1.3 cm) materials were used for six of the columns to ensure they would withstand dead load surcharges.

On Day 0, the volume of PASS-treated FFT, freshwater cap, and headspace in each column was as follows: 4 L, 0.5 L, and 1 L, respectively. Additional headspace was provided for each column through a series of gas collection bottles which were connected to the column headspace through tubing. This gas collection system also ensured that the column headspace remained at atmospheric pressure. Headspace was sampled through a Chemglass butyl rubber septum embedded into the center of each lid. Columns were kept under anaerobic conditions (similar to the anaerobic

conditions that exist in BML FFT (Dompierre et al. 2016)) by flushing the headspace with nitrogen gas and sealing the lids with silicon to ensure the columns were airtight. All columns were pressure tested multiple times throughout the experiment to ensure anaerobic conditions were maintained. While the anaerobic conditions in the columns mimic that of FFT in pit lakes, pit lake water caps may be aerobic (depending on the season) (Lawrence et al. 2016; Risacher et al. 2018). As such this study does not evaluate aerobic biogeochemical processes that may occur in pit lake water caps (such as oxidation of sulfur species or aerobic methanotrophy) (Chen et al. 2020; Risacher et al. 2018). Columns were also stored in the dark under black tarps, because light does not penetrate BML FFT, and at room temperature, though the average annual temperature of BML FFT is roughly 10°C (Dompierre et al. 2016; Tedford et al. 2019). All columns were set up in February 2022 and monitored for roughly 360 d.

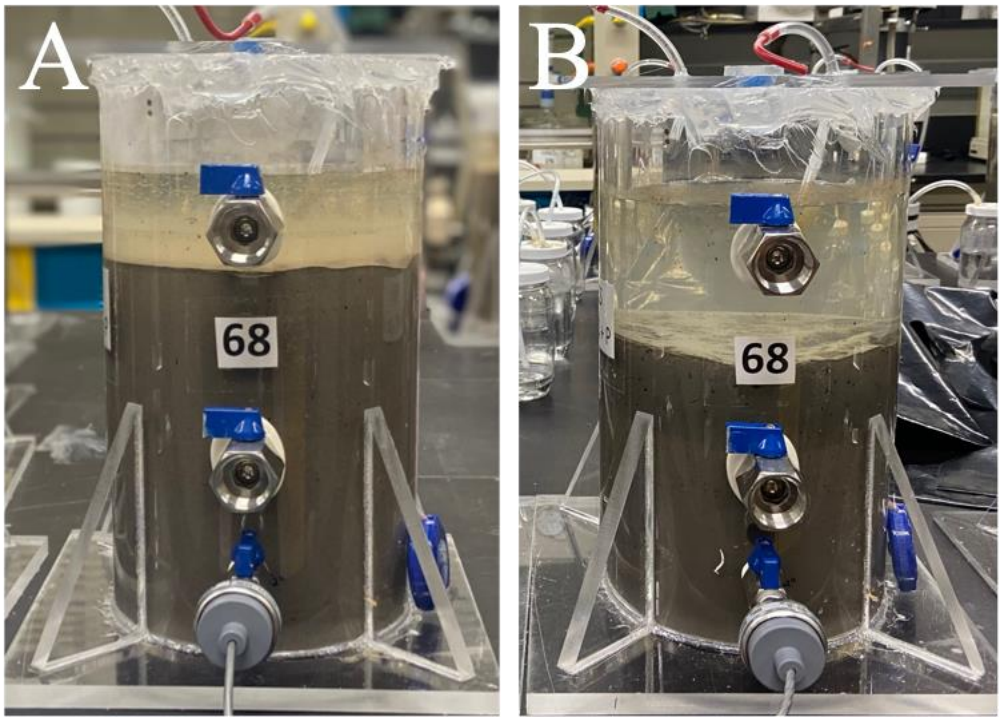

Figure 5-1. A: Day 0 photo of a 5.5 L column containing PASS-treated FFT and a freshwater cap and B: Day 60 photo of the same column after undergoing self-weight consolidation.

Table 5-1 summarizes the 12 columns that were set up in triplicate and the two factors tested (hydrocarbon amendments and pressure) as part of this experiment. Tailings in six of the columns

were amended with a hydrocarbon mixture similar to that of fresh naphtha diluent (Kuznetsov et al. 2023; Mohamad Shahimin and Siddique 2017a). The purpose of hydrocarbon amendments was to i) accelerate microbial activity and subsequent biogeochemical cycling processes in the columns in order to evaluate these processes in the laboratory in a timely manner and ii) evaluate the biogeochemical implications of applying the PASS-treatment process to tailings that contain diluent (i.e. FTT). Based on previous research by Kuznetsov et al. (2023), a mixture of BTEX compounds (150 ppm toluene, 50 ppm o-xylene, 50 ppm m-xylene, 50 ppm p-xylene), n-alkanes (500 ppm n-octane, 500 ppm n-decane), and iso-alkanes (500 ppm 2-methylpentane, 500 ppm 3-methylhexane) was selected as the carbon source for microorganisms in PASS-treated FFT. For each of the six columns containing hydrocarbon amended tailings, the hydrocarbons were added to 4 L of PASS-treated FFT as a free phase. The tailings were then mixed thoroughly (by hand for approximately 1 min.) and placed in a column.

Table 5-3. Summary of 12 columns set up in triplicate for pressure experiments.

Column	Tailings Treatment (PASS)	Hydrocarbon (HC) Amendments	Pressure (P) Applied (0.3 to 5.1 kPa)
PASS, No HC + No P	✓		
PASS, No HC + P	✓		✓
PASS, HC + No P	✓	✓	
PASS, HC + P	✓	✓	✓

Tailings in all 12 columns underwent self-weight consolidation during the first 60 d of the experiment. After self-weight consolidation, tailings in six of the columns were subjected to a series of dead loads (0.3, 0.6, 1.2, 2.4, and 5.1 kPa). On Day 60, the lightest dead load (0.3 kPa) was placed on the tailings and pore pressure dissipation and vertical deformation of the tailings were monitored for roughly 60 d. A circular cast acrylic disc with drainage holes was placed between the tailings and dead load to ensure pressure was applied evenly over the tailings surface. Every 60 d (by which point pore pressure and vertical deformation should have plateaued), the dead load was doubled. This multi-step loading scheme allowed the FFT to gain strength before the application of higher loads. Sand was used for the lightest two dead loads (0.3 and 0.6 kPa) while custom-made carbon steel cylinders (13 cm diameter, varying thicknesses, GC Custom

Metal Fabrication Ltd., Edmonton, CA) were used for the 1.2, 2.4, and 5.1 kPa dead loads. The sand and carbon steel dead loads were sealed in plastic bags prior to being placed in the columns to limit the impact of the dead load applications on water cap chemistry (as the dead loads were at least partially submerged in the water caps). In order to apply dead loads to the tailings surface, each column had to be unsealed and resealed every 60 d. After resealing, the column headspaces and gas collection systems were flushed with nitrogen to ensure anaerobic conditions. To be consistent, the headspace in all 12 columns was flushed every 60 d, regardless of whether or not the columns had been recently unsealed/resealed.

5.2.2.1 Evaluating Behavior of Two Different PASS-treated Oil Sands Tailings

In addition to the 12 columns detailed above, three 1 L columns containing the PASS-treated FFT and BCR water described in subsection 5.2.1 were also set up as part of the experiment. The 1 L columns contained the same proportions of tailings, fresh water, and headspace as the 1 L columns in Chapter 4 (0.75 L PASS-treated FFT, 0.3 L BCR water, and 0.13 L headspace). The purpose of setting up these triplicate columns was to compare the effects of two different types of oil sands tailings on the geotechnical and biogeochemical behavior of PASS-treated FFT, given that the PASS-treated FFT in Chapter 4 consolidated at a slower rate than untreated FFT and produced little to no methane. The columns were monitored for 360 d and were stored in the dark, at room temperature, and under anaerobic conditions. As such, these columns were comparable to the 1 L PASS S20 columns presented in Chapter 4.

5.2.3 Column Monitoring and Measurements

5.2.3.1 Geotechnical Parameters

Solids, water, and bitumen content, bulk density, and yield stress were measured in Day 0 samples of both PASS-treated and untreated FFT. The elemental composition of the tailings solids was determined for Day 0 samples of PASS-treated FFT. Day 0 samples of the untreated FFT were also measured for PSD, which provides SFR and D_{50}, and MBI, which indicates clay content and activity. PSD and MBI of the PASS-treated FFT were not measured because these parameters are assumed to be the same in both the untreated and PASS-treated FFT. Tailings collected from all columns on Day 360 were also measured for solids, water, and bitumen content, and elemental composition of the solids.

Solids and water content were determined using oven analysis (105°C, 24 hr) following the procedure in ASTM D2216 (2019). Bitumen content was conducted at NAIT following the method developed by Dean and Stark (1920). Yield stress was measured with a Brookfield rheometer (shear rate 0.1 rpm, DV3T, CAN-AM Instruments Ltd., Oakville, CA) and V-71 and V-72 spindles (Brookfield Engineering Labs Ltd., Middleboro, US). The elemental composition of the tailings solids was determined using XRF which was conducted at NAIT using an S8 Tiger Wavelength Dispersive XRF Spectrometer (Bruker AXS, US). The purpose of XRF was to evaluate the precipitation of sulfur species over the course of the experiment. Prior to XRF analysis, tailings samples were mixed with Celleox, a cellulose based binder, to create a paste-like consistency and minimize surface interference of water. Hydrometer tests were conducted to determine the PSD of the untreated FFT, following ASTM D79828 (2017) and using dispersed conditions (4% sodium metaphosphate dispersant) and a 152H hydrometer (Fisherbrand, Buena, US). MBI measurements of the untreated FFT were performed at NAIT following the method developed by Sethi (1995). Full details on the Dean-Stark, XRF, hydrometer test, and MBI procedures are available in subsection 4.2.3.1.

Consolidation of the tailings in each column was continuously monitored by measuring settlement of the FFT-water interface (every 1 to 7 d, as appropriate) and pore pressure at the base of the columns (every 30 min). Interface settlement was used to i) determine the end of a consolidation phase (after which a higher dead load could be applied) and ii) calculate the NWR from the tailings (see Equation 4-1 in subsection 4.2.3.1). The purpose of collecting pore pressure data was to monitor pore pressure dissipation, which can also be used to determine the end of a consolidation phase. Pore pressure transducers near the base of each column were connected to a Keysight data logger (DAQ973A Data Acquisition System and Keysight DAQM901A 20 channel multiplexers, Santa Rosa, US). Time intervals for pore pressure data collection were set at 30 min, though intervals were decreased during the application of a new dead load to capture sudden changes in pore pressure.

5.2.3.2 Water Chemistry Parameters

Water cap and pore water samples were collected from all columns on Day 0 and every 60 d thereafter (prior to the application of a new dead load). Water cap and pore water samples were analyzed for the following: pH, cations (Na^+, K^+, Ca^{2+}, Mg^{2+}, Fe, and Al), anions (Cl^- and SO_4^{2-}), aqueous total sulfide species (H_2S, HS^-, S^{2-}), total alkalinity, DOC, COD, and ammonia/ammonium (NH_3/NH_4^+). Pore water samples and select Day 360 water cap were also analyzed for PAM to determine if the parent compound was breaking down over the course of the experiment. Charge balance calculations were conducted every 60 d using the average concentrations of all measured cations and anions in the pore water and water caps to confirm the accuracy of the water chemistry results.

The pH of the water cap and tailings were measured through the column sampling ports using an E-135M pH probe (Gain Express) and a Thermo Scientific Orion Dual Star pH/ISE Benchtop. Cations and anions were measured in 0.45 µm nylon filtered samples at the University of Alberta's NRAL. Cations were measured using a Thermo iCAP6300 Duo ICP-OES (Thermo Fisher Corp., Cambridge, UK) and anions were measured using a colormetric autoanalyzer (Thermo Gallery Plus Beermaster AutoAnalyzer, Thermo Scientific, Vantaa, FI). Total sulfide species were measured using HACH's DR 900 Multiparameter Portable Colorimeter and Sulfide Reagent Kit (Loveland, US), following the USEPA Methylene Blue Method (HACH Method 8131). Sulfide species can quickly oxidize following sample collection from anaerobic columns. As such this analysis was time-sensitive and measurements were likely underestimated for pore water samples, which had to be centrifuged prior to sulfide species analysis.

A Metrohm Eco Titrator (Herisau, CH) was used to measure total alkalinity in unfiltered samples (0.02 N H_2SO4 titrant, pH 4.5 endpoint). The non-volatile DOC content of 0.45 µm nylon filtered samples was measured with a Shimazdu Model TOC-L_{CPH} (Kyoto, JP). The HACH DR 900 Multiparameter Portable Colorimeter (Loveland, US) was also used to measure COD and ammonia/ammonium in the samples. COD measurements were conducted on unfiltered samples using HACH Digestion Vials (high range, 20 – 1500 mg/L, US) and a HACH Digital Reactor Box 200 (Loveland, US), following the procedure outlined in the USEPA Reactor Digestion Method (HACH Method 8000). Measurements of ammonia and ammonium (combined, measured as NH_3-

N) used the HACH AmVer™ (high range, 0.4 to 50.0 mg/L) ammonia nitrogen Test 'N Tube™ Reactor Tubes and Reagent Set (London, CA) and followed the procedure outlined in the AmVer™ Salicylate Test 'N Tube™ Method (Hach Method 10031).

PAM was measured in 0.45 µm nylon filtered pore water and water cap samples using size exclusion – high performance liquid chromatography (SEC-HPLC) (Agilent 1200 Infinity HPLC, Santa Clara, US) with an Agilent PL Aquagel-OH Mixed-H column (8 µm, 300 x 7.5 mm, Santa Clara, US) and an Agilent PL Aquagel-OH Guard column (8 µm, 50 x 7.5 mm, Santa Clara, US). Size exclusion chromatography was used to determine if the parent compound had been degraded into compounds of lower molecular weight. The mobile phase was 0.01 M NaH_2PO_4 + 0.1 M NaCl with pH adjusted to 7.0 and the column flow rate was set to 0.75 mL/min. The sample injection volume was 20 µL and run time was 20 min per sample. SEC-HPLC separates compounds based on molecular weight and as such, it would be difficult to determine the difference between the parent compound and biodegradation products of similar molecular weights (such as polyacrylic acid) using this method, particularly in a degraded sample.

5.2.3.3 Microbial Activity and Communities

Biogenic gas emissions (of H_2S, CO_2, and CH_4) and 16S sequencing were used to evaluate microbial activity and microbial communities in the columns. Biogenic gases were measured in the column headspace every 60 d (prior to the addition of a new dead load). Similarly, 1.5 mL tailings samples were collected every 60 d for DNA extraction and sequencing. Hydrocarbon concentrations (of toluene, o-xylene, m-xylene, p-xylene, octane, decane, 2-methylpentane, and 3-methylhexane) in the tailings were also measured on Day 0 and 360 to confirm that the hydrocarbons added to six of the columns were degraded by microbial communities over the course of the experiment.

H_2S gas was measured in 30 mL headspace samples at AGAT Laboratories (Calgary, CA) using GC-SCD. CO_2 and CH_4 gas were measured in 0.1 mL headspace samples using a GC-TCD (Agilent 7890+ GC, Agilent HP-PLOT/Q column: 30 m x 320 µm x 0.2 µm) and GC-FID (Agilent 7890+ GC, Agilent HP-5MS column: 30 m x 250 µm x 0.25 µm), respectively. Full details on the GC-TCD and GC-FID operating conditions are available in subsection 4.2.3.3. Hydrocarbon

concentrations in the tailings were determined using the methane extraction and GC-MS protocol developed by the University of Alberta's Soil Chemistry and Environmental Microbiology Laboratory and described in subsection 4.2.3.3.

Tailings samples collected for DNA extraction were centrifuged twice (5000 rpm, 5 min, 4°C) and stored at -20°C until the extractions were performed. FastDNA^{TM} Spin Kits for Soils (MP Biomedical, Solon, US) were used to complete the DNA extractions. Triplicate samples of extracted DNA were pooled prior to being sent to the University of Alberta's MBSU for PCR amplification and amplicon sequencing. Based on previous research of bacteria and archaea in oil sands tailings (An et al. 2013), the following universal primers were selected to target the V6 to V8 regions of bacterial and archaeal 16S rRNA genes: 926F (AAACTYAAAKGAATWGRCGG) and 1392R (ACGGGCGGTGWGTRC). Subsequent amplicon sequencing was performed using an Illumina MiSeq instrument and MiSeq Reagent Kit v3 (600 cycle, PE300, Cat# MS-102-3003, San Diego, US). Raw data from amplicon sequencing was processed with the MetaAmp pipeline (97% similarity cut-off, 300 bp amplicon length), which uses the SILVA database (Dong et al. 2017).

5.2.4 Statistical Analysis

Multi-factor analysis of variance (ANOVA) was computed with XLSTAT software in Microsoft Excel and used to determine the statistical significance (at $\alpha = 0.05$) of differences in measurements of geotechnical and biogeochemical parameters in the columns. ANOVA was used to determine the effects of pressure and/or hydrocarbon amendments on the geotechnical and biogeochemical parameters measured in the tailings and water caps. Statistical significance was analyzed using the Day 360 measurements of all parameters. Select parameters were also analyzed for statistical significance on Day 60, 120, 180, 240 and/or 300 if it was suspected that the statistical significance results would be different for Day 360 versus other measurement days. Statistical significance results are based on Type III Sum of Squares, which accounts for any interaction between the two independent variables. All statistically significant factors for each parameter are provided in Appendix C1, Table C-1, along with F and p values.

5.3 Results and Discussion

5.3.1 Initial Characterization of Materials

Day 0 geotechnical characterization of the PASS-treated FFT used in the columns is presented in Table 5-2. Day 0 water chemistry characterization of tailings pore water and BCR fresh water is provided in Table 5-3. Characterization data of untreated FFT is also provided in Tables 5-2 and 5-3 for comparison, though all columns contained PASS-treated FFT. All measurements presented in Tables 5-2 and 5-3 were taken prior to hydrocarbon amendments (if applicable), though these amendments would not substantially impact the values presented in the two tables because the volume of hydrocarbons added was small (12.8 mL) and the hydrocarbons likely mixed with and became soluble in the bitumen phase. In future studies, SARA (saturate, aromatic, resin, and asphaltene) analysis of the bitumen before and after hydrocarbon addition could confirm that the hydrocarbons mixed with the bitumen phase.

Table 5-2. Day 0 **geotechnical characterization** of PASS-treated FFT. Geotechnical characterization of the untreated FFT (prior to PASS treatment) is provided for comparison. Results are presented as average ± standard deviation of replicates (three or more). Measurements were taken prior to hydrocarbon amendments, if applicable. Modified from Cossey and Ulrich (2022).

Geotechnical Parameters	PASS-treated FFT	Untreated FFT
Solids content (oven analysis, wt%)	33.4 ± 0.0	36.7 ± 0.1
Water content (oven analysis, wt%)	66.6 ± 0.0	63.3 ± 0.1
Bitumen content (Dean-Stark, wt%)	3.3 *	2.6 ± 0.5
Bulk density (g/mL)	1.2 ± 0.0	1.2 ± 0.0
Yield stress (Pa)	7.8 ± 0.9	2.7 ± 0.1
Sand to fines ratio (SFR)	**	0.3 ± 0.1
Median particle diameter (D_{50}) (μm)	**	6.3 ± 1.1
Methylene blue index (MBI) (meq/100 g)	**	5.8 ± 0.1
Sulfur content (solid phase, %)	0.7 ± 0.3	-

** Parameter only measured once due to sample volume limitations*

*** Parameter measured in untreated FFT but assumed to be the same in PASS-treated FFT*

Table 5-3. Day 0 **water chemistry characterization** of PASS-treated FFT and BCR water. Water chemistry characterization of the untreated FFT (prior to PASS treatment) is provided for comparison. Results are presented as average ± standard deviation of replicates (three or more). Measurements were taken prior to hydrocarbon amendments, if applicable. Modified from Cossey and Ulrich (2022).

Water Chemistry Parameters	PASS-treated FFT	Untreated FFT	BCR Water
pH	7.1 ± 0.1	7.6 ± 0.0	8.5 ± 0.0
Sodium, Na^+ (mg/L)	322.3 ± 2.6	284.7 ± 1.6	42.4 ± 0.5
Potassium, K^+ (mg/L)	25.2 ± 0.2	18.3 ± 0.1	2.2 ± 0.1
Calcium, Ca^{2+} (mg/L)	57.5 ± 0.5	27.0 ± 0.2	22.4 ± 0.2
Magnesium, Mg^{2+} (mg/L)	31.0 ± 0.3	17.6 ± 0.4	11.8 ± 0.2
Iron, Fe (mg/L)	0.000 ± 0.000	0.002 ± 0.002	0.008 ± 0.003
Aluminum, Al (mg/L)	BDL*	BDL*	BDL*
Chloride, Cl^- (mg/L)	126.5 ± 0.4	123.6 ± 0.3	7.3 ± 0.1
Sulfate, SO_4^{2-} (mg/L)	437.6 ± 2.8	11.9 ± 0.5	17.4 ± 0.2
Sulfide species, H_2S, HS^-, S^{2-} (mg/L)	0.0 ± 0.0	0.0 ± 0.0	0.0 ± 0.0
Total alkalinity (mg $CaCO_3$/L)	365.7 ± 1.8	635.8 ± 2.2	194.4 ± 3.0
Bicarbonate, HCO_3^- (mg/L)	446.1 ± 2.1	775.6 ± 2.7	237.2 ± 3.7
Dissolved organic carbon (DOC) (mg/L)	31.1 ± 1.1	36.1 ± 1.4	18.0 ± 0.3
Chemical oxygen demand (COD) (mg O_2/L)	139 ± 4	**	36 ± 5
Ammonium, NH_4^+ (mg/L)	0.0 ± 0.0	0.0 ± 0.0	0.0 ± 0.0

** BDL indicates below detection limit*

*** Parameter not measured in untreated FFT*

PASS treatment lowered the solids content of the tailings, as seen in Table 5-2, because the polymer solution added during PASS treatment increased the amount of water in the tailings. Interestingly, the PASS treatment process appeared to increase the bitumen content of the sample. However, this value is likely not representative of the bulk sample because i) it is based on a single measurement, ii) bitumen content is notoriously difficult to determine as bitumen is not homogenously mixed throughout the sample, and iii) if anything, bitumen content should decrease following PASS treatment as bitumen visibly adheres to equipment during coagulation/flocculation and shearing.

As shown in Table 5-3, PASS treatment lowered the pH of the tailings, from 7.6 to 7.1, which was likely a result of alum consuming alkalinity. Alum addition in PASS treatment also increased pore water sulfate concentrations by roughly 425 mg/L. The concentration of DOC in the PASS-treated FFT pore water (31.1 ± 1.1 mg/L) was lower than that of untreated FFT (36.1 ± 1.4 mg/L). One purpose of PASS treatment is to reduce the mobility of organics, which may theoretically be achieved by lowering the pH, thereby increasing the dissolution of calcium carbonate and immobilizing NAFCs in the form of calcium naphthenate. However, there is no publicly available literature which demonstrates calcium naphthenate formation as a result of PASS treatment. Another possible reason for the lower DOC concentration following PASS treatment is the water chemistry of the polymer solution (which was made up of PAM and FFT pore water). The FFT pore water used in the polymer solution was similar to that of the untreated FFT pore water seen in Table 5-3, though there were some differences, particularly with regards to cation concentrations. As such, these differences may have contributed to both the lower DOC and higher cation concentrations in the tailings following PASS treatment. The BCR water that made up the column water caps on Day 0 had a higher pH than the PASS-treated FFT, but lower or equal concentrations of all other parameters presented in Table 5-3, except dissolved iron.

5.3.2 Geotechnical Parameters

Figure 5-2 shows the average NWR from the columns over 360 d. Dead load applications (0.3, 0.6, 1.2, 2.4, and 5.1 kPa) are indicated by arrows and occurred roughly every 60 d. All columns had a negative NWR on Day 0, which accounts for the polymer solution added to the tailings during PASS treatment. NWR quickly increased in all columns, becoming positive on Day 3 and surpassing 20% on Day 12. This means that by Day 12, 20% of the pore water had been released from the tailings in each column. During the first 60 d of the experiment, tailings in all 12 columns underwent self-weight consolidation. Tailings in six of the columns (PASS, No HC + No P and PASS, HC + No P) continued to undergo self-weight consolidation for the duration of the experiment. Though the rate of NWR slowed substantially after Day 12, these columns eventually reached a NWR of roughly 35% on Day 360. Tailings in the other six columns (PASS, No HC + P and PASS, HC + P) were placed under a series of five dead loads. As seen in Figure 5-2, after each dead load NWR spiked and then quickly plateaued. By Day 360, the PASS, No HC + No P columns had a NWR of 56% while the PASS, HC + P columns had a slightly lower NWR of 54%.

NWR was likely underestimated in most columns because of the production of biogenic gases in the tailings. Some of these biogenic gases were trapped in the tailings, as shown in Figure C-1 in Appendix C2, creating unsaturated pockets or channels. Because NWR was calculated using interface settlement rather than the volume of water released, these unsaturated zones resulted in a lower NWR. Biogenic gas emissions were highest in columns under pressure (PASS, No HC + P and PASS, HC + P), and as such, NWR may have been underestimated to a greater extent in these columns. However, this may have been offset by the increased solubility of gas in the tailings under pressure.

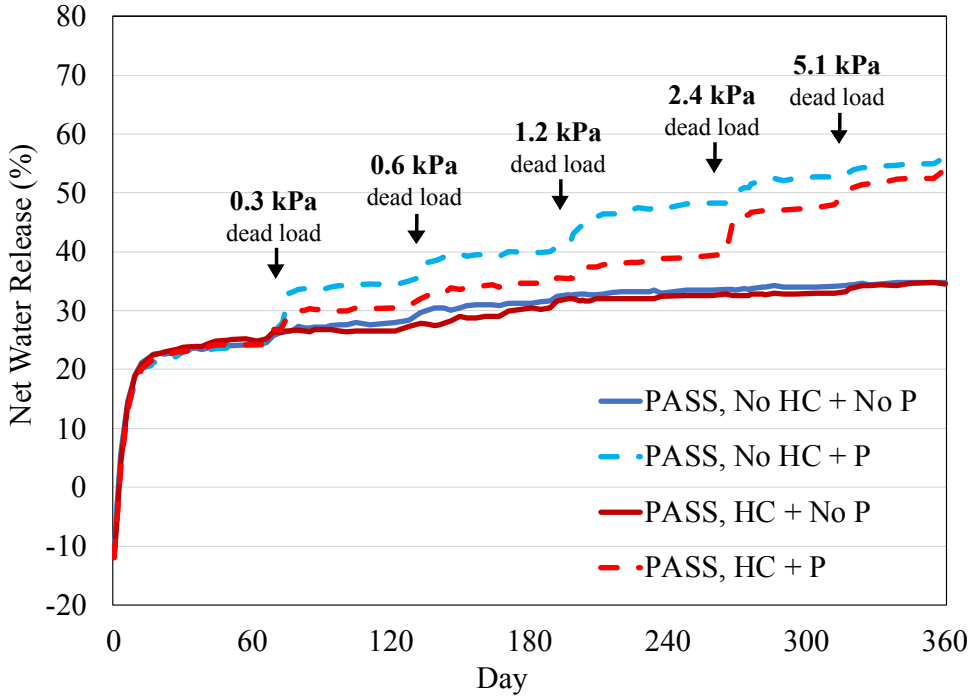

Figure 5-2. Net water release from PASS-treated FFT in 5.5 L columns over 360 d. Dead load (pressure) applications are indicated by arrows and occurred roughly every 60 d. Results are averaged from triplicate columns. Label HC refers to hydrocarbon amended tailings; P refers to tailings under pressure.

Pressure (dead load application) had a statistically significant influence on the Day 360 NWR from the tailings ($p < 0.0001$) while hydrocarbon amendments did not significantly impact NWR. However, hydrocarbon amendments slightly hindered NWR from the tailings over the course of the experiment, particularly in PASS, HC + P columns. The PASS, HC + P columns generated

more biogenic gas than all other columns, especially after Day 60. As such, the lower NWR in PASS, HC + P columns (relative to PASS, No HC + P columns) is presumably due to a higher volume of gas trapped in the tailings. This theory is supported by the Day 360 solids content measurements presented in Figure 5-3, which shows that the solids content of the tailings in PASS, No HC + P and PASS, HC + P columns are essentially the same on Day 360. Pressure had a statistically significant ($p < 0.0001$) influence on Day 360 solids content measurements, which is consistent with the NWR trends seen in Figure 5-2. Conversely, hydrocarbon amendments did not have a statistically significant influence on solids content. These results suggest that if bioconsolidation occurred in the columns, it was not significantly influenced by hydrocarbon amendments. Bioconsolidation (particularly via a methanogenic pathway) could have been enhanced by pressure, but pore water concentrations of divalent cations do not support this theory. Further, it is likely that dead loads would have had a stronger influence on FFT consolidation than bioconsolidation.

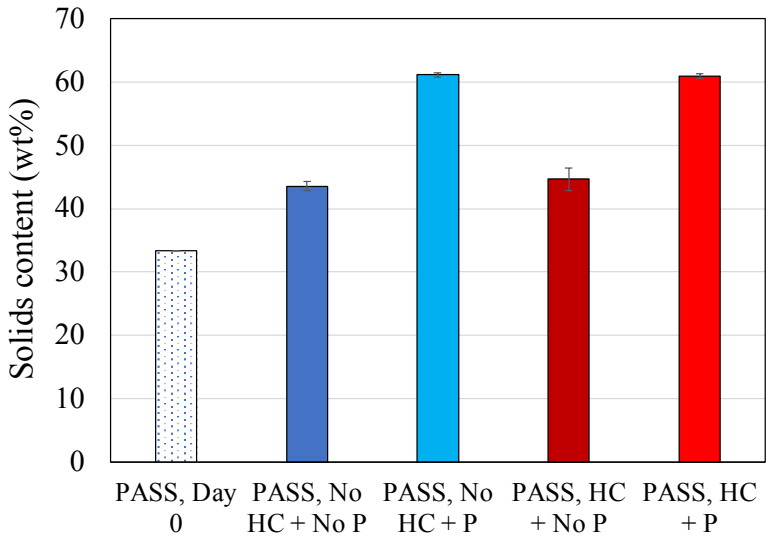

Figure 5-3. Solids content of PASS-treated FFT on 360 d. The solids content of PASS-treated FFT on Day 0 is provided for comparison. Results are averaged from triplicate columns and error bars represent one standard deviation of triplicates. Label HC refers to hydrocarbon amended tailings; P refers to tailings under pressure.

Pore pressure was monitored in all columns over the 360 d and the data is presented in Appendix C2, Figure C-2. Unfortunately, pore pressure measurements were erroneous and could not be used to determine the end of a consolidation phase. As such, dead loads were applied every 60 d to be

consistent with the length of time selected for the self-weight consolidation phase and to ensure consolidation was sufficient before doubling the dead load.

Bitumen content of the tailings on Day 360 (see Appendix C2, Figure C-3) was significantly ($p = 0.000$) and positively influenced by hydrocarbon amendments. This is likely due to a decrease in bitumen viscosity in the presence of hydrocarbon solvents (Zhang 2012), which would subsequently cause increased mixing and mobility of bitumen in hydrocarbon amended tailings (and seemingly increase bitumen content). It is also possible that the positive influence of hydrocarbon amendments on bitumen content was the result of bitumen being biodegraded in unamended tailings. Anaerobic biodegradation of bitumen was recently reported in a 945 d laboratory study, though degradation rates were low and the authors estimated it would take between 2200 and 9000 years to degrade 1 L of bitumen (Pannekens et al. 2021).

5.3.3 Biogeochemical Parameters

Figure 5-4 shows sulfate concentrations in the pore water (Figure 5-4A) and water cap (Figure 5-4B) of all columns over 360 d. Pore water sulfate concentrations decreased quickly, especially in hydrocarbon amended columns. By Day 60, average pore water sulfate concentrations had decreased from 438 mg/L (on Day 0) to approximately 11 mg/L in hydrocarbon amended tailings and 164 mg/L in unamended tailings. Pore water sulfate concentrations continued to decrease in unamended tailings, dropping to an average of 15 mg/L by Day 180. Hydrocarbon amendments had the most significant influence on pore water sulfate concentrations on Day 60 ($p < 0.0001$) and Day 120 ($p = 0.020$). This is consistent with the findings of Gee et al. (2017), who found that diluent stimulated sulfate reduction in FFT which subsequently increased RSC generation. Further, these results suggest that if PASS treatment is applied to diluent impacted FFT (FTT) in the future, the tailings will undergo complete sulfate reduction relatively quickly (though the bioavailability of hydrocarbons in columns containing hydrocarbon amended PASS-treated FFT is likely different than that of FTT in the field). Pressure also significantly influenced (decreased) Day 120 pore water sulfate concentrations ($p = 0.029$), though greater than 97% and 63% of the sulfate had already been reduced in the hydrocarbon amended and unamended tailings, respectively, by the time pressure was applied on Day 60.

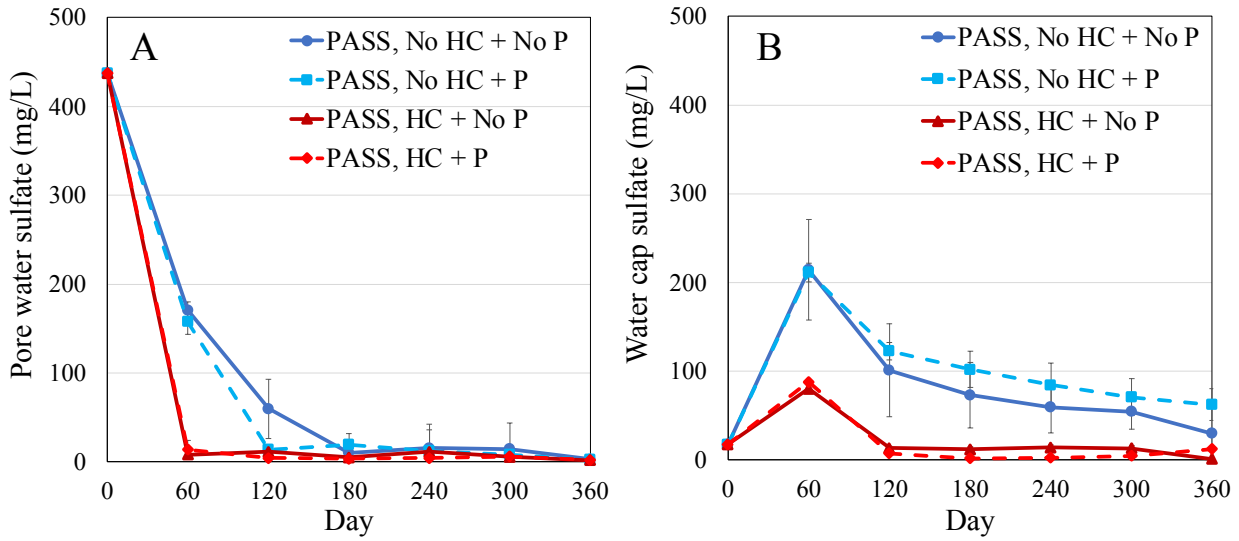

Figure 5-4. Sulfate concentrations in the pore water (A) and water cap (B) in PASS-treated FFT columns over 360 d. Results are averaged from triplicate columns and error bars represent one standard deviation of triplicates. Label HC refers to hydrocarbon amended tailings; P refers to tailings under pressure.

Water cap sulfate concentrations increased during the first 60 d and were highest in the unamended columns ($p = 0.042$). This is consistent with the high NWR during this period as well as the slower sulfate reduction in unamended tailings. Sulfate concentrations decreased in all water caps after Day 60, likely a result of sulfate reduction in the anaerobic water cap (though the majority of SRB would be contained in the tailings) and slower NWR.

Total aqueous sulfide species (H_2S, HS^-, S^{2-}), generated as a result of sulfate reduction, are shown in Figure 5-5. Total sulfide species were present in the pore water and water caps in all columns over the course of the experiment (except on Day 0), but concentrations were highest on Day 60. Further, columns with hydrocarbon amendments generally had higher concentrations of sulfide species in both the pore water and water caps, which is consistent with the rapid and extensive sulfate reduction seen in Figure 5-4A. Concentrations of sulfide species were generally higher in the water cap than in the pore water during the first 120 d and this is presumably due to i) the rapid NWR during the first 60 d, ii) the time-sensitive nature of aqueous sulfide species measurements, which likely underestimated pore water concentrations, and iii) precipitation of sulfide species in the tailings.

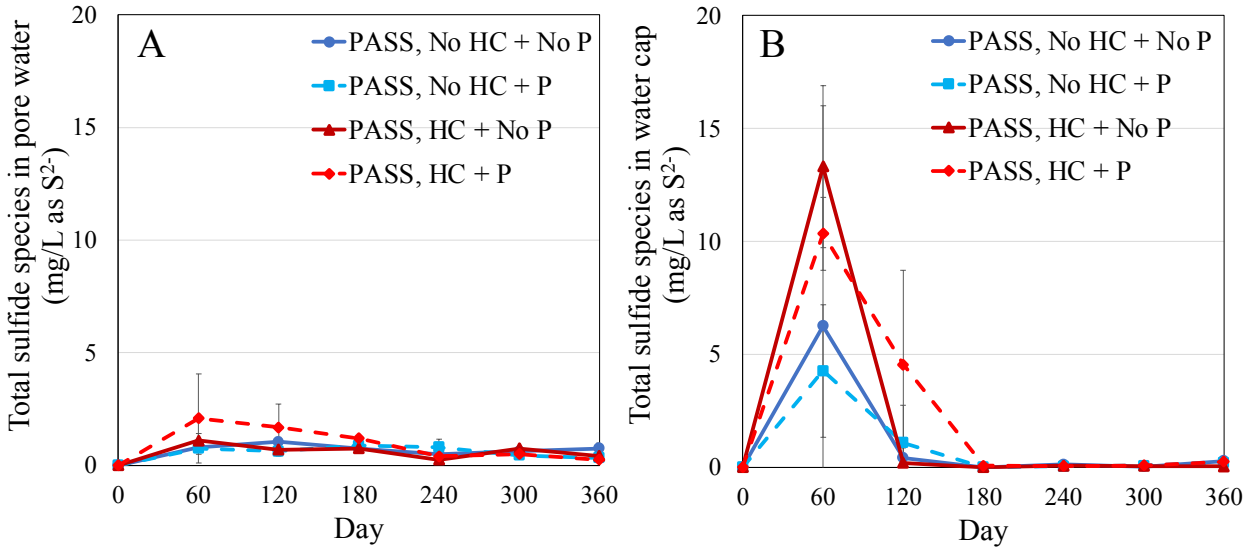

Figure 5-5. Total sulfide species (S^{2-}, HS^-, H_2S) concentrations in the pore water (A) and water cap (B) in PASS-treated FFT columns over 360 d. Results are averaged from triplicate columns and error bars represent one standard deviation of triplicates. Label HC refers to hydrocarbon amended tailings; P refers to tailings under pressure.

Figure 5-6 presents the sulfur content of the PASS-treated FFT on Day 540; the sulfur content of PASS-treated FFT on Day 0 is provided for comparison. By Day 540, the sulfur content of the tailings had increased in all columns but especially in columns with pressure and/or hydrocarbon amendments, though these differences were not statistically significant. This increase in solid phase sulfur over the course of the experiment is expected to be primarily due to the precipitation of sulfide species (generated through sulfate reduction) as metal sulfides. Numerous laboratory and field studies have also reported sulfide species precipitation as a result of sulfate reduction (Chen et al. 2013; Dompierre et al. 2016; Stasik et al. 2014; Warren et al. 2016). Some of the triplicate results presented in Figure 5-6 have large standard deviations and this is due to the volatility of reduced sulfur which can underestimate XRF measurements of sulfur. Further, reduced sulfur likely existed in multiple phases throughout each of the columns, which would have also contributed to the variability in the results.

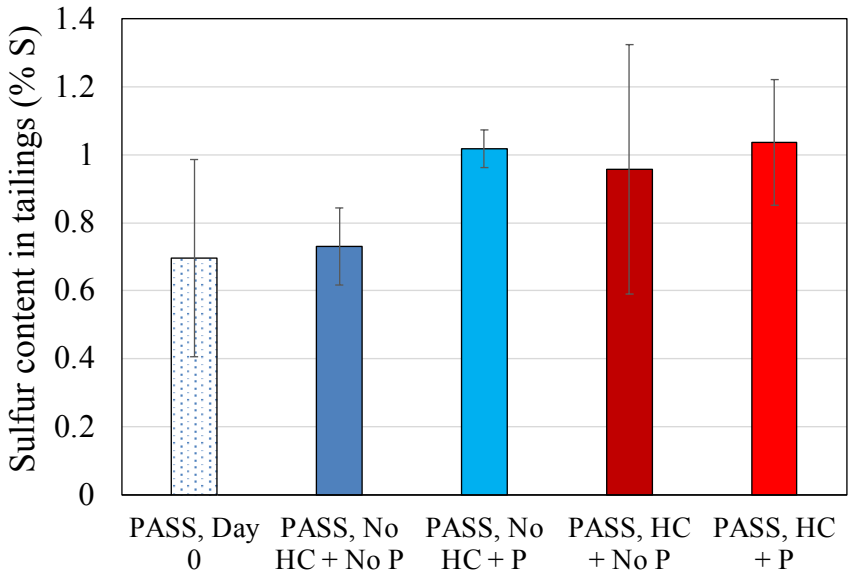

Figure 5-6. Sulfur (S) content in the tailings in PASS-treated FFT columns on Day 540. Data is presented as the percentage of elements in the solid phase that are sulfur. Sulfur content of PASS-treated FFT on Day 0 is provided for comparison. Results are averages of triplicate columns and error bars represent one standard deviation of triplicates. Label HC refers to hydrocarbon amended tailings; P refers to tailings under pressure.

Gaseous RSC generation in the columns was monitored by measuring gaseous H_2S in the headspace, though it is possible that sulfate reduction generated other RSCs as well (Gee et al. 2017). Gaseous H_2S measurements are provided in Appendix C2, Table C-2. Gaseous H_2S was highest on Day 60 where it was detected in 100% of the hydrocarbon amended columns and 50% of the unamended columns. This is consistent with the timing and trends in both sulfate reduction and total sulfide species generation. Average headspace concentrations of H_2S on Day 60 ranged from 1.2 to 32.2 ppmv. Headspaces were flushed every 60 d and gaseous H_2S was below detection (<0.1 ppmv) in almost all columns after Day 60. As such, any sulfide species generated after Day 60 must have remained in the solid or aqueous phases or were present as RSCs other than H_2S.

Figure 5-7 presents alkalinity in the pore water (A) and water caps (B) in all columns over 360 d. Hydrocarbon amendments had a statistically significant influence on alkalinity in the pore water (Day 360, $p = 0.001$) and water caps (Day 360, $p < 0.0001$). Pore water alkalinity increased during the first 60 d, especially in the hydrocarbon amended tailings, which is consistent with sulfate reduction (Wersin et al. 2011a,b). Pore water alkalinity continued to increase in unamended

tailings up to Day 120 (in PASS, No HC + P columns) and Day 180 (in PASS, No HC + No P columns), at which point sulfate reduction in the tailings was largely complete. Water cap alkalinity was initially highest in columns with hydrocarbon amended tailings, which also agrees with sulfate trends. Further, during the first 60 d of the experiment, the pH of the tailings (see Appendix C2, Figure C-4) decreased by an average of 0.2 pH units in all columns, consistent with sulfate reduction. Concentrations of major cations (sodium, calcium, magnesium, and potassium) and chloride are also provided in Appendix C2. Trends are generally consistent with NWR though there was an initial drop in pore water concentrations of divalent cations which is consistent with carbonate mineral precipitation as a result of sulfate reduction (as discussed in Chapter 4). Fifty charge balance calculations were performed and all were within allowable limits (± 5%) with three exceptions, though these can be attributed to cation or anion measurement errors.

In addition to hydrocarbon amendments and sulfate reduction, alkalinity was also influenced by pressure. Pore water alkalinity was generally higher in columns with pressure than comparable columns without pressure. Further, pressure had the greatest influence on water cap alkalinity (Day 360, $p < 0.0001$). In columns with pressure, water cap alkalinity continued to increase over the course of the experiment, even after pore water sulfate was depleted in all columns, and surpassed pore water alkalinity around Day 180. By Day 360, water cap alkalinity had surpassed pore water alkalinity by roughly 73 mg/L in PASS, No HC + P columns and by 118 mg/L in PASS, HC + P columns. This cannot be explained by NWR or diffusive fluxes (due to a lack of concentration gradient). Sulfate reduction in the water cap also cannot explain the high alkalinity in PASS, HC + P water caps because water cap sulfate was essentially depleted after Day 120. Instead, alkalinity differences in columns with and without pressure are likely the combined result of several biogeochemical differences between these columns, including pCO_2 and $CO_{2(g)}$ generation, both of which were higher in columns with pressure. The lower alkalinity in the pore water than the water cap of columns with pressure might be explained by uptake of CO_2 by microorganisms in the tailings.

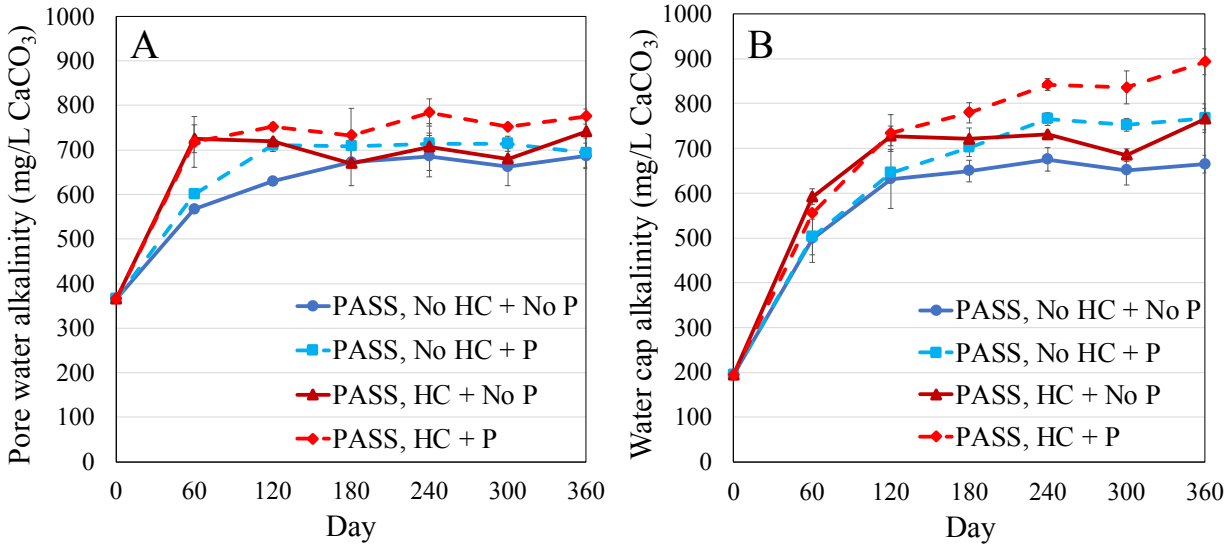

Figure 5-7. Total alkalinity (in mg $CaCO_3$/L) in the pore water (A) and water cap (B) in PASS-treated FFT columns over 360 d. Results are averaged from triplicate columns and error bars represent one standard deviation of triplicates. Label HC refers to hydrocarbon amended tailings; P refers to tailings under pressure.

Pressure applied to the tailings influenced the generation of biogenic CO_2 and CH_4, as shown in Figure 5-8. The range of volumes shown on the y-axes are different for Figure 5-8A and 5-8B, with the CH_4 figure (5-8B) having a much greater range (0 to 1200 mL) than the CO_2 figure (5-8A, 0 to 400 mL). Applying pressure to the tailings increased the amount of CO_2 and CH_4 generated in the columns. By Day 360, PASS, No HC + P columns had generated 42% more CO_2 and 345% more CH_4 than PASS, No HC + No P columns. Similarly, PASS, HC + P columns had generated 60% more CO_2 and 25% more CH_4 than PASS, HC + No P columns by Day 360. There was a large increase in CH_4 generation from the PASS, HC + No P columns after Day 300, but prior to Day 300, PASS, HC + P columns had generated 135% more CH_4 than PASS, HC + No P columns. Further, pressure had the most influence on Day 360 headspace CO_2 measurements ($p < 0.0001$) and on Day 120 ($p = 0.000$), Day 180 ($p = 0.000$), Day 240 ($p < 0.0001$), and Day 300 ($p < 0.0001$) headspace CH_4 measurements. Pressure clearly enhanced methanogenesis even though the higher solids content in tailings under pressures (+16% by Day 360) may have reduced the diffusion of microbial substrates and intermediates through the tailings (Cazier et al. 2015).

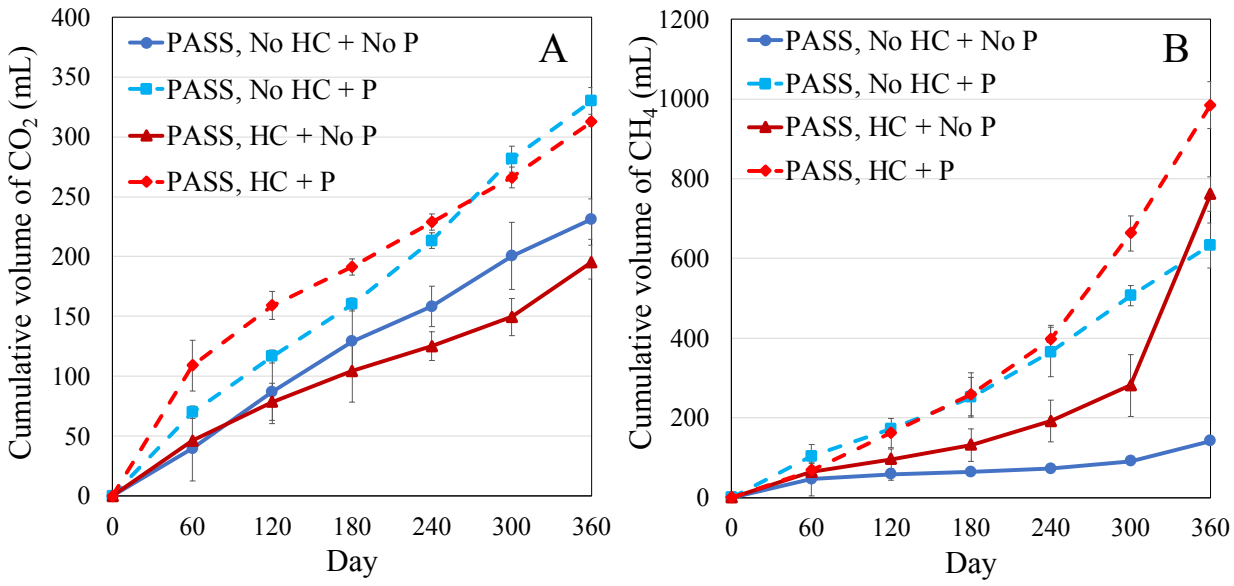

Figure 5-8. Cumulative volume of carbon dioxide (A) and methane (B) generated in the headspace of 5.5 L PASS-treated FFT columns over 360 d. Results are averaged from triplicate columns and error bars represent one standard deviation of triplicates. Label HC refers to hydrocarbon amended tailings; P refers to tailings under pressure.

The most likely explanation for the positive effect of pressure (0.3 to 5.1 kPa) on microbial activity in oil sands tailings is that the relatively low pressures used in this work enhanced the solubility of biologically important gases, such as CO_2 and H_2, and volatile organic compounds involved in microbial metabolism, thereby increasing the bioavailability of substrates (Cassarini et al. 2019; Meredith and Tfaily 2022). Increasing substrate and metabolite solubility would make applicable microbially-mediated reactions more thermodynamically favorable and enhance microbial growth and activity. This can be explained theoretically by Henry's Law (Equation 5-1), which shows that as the partial pressure (Pi) of a compound increases, so does its solubility:

$$K_H = \frac{P_i}{C_l} \tag{5-1}$$

where K_H is the Henry's Law Constant, P_i is the partial pressure of a compound in the gaseous phase, and C_l is the concentration (solubility) of the same compound in the liquid phase. The application of Henry's Law in this scenario is not perfect (for example, Henry's Law is for ideal dilute solutions) and is dependent on temperature but the general concept can be used to describe

the direct effect of pressure on the biogeochemistry of the tailings. As an example, in hydrogenotrophic methanogenesis (Equation 5-2), increasing the partial pressure and thereby dissolved concentration of CO_2 decreases the Gibb's free energy of the reaction (Mayumi et al. 2013), which makes the reaction in Equation 5-2 more energetically favorable and should theoretically lead to increased CH_4 production (assuming H_2 is also readily available).

$$CO_2 + 4H_2 \rightarrow CH_4 + 2H_2O \quad (5\text{-}2)$$

Previous microcosm studies by Cassarini et al. (2019) and Meulepas et al. (2010) investigated the effects of pCH_4 on anaerobic CH_4 oxidation and sulfate reduction and found that in general, increasing partial pressure (from 0.1 to 0.45 MPa in Cassarini et al. (2019) and from 0.1 to 10 MPa in Meulepas et al. (2010)) was associated with increased CH_4 oxidation and sulfate reduction. Another microcosm study investigated the effect of pCO_2 on methanogenesis with acetate as the carbon source (Mayumi et al. 2013). The authors found that the application of 200 kPa pCO_2 enhanced CH_4 production via acetoclastic methanogenesis relative to that of control microcosms which produced CH_4 at a slower rate via acetate oxidation coupled with hydrogenotrophic methanogenesis (Mayumi et al. 2013). This shift in microbial methanogenic communities occurred because acetoclastic methanogenesis was more thermodynamically favorable than acetate oxidation in the microcosms injected with CO_2. While the microbially-mediated reactions and partial pressures in these microcosms studies are not necessarily the same as in this experiment, these studies demonstrate that increased partial pressures can influence and enhance microbial activity.

At a given temperature and pressure, the solubility of CO_2 in water is roughly 10 times higher than that of CH_4 (Austegard et al. 2006), and thus the solubility of CO_2 would have been greater than that of CH_4 in columns with and without pressure. Nevertheless, pCH_4 would have also increased to some extent due to the pressures used in this experiment. This might seemingly inhibit methanogenesis (though Meulepas et al. (2010) found that a pCH_4 of 10 MPa only slightly inhibited methanogenesis in granular sludge). However, in this experiment, pressure enhanced CH_4 production. This highlights the complex biogeochemical reactions involved in CH_4

production in FFT and suggests that pressure enhanced the solubility of numerous substrates and metabolites involved in methanogenic pathways.

Methanogenesis is assumed to be the primary reason for the generation of CO_2 and CH_4 in the headspace of all columns as seen in Figure 5-8, though sulfate reduction would have also contributed to CO_2 generation in the first 60 to 180 d of the experiment. Some researchers have found that the presence of sulfate inhibits methanogenesis in FFT (Fedorak et al. 2002; Holowenko et al. 2000; Ramos-Padrón et al. 2011), while others have reported that sulfate reduction and methanogenesis can occur simultaneously (Stasik and Wendt-Potthoff 2014, 2016; Stasik et al. 2014). While SRB have a thermodynamic and kinetic advantage over methanogens, they can co-exist and thrive if there are abundant electron donors and acceptors. Stasik and Wendt-Potthoff (2016) found that SRB co-existed with hydrogenotrophic methanogens in FFT, possibly because SRB converted acetate to CO_2 (through syntrophic oxidation), which was then utilized by hydrogenotrophic methanogens to generate CH_4. In this experiment, the majority of the sulfate reduction in the tailings occurred during the first 60 d, though in some unamended columns sulfate reduction continued until Day 180. CH_4 was produced in all 12 columns during the first 60 d, which suggests that methanogenesis and sulfate reduction occurred at the same time, especially because sulfate reduction continued beyond Day 60 in the unamended columns. As such, there must have been ample electron donors/substrates in the tailings and/or they were used non-competitively.

The effect of hydrocarbon amendments on CO_2 and CH_4 generation over the 360 d was not as pronounced as that of similar experiments by Siddique et al. (2014a) and Kuznetsov et al. (2023), though hydrocarbon amendments had the most influence on Day 360 measurements of headspace CH_4 ($p < 0.0001$). The 'dampened' effect of hydrocarbons in this experiment likely occurred because the microorganisms in the tailings needed time to adjust to their new carbon sources, as they would have been more accustomed to hydrocarbons in paraffinic diluents (Mohamad Shahimin et al. 2016, 2021). This would explain the sharp rise in CH_4 generation in PASS, HC + No P and PASS, HC + P columns after Day 300 and 240, respectively. By Day 360, >95% of each of the hydrocarbons added to the tailings on Day 0 (toluene, o-xylene, m-xylene, p-xylene, octane, decane, 2-methlypentane, and 3-methylhexane) had been degraded. Hydrocarbon concentrations

in the amended tailings ranged from 0.1 to 13.8 ppm on Day 360 (full details provided in Appendix C3, Table C-3), indicating that the microorganisms were capable of degrading hydrocarbons typical of naphtha diluent.

Figure 5-9 presents the relative abundance of microbial communities (at the order level) in the tailings on Day 60 and Day 360, as indicated. Microbial communities in the PASS-treated FFT on Day 0 are included in Figure 5-9 for comparison. On Day 0, the PASS-treated FFT consisted predominately of known methanogens. *Methanomicrobiales (*genus *Methanoregula)* made up 31.3% of the total microbial community while *Methanosarcinales (*genus *Methanosaeta)* accounted for 15.4%. *Methanoregula* are hydrogenotrophic methanogens (consume H_2 and CO_2) while *Methanosaeta* are acetoclastic methanogens (consume acetate) (Pyzik et al. 2018). These methanogenic microbial communities are consistent with archaea previously reported in FFT (Foght et al. 2017). Bacteria in the Day 0 PASS-treated FFT consisted primarily of *Burkholderiales* (16.2%, class *Gammaproteobacteria*), *Anaerolineales* (4.5%), *Desulfotomaculales* (2.7%), and *Thermodesulfovibrionia* (2.7%, class level). *Burkholderiales* contains genera known to be capable of aerobic hydrocarbon degradation, though the order also includes facultative anaerobes (An et al. 2013; Pérez-Pantoja et al. 2011). *Anaerolineales* (family *Anaerolineaceae*) are fermenters and contribute to anaerobic hydrocarbon degradation (Foght et al. 2017; Liang et al. 2015; Mohamad Shahimin and Siddique 2017a; Mohamad Shahimin et al. 2016), *Desulfotomaculales* (genus *Pelotomaculum*) are syntrophs (Foght et al. 2017), and *Thermodesulfovibrionia* contains SRB and microorganisms capable of sulfur disproportionation (D'Angelo et al. 2023).

By Day 60, the relative abundance of methanogenic communities in the tailings had decreased by between 2.5 to 6.0%, likely the result of an increase in microorganisms involved in sulfur cycling. *Desulfotomaculales* increased in all columns to roughly 6% and columns with hydrocarbon amendments also saw an increase in *Desulfobulbales* (to roughly 3.5%, genus *Desulfoprunum*) and *Pseudomonodales* (to 1%, genus *Pseudomonas*). *Desulfoprunum* is a known SRB and has been associated with hydrocarbon (toluene and ethylbenzene) degradation (Ahmar Siddiqui et al. 2022; Wu et al. 2022). *Pseudomonas*, which includes aerobic and facultative anaerobic species, has been found in numerous oil-contaminated sites and may be involved in hydrocarbon degradation (Das and Kazy 2014; Ren et al. 2011; Wang et al. 2013). Columns without hydrocarbon amendments

saw an increase in *Geobacterales* (to 1.3%, family *Geobacteraceae*) and *Desulfatiglandales* (to 1.2%). *Geobacteraceae* are responsible for Fe(III) reduction (Holmes et al. 2002, 2004) while *Desulfatiglandales* contains SRB (Csapo et al. 2022). The presence of SRB in all columns is consistent with the extensive sulfate reduction seen in the first 60 d of the experiment. Further, differences in the SRB communities in columns with and without hydrocarbon amendments is consistent with the different carbon sources available in these columns.

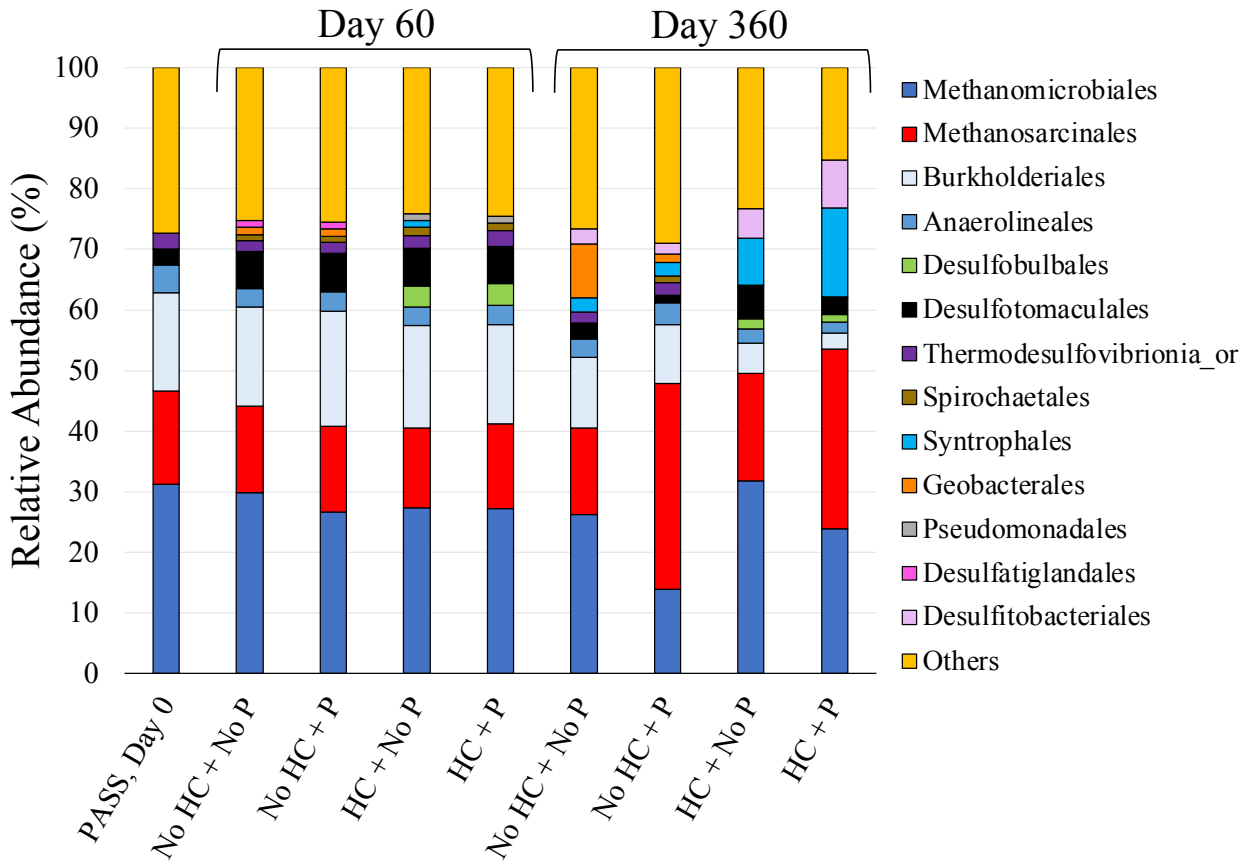

Figure 5-9. Stacked bars illustrating the relative abundances of microorganisms at the order level, represented by the percentage of the 16S rRNA read counts within each group. A relative abundance of less than 1.0% is assigned to 'Others'. Bars represent tailings samples collected on Day 60 or Day 360, as indicated. PASS, Day 0 is also provided for comparison. Label HC refers to hydrocarbon amended tailings; P refers to tailings under pressure.

There were notable differences in the relative abundance of microbial communities in the columns on Day 60 versus Day 360. Microbial communities still consisted predominately of methanogens on Day 360, though the relative abundance of *Methanomicrobiales* decreased in most of the

columns (by 3.5% in PASS, No HC + No P; 12.8% in PASS, No HC + P; 3.3% in PASS, HC + P) except in PASS, HC + No P which saw an increase of 4.4%. The relative abundance of *Methanosarcinales* remained unchanged in PASS, No HC + No P columns while all other columns saw an increase (of 19.9% in PASS, No HC + P; 4.5% in PASS, HC + No P; 15.7% in PASS, HC + P). Evidently, columns with pressure underwent a shift in methanogenic microbial communities from hydrogenotrophic methanogens to acetoclastic methanogens. The pressures applied to the tailings likely impacted intermediate substrates and metabolites involved in methanogenic pathways such that acetoclastic methanogenesis (Equation 5-3) became more thermodynamically favorable. The presumed increase in pCO_2 (and the partial pressure of H_2) as a result of pressure application might theoretically enhance hydrogenotrophic methanogenesis (Equation 5-2), however, depending on the hydrogenotrophic methanogenic pathway occurring in the tailings, this may not be the case. For example, if syntrophic acetate oxidation (Equation 5-4) was necessary prior to hydrogenotrophic methanogenesis, enhancing the solubility of CO_2 and/or H_2 would have an inhibitory effect on syntrophic acetate oxidation, limiting the activity of hydrogenotrophic methanogens (Mayumi et al. 2013). Another explanation for the shift in methanogenic microbial communities may be that ammonia (see Figure 5-11) toxicity impacted the activity of hydrogenotrophic methanogens, though ammonia inhibition is unlikely given the relatively low ammonium/ammonia concentrations in this experiment (Fotidis et al. 2012; Wang et al. 2022).

$$CH_3COO^- + H^+ \rightarrow CH_4 + CO_2 \quad (5\text{-}3)$$

$$CH_3COO^- + H^+ + 2H_2O \rightarrow 4H_2 + 2CO_2 \quad (5\text{-}4)$$

The relative abundance of some bacteria had also changed by Day 360. The relative abundance of *Burkholderiales* had decreased in all columns, though more so in columns with pressure. *Desulfotomaculales* decreased by roughly 3% in all columns except for PASS, HC + No P columns and *Thermodesulfovibrionia* were no longer detected in hydrocarbon amended tailings. *Syntrophale*s, which were previously only present in PASS, HC + No P columns on Day 60, were present in all columns on Day 360. Hydrocarbon amended tailings had higher proportions of *Syntrophales* than unamended tailings. It is thought that microorganisms in the order *Syntrophales* work in synergy with methanogens, providing them with various fermentation products (Langwig

et al. 2022; Mercado et al. 2023). *Desulfitobacteriales* were found in all columns on Day 360, though they were previously present at a relative abundance of <1% on Day 60. *Desulfitobacteriales,* which contain known SRB, were highest in hydrocarbon amended tailings (Pester et al. 2012). It is interesting that the relative abundance of *Desulfitobacteriales* increased from Days 60 to 360, when the majority of the sulfate reduction in the tailings was complete by Day 60. One possible explanation is that diffusion of sulfate from the water cap to the tailings after Day 60 stimulated the growth of *Desulfitobacteriales,* though they are known to thrive in both low and high sulfate environments (Pester et al. 2012). Another possibility is that anaerobic oxidation of reduced sulfur species and/or sulfide minerals in the tailings generated electron acceptors for *Desulfitobacteriales*, promoting their growth (Stasik et al. 2021).

Figure 5-10 presents DOC concentrations in the pore water (A) and water cap (B) of the columns over 360 d. During the first 60 d, DOC in both the pore water and water cap was highest in columns with hydrocarbon amended tailings, which is consistent with microbial activity in general. For the remainder of the experiment, columns with pressure had the highest DOC concentrations both in the pore water (Day 240, $p < 0.0001$; Day 300, $p < 0.0001$) and water cap (Day 360, $p < 0.0001$). DOC concentrations provide an indication of the production and/or decomposition of soluble, microbial metabolites (Campbell et al. 2022). As such, the higher DOC concentrations in the columns with pressure are consistent with the enhanced microbial activity seen in these columns. Further, in columns with pressure, DOC concentrations were higher in the water cap than in the pore water. This reflects both the high NWR in these columns and the enhanced microbial activity and DOC utilization/degradation in the tailings relative to the water caps. Other possible explanations for the high DOC in columns with pressure include lysis of some microbial cells due to compressive stress, which would cause a release of intracellular material that could subsequently be used to support microbial growth (Gonzalez-Rodriguez et al. 2016; Malone et al. 2002). However, the pressures used in this work are likely too low to cause cell lysis. Another possibility is that pressure increased the adsorption of gases to tailings solids, which in turn caused the desorption of organics from the tailings and contributed to higher DOC in these columns (Guo 2013). While gas adsorption may explain the DOC trends in columns with pressure, it is also likely that the higher DOC in columns with pressure is an indirect result of the enhanced gas solubility, and subsequent microbial activity, in these columns. COD trends in the pore water and water cap

(see Appendix C2, Figure C-10) mirror that of the DOC trends in Figure 5-10, and further indicate that the columns with pressure had higher concentrations of organic compounds and more microbial activity.

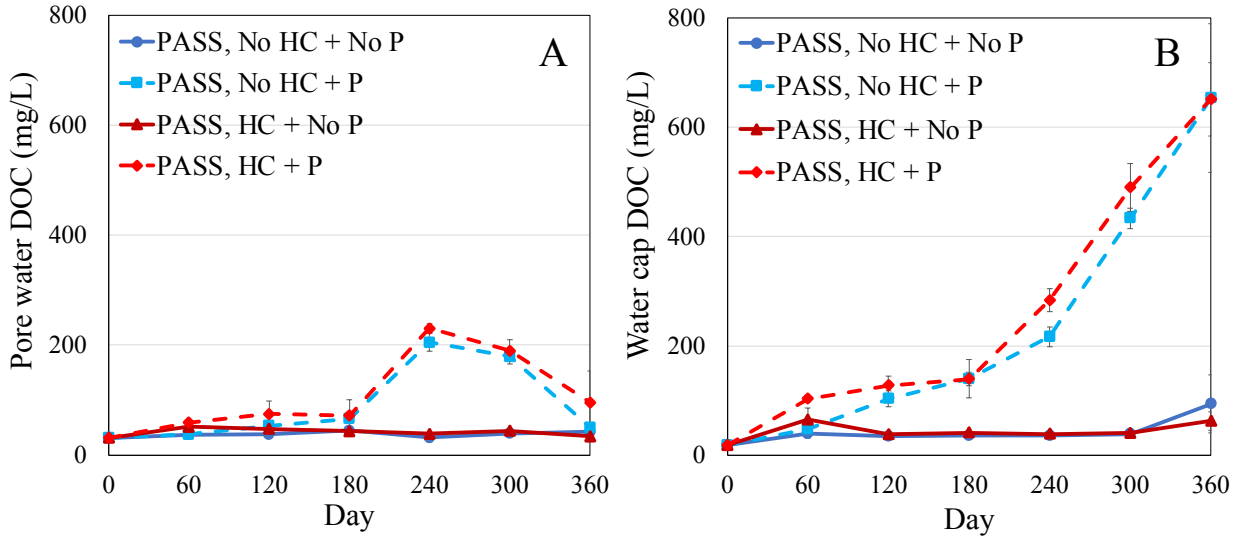

Figure 5-10. Dissolved organic carbon concentrations in the pore water (A) and water cap (B) in PASS-treated FFT columns over 360 d. Results are averaged from triplicate columns and error bars represent one standard deviation of triplicates. Label HC refers to hydrocarbon amended tailings; P refers to tailings under pressure.

PAM was measured in pore water samples every 60 d (with the exception of Day 60) and in select Day 360 water cap samples. PAM concentrations were below detection (< 10 mg/L) in all pore water and water cap samples and as such it was not possible to tell if the parent compound had been degraded into lower molecular weight compounds. Further, PAM concentrations were below detection in samples of Day 0 PASS-treated FFT pore water. This highlights the difficulties in separating PAM from the solid phase via centrifugation and unfortunately means it is not possible to determine whether or not PAM was degraded over the 360 d. Previous research has found that anionic PAM, and the intermediate products (polyacrylate and/or polyacrylic acids) that would result from PAM being utilized as a nitrogen source, sorb strongly to soil, particularly if the soil has a high clay content and/or high concentrations of cations (Duis et al. 2021; Guezennec et al. 2015; Lu et al. 2002). The findings from previous research are consistent with the lack of detectable PAM in all of the pore water and water cap samples analyzed in this experiment.

The ammonium generation shown in Figure 5-11 might suggest that PAM was degraded through hydrolysis of the amide nitrogen, particularly in columns with pressure (Cossey et al. 2021a; Grula et al. 1994; Guezennec et al. 2015; Haveroen et al. 2005; Hu et al. 2018; Li et al. 2023). Metabolite formation from the PAM biodegradation process would then contribute to the DOC and COD observed in columns with pressure. Haveroen et al. (2005) found that PAM could stimulate methanogenesis in MFT and thickened tailings (flocculated FFT), likely because ammonium generated through the deamination of PAM served as a nitrogen source and stimulated microbial metabolism and growth. However, in the study by Haveroen et al. (2005), serial dilutions were performed to ensure that PAM was the only fixed nitrogen source available in the microcosms. The findings of Haveroen et al. (2005) are in contrast to that of Collins et al. (2016) who found that with a microcosm headspace made up of 30% CO_2 balance N_2, PAM did not serve as a nitrogen source in MFT and rather N_2 fixation occurred in conjunction with methanogenesis. The 12 columns in this experiment also had an N_2 headspace and as such N_2 fixation is a likely explanation for the ammonium generation shown in Figure 5-11. Though anaerobic N_2 fixing bacteria, such as *Clostridium,* do not appear to have been present in the columns in substantial amounts (see Figure 5-9), methanogenic species are known to be capable of N_2 fixation (Bae et al. 2018; Leigh 2000). As such, the methanogens present in the tailings could have contributed to N_2 fixation and the ammonia/ammonium generation in Figure 5-11. Given the pH of the tailings and water cap in each column (see Appendix C2, Figure C-4), the majority of these aqueous species would be ammonium rather than ammonia.

Pressure had the most influence on Day 360 water cap ammonium concentrations ($p = 0.000$) and on Day 180 ($p < 0.0001$), Day 240 ($p = 0.000$), and Day 300 ($p < 0.0001$) pore water ammonium concentrations. There was a spike in ammonium concentrations in columns without pressure after Day 300, which coincides with the increase in CH_4 production in these columns (especially in PASS, HC + No P) after Day 300. As such hydrocarbon amendments had the most influence on Day 360 pore water ammonium concentrations ($p = 0.030$). It is possible that the columns with pressure had higher pore water ammonium concentrations simply because of the higher solubility of ammonia gas under pressure, however, this cannot account for all of the NH_4^+ generation shown in Figure 5-11. As such, the relatively high ammonium concentrations in both the pore water and water caps of columns with pressure agrees with the biogenic gas, DOC, and COD trends and

supports the theory that columns with pressure had enhanced microbial activity. To meet the demands of the enhanced microbial growth and metabolism in columns with pressure, the microorganisms in these columns likely utilized PAM and/or N_2 fixation as a nitrogen source. PAM degradation and/or N_2 fixation likely also occurred in columns without pressure, but there was a roughly 300 d lag in this microbial activity. Water cap concentrations of ammonium were higher than pore water concentrations in almost all cases, which suggests that ammonium in the pore water was largely being consumed as a nitrogen source.

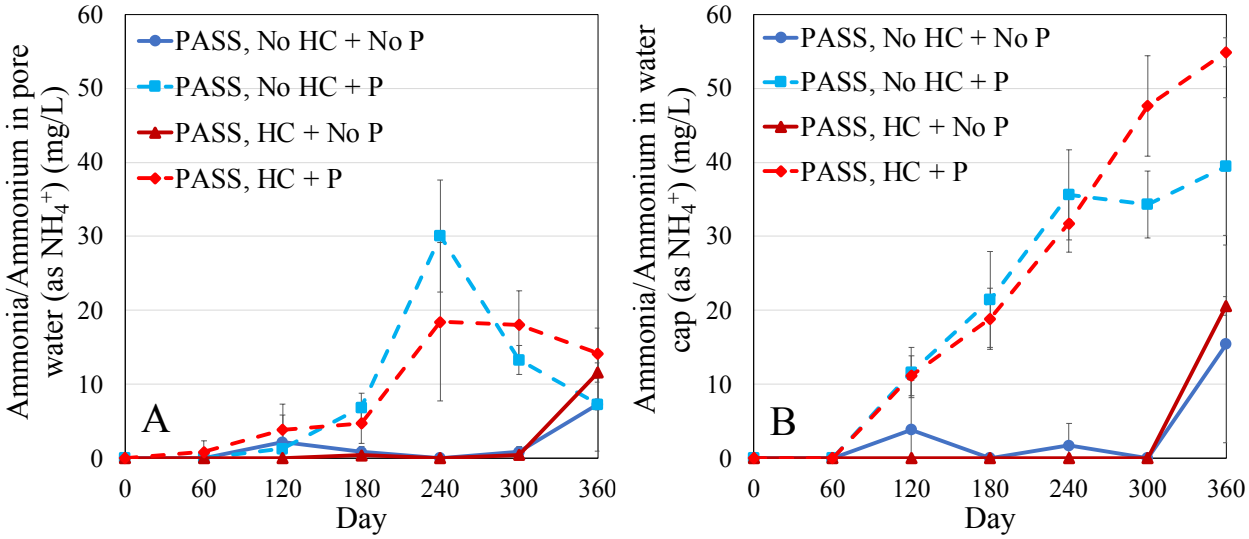

Figure 5-11. Ammonia and ammonium (as NH_4^+) concentrations in the pore water (A) and water cap (B) in PASS-treated FFT columns over 360 d. Results are averaged from triplicate columns and error bars represent one standard deviation of triplicates. Label HC refers to hydrocarbon amended tailings; P refers to tailings under pressure.

5.3.4 Differences in Geotechnical and Biogeochemical Behavior of Two Different Oil Sands Tailings

Oil sands tailings from different operators were used in Chapters 4 and 5, and this resulted in differences in geotechnical and biogeochemical behavior, most notably NWR and methanogenesis. Figure 5-12 compares NWR from triplicate 1 L columns each containing the same ratio of PASS-treated FFT, BCR water, and headspace. All six columns were stored under the same room temperature, dark, and anaerobic conditions; the only difference in the columns is that three of them contained PASS-treated FFT from Chapter 4 and the other three contained PASS-treated FFT from Chapter 5. The alum and PAM dosage for each of the PASS-treated

tailings was different (PAM dose of 2.43 g/kg of FFT solids in Chapter 4 and 1.015 g/kg of FFT solids in Chapter 5) but in both instances the dosage was optimized before applying it to the tailings. Despite this optimization, the PASS-treated FFT in Chapter 5 had 12% higher NWR than the PASS-treated FFT in Chapter 4 on Day 360. There are numerous material properties that impact FFT consolidation, such as solids content, clay content, SFR, void ratio, clay mineralogy, and water chemistry (Jeeravipoolvarn et al. 2009; Mikula and Omotoso 2006). Further, there are numerous material properties and factors that impact flocculation performance such as clay, sand, solids, and bitumen contents, polymer dosage, and mixing (Li et al. 2021). A combination of these factors and properties likely contributed to the differences seen in Figure 5-12. This highlights the challenges in applying treatment technologies to FFT and achieving the desired consolidation performance because feed material properties and treatment methodologies can have a substantial impact on performance.

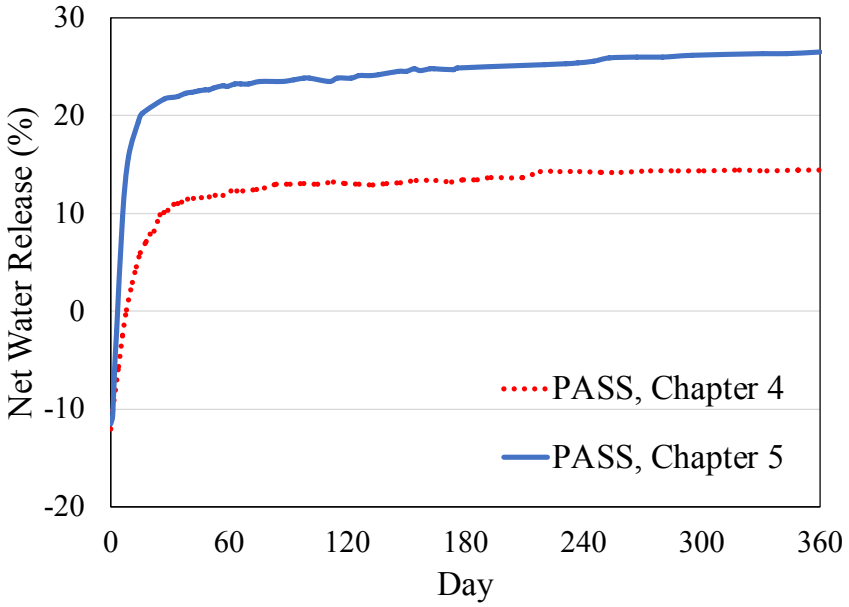

Figure 5-12. Net water release from two different PASS-treated oil sands tailings in 1 L columns over 360 d. Results are averaged from triplicate columns.

In both Chapters 4 and 5, the PASS-treated FFT that was amended with hydrocarbons underwent almost complete sulfate reduction in 120 d. Further, sulfate in the unamended PASS-treated FFT in Chapter 5 was almost completely reduced (from 437 mg/L to 15 mg/L) in 180 d. Sulfate in the unamended PASS-treated FFT in Chapter 4 was reduced by 242 mg/L after 540 d. The sulfate

reduction in unamended PASS-treated FFT in Chapter 5 was faster and occurred to a greater extent than that of Chapter 4. This is likely due to several factors including differences in microbial communities and the availability of suitable carbon sources in unamended tailings. While sulfate reduction was reasonably similar between the two experiments, methanogenesis, and the extent to which it occurred, was substantially different for the two types of PASS-treated FFT. Figure 5-13 presents CO_2 (A) and CH_4 (B) in the triplicate 1 L columns containing PASS-treated FFT from Chapters 4 or 5. The volume of CO_2 produced over the course of 360 d is similar for both types of tailings and indicative of microbial activity in general. However, Chapter 4 PASS-treated FFT did not produce CH_4 while Chapter 5 PASS-treated FFT produced 30 mL of CH_4 (the total headspace was 130 mL). There are numerous explanations for the inconsistency in methanogenic microbial activity between these two types of PASS-treated FFT, including differences in i) established microbial communities, ii) carbon sources the microbial communities were accustomed to (though both communities should have been accustomed to paraffinic diluent), and iii) age of the tailings, as fresher tailings would be less likely to have established methanogenic microbial communities (Foght et al. 2017; Mohamad Shahimin et al. 2016, 2021). Further, the development of microbial communities would have been impacted by differences in how the tailings were processed, stored, and handled (such as temperature, oxygen exposure, etc.) prior to being sent to the University of Alberta (Foght et al. 2017; Lyu and Lu 2018). Comparing the microbial communities present in the tailings on Day 0, there were no methanogens detected in the Chapter 4 PASS-treated FFT whereas methanogens made up 46.7% of the total microbial community in the Chapter 5 PASS-treated FFT. As such, differences in the methanogenic microbial activity observed in these two column studies can be attributed primarily to differences in the previously established microbial communities.

The differences in geotechnical behavior and microbial activity seen in Figures 5-12 and 5-13 indicate the importance of considering the source of the tailings when evaluating treatment technologies, geotechnical behavior, and biogeochemistry in the lab or field as different material properties and/or treatment methodologies can provide vastly different results. Further, this highlights the need to complete a thorough characterization of all feed materials and to provide this data in publications so that the results can be evaluated (and generalized) appropriately.

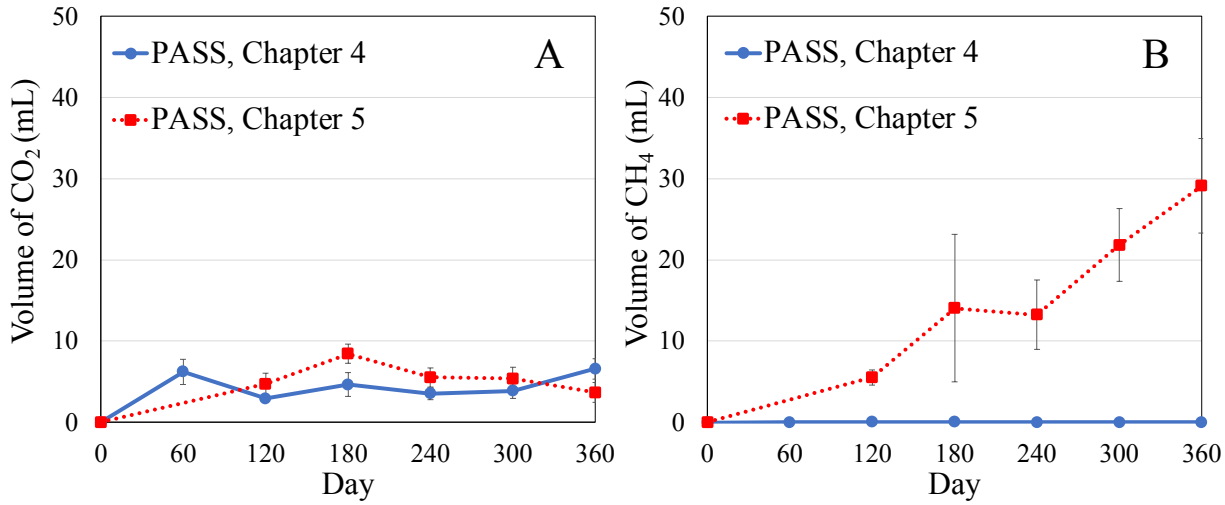

Figure 5-13. Volume of carbon dioxide (A) and methane (B) generated in the headspace of triplicate 1 L columns containing two different types of PASS-treated tailings. Results were collected over 360 d and averaged from triplicate columns. Error bars represent one standard deviation of triplicates.

5.4 Conclusions

This column study is the first to investigate the effects of pressure on the biogeochemistry of oil sands tailings. The relatively low pressures (0.3 to 5.1 kPa) used in this work impacted both the biogeochemical and geotechnical behavior of PASS-treated FFT and these findings can be used to develop additional studies which investigate the effects of higher pressures (up to 1 MPa) on the biogeochemistry of oil sands tailings deposited in pit lakes. Applying pressure (up to 5.1 kPa) to the tailings led to roughly 20% higher NWR compared to tailings that only underwent self-weight consolidation. The higher NWR from tailings under pressure is to be expected and agrees with the higher solids contents in these tailings on Day 360. In contrast, hydrocarbon amendments did not impact NWR or solids content.

The primary impact of the hydrocarbon amendments appeared to be on sulfate reduction rather than methanogenesis, though this may be because the hydrocarbon amendments resembled naphtha diluent while the microbial communities were likely more accustomed to paraffinic diluent. By Day 60, pore water sulfate concentrations were reduced by roughly 97% in hydrocarbon amended tailings and by 63% in unamended tailings. Sulfate reduction continued past Day 60 in unamended columns and by Day 180, pore water sulfate concentrations were reduced

by >96% in these columns. Sulfate reduction led to the generation of aqueous sulfide species throughout the pore water and water caps in all columns. Sulfate reduction was also presumably responsible for the increase in sulfur content in the tailings on Day 540, which is indicative of metal sulfide species precipitation. Further, by Day 360, over 80% of the columns had generated H_2S gas. The rapid sulfate reduction in hydrocarbon amended PASS-treated FFT and the generation of reduced sulfur in the solid, aqueous, and gaseous phases has implications for PASS treatment and suggests that applying the PASS treatment process to diluent impacted FFT (i.e. FTT) would lead to rapid and extensive sulfate reduction. The majority of the sulfate reduction occurred by Day 60, at which time pressure was applied to the tailings. As such, it is not possible to understand the full effect of pressure on sulfate reduction, though pressure did significantly decrease Day 120 pore water sulfate concentrations in unamended tailings. It is suspected that sulfate reduction would have been further enhanced by pressure, had pressure been applied earlier in the study (Meulepas et al. 2010).

Applying pressure to the tailings enhanced microbial activity in the columns. Columns with pressure generated significantly more CO_2 and CH_4 over the course of the study. Further, these columns had significantly higher concentrations of DOC and COD throughout the pore water and water caps, both of which are indicative of microbial activity. The most likely explanation for this behavior is that pressure increased the solubility of microbial substrates and metabolites in the tailings, which led to increased bioavailability of these compounds and enhanced microbial growth and activity. Pressure also caused a shift in methanogenic microbial communities, from hydrogenotrophic methanogens to predominately acetoclastic methanogens. The pressures applied to the tailings must have impacted substrates and metabolites involved in methanogenic pathways such that acetoclastic methanogenesis became more thermodynamically favorable. Future work in the near term will include qPCR for total quantification of both bacteria and archaea to further elucidate the impact of pressure on microbial growth, as well as measurements of microbial metabolites and intermediate substrates (starting with volatile fatty acids), and in the longer term will include a metagenomics-metabolomics study. Columns with pressure also had significantly higher concentrations of ammonium throughout the pore water and water caps, which suggests that in order to meet the demands of the enhanced microbial growth and metabolism in these columns, the microorganisms utilized PAM and/or N_2 fixation as a nitrogen source. Taken

together, these findings demonstrate the significant impact of relatively low pressures (0.3 to 5.1 kPa) on biogeochemical cycling and microbial activity in oil sands tailings.

There were notable differences in the geotechnical and biogeochemical behavior of the similarly PASS-treated FFT used in Chapters 4 and 5. The tailings used in these two chapters were sourced from different operators and underwent PASS treatment at NAIT. The PASS-treated FFT used in Chapter 5 had a 12% higher NWR and produced 30 times more CH_4 than comparable columns containing PASS-treated FFT from Chapter 4. These differences highlight the influence of the source of tailings on observed geotechnical and biogeochemical behaviors.

5.5 References

Abe, F. Exploration of the effects of high hydrostatic pressure on microbial growth, physiology and survival: perspectives from piezophysiology. *Biosci. Biotechnol. Biochem.* **2007**, *71*, 2347-2357.

Ahmar Siddiqui, M.; Biswal, B.K.; Heynderickx, P.M.; Kim, J.; Khanal, S.K.; Chen, G.; Wu, D. Dynamic anaerobic membrane bioreactor coupled with sulfate reduction (SrDMBR) for saline wastewater treatment. *Bioresour. Technol.* **2022**, *346*, 126447.

Alberta Energy Regulator (AER). State of Fluid Tailings Management for Mineable Oil Sands, 2021; Alberta Energy Regulator: Calgary, CA, 2022; Available online: https://static.aer.ca/prd/documents/reports/State-Fluid-Tailings-Management-Mineable-OilSands.pdf

American Standard for Testing Materials (ASTM). Standard Test Methods for Particle-Size Distribution (Gradation) of Fine-grained Soils Using the Sedimentation (Hydrometer) D7928-17; ASTM International: West Conshohocken, US, 2017.

American Standard for Testing Materials (ASTM). Standard Test Methods for Laboratory Determination of Water (Moisture) Content of Soil and Rock by Mass D2216-19; ASTM International: West Conshohocken, US, 2019.

An, D.; Caffrey, S.M.; Soh, J.; Agrawal, A.; Brown, D.; Budwill, K.; Dong, X.; Dunfield, P.F.; Foght, J.; Gieg, L.M.; et al. Metagenomics of hydrocarbon resource environments indicates aerobic taxa and genes to be unexpectedly common. *Environ. Sci. Technol.* **2013**, *47*, 10708-10717.

Austegard, A.; Solbraa, E.; De Koeijer, G.; Mølnvik, M.J. Thermodynamic models for calculating mutual solubilities in H_2O-CO_2-CH_4 mixtures. *Chem. Eng. Res. Des.* **2006***, 84*, 781-794.

Bae, H.S.; Morrison, E.; Chanton, J.P.; Ogram, A. Methanogens are major contributors to nitrogen fixation in soils of the Florida Everglades. *Appl. Environ. Microbiol.* **2018**, *84*, e02222-17.

Barbato, M.; Scoma, A. Mild hydrostatic-pressure (15 MPa) affects the assembly, but not the growth, of oil-degrading coastal microbial communities tested under limiting conditions (5°C, no added nutrients). *FEMS Microbiol. Ecol.* **2020**, *96*, fiaa160.

Campbell, T.P.; Ulrich, D.E.M.; Toyoda, J.; Thompson, J.; Munsky, B.; Albright, M.B.N.; Bailey, V.L.; Tfaily, M.M.; Dunbar, J. Microbial communities influence soil dissolved organic carbon concentration by altering metabolite composition. *Front. Microbiol.* **2022**, *12*, 799014.

Capo, E.; Broman, E.; Bonaglia, S.; Bravo, A.G.; Bertilsson, S.; Soerensen, A.L.; Pinhassi, J.; Lundin, D.; Buck, M.; Hall, P.O.J.; et al. Oxygen-deficient water zones in the Baltic Sea promote uncharacterized Hg methylating microorganisms in underlying sediments. *Limnol. Oceanogr.* **2022**, *67*, 135-146.

Cassarini, C.; Zhang, Y.; Lens, P.N.L. Pressure selects dominant anaerobic methanotrophic phylotype and sulfate reducing bacteria in coastal marine Lake Grevelingen sediment. *Front. Environ. Sci.* **2019**, *6*, 162.

Cazier, E.A.; Trably, E.; Steyer, J.P.; Escudie, R. Biomass hydrolysis inhibition at high hydrogen partial pressures in solid-state anaerobic digestion. *Bioresour. Technol.* **2015**, *190*, 106-113.

Chen, L.X.; Méheust, R.; Crits-Christoph, A.; McMahon, K.D.; Colenbrander Nelson, T.; Slater, G.F.; Warren, L.A.; Banfield, J.F. Large freshwater phages with the potential to augment aerobic methane oxidation. *Nat. Microbiol.* **2020**, *5*, 1504–1515.

Chen, M.; Walshe, G.; Chi Fru, E.; Ciborowski, J.J.H.; Weisener, C.G. Microcosm assessment of the biogeochemical development of sulfur and oxygen in oil sands fluid fine tailings. *Appl. Geochem.* **2013**, *37*, 1–11.

Collins, C.E.V.; Foght, J.M.; Siddique, T. Co-occurrence of methanogenesis and N_2 fixation in oil sands tailings. *Sci. Total Environ.* **2016**, *565*, 306–312.

Cossey, H.L.; Batycky, A.E.; Kaminsky, H.; Ulrich, A.C. Geochemical stability of oil sands tailings in mine closure landforms. *Minerals* **2021a**, *11*, 830.

Cossey, H.L.; Ulrich A.C. Biogeochemical and geotechnical behavior of treated tailings in oil sands end pit lakes. In Proceedings of the 26th International Conference on Tailings and Mine Waste, Denver, US, 6-9 November 2022.

D'Angelo, T.; Goordial, J.; Lindsay, M.R.; McGonigle, J.; Booker, A.; Moser, D.; Stepanauskus, R.; Orcutt, B.N. Replicated life-history patterns and subsurface origins of the bacterial sister phyla *Nitrospirota* and *Nitrospinota*. *ISME J.* **2023**, *17*, 891-902.

Dai, X.; Luo, F.; Yi, J.; He, Q.; Dong, B. Biodegradation of polyacrylamide by anaerobic digestion under mesophilic condition and its performance in actual dewatered sludge system. *Bioresour. Technol.* **2014**, *153*, 55–61.

Dai, X.; Luo, F.; Zhang, D.; Dai, L.; Chen, Y.; Dong, B.Waste-activated sludge fermentation for polyacrylamide biodegradation improved by anaerobic hydrolysis and key microorganisms involved in biological polyacrylamide removal. *Sci. Rep.* **2015**, *5*, 11675.

Das, R.; Kazy, S.K. Microbial diversity, community composition and metabolic potential in hydrocarbon contaminated oily sludge: prospects for in situ bioremediation. *Environ. Sci. Pollut, Res.* **2014**, *21*, 7369-7389.

Dean, E.W.; Stark, D.D. A convenient method for the determination of water in petroleum and other organic emulsions. *Ind. Eng. Chem.* **1920**, *12(5), 486-490.*

Dompierre, K.A.; Lindsay, M.B.J.; Cruz-Hernández, P.; Halferdahl, G.M. Initial geochemical characteristics of fluid fine tailings in an oil sands end pit lake. *Sci. Total Environ.* **2016**, *556*, 196–206.

Dong, X.; Kleiner, M.; Sharp, C.E.; Thorson, E.; Li, C.; Liu, D.; Strous, M. Fast and simple analysis of MiSeq amplicon sequencing data with MetaAmp. *Front. Microbiol.* **2017**, *8*, 1461.

Duis, K.; Junker, T.; Coors, A. Environmental fate and effects of water-soluble synthetic organic polymers used in cosmetic products. *Environ. Sci. Eur.* **2021**, *33*, 21.

Fedorak, P.M.; Coy, D.L.; Salloum, M.J.; Dudas, M.J. Methanogenic potential of tailings samples from oil sands extraction plants. *Can. J. Microbiol.* **2002**, *48,* 21-33.

Fichtel, K.; Logemann, J.; Fichtel, J.; Rullkötter, Cypionka, H.; Engelen, B. Temperature and pressure adaptation of sulfate reducer from the deep subsurface. *Front. Microbiol.* **2015**, *6*, 1078.

Foght, J.M.; Gieg, L.M.; Siddique, T. The microbiology of oil sands tailings: Past, present, future. *FEMS Microbiol. Ecol.* **2017**, *93*, fix034.

Fotidis, I.A.; Karakashev, D.; Kotsopoulos, T.A.; Martzopoulos, G.G.; Angelidaki, I. Effect of ammonium and acetate on methanogenic pathway and methanogenic community composition. *FEMS Microbiol. Ecol.* **2012**, *83*, 38-48.

Gee, K.; Poon, H.Y.; Hashisho, Z.; Ulrich, A.C. Effect of naphtha diluent on greenhouse gases and reduced sulfur compounds emissions from oil sands tailings. *Sci. Total Environ.* **2017**, *598*, 916-924.

Gonzalez-Rodriguez, D.; Guillou, L.; Cornat, F.; Lafaurie-Janvore, J.; Babataheri, A.; de Langre, E.; Barakat, A.I.; Husson, J. Mechanical criterion for the rupture of a cell membrane under compression. *Biophys. J.* **2016***, 111*, 2711-2721.

Grula, M.M.; Huang, M.; Sewell, G. Interactions of certain polyacrylamides with soil bacteria. *Soil Sci.* **1994**, *158*, 291–300.

Guezennec, A.G.; Michel, C.; Bru, K.; Touze, S.; Desroche, N.; Mnif, I.; Motelica-Heino, M. Transfer and degradation of polyacrylamide-based flocculants in hydrosystems: a review. *Environ. Sci. Pollut. Res.* **2015**, *22*, 6390–6406.

Guo, S. Experimental study on isothermal adsorption of methane gas on three shale samples from Upper Paleozoic strata of the Ordos Basin. *J. Pet. Sci. Eng.* **2013**, *110*, 132-138.

Haveroen, M.E.; MacKinnon, M.D.; Fedorak, P.M. Polyacrylamide added as a nitrogen source stimulates methanogenesis in consortia from various wastewaters. *Water Res.* **2005**, *29*, 3333–3341.

Holmes, D.E.; Finneran, K.T.; O'Neil, R.A.; Lovley, D.R. Enrichment of members of the family *Geobacteraceae* associated with stimulation of dissimilatory metal reduction in uranium-contaminated aquifer sediments. *Appl. Environ. Microbiol.* **2002**, *68*, 2300-2306.

Holmes, D.E.; Nevin, K.P.; Lovley, D.R. Comparison of 16S rRNA, *nifD, recA, gyrB, rpoB* and *fusA* genes within the family *Geobacteraceae* fam. nov. *IJSEM* **2004**, *54*, 1591-1599.

Holowenko, F.M.; MacKinnon, M.D.; Fedorak, P.M. Methanogens and sulfate-reducing bacteria in oil sands fine tailings waste. *Can. J. Microbiol.* **2000**, *46*, 927–937.

Hu, H.; Liu, J.F.; Li, C.Y.; Yang, S.Z.; Gu, J.D.; Mu, B.Z. Anaerobic biodegradation of partially hydrolyzed polyacrylamide in long-term methanogenic enrichment cultures from production water of oil reservoirs. *Biodegradation*, **2018**, *29*, 233-243.

Jeeravipoolvarn, S.; Scott, J.D.; Chalaturnyk, R.J. 10 m standpipe tests on oil sands tailings: Long-term experimental results and prediction. *Can. Geotech. J*. **2009**, *46*, 875–888.

Kaminsky, H. Demystifying the methylene blue index. In Proceedings of the 4th International Oil Sands Tailings Conference, Lake Louise, CA, 7–10 December 2014.

Kuznetsov, P.; Wei, K.; Kuznetsova, A.; Foght, J.; Ulrich, A.; Siddique, T. Anaerobic microbial activity may affect development and sustainability of end-pit lakes: a laboratory study of biogeochemical aspects of oil sands mine tailings. *ACS EST Water*. **2023**, *3*, 1039-1049.

Langwig, M.V.; De Anda, V.; Dombrowski, N.; Seitz, K.W.; Rambo, I.M.; Greening, C.; Testke, A.P.; Baker, B.J. Large-scale protein level comparison of Deltaproteobacteria reveals cohesive metabolic groups. *ISME J.* **2022**, *16*, 307-320.

Lawrence, G.A.; Tedford, E.W. Pieters, R. Suspended solids in an end pit lake: Potential mixing mechanisms. *Can. J. Civ. Eng.* **2016**, *43*, 211–217.

Leigh, J.A. Nitrogen fixation in methanogens: the archaeal perspective. *Curr. Issues Mol. Biol.* **2000**, *2*, 125-131.

Li, J.; How, Z.T.; El-Din, M.G. Aerobic degradation of anionic polyacrylamide in oil sands tailings: impact factor, degradation effect, and mechanism. *Sci. Total Environ.* **2023***, 856*, 159079.

Li, Y.; Kaminsky, H.; Gong, X.Y.; Sun, Y.S.; Ghuzi, M.; Sadighian, A. What affects dewatering performance of high density slurry? *Minerals* **2021**, *11*, 761.

Liang, B.; Wang, L.Y.; Mbadinga, S.M.; Liu, J.F.; Yang, S.Z.; Gu, J.D.; Mu, B.Z. *Anaerolineaceae* and *Methanosaeta* turned to be the dominant microorganisms in alkanes-dependent methanogenic culture after long-term of incubation. *AMB Express* **2015**, *5*, 37.

Lu, J.H.; Wu, L.; Letey, J. Effects of soil and water properties on anionic polyacrylamide sorption. *Soil Sci. Soc. Am. J.* **2002***, 66*, 578-584.

Lyu, Z.; Lu, Y. Metabolic shift at the class level sheds light on adaptation of methanogens to oxidative environments. *ISME J.* **2018***, 12*, 411-423.

Malone, A.S.; Shellhammer, T.H.; Courtney, P.D. Effects of high pressure on the viability, morphology, lysis, and cell wall hydrolase activity of *Lactococcus lactis* subsp. *cremoris*. *Appl. Environ. Microbiol.* **2002**, *68*, 4357-4363.

Mayumi, D.; Dolfing, J.; Sakata, S.; Maeda, H.: Miyagawa, Y.; Ikarashi, M.; Tamaki, H.; Takeuchi, M.; Nakatsu, C.H.; Kamagata, Y. Carbon dioxide concentration dictates alternative methanogenic pathways in oil reservoirs. *Nat. Commun.* **2013**, *4*, 1998.

Mercado, J.V.; Koyama, M.; Nakasaki, K. Complexity of acclimatization substrate affects anaerobic digester microbial community response to organic load shocks. *Environ. Res.* **2023**, *216*, 114722.

Meredith, L.K.; Tfaily, M.M. Capturing the microbial volatilome: an oft overlooked 'ome'. *Trends Microbiol.* **2022**, *30*, 623-631.

Meulepas, R.J.W.; Jagersma, C.G.; Zhang, Y.; Petrillo, M.; Cai, H.; Buisman, C.J.N.; Stams, A.J.M.; Lens, P.N.L. Trace methane oxidation and the methane dependency of sulfate reduction in anaerobic granular sludge. *FEMS Microbiol. Ecol.* **2010**, *72*, 261-271.

Mikula, R.; Omotoso, O. Role of clays in controlling tailings behavior in oil sands processing. *Clay Sci.* **2006**, *12*, 177-182.

Mohamad Shahimin, M.F.; Foght, J.M.; Siddique, T. Preferential methanogenic biodegradation of short-chain *n*-alkanes by microbial communities from two different oil sands tailings ponds. *Sci. Total Environ.* **2016**, *553*, 250-257.

Mohamad Shahimin, M.F.; Foght, J.M.; Siddique, T. Methanogenic biodegradation of *iso*- alkanes by indigenous microbes from two different oil sands tailings ponds. *Microorganisms* **2021**, *9*, 1569.

Mohamad Shahimin, M.F.; Siddique, T. Sequential biodegradation of complex naphtha hydrocarbons under methanogenic conditions in two different oil sands tailings. *Environ. Pollut.* **2017a**, *221*, 398–406.

Pannekens, M.; Voskuhl, L.; Mohammadian, S.; Köster, D.; Meier, A.; Köhne, J.M.; Kulbatzki, M.; Akbari, A.; Haque, S.; Meckenstock, R.U. Microbial degradation rates of natural bitumen. *Environ. Sci. Technol.* **2021**, *55*, 8700-8708.

Pérez-Pantoja, D.; Donoso, R.; Agulló, L.; Córdova, M.; Seeger, M.; Pieper, D.H.; González, B. Genomic analysis of the potential for aromatic compounds biodegradation in *Burkholderiales*, *Environ. Microbiol.* **2011**, *14*, 1091-1117.

Pester, M.; Brambilla, E.; Alazard, D.; Rattei, T.; Weinmaier, T.; Han, J.; Lucas, S.; Lapidus, A.; Cheng, J.F.; Goodwin, L.; et al. Complete genome sequences of *Desulfosporosinus orientis* DSM765^T, *Desulfosporosinus youngiae* DSM17734^T, *Desulfosporosinus meridiei* DSM13257^T, and *Desulfosporosinus acidiphilus* DSM22704^T. *J. Bacteriol.* **2012**, *194*, 6300-6301.

Pope, D.H.; Berger, L.R. Inhibition of metabolism by hydrostatic pressure: what limits microbial growth? *Arch. Mikrobiol.* **1973**, *93*, 367-370.

Pyzik, A.; Ciezkowska, M.; Krawczyk, P.S.; Sobczak, A.; Drewniak, L.; Dziembowski, A.; Lipinski, L. Comparative analysis of deep sequenced methanogenic communities: identification of microorganisms responsible for methane production. *Microb. Cell Factories* **2018**, *17*, 197.

Ramos-Padrón, E.; Bordenave, S.; Lin, S.; Bhaskar, I.M.; Dong, X.; Sensen, C.W.; Fournier, J.; Vourdouw, G.; Gieg, L.M. Carbon and sulfur cycling by microbial communities in a gypsum-treated oil sands tailings pond. *Environ. Sci. Technol.* **2011**, *45*, 439–446.

Reid, M.L.; Warren, L.A. S reactivity of an oil sands composite tailings deposit undergoing reclamation wetland construction. *J. Environ. Manag.* **2016**, *166*, 321–329.

Ren, H.Y.; Zhang, X.J.; Song, Z.Y.; Rupert, W.; Gao, G.J.; Guo, A.X.; Zhao, L.P. Comparison of microbial community compositions of injection and production well samples in a long-term water-flooded petroleum reservoir. *PLoS One* **2011**, *6*, e23258.

Risacher, F.F.; Morris, P.K.; Arriaga, D.; Goad, C.; Colenbrander Nelson, T.; Slater, G.F.; Warren, L.A. The interplay of methane and ammonia as key oxygen consuming constituents in early stage development of Base Mine Lake, the first demonstration oil sands pit lake. *Appl. Geochem.* **2018**, *93*, 49–59.

Scoma, A.; Heyer, R.; Rifal, R.; Dandyk, C.; Marshall, I.; Kerckhof, F.M.; Marietou, A.; Boshker, H.T.S.; Meysman, F.J.R.; Malmos, K.G.; et al. Reduced TCA cycle rates at high hydrostatic pressure hinder hydrocarbon degradation and obligate oil degraders in natural, deep-sea microbial communities. *ISME J.* **2019**, *13*, 1005-1018.

Sethi, A.J. Methylene Blue Test for Clay Activity Determination in Fine Tails, MRRT Procedures, 1995.

Siddique, T.; Kuznetsov, P.; Kuznetsova, A.; Arkell, N.; Young, R.; Li, C.; Guigard, S.; Underwood, E.; Foght, J.M. Microbially-accelerated consolidation of oil sands tailings. Pathway I: changes in porewater chemistry. *Front. Microbiol.* **2014a**, *5*, Article 106.

Song, W.; Zhang, Y.; Gao, Y.; Chen, D.; Yang, M. Cleavage of the main carbon chain backbone of high molecular weight polyacrylamide by aerobic and anaerobic biological treatment. *Chemosphere* **2017**, *189*, 277–283.

Song, W.; Zhang, Y.; Hamidian, A.H.; Yang, M. Biodegradation of low molecular weight polyacrylamide under aerobic and anaerobic conditions: effect of the molecular weight. *Water Sci. Technol.* **2020**, *81*, 301-308.

Stasik, S.; Loick, N.; Knöller, K.; Weisener, C.; Wendt-Potthoff, K. Understanding biogeochemical gradients of sulfur, iron and carbon in an oil sands tailings pond. *Chem. Geol*. **2014**, *382*, 44–53.

Stasik, S.; Schmidt, J.; Wendt-Potthoff, K. High potential for anaerobic microbial sulfur oxidation in oil sands tailings ponds. *Microorganisms* **2021***, 9*, 2529.

Stasik, S.; Wendt-Potthoff, K. Interaction of microbial sulphate reduction and methanogenesis in oil sands tailings ponds. *Chemosphere* **2014**, *103*, 59–66.

Stasik, S.; Wendt-Potthoff, K. Vertical gradients in carbon flow and methane production in a sulfate-rich oil sands tailings pond. *Water Res*. **2016**, *106*, 223–231.

Suncor Energy Operating Inc. (Suncor). 2021 Fort Hills Fluid Tailings Management Report; Suncor Energy Operating Inc. on behalf of Fort Hills Energy Corporation; Calgary, CA, 2022b.

Tedford, E.; Halferdahl, G.; Pieters, R.; Lawrence, G.A. Temporal variations in turbidity in an oil sands pit lake. *Environ. Fluid Mech.* **2019**, *19*, 457–473.

Tholosan, O.; Garcin, J.; Bianchi, A. Effects of hydrostatic pressure on microbial activity through a 2000 m deep water column in the NW Mediterranean Sea. *Mar. Ecol. Prog. Ser.* **1999***, 183*, 49-57.

Wang, Z.; Wang, S.; Hu, Y.; Du, B.; Meng, J.; Wu, G.; Liu, H.; Zhan, X. Distinguishing responses of acetoclastic and hydrogenotrophic methanogens to ammonia stress in mesophilic mixed cultures. *Water Res.* **2022**, *224*, 119029.

Wang, H.; Wang, C.; Lin, M.; Sun, X.; Wang, C.; Hu, X. Phylogenetic diversity of bacterial communities associated with bioremediation of crude oil in microcosms. *Int. Biodeterior. Biodegrad.* **2013**, *85*, 400-406.

Warren, L.A.; Kendra, K.E.; Brady, A.L.; Slater, G.F. Sulfur biogeochemistry of an oil sands composite tailings deposit. *Front. Microbiol.* **2016**, *6*, 1–14.

Wersin, P.; Leupin, O.X.; Mettler, S.; Gaucher, E.C.; Mäder, U.; De Cannière, P.; Vinsot, A.; Gäbler, H.E.; Kunimaro, T.; Kiho, K.; et al. Biogeochemical processes in a clay formation in situ experiment: part A – overview, experimental design and water data of an experiment in the Opalinus Clay at the Mont Terri Underground Research Laboratory, Switzerland. *Appl. Geochem.* **2011a**, *26,* 931-953.

Wersin, P.; Stroes-Gascoyne, S.; Pearson, F.J.; Tournassat, C.; Leupin, O.X.; Schwyn, B. Biogeochemical processes in a clay formation in situ experiment: part G – key interpretations and conclusions. Implications for repository safety. *Appl. Geochem.* **2011b**, *26,* 1023-1034.

Wu, Z.; Guiping, L.; Ji, Y.; Li, P.; Yu, X.; Qiao, X.; Wang, B.; She, K.; Liu, W.; Liang, B.; et al. Electron acceptors determine the BTEX degradation capacity of anaerobic microbiota via regulating the microbial community. *Environ. Res.* **2022**, *215*, 114420.

Zhang, M. Role of Bitumen Viscosity in Bitumen Recovery from Athabasca Oil Sands. M.Sc. Thesis, University of Alberta, Edmonton, CA, 2012.

6 CONCLUSIONS AND RECOMMENDATIONS

6.1 Summary of Key Findings

The overall purpose of this research, as described in Chapter 1, was to evaluate and improve upon pit lakes which are a proposed oil sands tailings reclamation strategy. Three laboratory studies were designed to i) improve pit lake water chemistry by mitigating turbidity generation (Chapter 3) and ii) evaluate the biogeochemical and geotechnical behavior of untreated and treated FFT in pit lakes (Chapters 4 and 5). These studies provide valuable information regarding a biological turbidity mitigation mechanism that was successful at the laboratory scale, as well as key biogeochemical and geotechnical behaviors of untreated and treated FFT that will be important to mitigate, monitor, and/or manage in the field as part of ensuring successful reclamation of oil sands tailings in pit lakes.

The overall purpose of this research was achieved through three objectives which correspond to the laboratory studies presented in Chapters 3 to 5. A summary of the key findings associated with each of the research objectives is provided below.

Objective 1. Mitigate turbidity in oil sands pit lakes using biofilms (Chapter 3)

The laboratory study presented in Chapter 3 is the first to demonstrate biostabilization via mudline biofilms as a mechanism of turbidity mitigation in oil sands pit lakes. Mudline biofilms reduced turbidity generation by up to 99% during physical mixing experiments. Biofilms mitigated turbidity generation during two mixing tests, 35 d apart, and at multiple mixing speeds (80 to 200 rpm) relative to controls without biofilms (sterilized FFT). Further, biofilms accelerated turbidity dissipation due in part to the visibly larger size of any suspended particles/flocs. Turbidity increased in all jars during the second mixing test (relative to the first mixing test), though biofilms still substantially reduced turbidity generation relative to controls. Multiple factors likely contributed to the higher turbidity generation in biofilm jars during the second mixing test, including death and decay of older biofilm layers, reduced biofilm integrity due to physical mixing in the water cap, and decreased photosynthesis due to turbidity. Biofilm age was also investigated in this study (10 versus 20-week-old biofilms). Older biofilms had visibly weaker attachment to the underlying FFT due to gas release and microbial death and decay. While younger biofilms

performed better, with 93 and 99% turbidity reduction during two mixing tests, older biofilms still showed substantial improvement over controls, with 69 to 95% turbidity reduction during two mixing tests.

In this study, mudline biofilms were made up of multiple layers of diverse microbial communities indigenous to oil sands tailings, including photoautotrophic cyanobacteria and green algae as well as facultative or anaerobic heterotrophs. It is likely that these communities of photoautotrophs and heterotrophs had mutually beneficial relationships which further enhanced biostabilization. In the field, the microbial communities that make up mudline biofilms would largely depend on light penetration and the depth of the mudline but would also be influenced by temporal seasonal changes and nutrient/substrate availability. Mudline biofilms in littoral zones may consist predominately of algae or photoautotrophic cyanobacteria. Conversely, mudline biofilms that develop at greater depths or in turbid zones may consist primarily of facultative or anaerobic heterotrophs. While these differences in microbial community structure may impact biostabilization in the field (for example, different microorganisms have different attachment/binding styles which can impact adhesion to sediments (Gerbersdorf and Wieprecht 2015)), this research clearly demonstrates that biostabilization of FFT is a promising mechanism of turbidity mitigation in pit lakes.

Objective 2. Evaluate the biogeochemical and geotechnical behavior of untreated and PASS-treated oil sands tailings in pit lakes (Chapter 4)

The column study presented in Chapter 4 revealed the influence of PASS treatment, hydrocarbon amendments, and column size on the biogeochemical and geotechnical behavior of FFT; temperature and CO_2 addition were not as significant as the other three factors evaluated in this study. The tailings in all 64 columns underwent self-weight consolidation and achieved a higher solids content over 540 d. NWR from the tailings was impacted by column size, with 1 L columns undergoing rapid initial NWR before plateauing around Day 60. Conversely, 19 L columns underwent long-term settlement and consolidation and some of these columns were still undergoing self-weight consolidation (based on continual NWR) by Day 540. NWR from tailings in the 19 L columns eventually exceeded that of comparable 1 L columns due to the higher total

stress in the 19 L columns. PASS treatment also influenced geotechnical behavior and resulted in a lower NWR and lower solids content compared to untreated FFT. PASS treatment was designed in part to improve FFT dewatering and as such, this study highlights difficulties in achieving the desired flocculation and dewatering performance, even in a controlled laboratory setting.

During the 540 d study, the dominant microbial process in all columns was sulfate reduction. This may be in part due to the lack of methanogens in the tailings on Day 0 and the time needed for these communities to develop. The most extensive sulfate reduction occurred in columns with hydrocarbon amendments and/or PASS-treated FFT and PASS-treated FFT had a greater relative abundance of known SRB. Pore water sulfate concentrations were reduced by >99% in hydrocarbon amended tailings (equivalent to a sulfate reduction of 628 mg/L and 315 mg/L in PASS-treated and untreated FFT, respectively). In unamended tailings, pore water sulfate concentrations were reduced by 242 mg/L and 71 mg/L in PASS-treated and untreated FFT, respectively. Aqueous sulfide species, generated through sulfate reduction, were present throughout the pore water and/or water caps in >90% of the columns containing PASS-treated FFT, as well as in some columns containing untreated FFT. Sulfate reduction also led to significant increases in alkalinity and $CO_{2(g)}$, as well as lower pore water concentrations of divalent cations (presumably a result of carbonate mineral precipitation).

Water cap chemistry in the columns was influenced by consolidation-driven advection, diffusion, and biogeochemical reactions in the tailings. The combination of these processes generally increased concentrations of ions and organics in the column water caps. Diffusion was significantly influenced by column size and caused water cap concentrations to continually increase in the 1 L columns, despite a plateau in NWR. By Day 540, the 1 L columns had higher water cap concentrations of pore water constituents (such as Na^+) , even though the 19 L columns had higher NWR.

In summary, over the course of the experiment the tailings in all 64 columns underwent self-weight consolidation, which caused advective fluxes of pore water into the water cap. Water cap concentrations of pore water constituents also increased over time due to diffusion (though this primarily occurred in the 1 L columns). The dominant microbial process in all columns was sulfate

reduction, which subsequently influenced alkalinity, $CO_{2(g)}$, and divalent cations. Column size had a significant influence on NWR (higher in 19 L columns) and diffusion (higher in 1 L columns). Meanwhile, PASS treatment negatively impacted NWR and both PASS treatment and hydrocarbon amendments enhanced sulfate reduction.

Objective 3. Evaluate the effects of pressure on the biogeochemical and geotechnical behavior of PASS-treated oil sands tailings in pit lakes (Chapter 5)

The column study presented in Chapter 5 is the first to evaluate and elucidate the effects of pressure on the biogeochemical behavior of oil sands tailings. Moreover, this study revealed that pressure (0.3 to 5.1 kPa) significantly influences both the geotechnical and biogeochemical behavior of PASS-treated FFT.

As expected, pressure significantly enhanced consolidation of the tailings. By Day 360, PASS-treated FFT under pressure had a 20% higher NWR and 16 wt% higher solids content than PASS-treated FFT undergoing self-weight consolidation. Pressure also enhanced microbial activity in the tailings. This was evidenced by the generation of significantly more $CO_{2(g)}$ and $CH_{4(g)}$ in columns with pressure, as well as higher concentrations of DOC and COD throughout these columns. It is likely that applying pressure to the tailings increased the solubility of microbial substrates and metabolites, which subsequently enhanced microbial growth and activity. Pressure also impacted microbial community structure and there was a shift from hydrogenotrophic methanogens to acetoclastic methanogens in columns with pressure, indicating that pressure made the acetoclastic methanogenic pathway more thermodynamically favorable. Finally, columns with pressure generated significantly higher concentrations of ammonium. It is suspected that in columns with pressure, microorganisms generated nitrogen through PAM degradation and/or N_2 fixation to meet the nutrient demands of the enhanced microbial growth and activity.

Sulfate reduction also occurred in all columns, though the majority of the sulfate reduction occurred prior to pressure application (Day 60). While it is not possible to evaluate the full effect of pressure on sulfate reduction, it is suspected that pressure would have enhanced sulfate reduction as well, given that pressure significantly decreased pore water sulfate concentrations in

PASS, No HC + P columns between Days 60 to 120. Similar to the results of Chapter 4, rapid sulfate reduction occurred in hydrocarbon amended tailings, with 97% of the pore water sulfate reduced in these columns by Day 60. In unamended tailings, sulfate reduction continued beyond Day 60 and pore water sulfate concentrations were reduced by greater than 96% by Day 180. Aqueous sulfide species, generated from sulfate reduction, were present throughout the pore water and water caps in all columns. In addition, $H_2S_{(g)}$ was detected in more than 80% of the columns during the 360 d study.

Comparing the different geotechnical and biogeochemical behaviors seen in Chapters 4 and 5 for similarly PASS-treated FFT highlights the influence of the source of tailings on observed behavior as well as the importance of providing a thorough characterization of all feed materials in publications. The FFT in Chapter 5 was more microbially active than the FFT used in Chapter 4, likely due to differences in the microbial communities that had established in the tailings prior to commencing the column studies as well as the availability of suitable carbon sources in the tailings. These differences resulted in almost complete sulfate reduction (from 437 mg/L to 15 mg/L) in the unamended PASS-treated FFT in Chapter 5 after 180 d whereas in Chapter 4, roughly 390 mg/L of sulfate remained in the unamended PASS-treated FFT after 540 d. Further, 1 L columns containing PASS-treated FFT from Chapter 5 produced 30 times more CH_4 and had a 12% higher NWR than comparable 1 L columns containing PASS-treated FFT from Chapter 4. Thus, the biogeochemical and geotechnical behaviors observed in these laboratory studies are highly dependent on the source of the tailings.

6.2 Recommendations for Future Research

Turbidity is an ongoing issue in BML and recent research has found that alum addition to the water cap had unintended consequences, including expansion of the water cap's anoxic layer (Jessen et al. 2022). As such, a biological mechanism of turbidity mitigation may be the best strategy for BML and/or future oil sands pit lakes. The findings from Chapter 3 clearly demonstrate that biofilms are a promising mechanism of turbidity mitigation in pit lakes. However, there are a number of factors that could impact the development of mudline biofilms in the field that should be investigated further. Firstly, future work should investigate biofilms grown under aerobic versus anaerobic conditions and physical mixing tests should be conducted to determine how these

different microbial community structures influence biostabilization and turbidity mitigation. The influences of temporal seasonal changes, such as lake turnover and ice cover, on biostabilization should also be investigated. In this study biofilms were grown under quiescent conditions, however, physical mixing events such as spring/fall turnover may impact the growth and integrity of mudline biofilms. Further, it would be valuable to investigate the effects of ice cover on biofilm growth as turbidity is still present in BML during ice cover due to gas ebullition from FFT (Tedford et al. 2019; Zhao et al. 2022). While ice cover would reduce oxygen concentrations and light penetration (Lawrence et al. 2016), thereby impacting photoautotrophic biofilms in the littoral zone, it would be important to maintain the growth and development of heterotrophic biofilms during winter. In Chapter 3, gas ebullition contributed to lifting and layering and weaker sediment attachment in older biofilms, however, the effects (if any) of gas ebullition on biofilm growth are unclear. Further, consolidation, and thereby pore water expression, were minimal during this biofilm study and as such, the effects of pore water expression on biofilm growth and structure should also be evaluated. The growth conditions that were not accounted for in this work (aerobic vs. anaerobic, gas ebullition, pore water fluxes, seasonal events) could influence biostabilization in the field and should be the focus of future FFT biostabilization studies.

The column studies in Chapters 4 and 5 showed numerous biogeochemical changes that can occur in FFT under anaerobic conditions over a relatively short period of time (1 to 1.5 yr). Shortening sampling time periods in future laboratory studies could help to further elucidate some of these complex biogeochemical changes. For example, sampling periods of 15 to 30 d would be better for capturing the rapid sulfate reduction that was seen in Chapters 4 and 5 for hydrocarbon amended tailings. These columns studies also revealed that biogeochemical and geotechnical behaviors can be highly dependent on both the source of the tailings and the experimental set-up (for example, column size influences geotechnical behavior and chemical mass loading). Using multiple sources/types of tailings and experimental set-ups when evaluating treatment technologies and biogeochemical and geotechnical behavior would be ideal in order to better assess findings and apply them to broader scenarios. Further, including thorough characterization data in publications can help to ensure that results are evaluated (and generalized) appropriately.

Future studies should be conducted to further understand and explore the effects of pressure on microbial activity and biogeochemical cycling in oil sands tailings. In future work, qPCR should be conducted for total quantification of bacteria and archaea to better evaluate how pressure impacts microbial growth. Based on the findings in Chapter 5, it was suspected that concentrations of microbial metabolites and intermediate substrates would be higher in columns with pressure. Measuring microbial metabolites and intermediate substrates (such as volatile fatty acids) periodically throughout the study could confirm this theory. Future work should also include a metagenomics-metabolomics study which would provide a more detailed analysis of microbial communities and their functions and the metabolic pathways that are influenced or enhanced (indirectly) by pressure. Additional studies should also aim to reveal if PAM is being degraded and used as a nitrogen source and/or if N_2 fixation is occurring. A good starting point would be to evaluate the occurrence of N_2 fixation by using $^{15}N_2$ in the headspace and analyzing its uptake into microbial biomass and/or soluble ions (ammonium, nitrite, or nitrate), as outlined in Collins et al. (2016). Finally, this work used relatively low pressures (0.3 to 5.1 kPa) and additional studies should be developed to evaluate the effects of higher pressures on microbial activity and biogeochemical cycling in FFT. Depending on the 'type' of pressure being mimicked (total stress, effective stress, or hydrostatic pressure), pressures up to roughly 1 MPa may be appropriate.

6.3 References

Collins, C.E.V.; Foght, J.M.; Siddique, T. Co-occurrence of methanogenesis and N_2 fixation in oil sands tailings. *Sci. Total Environ.* **2016**, *565*, 306–312.

Gerbersdorf, S.U.; Wieprecht, S. Biostabilization of cohesive sediments: Revisiting the role of abiotic conditions, physiology and diversity of microbes, polymeric secretion, and biofilm architecture. *Geobiology* **2015**, *13*, 68–97.

Jessen, G.L.; Chen, L.-X.; Mori, J.F.; Nelson, Nelson, T.E.C.; Slater, G.F.; Lindsay, M.B.J.; Banfield, J.F.; Warren, L.A. Alum addition triggers hypoxia in an engineered pit lake. *Microorganisms* **2022**, *10*, 510.

Lawrence, G.A.; Tedford, E.W. Pieters, R. Suspended solids in an end pit lake: Potential mixing mechanisms. *Can. J. Civ. Eng.* **2016**, *43*, 211–217.

Tedford, E.; Halferdahl, G.; Pieters, R.; Lawrence, G.A. Temporal variations in turbidity in an oil sands pit lake. *Environ. Fluid Mech.* **2019**, *19*, 457–473.

Zhao, K.; Tedford, E.W.; Zare, M.; Lawrence, G.A. Impact of atmospheric pressure variations on methane ebullition and lake turbidity during ice-cover. *L&O Letters* **2021**, *6*, 253-261.

BIBLIOGRAPHY

Abe, F. Exploration of the effects of high hydrostatic pressure on microbial growth, physiology and survival: perspectives from piezophysiology. *Biosci. Biotechnol. Biochem.* **2007**, *71*, 2347-2357.

Ahmar Siddiqui, M.; Biswal, B.K.; Heynderickx, P.M.; Kim, J.; Khanal, S.K.; Chen, G.; Wu, D. Dynamic anaerobic membrane bioreactor coupled with sulfate reduction (SrDMBR) for saline wastewater treatment. *Bioresour. Technol.* **2022**, *346*, 126447.

Albakistani, E.A.; Nwosu, F.C.; Furgason, C.; Haupt, E.S.; Smirnova, A.V.; Verbeke, T.J.; Lee, E.S.; Kim, J.J.; Chan, A.; Ruhl, I.A.; et al. Seasonal dynamics of methanotrophic bacteria in a boreal oil sands end pit lake. *Appl. Environ. Microbiol.* **2022**, *88*, e01455-21.

Alberta Energy Regulator (AER). State of Fluid Tailings Management for Mineable Oil Sands, 2019; Alberta Energy Regulator: Calgary, CA, 2020.

Alberta Energy Regulator (AER). State of Fluid Tailings Management for Mineable Oil Sands, 2021; Alberta Energy Regulator: Calgary, CA, 2022; Available online: https://static.aer.ca/prd/documents/reports/State-Fluid-Tailings-Management-Mineable-OilSands.pdf

American Standard for Testing Materials (ASTM). Standard Test Methods for Particle-Size Distribution (Gradation) of Fine-grained Soils Using the Sedimentation (Hydrometer) D7928-17; ASTM International: West Conshohocken, US, 2017.

American Standard for Testing Materials (ASTM). Standard Test Methods for Laboratory Determination of Water (Moisture) Content of Soil and Rock by Mass D2216-19; ASTM International: West Conshohocken, US, 2019.

Amoako, K. Geotechnical Behaviour of Two Novel Polymer Treatments of Oil Sands Fine Tailings. M.Sc. Thesis, University of Alberta, Edmonton, CA, 2020.

Amos, C.L.; Bergamasco, A.; Umgiesser, G.; Cappucci, S.; Cloutier, D.; DeNat, L.; Flindt, M.; Bonardi, G.; Cristante, S. The stability of tidal flats in Venice Lagoon—The results of in-situ measurements using two benthic annular flumes. *J. Mar. Syst.* **2004**, *51*, 211–241.

An, D.; Caffrey, S.M.; Soh, J.; Agrawal, A.; Brown, D.; Budwill, K.; Dong, X.; Dunfield, P.F.; Foght, J.; Gieg, L.M.; et al. Metagenomics of hydrocarbon resource environments indicates aerobic taxa and genes to be unexpectedly common. *Environ. Sci. Technol.* **2013**, *47*, 10708-10717.

Andersen, R.A.; Kawachi, M. Traditional microalgae isolation techniques. In *Algal Culturing Techniques*, 1st ed.; Andersen, R.A., Ed.; Elsevier, Inc.: San Diego, US, 2005; pp. 83–100.

Anishchenko, O.V.; Gladyshev, M.I.; Kravchuk, E.S.; Ivanova, E.A.; Gribovskaya, L.V.; Sushchik, N.N. Seasonal variations of metal concentrations in periphyton and taxonomic composition of the algal community at a Yenisei River littoral site. *Cent. Eur. J. Biol.* **2010**, *5*, 125–134.

Arriaga, D.; Colenbrander Nelson, T.; Risacher, F.F.; Morris, P.K.; Goad, C.; Slater, G.F.; Warren, L.A. The co-importance of physical mixing and biogeochemical consumption in controlling water cap oxygen levels in Base Mine Lake. *Appl. Geochem.* **2019**, *111*, 104442.

Austegard, A.; Solbraa, E.; De Koeijer, G.; Mølnvik, M.J. Thermodynamic models for calculating mutual solubilities in H_2O-CO_2-CH_4 mixtures. *Chem. Eng. Res. Des.* **2006***, 84*, 781-794.

Australian and New Zealand Environment and Conservation Council & Agriculture and Resource Management Council of Australia and New Zealand (ANZECC & ARMCANZ). Australian and New Zealand Guidelines for Fresh and Marine Water Quality; ANZECC & ARMCANZ: Canberra, AU, 2000.

Bae, H.S.; Morrison, E.; Chanton, J.P.; Ogram, A. Methanogens are major contributors to nitrogen fixation in soils of the Florida Everglades. *Appl. Environ. Microbiol.* **2018**, *84*, e02222-17.

Bakhtiari, M.T. Role of Sodium Hydroxide in Bitumen Extraction: Production of Natural Surfactants and Slime Coating. Ph.D. Thesis, University of Alberta, Edmonton, CA, 2015.

Ball, J. W.; Nordstrom, D. K. User's Manual for WATEQ4F, with Revised Thermodynamic Data Base and Text Cases for Calculating Speciation of Major, Trace, and Redox Elements in Natural Waters, U.S. Geological Survey: Menlo Park, US, 1991.

Bao, M.; Chen, Q.; Li, Y.; Jiang, G. Biodegradation of partially hydrolyzed polyacrylamide by bacteria isolated from production water after polymer flooding in an oil field. *J. Hazard. Mater.* **2010**, *184*, 105–110.

Baotian, W.; Shuaijie, G.; Funhai, Z. Research on deposition and consolidation behavior of cohesive sediment with settlement column experiment. *Eur. J. Environ. Civ. Eng.* **2013***, 17*, s144-s157.

Barbato, M.; Scoma, A. Mild hydrostatic-pressure (15 Mpa) affects the assembly, but not the growth, of oil-degrading coastal microbial communities tested under limiting conditions (5°C, no added nutrients). *FEMS Microbiol. Ecol.* **2020**, *96*, fiaa160.

Begmatov, S.; Beletsky, A.V.; Dedysh, S.N.; Mardanov, A.V.; Ravin, N.V. Genome analysis of the candidate phylum MBNT15 bacterium from a boreal peatland predicted its respiratory versatility and dissimilatory iron metabolism. *Front. Microbiol.* **2022**, *13*, 951761.

Beier, N.A. Development of a Tailings Management Simulation and Technology Evaluation Tool. Ph.D. Thesis, University of Alberta, Edmonton, CA, 2015.

Berdugo-Clavijo, C.; Sen, A.; Seyyedi, M.; Quintero, H.; O'Neil, B.; Gieg, L.M. High temperature utilization of PAM and HPAM by microbial communities enriched from oilfield produced water and activated sludge. *AMB Express* **2019**, *9*, 1–10.

BGC Engineering Inc. Oil Sands Tailings Technology Review; Oil Sands Research and Information Network, University of Alberta: Edmonton, CA, 2010.

Biagi, K.M.; Carey, S.K. The hydrochemical evolution of a constructed peatland in a post-mining landscape six years after construction. *J. Hydrol. Reg. Stud.* **2022**, *39*, 100978.

Biagi, K.M.; Clark, M.G.; Carey, S.K. Hydrological functioning of a constructed peatland watershed in the Athabasca oil sands region: Potential trajectories and lessons learned. *Ecol. Eng.* **2021**, *166*, 106236.

Biagi, K.M.; Oswald, C.J.; Nicholls, E.M.; Carey, S.K. Increases in salinity following a shift in hydrologic regime in a constructed wetland watershed in a post-mining oil sands landscape. *Sci. Total Environ.* **2019**, *653*, 1445–1457.

Birtwell, I.K.; Farrell, M.; Jonsson, A. The Validity of Including Turbidity Criteria for Aquatic Resource Protection in Land Development Guideline (Pacific and Yukon Region); Fisheries and Oceans Canada: Vancouver, CA, 2008. Available online: https://publications.gc.ca/collections/collection_2014/mpo-dfo/Fs97-4-2852-eng.pdf

Blanchette, M.L.; Lund, M.A. Pit lakes are a global legacy of mining: an integrated approach to achieving sustainable ecosystems and value for communities. *Curr. Opin. Environ. Sustain.* **2016**, *23,* 28-34.

Boldt-Burisch, K.; Naeth, M.A.; Schneider, U.; Schenider, B.; Hüttl, R.F. Plant growth and arbuscular mycorrhizae development in oil sands processing by-products. *Sci. Total Environ.* **2018**, *621*, 30–39.

Bordenave, S.; Ramos, E.; Lin, S.; Voordouw, G.; Gieg, L.; Guo, C.; Wells, S. Use of calcium sulfate to accelerate densification while reducing greenhouse gas emissions from oil sands

tailings ponds. In Proceedings of the Canadian International Petroleum Conference, Calgary, CA, 16–18 June 2009.

Bordenave, S.; Kostenko, V.; Dutkoski, M.; Grigoryanm, A.; Martinuzzi, R.J.; Voordouw, G. Relation between the activity of anaerobic microbial populations in oil sands tailings ponds and the sedimentation of tailings. *Chemosphere* **2010**, *81*, 663–668.

Bornstein, J.; Hedstrom, W.E.; Scott, F.R. Oxygen Diffusion Rate Relationships under Three Soil Conditions; Life Sciences and Agriculture Experiment Station, University of Maine: Orono, US, 1980; Volume 98, pp. 1–14.

Brown, L.D.; Ulrich, A.C. Oil sands naphthenic acids: A review of properties, measurement, and treatment. *Chemosphere* **2015**, *127*, 276–290.

Burkus, Z.; Wheler, J.; Pletcher, S. GHG Emissions from oil sands tailings ponds: Overview and modelling based on fermentable substrates. In Part I: Review of Tailings Pond Facts and Practices; Alberta Environment and Sustainable Resource Development: Edmonton, CA, 2014.

Burow, L.C.; Woebken, D.; Marshall, I.P.G.; Singer, S.W.; Pett-Ridge, J.; Prufert-Bebout, L.; Spormann, A.M.; Bebout, B.M.; Weber, P.K.; Hoehler, T.M. Identification of *Desulfobacterales* as primary hydrogenotrophs in a complex microbial mat community. *Geobiology* **2014**, *12*, 221-230.

Callahan, B.J.; McMurdie, P.J.; Rosen, M.J.; Han, A.W.; Johnson, A.J.A.; Holmes, S.P. DADA2: High-resolution sample interference from Illumina amplicon data. *Nat. Methods* **2016**, *13*, 581–583.

Campbell, T.P.; Ulrich, D.E.M.; Toyoda, J.; Thompson, J.; Munsky, B.; Albright, M.B.N.; Bailey, V.L.; Tfaily, M.M.; Dunbar, J. Microbial communities influence soil dissolved organic carbon concentration by altering metabolite composition. *Front. Microbiol.* **2022**, *12*, 799014.

Canada's Oil Sands Innovation Alliance (COSIA). 2019 Water Mining Research Report; Canada's Oil Sands Innovation Alliance: Calgary, CA, 2020.

Canada's Oil Sands Innovation Alliance (COSIA). Pit Lakes: A Surface Mining Perspective; Canada's Oil Sands Innovation Alliance: Calgary, CA, 2021; Available online: https://cosia.ca/sites/default/files/attachments/Park%20-%20COSIA%20-%20Pit%20Lakes%20- %20Final.pdf

Capo, E.; Broman, E.; Bonaglia, S.; Bravo, A.G.; Bertilsson, S.; Soerensen, A.L.; Pinhassi, J.; Lundin, D.; Buck, M.; Hall, P.O.J.; et al. Oxygen-deficient water zones in the Baltic Sea promote uncharacterized Hg methylating microorganisms in underlying sediments. *Limnol. Oceanogr.* **2022**, *67*, 135-146.

Caporaso, J.G.; Lauber, C.L.; Walters, W.A.; Berg-Lyons, D.; Lozupone, C.A.; Turnbaugh, P.J.; Fierer, N.; Knight, R. Global patterns of 16S rRNA diversity at a depth of millions of sequences per samples. *PNAS* **2011**, *108 (*Suppl. S1*)*, 4516–4522.

Casco, M.A.; Mac Donagh, M.E.; Cano, M.G.; Solari, L.C.; Claps, M.C.; Gabellone, N.A. Phytoplankton and Epipelon responds to clear and turbid phases in a seepage lake (Buenos Aires, Argentina). *Internat. Rev. Hydrobiol.* **2009**, *94*, 153–168.

Cassarini, C.; Zhang, Y.; Lens, P.N.L. Pressure selects dominant anaerobic methanotrophic phylotype and sulfate reducing bacteria in coastal marine Lake Grevelingen sediment. *Front. Environ. Sci.* **2019**, *6*, 162.

Caulfield, M.J.; Qiao, G.G.; Solomon, D.H. Some aspects of the properties and degradation of polyacrylamides. *Chem. Rev.* **2002**, *102*, 3067–3083.

Cazier, E.A.; Trably, E.; Steyer, J.P.; Escudie, R. Biomass hydrolysis inhibition at high hydrogen partial pressures in solid-state anaerobic digestion. *Bioresour. Technol.* **2015**, *190*, 106-113.

Chalaturnyk, R.J.; Scott, J.D.; Özüm, B. Management of oil sands tailings. *Pet. Sci. Technol.* **2002**, *20*, 1025–1046.

Charette, T.; Castendyk, D.; Hrynshyn, J.; Kupper, A.; McKenna, G.; Mooder, B. End Pit Lakes Guidance Document 2012; Cumulative Environmental Management Association: Fort McMurray, CA, 2010.

Chen, L.X.; Méheust, R.; Crits-Christoph, A.; McMahon, K.D.; Colenbrander Nelson, T.; Slater, G.F.; Warren, L.A.; Banfield, J.F. Large freshwater phages with the potential to augment aerobic methane oxidation. *Nat. Microbiol.* **2020**, *5*, 1504–1515.

Chen, M.; Walshe, G.; Chi Fru, E.; Ciborowski, J.J.H.; Weisener, C.G. Microcosm assessment of the biogeochemical development of sulfur and oxygen in oil sands fluid fine tailings. *Appl. Geochem.* **2013**, *37*, 1–11.

Chou, L.; Garrels, R.M.; Wollast, R. Comparative study of the kinetics and mechanics of dissolution of carbonate minerals. *Chem. Geol.* **1989**, *78*, 269-282.

Chow, D.L.; Nasr, T.N.; Chow, R.S.; Sawatzky, R.P. Recovery techniques for Canada's heavy oil and bitumen resources. *J. Can. Petrol. Technol.* **2008**, *47*, 12–17.

Clark, K.A.; Pasternack, D.S. Hot water separation of bitumen from Alberta bituminous sand. *Ind. Eng. Chem.* **1932**, *24*, 1410–1416.

Clark, M.G.; Drewitt, G.B.; Carey, S.K. Energy and carbon fluxes from an oil sands pit lake. *Sci. Total Environ.* **2021**, *752*, 141966.

Clark, M.G.; Humphreys, E.R.; Carey, S.K. The initial three years of carbon dioxide exchange between the atmosphere and a reclaimed oil sands wetland. *Ecol. Eng.* **2019**, *17*, 667–682.

Clark, M.G.; Humphreys, E.R.; Carey, S.K. Low methane emissions from a boreal wetland constructed on oil sands mine tailings. *Biogeosciences* **2020**, *135*, 116–126.

Clemente, J.S.; MacKinnon, M.D.; Fedorak, P.M. Aerobic biodegradation of two commercial naphthenic acids preparations. *Environ. Sci. Technol.* **2004**, *38*, 1009–1016.

Collins, C.E.V.; Foght, J.M.; Siddique, T. Co-occurrence of methanogenesis and N_2 fixation in oil sands tailings. *Sci. Total Environ.* **2016**, *565*, 306–312.

Comiti, J.; Renaud, M. A new model for determining mean structure parameters of fixed beds from pressure drop measurements, with application to beds packed with parallelepipedal particles. *Chem. Eng. Sci.* **1989**, *44*, 1539–1545.

Cossey, H.L.; Batycky, A.E.; Kaminsky, H.; Ulrich, A.C. Geochemical stability of oil sands tailings in mine closure landforms. *Minerals* **2021a**, *11*, 830.

Cossey, H.L., Kaminsky, H., Ulrich, A.C. Evaluating the long-term behavior of an oil sands tailings reclamation strategy. In Proceedings of Mine Closure 2022, Brisbane AU, 4-6 October 2022.

Cossey, H.L.; Kuznetsov, P.V.; Ulrich A.C. Evaluating the biogeochemical and consolidation behavior of oil sands end pit lakes with accelerated aging. In Proceedings of the 25th International Conference on Tailings and Mine Waste, Banff, CA, 7-10 November 2021b.

Cossey, H.L.; Ulrich A.C. Biogeochemical and geotechnical behavior of treated tailings in oil sands end pit lakes. In Proceedings of the 26th International Conference on Tailings and Mine Waste, Denver, US, 6-9 November 2022.

D'Angelo, T.; Goordial, J.; Lindsay, M.R.; McGonigle, J.; Booker, A.; Moser, D.; Stepanauskus, R.; Orcutt, B.N. Replicated life-history patterns and subsurface origins of the bacterial sister phyla *Nitrospirota* and *Nitrospinota*. *ISME J.* **2023**, *17*, 891-902.

Dai, X.; Luo, F.; Yi, J.; He, Q.; Dong, B. Biodegradation of polyacrylamide by anaerobic digestion under mesophilic condition and its performance in actual dewatered sludge system. *Bioresour. Technol.* **2014**, *153*, 55–61.

Dai, X.; Luo, F.; Zhang, D.; Dai, L.; Chen, Y.; Dong, B. Waste-activated sludge fermentation for polyacrylamide biodegradation improved by anaerobic hydrolysis and key microorganisms involved in biological polyacrylamide removal. *Sci. Rep.* **2015**, *5*, 11675.

Das, R.; Kazy, S.K. Microbial diversity, community composition and metabolic potential in hydrocarbon contaminated oily sludge: prospects for in situ bioremediation. *Environ. Sci. Pollut, Res.* **2014**, *21*, 7369-7389.

de Brouwer, J.F.C.; Bjelic, S., de Deckere, E.M.G.T.; Stal, L.G. Interplace between biology and sedimentology in a mudflat (Biezelingse Ham, Westerschedle, The Netherlands). *Cont. Shelf Res.* **2000**, *20*, 1159–1177.

Dean, E.W.; Stark, D.D. A convenient method for the determination of water in petroleum and other organic emulsions. *Ind. Eng. Chem.* **1920**, *12(5), 486-490.*

Deusner, C.; Meyer, V.; Ferdelman, T.G. High-pressure systems for gas-phase free continuous incubation of enriched marine microbial communities performing anaerobic oxidation of methane. *Biotechnol. Bioeng.* **2010***, 105,* 524-533.

Dompierre, K.A.; Barbour, S.L. Characterization of physical mass transport through oil sands fluid fine tailings in an end pit lake: A multi-tracer study. *J. Contam. Hydrol.* **2016**, *189*, 12–26.

Dompierre, K.A.; Barbour, S.L.; North, R.L.; Carey, S.K.; Lindsay, M.B.J. Chemical mass transport between fluid fine tailings and the overlying water cover of an oil sands end pit lake. *Water Resour. Res.* **2017**, *53*, 4725–4740.

Dompierre, K.A.; Lindsay, M.B.J.; Cruz-Hernández, P.; Halferdahl, G.M. Initial geochemical characteristics of fluid fine tailings in an oil sands end pit lake. *Sci. Total Environ.* **2016**, *556*, 196–206.

Dong, X.; Kleiner, M.; Sharp, C.E.; Thorson, E.; Li, C.; Liu, D.; Strous, M. Fast and simple analysis of MiSeq amplicon sequencing data with MetaAmp. *Front. Microbiol.* **2017**, *8*, 1461.

Droppo, I. Biofilm structure and bed stability of five contrasting freshwater sediments. *Mar. Freshw. Res.* **2009**, *60*, 690–699.

Droppo, I.G.; Amos, C.L. Structure, stability and transformation of contaminated lacustrine surface fine-grained laminae. *J. Sediment. Res.* **2001**, *71*, 717–726.

Droppo, I.G.; Lau, Y.L.; Mitchell, C. The effect of depositional history on contaminated bed sediment stability. *Sci. Total Environ.* **2001**, *266*, 7–13.

Droppo, I.G.; Ross, N.; Skafel, M.; Liss, S.N. Biostabilization of cohesive sediment beds in a freshwater wave-dominated environment. *Limnol. Oceanogr.* **2007**, *52*, 577–589.

Duis, K.; Junker, T.; Coors, A. Environmental fate and effects of water-soluble synthetic organic polymers used in cosmetic products. *Environ. Sci. Eur.* **2021**, *33*, 21.

Dunmola, A.; Werneiwski, R.A.; McGowan, D.; Shaw, B.; Carrier. D. Geotechnical performance of fine tailings in an oil sands pit lake. *Can. Geotech. J.* **2023***, 60*, 595-610.

Fedorak, P.M.; Coy, D.L.; Dudas, M.J.; Simpson, M.J.; Renneberg, A.J.; MacKinnon, M.D. Microbially-mediated fugitive gas production from oil sands tailings and increased tailings densification rates. *J. Environ. Eng. Sci.* **2003**, *2*, 199–211.

Fedorak, P.M.; Coy, D.L.; Salloum, M.J.; Dudas, M.J. Methanogenic potential of tailings samples from oil sands extraction plants. *Can. J. Microbiol.* **2002**, *48,* 21-33.

Fichtel, K.; Logemann, J.; Fichtel, J.; Rullkötter, Cypionka, H.; Engelen, B. Temperature and pressure adaptation of sulfate reducer from the deep subsurface. *Front. Microbiol.* **2015**, *6*, 1078.

Flemming, H.C.; Wingender, J. The biofilm matrix. *Nature Rev. Microbiol.* **2010**, *8*, 623–633.

Foght, J.M.; Gieg, L.M.; Siddique, T. The microbiology of oil sands tailings: Past, present, future. *FEMS Microbiol. Ecol.* **2017**, *93*, fix034.

Fotidis, I.A.; Karakashev, D.; Kotsopoulos, T.A.; Martzopoulos, G.G.; Angelidaki, I. Effect of ammonium and acetate on methanogenic pathway and methanogenic community composition. *FEMS Microbiol. Ecol.* **2012**, *83*, 38-48.

Francis, D.J.; Barbour, S.L.; Lindsay, M.B.J. Ebullition enhances chemical mass transport across the tailings-water interface of oil sands pit lakes. *J. Contam. Hydrol.* **2022**, *245*, 103938.

Frederick, K.R. Productivity and carbon accumulation potential of transferred biofilms in reclaimed oil sands-affected wetlands. Master Thesis, University of Alberta, Edmonton, CA, 2011.

Friend, P.L.; Ciavola, P.; Cappucci, S.; Santos, R. Bio-dependent bed parameters as a proxy tool for sediment stability in mixed habitat intertidal areas. *Cont. Shelf Res.* **2003***, 23*, 1899–1917.

Gao, Y.F.; Zhang, Y.; Zhou, Y.; Li, D. Effects of column diameter on settling behavior of dredged slurry in sedimentation experiments. *Mar. Georesources Geotechnol.* **2016**, *34*, 431-439.

Garcia-Garcia, E.; Pun, J.; Perez-Estrada, L.A.; Din, M.G.E.; Smith, D.W.; Martin, J.W.; Belosevic, M. Commercial naphthenic acids and organic fraction of oil sands process water downregulate pro-inflammatory gene expression and macrophage antimicrobial responses. *Toxicol. Lett.* **2011**, *203*, 62–73.

Gee, K.; Poon, H.Y.; Hashisho, Z.; Ulrich, A.C. Effect of naphtha diluent on greenhouse gases and reduced sulfur compounds emissions from oil sands tailings. *Sci. Total Environ.* **2017**, *598*, 916-924.

Gerbersdorf, S.U.; Jancke, T.; Westrich, B.; Paterson, D.M. Microbial stabilization of riverine sediments by extracellular polymeric substances. *Geobiology* **2008**, *6*, 57–69.

Gerbersdorf, S.U.; Wieprecht, S. Biostabilization of cohesive sediments: Revisiting the role of abiotic conditions, physiology and diversity of microbes, polymeric secretion, and biofilm architecture. *Geobiology* **2015**, *13*, 68–97.

Gibson, R.E.; England, G.L.; Hussey, M.J.L. The theory of one-dimensional consolidation of saturated clays I, finite non-linear consolidation of thin homogeneous layers. *Géotechnique* **1967**, *17*, 261-273.

Golder Associates Ltd. Literature Review of Global Pit Lakes: Pit Lake – Case Studies; Report 1777450, Golder Associate Ltd: Calgary, CA, 2017; Available online: https://cosia.ca/sites/default/files/attachments/Literature%20Review%20of%20Global%20Pit%20Lakes_0.pdf

Gonzalez-Rodriguez, D.; Guillou, L.; Cornat, F.; Lafaurie-Janvore, J.; Babataheri, A.; de Langre, E.; Barakat, A.I.; Husson, J. Mechanical criterion for the rupture of a cell membrane under compression. *Biophys. J.* **2016***, 111*, 2711-2721.

Government of Alberta. Lower Athabasca Region: Tailings Management Framework for the Mineable Athabasca Oil Sands. Government of Alberta: Edmonton, CA, 2015; Available online: https://open.alberta.ca/publications/9781460121740

Government of Alberta. Environmental Quality Guidelines for Alberta Surface Waters; Water Policy Branch, Alberta Environment and Parks: Edmonton, CA, 2018.

Government of Alberta. Oil sands facts and statistics. 2023. Available online: https://www.alberta.ca/oil-sands-facts-and-

statistics.aspx#:~:text=Alberta's%20oil%20sands%20has%20the,165.4%20billion%20barrels%20(bbl) (accessed 6 February 2023).

Gröllmann, U.; Schnabel, W. Free radical-induced oxidative degradation of polyacrylamide in aqueous solution. *Polym. Degrad. Stab.* **1982**, 4, 203–212.

Grula, M.M.; Huang, M.; Sewell, G. Interactions of certain polyacrylamides with soil bacteria. *Soil Sci.* **1994**, *158*, 291–300.

Guezennec, A.G.; Michel, C.; Bru, K.; Touze, S.; Desroche, N.; Mnif, I.; Motelica-Heino, M. Transfer and degradation of polyacrylamide-based flocculants in hydrosystems: a review. *Environ. Sci. Pollut. Res.* **2015**, *22*, 6390–6406.

Guo, S. Experimental study on isothermal adsorption of methane gas on three shale samples from Upper Paleozoic strata of the Ordos Basin. *J. Pet. Sci. Eng.* **2013**, *110*, 132-138.

GWP Software Inc. FSCONSOL Slurry Consolidation Software User Manual. GWP Software Inc.: Edmonton, CA, 2007.

Hao, X.; Liu, R.; van Loosdrecht, M.C.M.; Cao, D. Batch influences of exogenous hydrogen on both acidogenesis and methanogenesis of excess sludge. *Chem. Eng. J.* **2017**, *317*, 544-550.

Hart, E.A.; Lovvorn, J.R. Vegetation dynamics and primary production in saline, lacustrine wetlands of a Rocky Mountain basin. *Aquat. Bot.* **2000**, *66*, 21–39.

Hartsock, J.A.; Piercey, J.; House, M.K.; Vitt, D.H. An evaluation of water quality at Sandhills Wetland: Implications for reclaiming wetlands above soft tailings deposits in northern Alberta, Canada. *Wetl. Ecol. Manag.* **2021**, *29*, 111–127.

Haveroen, M.E.; MacKinnon, M.D.; Fedorak, P.M. Polyacrylamide added as a nitrogen source stimulates methanogenesis in consortia from various wastewaters. *Water Res.* **2005**, *29*, 3333–3341.

He, J.; Zhang, Y.; Wu, X.; Yang, Y.; Xu, X.; Zheng, B.; Deng, W.; Shao, Z.; Lu, L.; Wang, L.; et al A study on the relationship between metabolism of Cyanobacteria and chemical oxygen demand in Dianchi Lake, China. *Water Environ. Res.* **2019**, *91*, 1650–1660.

Headley, J.V.; Peru, K.M.; Barrow, M.P. Advances in mass spectrometric characterization of naphthenic acids fraction compounds in oil sands environmental samples and crude oil—A review. *Mass Spectrom. Rev.* **2016**, *35*, 311–328.

Herman, D.C.; Fedorak, P.M.; Mackinnon, M.D.; Costerton, J.W. Biodegradation of naphthenic acids by microbial populations indigenous to oil sands tailings. *Can. J. Microbiol.* **1994**, *40*, 467–477.

Holmes, D.E.; Finneran, K.T.; O'Neil, R.A.; Lovley, D.R. Enrichment of members of the family *Geobacteraceae* associated with stimulation of dissimilatory metal reduction in uranium-contaminated aquifer sediments. *Appl. Environ. Microbiol.* **2002**, *68*, 2300-2306.

Holmes, D.E.; Nevin, K.P.; Lovley, D.R. Comparison of 16S rRNA, *nifD, recA, gyrB, rpoB* and *fusA* genes within the family *Geobacteraceae* fam. nov. *IJSEM* **2004**, *54*, 1591-1599.

Holowenko, F.M.; MacKinnon, M.D.; Fedorak, P.M. Methanogens and sulfate-reducing bacteria in oil sands fine tailings waste. *Can. J. Microbiol.* **2000**, *46*, 927–937.

Hu, H.; Liu, J.F.; Li, C.Y.; Yang, S.Z.; Gu, J.D.; Mu, B.Z. Anaerobic biodegradation of partially hydrolyzed polyacrylamide in long-term methanogenic enrichment cultures from production water of oil reservoirs. *Biodegradation*, **2018**, *29*, 233-243.

Imperial Oil Resources Ltd. (Imperial). Kearl Oil Sands Mine: Fluid Tailings Management Report; Imperial Oil Resources Ltd.: Calgary, CA, 2020.

Jarvie, H.P.; Neal, C.; Warwick, Aa.; White, J.; Neal, M.; Wickham, H.D.; Hill, L.K.; Andrews, M.C. Phosphorus uptake into algal blooms in a lowland chalk river. *Sci. Total Environ.* **2002**, *282-283*, 352–373.

Jeeravipoolvarn, S.; Chalaturnyk, R.J.; Scott, J.D. Consolidation modeling of oil sands fine tailings: history matching. In Proceedings of the 61st Canadian Geotechnical Conference, Edmonton, CA, 22–24 September 2008a.

Jeeravipoolvarn, S.; Scott, J.D.; Chalaturnyk, R.J. Multi-dimensional finite strain consolidation theory: modeling study. In Proceedings of the 61st Canadian Geotechnical Conference, Edmonton, CA, 22–24 September 2008b.

Jeeravipoolvarn, S.; Scott, J.D.; Chalaturnyk, R.J. 10 m standpipe tests on oil sands tailings: Long-term experimental results and prediction. *Can. Geotech. J.* **2009**, *46*, 875–888.

Jessen, G.L.; Chen, L.-X.; Mori, J.F.; Nelson, Nelson, T.E.C.; Slater, G.F.; Lindsay, M.B.J.; Banfield, J.F.; Warren, L.A. Alum addition triggers hypoxia in an engineered pit lake. *Microorganisms* **2022**, *10*, 510.

Joshi, S.; Abed, A. Biodegradation of polyacrylamide and its derivatives. *Environ. Process.* **2017**, *4*, 463–476.

Kaminsky, H. Demystifying the methylene blue index. In Proceedings of the 4th International Oil Sands Tailings Conference, Lake Louise, CA, 7–10 December 2014.

Kaminsky, H.; Omotoso, O. Variability in fluid fine tailings. In Proceedings of the 5th International Oil Sands Tailings Conference, Lake Louise, CA, 4–7 December 2016.

Kasperski, K.L.; Mikula, R.J. Waste streams of mined oil sands: Characteristics and remediation. *Elements* **2011**, *7*, 387–392.

Kavanagh, R.J.; Frank, R.A.; Oakes, K.D.; Servos, M.R.; Young, R.F.; Fedorak, P.M.; MacKinnon, M.D.; Solomon, K.R.; Dixon, D.G.; Van Der Kraak, G. Fathead minnow (*Pimephales promelas*) reproduction is impaired in aged oil sands process-affected waters. *Aquat. Toxicol.* **2011**, *101*, 214–220.

Kay-Shoemake, J.L.; Watwood, M.E.; Lentz, R.D.; Sojka, E.R. Polyacrylamide as an organic nitrogen source for soil microorganisms with potential effects on inorganic soil nitrogen in agricultural soil. *Soil Biol. Biochem*. **1998**, *30*, 1045–1052.

Keiluweit, M.; Fendorf, S. Texture-dependent anaerobic microsites constrain soil carbon oxidation rates. In Proceedings of the EGA General Assembly, Vienna, AT, 17–22 April 2016.

Kuznetsov, P.; Wei, K.; Kuznetsova, A.; Foght, J.; Ulrich, A.; Siddique, T. Anaerobic microbial activity may affect development and sustainability of end-pit lakes: a laboratory study of biogeochemical aspects of oil sands mine tailings. *ACS EST Water*. **2023**, *3*, 1039-1049.

Langwig, M.V.; De Anda, V.; Dombrowski, N.; Seitz, K.W.; Rambo, I.M.; Greening, C.; Testke, A.P.; Baker, B.J. Large-scale protein level comparison of Deltaproteobacteria reveals cohesive metabolic groups. *ISME J.* **2022**, *16*, 307-320.

Lawrence, G.A.; Tedford, E.W. Pieters, R. Suspended solids in an end pit lake: potential mixing mechanisms. *Can. J. Civ. Eng.* **2016**, *43*, 211–217.

Leigh, J.A. Nitrogen fixation in methanogens: the archaeal perspective. *Curr. Issues Mol. Biol.* **2000**, *2*, 125-131.

Leloup, M.; Nicolau, R.; Pallier, V.; Yéprémian, C.; Feuillade-Cathalifaud, G. Organic matter produced by algae and cyanobacteria: Quantitative and qualitative characterization. *J. Environ. Sci.* **2013**, *25*, 1089–1097.

Leriche, V.; Sibille, P.; Carpentier, B. Use of an enzyme-linked lectinsorbent assay to monitor the shift in polysaccharide composition in bacterial biofilms. *Appl. Environ. Microbiol.* **2000**, *66*, 1851–1856.

Li, J.; How, Z.T.; El-Din, M.G. Aerobic degradation of anionic polyacrylamide in oil sands tailings: impact factor, degradation effect, and mechanism. *Sci. Total Environ.* **2023***, 856*, 159079.

Li, Y.; Kaminsky, H.; Gong, X.Y.; Sun, Y.S.; Ghuzi, M.; Sadighian, A. What affects dewatering performance of high density slurry? *Minerals* **2021**, *11*, 761.

Li, Y.; Kaminsky, H.; Revington, A.; Sadighian, A. A protocol to assess and screen new flocculant for Suncor's PASS program planning. In Proceedings of the 7th International Oil Sands Tailings Conference, Edmonton, CA, 4-7 December 2022a.

Li, Y.; Kaminsky, H.; Sadighian, A.; Sun, Y.S.; Murphy, F.; Gong, X.Y.; Ghuzi, M.; Rima, U. Impact of chemical and physical treatments on freeze-thaw dewatering of fluid fine tailings. *Cold Reg. Sci. Technol.* **2022b**, *193*, 103385.

Liang, B.; Wang, L.Y.; Mbadinga, S.M.; Liu, J.F.; Yang, S.Z.; Gu, J.D.; Mu, B.Z. *Anaerolineaceae* and *Methanosaeta* turned to be the dominant microorganisms in alkanes-dependent methanogenic culture after long-term of incubation. *AMB Express* **2015**, *5*, 37.

Liang, J.; Guo, Z.; Deng, L.; Liu, Y. Oil Sands Mature Fine Tailings Consolidation Through Microbial Induced Calcite Precipitation, Oil Sands Research and Information Network: Edmonton, CA, 2014.

Lichtenthaler, H.K. Chlorophylls and cartenoids: Pigments of photosynthetic biomembranes. *Methods Enzymol.* **1987**, *148*, 350–382.

Lipp, D.; Kozakiewicz, J. Acrylamide polymers. In Kirk-Othmer Encyclopedia of Chemical Technology; Kroschwitz, J.I., Ed.; Wiley: Toronto, CA, 1991; pp. 266–287.

Liu, L.; Wang, Z.; Lin, K.; Cai, W. Microbial degradation of polyacrylamide by aerobic granules. *Environ. Technol.* **2012**, *33*, 1049–1054.

Liu, Q.; Montoya, B.M. Experimental study of consolidation behavior of mature fine tailings treated with microbial induced calcium carbonate precipitation. In Proceeding of Geo-Congress 2020, Minneapolis, US, 25-28 February 2020.

Lu, J.H.; Wu, L.; Letey, J. Effects of soil and water properties on anionic polyacrylamide sorption. *Soil Sci. Soc. Am. J.* **2002***, 66*, 578-584.

Lundkvist, M.; Grui, M.; Friend, P.L.; Flindt, M.R. The relative contributions of physical and microbiological factors to cohesive sediment stability. *Cont. Shelf Res.* **2007**, *27*, 1143–1152.

Lyu, Z.; Lu, Y. Metabolic shift at the class level sheds light on adaptation of methanogens to oxidative environments. *ISME J.* **2018***, 12*, 411-423.

MacKinnon, M.D. Development of the tailings pond at Syncrude's oil sands plant: 1978–1987. *AOSTRA J. Res.* **1989**, *5*, 109–133.

Mahdavi, H.; Prasad, V.; Liu, Y.; Ulrich, A.C. In situ biodegradation of naphthenic acids in oil sands tailings pond water using indigenous algae-bacteria consortium. *Bioresour. Technol.* **2015**, *187*, 97–105.

Malone, A.S.; Shellhammer, T.H.; Courtney, P.D. Effects of high pressure on the viability, morphology, lysis, and cell wall hydrolase activity of *Lactococcus lactis* subsp. *cremoris*. *Appl. Environ. Microbiol.* **2002**, *68*, 4357-4363.

Mayumi, D.; Dolfing, J.; Sakata, S.; Maeda, H.: Miyagawa, Y.; Ikarashi, M.; Tamaki, H.; Takeuchi, M.; Nakatsu, C.H.; Kamagata, Y. Carbon dioxide concentration dictates alternative methanogenic pathways in oil reservoirs. *Nat. Commun.* **2013**, *4*, 1998.

McDonald, D.; Price, M.N.; Goodrich, J.; Nawrocki, E.P.; DeSantis, T.Z.; Probst, A.' Andersen, G.L.; Knight, R.; Hugenholtz, P. An improved Greengenes taxonomy with explicit ranks for ecological and evolutionary analyses of bacteria and archaea. *ISME J.* **2012**, *6*, 610–618.

McKenna, G. Landscape design for mine reclamation. In Proceedings of the Tailings and Mine Waste '09, Banff, CA, 1–4 November 2009.

McKenna, G.; Mooder, B.; Burton, B.; Jamieson, A. Shear strength and density of oil sands fine tailings for reclamation of a boreal forest landscape. In Proceedings of the 5th International Oil Sands Tailings Conference, Lake Louise, CA, 4–7 December 2016.

Meister, P. Two opposing effects of sulfate reduction on carbonate precipitation in normal marine, hypersaline, and alkaline environments. *Geology* **2013**, *41*, 499-502.

Mercado, J.V.; Koyama, M.; Nakasaki, K. Complexity of acclimatization substrate affects anaerobic digester microbial community response to organic load shocks. *Environ. Res.* **2023**, *216*, 114722.

Meredith, L.K.; Tfaily, M.M. Capturing the microbial volatilome: an oft overlooked 'ome'. *Trends Microbiol.* **2022**, *30*, 623-631.

Meulepas, R.J.W.; Jagersma, C.G.; Zhang, Y.; Petrillo, M.; Cai, H.; Buisman, C.J.N.; Stams, A.J.M.; Lens, P.N.L. Trace methane oxidation and the methane dependency of sulfate reduction in anaerobic granular sludge. *FEMS Microbiol. Ecol.* **2010**, *72*, 261-271.

Mikula, R.; Omotoso, O. Role of clays in controlling tailings behavior in oil sands processing. *Clay Sci.* **2006**, *12*, 177-182.

Miles, S.M.; Asiedu, E.; Balaberda, A.; Ulrich, A.U. Oil sands process affected water sourced *Trichoderma harzianum* demonstrates capacity for mycoremediation of naphthenic acid fraction compounds. *Chemosphere* **2020**, *258*, 127281.

Mohamad Shahimin, M.F.; Foght, J.M.; Siddique, T. Preferential methanogenic biodegradation of short-chain *n*-alkanes by microbial communities from two different oil sands tailings ponds. *Sci. Total Environ.* **2016**, *553*, 250-257.

Mohamad Shahimin, M.F.; Foght, J.M.; Siddique, T. Methanogenic biodegradation of *iso*- alkanes by indigenous microbes from two different oil sands tailings ponds. *Microorganisms* **2021**, *9*, 1569.

Mohamad Shahimin, M.F.; Siddique, T. Sequential biodegradation of complex naphtha hydrocarbons under methanogenic conditions in two different oil sands tailings. *Environ. Pollut.* **2017a**, *221*, 398–406.

Mohamad Shahimin, M.F.; Siddique, T. Methanogenic biodegradation of paraffinic solvent hydrocarbons in two different oil sands tailings. *Sci. Total Environ.* **2017b**, *583*, 115–122.

Morandi, G.D.; Wiseman, S.B.; Pereira, A.; Mankidy, R.; Gault, I.G.M.; Martin, J.W.; Giesy, J.P. Effects-directed analysis of dissolved organic compounds in oil sands process-affected water. *Environ. Sci. Technol.* **2015**, *49*, 12395–12404.

Mori, J.F.; Chen, L.X.; Jessen, G.L.; Rudderham, S.G.; McBeth, J.M.; Lindsay, M.B.J.; Slater, G.F.; Banfield, J.F.; Warren, L.A. Putative mixotrophic nitrifying-denitrifying gammaproteobacterial implicated in nitrogen cycling within the ammonia/oxygen transition zone of an oil sands pit lake. *Front. Microbiol.* **2019**, *10*, 2435.

Murphy, C.L.; Biggerstaff, J.; Eichhorn, A.; Ewing, E.; Shahan, R.; Soriano, D.; Stewart, S.; VanMol, K.; Walker, R.; Walters, P.; et al. Genomic characterization of three novel Desulfobacterota classes expand the metabolic and phylogenetic diversity of the Phylum. *bioRxiv*. **2021**, doi:10.1101/2021.03.22.436540.

Nakamiya, K.; Kinoshita, S. Isolation of polyacrylamide-degrading bacteria. *J. Ferment. Bioeng.* **1995**, *80*, 418–420.

Neelakantan, R.; Vaezi, G.F.; Sanders, R.S. Effects of shear on the yield stress and aggregate structure of flocculant-dosed, concentrated kaolinite suspensions. *Miner. Eng.* **2018**, *123*, 95–103.

Neira, J.; Ortiz, M.; Morales, L.; Acevedo, E. Oxygen diffusion in soils: Understanding the factors and processes needed for modeling. *Chil. J. Agric. Res.* **2015**, *75*, 35–44.

Nozhevnikova, A.N.; Holliger, C.; Ammann, A.; Zehnder, A.J.B. Methanogenesis in sediments from deep lakes at different temperatures (2-70 °C). *Water Sci. Technol.* **1997**, *36*, 57-64.

Oil Sands Tailings Consortium (OSTC) and Canada's Oil Sands Innovation Alliance (COSIA). Technical Guide for Fluid Fine Tailings Management; OSTC and COSIA: Calgary, CA, 2012.

Op den Camp, J.J.M.; Islam, T.; Stott, M.B.; Harhangi, H.R.; Hynes, A.; Schouten, S.; Jettens, M.S.M.; Birkeland, N.; Pol, A.; Dunfield, P.F. Environmental, genomic and taxonomic perspectives on methanotrophic *Verrucomicrobia*. *Environ. Microbial. Rep.* **2009**, *1*, 293–306.

Parkhurst, D. L., & Appelo, C. A. J. Description of Input and Examples for PHREEQC Version 3 – A Computer Program for Speciation, Batch-reaction, One-Dimensional Transport, and Inverse Geochemical Calculations, U.S. Geological Survey: Denver, US, 2013.

Pannekens, M.; Voskuhl, L.; Mohammadian, S.; Köster, D.; Meier, A.; Köhne, J.M.; Kulbatzki, M.; Akbari, A.; Haque, S.; Meckenstock, R.U. Microbial degradation rates of natural bitumen. *Environ. Sci. Technol.* **2021**, *55*, 8700-8708.

Pavlostathis, S.G.; Zhuang, P. Effect of temperature on the development of anaerobic cultures from a contaminated subsurface soil. *Environ.Technol.* **1991**, *12*, 679-687.

Pei, Y.; Zhao, L.; Du, G.; Li, N.; Xu, K.; Yang, H. Investigation of the degradation and stability of acrylamide-based polymers in acid solution: Functional monomer modified polyacrylamide. *Petroleum* **2016**, *2*, 399–407.

Penner, T.J.; Foght, J.M. Mature fine tailings from oil sands processing harbour diverse methanogenic communities. *Can. J. Microbiol.* **2010***, 56*, 459-470.

Pérez-Pantoja, D.; Donoso, R.; Agulló, L.; Córdova, M.; Seeger, M.; Pieper, D.H.; González, B. Genomic analysis of the potential for aromatic compounds biodegradation in *Burkholderiales*, *Environ. Microbiol.* **2011**, *14*, 1091-1117.

Pester, M.; Brambilla, E.; Alazard, D.; Rattei, T.; Weinmaier, T.; Han, J.; Lucas, S.; Lapidus, A.; Cheng, J.F.; Goodwin, L.; et al. Complete genome sequences of *Desulfosporosinus orientis* DSM765^T, *Desulfosporosinus youngiae* DSM17734^T, *Desulfosporosinus meridiei* DSM13257^T, and *Desulfosporosinus acidiphilus* DSM22704^T. *J. Bacteriol.* **2012**, *194*, 6300-6301.

Poon, H.Y.; Brandon, J.T.; Yu, X.; Ulrich, A.C. Turbidity mitigation in an oil sands pit lake through pH reduction and fresh water addition. *J. Environ. Eng.* **2018**, *114,* 04018127.

Pope, D.H.; Berger, L.R. Inhibition of metabolism by hydrostatic pressure: what limits microbial growth? *Arch. Mikrobiol.* **1973**, *93*, 367-370.

Potter, M.C.; Wiggert, D.C.; Ramadan, B.H. Shih, T.I-P. *Mechanics of Fluids*, 4th ed.; Cengage Learning: Stamford, US, 2012.

Pyzik, A.; Ciezkowska, M.; Krawczyk, P.S.; Sobczak, A.; Drewniak, L.; Dziembowski, A.; Lipinski, L. Comparative analysis of deep sequenced methanogenic communities: identification of microorganisms responsible for methane production. *Microb. Cell Factories* **2018**, *17*, 197.

Quesnel, D.M.; Bhaskar, I.M.; Gieg, L.M.; Chua, G. Naphthenic acid biodegradation by the unicellular alga *Dunaliella tertiolecta*. *Chemosphere* **2011**, *84*, 504–511.

Quinlan, P.J.; Tam, K.C. Water treatment technologies for the remediation of naphthenic acids in oil sands process-affected water. *Chem. Eng. J.* **2015**, *279*, 696–714.

Ramos-Padrón, E.; Bordenave, S.; Lin, S.; Bhaskar, I.M.; Dong, X.; Sensen, C.W.; Fournier, J.; Vourdouw, G.; Gieg, L.M. Carbon and sulfur cycling by microbial communities in a gypsum-treated oil sands tailings pond. *Environ. Sci. Technol.* **2011**, *45*, 439–446.

Rao, F.; Liu, Q. Froth treatment in Athabasca oil sands bitumen recovery process: A review. *Energy Fuels* **2013**, *27*, 7199–7207.

Reid, M.L.; Warren, L.A. S reactivity of an oil sands composite tailings deposit undergoing reclamation wetland construction. *J. Environ. Manag.* **2016**, *166*, 321–329.

Reid, T.; VanMansel, D.; Droppo, I.G.; Weisener, C.G. The symbiotic relationship of sediment and biofilm dynamics at the sediment water interface of oil sands industrial tailings ponds. *Water Res.* **2016**, *100*, 337–347.

Ren, H.Y.; Zhang, X.J.; Song, Z.Y.; Rupert, W.; Gao, G.J.; Guo, A.X.; Zhao, L.P. Comparison of microbial community compositions of injection and production well samples in a long-term water-flooded petroleum reservoir. *PLoS One* **2011**, *6*, e23258.

Ripmeester, M.J.; Duford, D.A. Method for routine "naphthenic acids fraction compounds" determination in oil sands process-affected water by liquid-liquid extraction in dichloromethane and Fourier-Transform Infrared Spectroscopy. *Chemosphere* **2019**, *233*, 687–696.

Risacher, F.F.; Morris, P.K.; Arriaga, D.; Goad, C.; Colenbrander Nelson, T.; Slater, G.F.; Warren, L.A. The interplay of methane and ammonia as key oxygen consuming constituents in early stage development of Base Mine Lake, the first demonstration oil sands pit lake. *Appl. Geochem.* **2018**, *93*, 49–59.

Rochman, F.F.; Sheremet, A.; Tamas, I.; Saidi-Mehrabad, A.; Kim, J.J.; Dong, X.; Sensen, C.W.; Gieg, L.M.; Dunfield, P.F. Benzene and naphthalene degrading bacterial communities in an oil sands tailings pond. *Front. Microbiol.* **2017**, *8*, 1–12.

Roeselers, G.; van Loosdrecht, M.C.M.; Muyzer, G. Heterotrophic pioneers facilitate phototrophic biofilm development. *Microb. Ecol.* **2007**, *54*, 578–585.

Roeselers, G.; van Loosdrecht, M.C.M.; Muyzer, G. Phototrophic biofilms and their potential application. *J. Appl. Phycol.* **2008**, *20*, 227–235.

Rourke, H.; Hockley, D. Assessing oil sands tailings consolidation parameters relative to long-term reclamation. In Proceedings of the 22nd International Conference on Tailings and Mine Waste, Keystone, USA, 30 September – 2 October 2018.

Rudderham, S.B. Geomicrobiology and Geochemistry of Fluid Fine Tailings in an Oil Sands End Pit Lake. Master's Thesis, Department of Geological Sciences, University of Saskatchewan, Saskatoon, CA, 2019.

Saidi-Mehrabad, A.; He, Z.; Tamas, I.; Sharp, C.E.; Brady, A.L.; Rochman, F.F.; Bodrossy, L.; Abell, G.C.J.; Penner, T.; Dong, X.; et al. Methanotrophic bacteria in oilsands tailings ponds of northern Alberta. *ISME J.* **2013**, *7*, 908–921.

Sawamura, A.; Egoshi, N.; Setoguchi, Y.; Matsuo, H. Solubility of sodium chloride in water under high pressure. *Fluid Phase Equilib.* **2007**, *254*, 158.162.

Sawatsky, L.; Hyndman, A.; McKenna, G.; Vandenberg, J. Fluid fine tailings processes: disposal, capping, and closure alternatives. In Proceedings of the 6th International Oil Sands Tailings Conference, Edmonton, CA, 9–12 December 2018.

Scoma, A.; Heyer, R.; Rifal, R.; Dandyk, C.; Marshall, I.; Kerckhof, F.M.; Marietou, A.; Boshker, H.T.S.; Meysman, F.J.R.; Malmos, K.G.; et al. Reduced TCA cycle rates at high hydrostatic pressure hinder hydrocarbon degradation and obligate oil degraders in natural, deep-sea microbial communities. *ISME J.* **2019**, *13*, 1005-1018.

Scott, A.C.; Mackinnon, M.D.; Fedorak, P.M. Naphthenic acids in Athabasca oil sands tailings waters are less biodegradable than commercial naphthenic acids. *Environ. Sci. Technol.* **2005**, *39*, 8388–8394.

Sentenac, P.; Lynch, R.J.; Bolton, M.D. Measurement of a side-wall boundary effect in soil columns using fibre-optics sensing. *Int. J. Phys. Model. Geotech.* **2001**, *4*, 35–41.

Sethi, A.J. Methylene Blue Test for Clay Activity Determination in Fine Tails, MRRT Procedures, 1995.

Shen, X.; Sun, T.; Su, M.; Dang, Z.; Yang, Z. Short-term response of aquatic ecosystem metabolism to turbidity disturbance in experimental estuarine wetlands. *Ecol. Eng*. **2019**, *136*, 55–61.

Siddique, T.; Fedorak, P.M.; Foght, J.M. Biodegradation of short-chain n-alkanes in oil sands tailings under methanogenic conditions. *Environ. Sci. Technol.* **2006**, *40*, 5459-5464.

Siddique, T.; Fedorak, P.M.; Mackinnon, M.D.; Foght, J.M. Metabolism of BTEX and naphtha compounds to methane in oil sands tailings. *Environ. Sci. Technol.* **2007**, *41*, 2350–2356.

Siddique, T.; Kuznetsov, P.; Kuznetsova, A.; Arkell, N.; Young, R.; Li, C.; Guigard, S.; Underwood, E.; Foght, J.M. Microbially-accelerated consolidation of oil sands tailings. Pathway I: changes in porewater chemistry. *Front. Microbiol.* **2014a**, *5*, Article 106.

Siddique, T.; Kuznetsov, P.; Kuznetsova, A.; Li, C.; Young, R.; Arocena, J.M.; Foght, J.M. Microbially-accelerated consolidation of oil sands tailings. Pathway II: Solid phase biogeochemistry. *Front. Microbiol.* **2014b,** *5*, 107.

Siddique, T.; Mohamad Shahimin, M.F.; Zamir, S.; Semple, K.; Li, C.; Foght, J.M. 2015. Long-term incubation reveals methanogenic biodegradation of C_5 and C_6 iso-alkanes in oil sands tailings. *Environ. Sci. Technol.* **2015,** *49*, 14732-14739.

Siddique, T.; Penner, T.; Semple, K.; Foght, J.M. Anaerobic biodegradation of longer-chain n-alkanes coupled to methane production in oil sands tailings. *Environ. Sci. Technol.* **2011**, *45*, 5892–5899.

Siddique, T.; Semple, K.; Li, C.; Foght, J.M. Methanogenic biodegradation of *iso*-alkanes and cycloalkanes during long-term incubation with oil sands tailings. *Environ. Pollut.* **2020,** *258*, 113768.

Sim, L.L.; David, J.A.; Chambers, J.M. Ecological regime shifts in salinized wetland systems. II. Factors affecting the dominance of benthic microbial communities. *Hydrobiologia* **2006**, *573*, 109–131.

Slater, G.F.; Goad, C.A.; Lindsay, M.B.J.; Mumford, K.G.; Colenbrander Nelson, T.E.; Brady, A.L.; Jessen, G.L.; Warren, L.A. Isotopic and chemical assessment of the dynamics of methane sources and microbial cycling during early development on an oil sands pit lake. *Microorganisms* **2021***, 9*, 2509.

Small, C.C.; Cho, S.; Hashisho, Z.; Ulrich, A.C. Emissions from oil sands tailings ponds: Review of tailings pond parameters and emission estimates. *J. Petrol. Sci. Eng.* **2015**, *127*, 490–501.

Song, T.; Li, S.; Ding, W.; Li, H.; Bao, M.; Li, Y. Biodegradation of hydrolyzed polyacrylamide by the combined expanded granular sludge bed reactor-aerobic biofilm reactor biosystem and key microorganisms involved in this bioprocess. *Bioresour. Technol.* **2018**, *263*, 153–162.

Song, W.; Zhang, Y.; Gao, Y.; Chen, D.; Yang, M. Cleavage of the main carbon chain backbone of high molecular weight polyacrylamide by aerobic and anaerobic biological treatment. *Chemosphere* **2017**, *189*, 277–283.

Song, W.; Zhang, Y.; Hamidian, A.H.; Yang, M. Biodegradation of low molecular weight polyacrylamide under aerobic and anaerobic conditions: effect of the molecular weight. *Water Sci. Technol.* **2020**, *81*, 301-308.

Sorta, A.; Beier, N.; Kabwe, L.K.; Scott, J.D.; Wilson, G.W. The case for using fines void ratio. In Proceedings of the 68th Canadian Geotechnical Conference, Quebec City, CA, 21–23 September 2015.

Sorta, A.R.; Sego, D.C.; Wilson, W. Physical modelling of oil sands tailings consolidation. *Int. J. Phys. Model. Geotech.* **2016**, *16*, 47–64.

Spormann, A.M.; Widdel, F. Metabolism of alkylbenzenes, alkanes, and other hydrocarbons in anaerobic bacteria. *Biodegradation* **2000***, 11,* 85 – 105.

Squires, M.M.; Lesack, L.E. Benthic algal response to pulsed versus distributed inputs of sediment and nutrients in a Mackenzie Delta Lake. *J. N. Am. Benthol. Soc*. **2001**, *20*, 369–384.

Stasik, S.; Loick, N.; Knöller, K.; Weisener, C.; Wendt-Potthoff, K. Understanding biogeochemical gradients of sulfur, iron and carbon in an oil sands tailings pond. *Chem. Geol*. **2014**, *382*, 44–53.

Stasik, S.; Schmidt, J.; Wendt-Potthoff, K. High potential for anaerobic microbial sulfur oxidation in oil sands tailings ponds. *Microorganisms* **2021***, 9*, 2529.

Stasik, S.; Wendt-Potthoff, K. Interaction of microbial sulphate reduction and methanogenesis in oil sands tailings ponds. *Chemosphere* **2014**, *103*, 59–66.

Stasik, S.; Wendt-Potthoff, K. Vertical gradients in carbon flow and methane production in a sulfate-rich oil sands tailings pond. *Water Res*. **2016**, *106*, 223–231.

Stasik, S.; Wick, L.Y.; Wendt-Potthoff, K. Anaerobic BTEX degradation in oil sands tailings ponds: Impact of labile organic carbon and sulfate-reducing bacteria. *Chemosphere* **2015**, *138*, 133–139.

Stawiński, J.; Wierzchoś, J.; Garoa-Gonzalez, M.T. Influence of calcium and sodium concentration on the microstructure of bentonite and kaolin. *Clays Clay Min.* **1990***, 38*, 617-622.

Suncor Energy Inc. (Suncor). 2021 Base Plant Fluid Tailings Management Report; Suncor Energy Inc: Calgary, CA, 2022a.

Suncor Energy Operating Inc. (Suncor) 2021 Fort Hills Fluid Tailings Management Report; Suncor Energy Operating Inc. on behalf of Fort Hills Energy Corporation; Calgary, CA, 2022b.

Suncor Energy Inc. (Suncor). Fort Hills. 2023a. Available online: https://www.suncor.com/en-ca/what-we-do/oil-sands/fort-hills (accessed on 31 May 2023).

Suncor Energy Inc. (Suncor). 2022 Base Plant Fluid Tailings Management Report; Suncor Energy Inc.: Calgary, CA, 2023b.

Suncor Energy Operating Inc. (Suncor). 2022 Fort Hills Fluid Tailings Management Report; Suncor Energy Operating Inc.; Calgary, CA, 2023c.

Suncor Energy (Syncrude) Operating Inc. (Syncrude). 2022 Pit Lake Monitoring and Research Report (Base Mine Lake Demonstration Summary: 2012-2021); Suncor Energy (Syncrude) Operating Inc.: Fort McMurray, CA, 2022.

Suncor Energy (Syncrude) Operating Inc. (Syncrude). 2022 Mildred Lake Tailings Management Report; Suncor Energy (Syncrude) Operating Inc.: Fort McMurray, CA, 2023.

Suthaker, N.N.; Scott, J.D. Large scale consolidation testing of oil sand fine tails. In Proceedings of the 1st International Congress on Environmental Geotechnics, Edmonton, CA, 10–15 July 1994.

Sutherland, T.F.; Grant, J.; Amos, L.L. The effect of carbohydrate production by diatom *Nitzchia curvilineata* on the erodibility of sediment. *Limnol. Oceanogr.* **1998**, *43*, 65–72.

Syncrude Canada Ltd. (Syncrude). 2019 Base Mine Lake Monitoring and Research Summary Report: Results from 2013-2018; Syncrude: Fort McMurray, CA, 2019.

Syncrude Canada Ltd. (Syncrude). 2019 Mildred Lake Tailings Management Report; Syncrude Canada Ltd.: Fort McMurray, CA, 2020.

Syncrude Canada Ltd. (Syncrude). 2021 Pit Lake Monitoring and Research Report (Base Mine Lake Demonstration Summary: 2021-2020); Syncrude Canada Ltd: Fort McMurray, CA, 2021.

Tan, B.F.; Semple, K.; Foght, J. Anaerobic alkane biodegradation by cultures enriched from oil sands tailings ponds involves multiple species capable of fumarate addition. *FEMS Microbiol. Ecol.* **2015**, *91*, fiv042.

Tedford, E.; Halferdahl, G.; Pieters, R.; Lawrence, G.A. Temporal variations in turbidity in an oil sands pit lake. *Environ. Fluid Mech.* **2019**, *19*, 457–473.

Tholosan, O.; Garcin, J.; Bianchi, A. Effects of hydrostatic pressure on microbial activity through a 2000 m deep water column in the NW Mediterranean Sea. *Mar. Ecol. Prog. Ser.* **1999***, 183*, 49-57.

Thompson, R.C.; Tobin, M.L.; Hawkins, S.J.; Norton, T.A. Problems in extraction and spectrophotometric determination of chlorophyll from epilithic microbial biofilms: Towards a standard method. *J. Mar. Biol. Ass. UK* **1999**, *79*, 551–558.

Timmers, P.H.A.; Gieteling, J.; Widjaja-Greefkes, H.C.A.; Plugge, C.M.; Stams, A.J.M.; Lens, P.N.L.; Meulepas, R.J.W. Growth of anaerobic methane-oxidizing archaea and sulfate-

reducing bacteria in a high-pressure membrane capsule bioreactor. *Appl. Environ. Microbiol.* **2015**, *81*, 1286-1296.

Tolhurst, T.J.; Reithmueller, P.; Paterson, D.M. In situ versus laboratory analysis of sediment stability from intertidal mudflats. *Cont. Shelf Res.* **2000***, 10/11*, 1317–1334.

United States Environmental Protection Agency (USEPA). Quality Criteria for Water; United States Department of Commerce, National Technical Information Service, USEPA: Springfield, US, 1986.

Uranta, K.G.; Rezaei-Gomari, S.; Russell, P.; Hamad, F. Studying the effectiveness of polyacrylamide (PAM) application in hydrocarbon reservoirs at different operational conditions. *Energies* **2018**, *11*, 2201.

Vadeboncoeur, Y.; Kalff, J.; Christoffersen, K.; Jeppesen, E. Substratum as a driver of variation in periphyton chlorophyll and productivity in lakes. *J. N. Am. Benthol. Soc.* **2006**, *25*, 378–392.

van Gemerden, H. Microbial mats: A joint venture. *Mar. Geol.* **1993**, *113*, 3–25.

Vandenberg, J.; Schultze, M.; McCullough, C.D.; Castendyk, D. The future direction of pit lakes: part 2, corporate and regulatory closure needs to improve management. *Mine Water Environ.* **2022**, *41,* 544-556.

Vedoy, D.R.J.; Soares, J.B.P. Water-soluble polymers for oil sands tailing treatment: A review. *Can. J. Chem. Eng.* **2015**, *93*, 888–904.

Vitt, D.H.; House, M.; Hartsock, J.A. Sandhill Fen, an initial trial for wetland species assembly on in-pit substrates: Lessons after three years. *Botany* **2016**, *94*, 1015–1025.

Wang, H.; Wang, C.; Lin, M.; Sun, X.; Wang, C.; Hu, X. Phylogenetic diversity of bacterial communities associated with bioremediation of crude oil in microcosms. *Int. Biodeterior. Biodegrad.* **2013**, *85*, 400-406.

Wang, Z.; Wang, S.; Hu, Y.; Du, B.; Meng, J.; Wu, G.; Liu, H.; Zhan, X. Distinguishing responses of acetoclastic and hydrogenotrophic methanogens to ammonia stress in mesophilic mixed cultures. *Water Res.* **2022**, *224*, 119029.

Warren, L.A.; Kendra, K.E.; Brady, A.L.; Slater, G.F. Sulfur biogeochemistry of an oil sands composite tailings deposit. *Front. Microbiol.* **2016**, *6*, 1–14.

Wei, K.; Cossey, H.L.; Ulrich, A.C. Effects of calcium and aluminum on particle settling in an oil sands end pit lake. *Mine Water Environ.* **2021**, *40*, 1025-1036.

Wen, Q.; Chen, Z.; Zhao, Y.; Zhang, H.; Feng, Y. Biodegradation of polyacrylamide by bacteria isolated from activated sludge and oil-contaminated soil. *J. Hazard. Mater.* **2010**, *175*, 955–959.

Werner, J.J.; Koren, O.; Hugenholtz, P.; DeSantis, T.Z.; Walters, W.A.; Caporaso, J.G.; Angenent, L.T.; Knight, R.; Ley, R.E. Impact of training sets on classification of high-throughput bacterial 16s rRNA gene surveys. *ISME J*. **2012**, *6*, 94–103.

Wersin, P.; Leupin, O.X.; Mettler, S.; Gaucher, E.C.; Mäder, U.; De Cannière, P.; Vinsot, A.; Gäbler, H.E.; Kunimaro, T.; Kiho, K.; et al. Biogeochemical processes in a clay formation in situ experiment: part A – overview, experimental design and water data of an experiment in the Opalinus Clay at the Mont Terri Underground Research Laboratory, Switzerland. *Appl. Geochem.* **2011a**, *26,* 931-953.

Wersin, P.; Stroes-Gascoyne, S.; Pearson, F.J.; Tournassat, C.; Leupin, O.X.; Schwyn, B. Biogeochemical processes in a clay formation in situ experiment: part G – key interpretations and conclusions. Implications for repository safety. *Appl. Geochem.* **2011b**, *26,* 1023-1034.

Westcott, F.; Watson, L. End pit Lakes Technical Guidance Document; Clearwater Environmental Consultants for Cumulative Effects; Project 2005-61; Management Association End Pit Lakes Subgroup: Calgary, CA, 2007.

White, K.B.; Liber, K. Early chemical and toxicological risk characterization of inorganic constituents in surface water from the Canadian oil sands first large-scale end pit lake. *Chemosphere* **2018**, *211*, 745–757.

Widdows, J.; Friend, P.L.; Bale, A.J.; Brinsley, M.D.; Pope, N.D.; Thompson, C.E.L. Inter-comparison between five devices for determining erodibility of intertidal sediments. *Cont. Shelf Res.* **2007***, 27*, 1174–1189.

Wilson, G.W.; Kabwe, L.K.; Beier, N.A.; Scott, J.D. Effect of various treatments on consolidation of oil sands fluid fine tailing. *Can. Geotech. J.* **2018**, *55*, 1059–1066.

Wong, M.; An, D.; Caffrey, S.M.; Soh, J.; Dong, X.; Sensen, C.W.; Oldenburg, T.B.P.; Larter, S.R.; Voordouw, G. 2015. Roles of thermophiles and fungi in bitumen degradation in mostly cold oil sands outcrops. *Appl. Environ. Microbiol.* **2015**, *81*, 6825-6838.

Woodrow, J.E.; Seiber, J.N.; Miller, G.C. Acrylamide release resulting from sunlight irradiation of aqueous polyacrylamide/iron mixtures. *J. Agric. Food Chem.* **2008**, *56*, 2773–2779.

Wotton, R.S. The essential role of exopolymers (EPS) in aquatic systems. *Oceanogr. Mar. Biol.* **2004***, 42*, 57–94.

Wu, Z.; Guiping, L.; Ji, Y.; Li, P.; Yu, X.; Qiao, X.; Wang, B.; She, K.; Liu, W.; Liang, B.; et al. Electron acceptors determine the BTEX degradation capacity of anaerobic microbiota via regulating the microbial community. *Environ. Res.* **2022**, *215*, 114420.

Xiong, B.; Dettam Loss, R.; Shields, D.; Pawlik, R.; Hochreiter, R.; Zydney, A.L.; Kumar, M. Polyacrylamide degradation and its implications in environmental systems. *NPJ Clean Water* **2018a**, *1*, 17.

Xiong, B.; Miller, Z.; Roman-White, S.; Tasker, T.; Farina, B.; Piechowicz, B.; Burgos, W.D.; Joshi, P.; Zhu, L.; Gorski, C.A.; et al. Chemical Degradation of Polyacrylamide during Hydraulic Fracturing. *Environ. Sci. Technol.* **2018b**, *52*, 327–336.

Xiong, B.; Purswani, P.; Pawlik, T.; Samineni, L.; Karpyn, Z.T.; Zydney, A.L.; Kumar, M. Mechanical degradation of polyacrylamide at ultra high deformation rates during hydraulic fracturing. *Environ. Sci. Water Res. Technol*. **2020**, *6*, 166–172.

Yan, Y.; Colenbrander Nelson, T.E.; Twible, L.; Whaley-Martin, K.; Jarolimek, C.V.; King, J.J.; Apte, S.C.; Arrey, J.; Warren, L.A. Sulfur mass balance and speciation in the water cap during early-stage development in the first pilot pit lake in the Alberta oil sands. *Environ. Chem.* **2022**, *19*, 236-253.

Yu, X. Improving Cap Water Quality in an Oil Sands End Pit Lake with Microbial Applications. PhD Thesis, University of Alberta, Edmonton, CA, 2019.

Yu, X.; Lee, K.; Ma, B.; Asiedu, E.; Ulrich, A.C. Indigenous microorganisms residing in oil sands tailings biodegrade residual bitumen. *Chemosphere* **2018**, *209*, 551–559.

Yu, X.; Lee, K.; Ulrich, A.C. Model naphthenic acids removals by microalgae and Base Mine Lake cap water microbial inoculum. *Chemosphere* **2019**, *234*, 796–805.

Zhang, S. The relationship between organoclastic sulfate reduction and carbonate precipitation/dissolution in marine sediments. *Mar. Geol.* **2020**, *428,* 106284.

Zhao, K.; Tedford, E.W.; Zare, M.; Lawrence, G.A. Impact of atmospheric pressure variations on methane ebullition and lake turbidity during ice-cover. *L&O Letters* **2021**, *6*, 253-261.

Znidarcic, D.; Van Zyl, D.; Ramirez, M.; Mittal, K.; Kaminsky, H. Consolidation characteristics of flocculated MFT – experimental column and SICT data. In Proceedings of the 5th International Oil Sands Tailings Conference, Lake Louise, CA, 4-7 December 2016.

APPENDIX A:

SUPPLEMENTARY INFORMATION FOR CHAPTER 3

Appendix A1: Supplementary Tables and Figures

This supplement includes turbidity data from preliminary mixing tests (Table A-1) and water chemistry data for the initial BML surface water and initial FFT pore water used in this work (Table A-2).

Table A-1. Turbidity measurements from preliminary mixing tests to confirm the threshold velocity of 40 rpm and compare turbidity generation from stationary versus moving impellers.

Mixing speed (rpm)	Turbidity after 1 hour (NTU)	
	Stationary Impeller	Moving Impeller
20	12.2	16.7
30	17.3	19.5
40	87.0	91.1

Table A-2. Water chemistry data for initial BML surface water and initial FFT pore water prior to biofilm growth and mixing tests. Results are presented as average ± one standard deviation of triplicates.

Parameter	Initial BML Surface Water	FFT Pore Water
pH	8.52 ± 0.04	8.18 ± 0.03
EC (mS/cm)	2.36 ± 0.01	2.95 ± 0.01
DO (mg/L)	6.96 ± 0.11	1.96 ± 0.07 *
NH_4-N (mg/L)	0.329 ± 0.004	7.12 ± 0.17
NO_2-N (µg/L)	0.181 ± 0.032	12.8 ± 11.9
NO_3-N (mg/L)	0.461 ± 0.097	0.168 ± 0.029
PO_4-P (µg/L)	2.96 ± 0.11	112.6 ± 47.4
SO_4-S (mg/L)	60.4 ± 0.5	18.8 ± 1.7
Cl^- (mg/L)	334.4 ± 2.4	476.3 ± 5.1
Na^+ (mg/L)	546.0 ± 2.4	791.5 ± 7.4
K^+ (mg/L)	14.2 ± 0.1	21.0 ± 1.4
Ca^{2+} (mg/L)	23.5 ± 0.1	22.0 ± 2.1
Mg^{2+} (mg/L)	11.9 ± 0.1	12.9 ± 0.1
NAFCs (mg/L)	45.3 ± 6.7	70.5 ± 11.7
Turbidity (NTU)	2.75 ± 0.96	-

*Measured in FFT (includes both solids and pore water)

Figure A-1 shows pictures of Biofilm10 and Biofilm20 jars prior to mixing tests. Figure A-2 shows pictures of a gas bubble in a Biofilm 20 jar, and the subsequent lifting and layering of Biofilm20 after the gas bubble was released. Figure A-3 provides a comparison of Eukaryote abundance at the species level in Biofilm 10a and Biofilm 20a. Figure A-4 compares the initial turbidity generated during the first and second 1 hr mixing periods using percent difference. DO and pH measurements taken over the 70 d experiment are available in Figures A-5 and A-6, respectively.

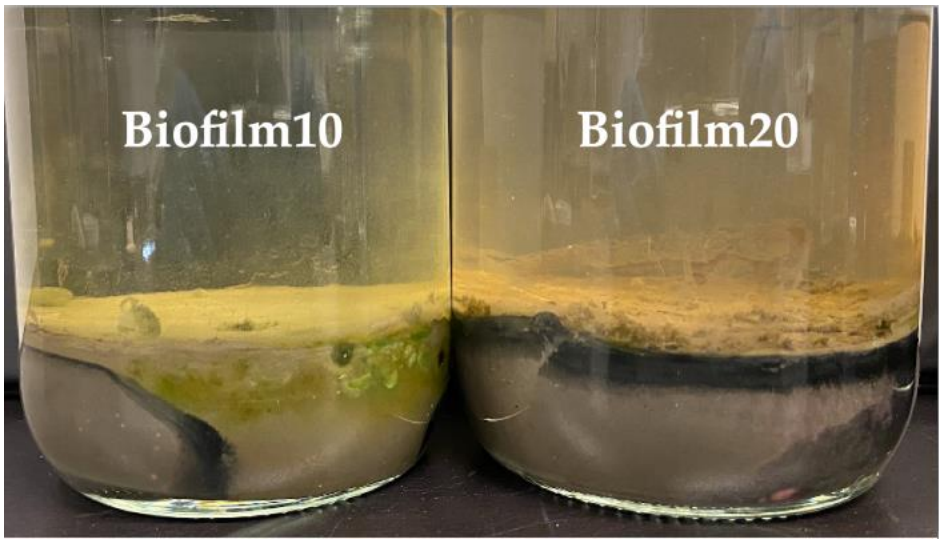

Figure A-1. Picture of a Biofilm10 (left) jar and a Biofilm20 (right) jar after 10-week and 20-week growth periods, respectively, but prior to mixing tests. Biofilm10 corresponds to 10-week-old biofilms; Biofilm20 corresponds to 20-week-old biofilms.

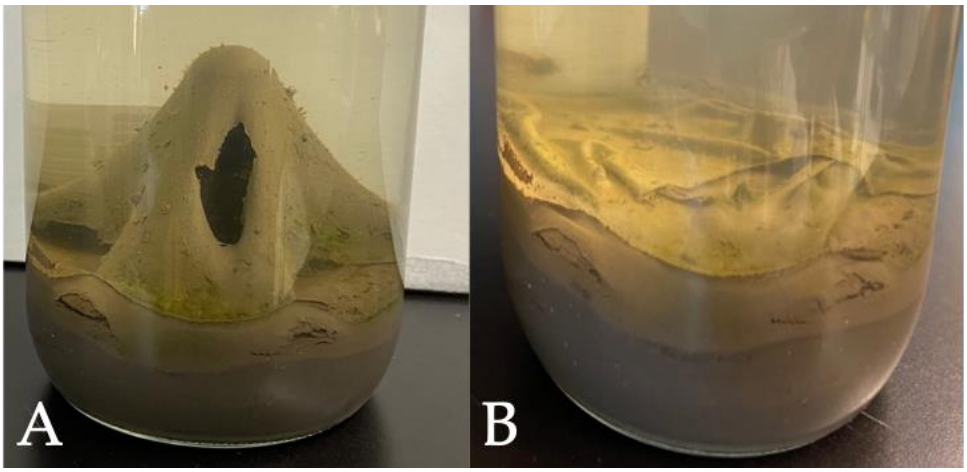

Figure A-2. Picture of A: Gas bubble in a Biofilm20 jar and B: Subsequent lifting and layering of Biofilm20 after gas bubble release during 20-week growth period.

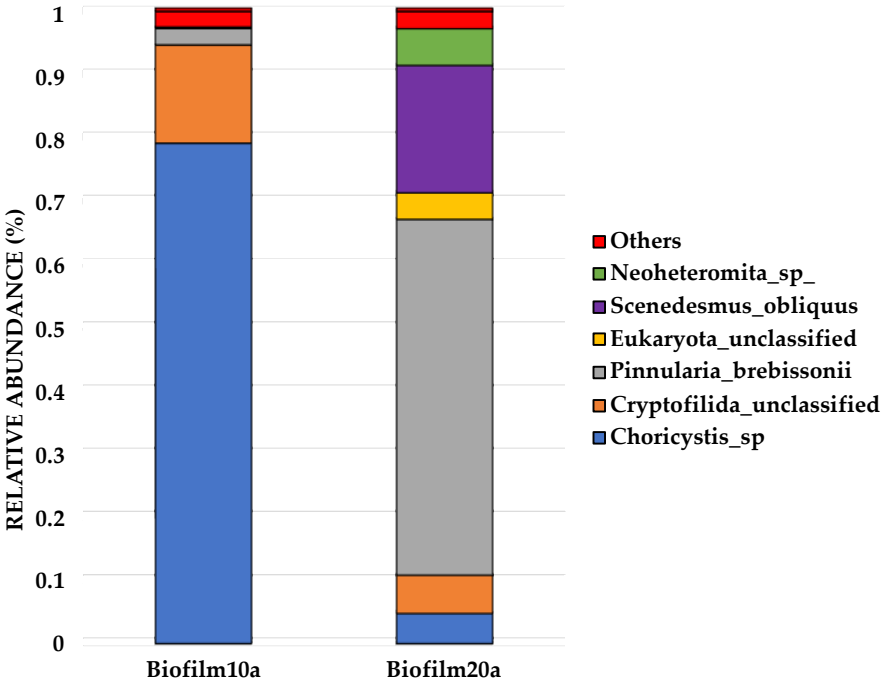

Figure A-3. A comparison of Eukaryote abundance at the species level in Biofilm10a and Biofilm20a, revealed by 18S sequencing. Biofilm10 corresponds to 10-week-old biofilms; Biofilm20 corresponds to 20-week-old biofilms. Biofilm 10a and Biofilm 20a refer to biofilm samples taken from the top layers of the biofilms.

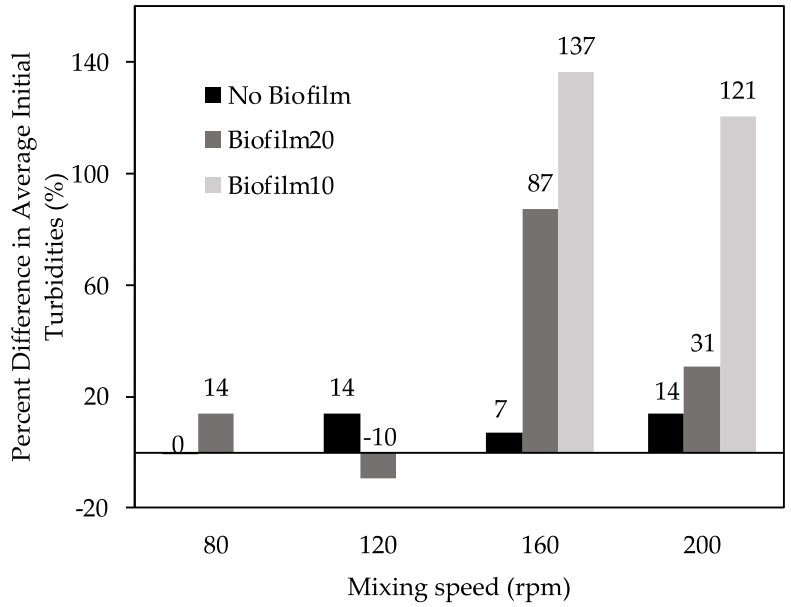

Figure A-4. Percent difference in average initial turbidity generated during the first and second 1 hr mixing periods for No Biofilm, Biofilm10, and Biofilm20 jars. Biofilm10 corresponds to 10-week-old biofilms; Biofilm20 corresponds to 20-week-old biofilms.

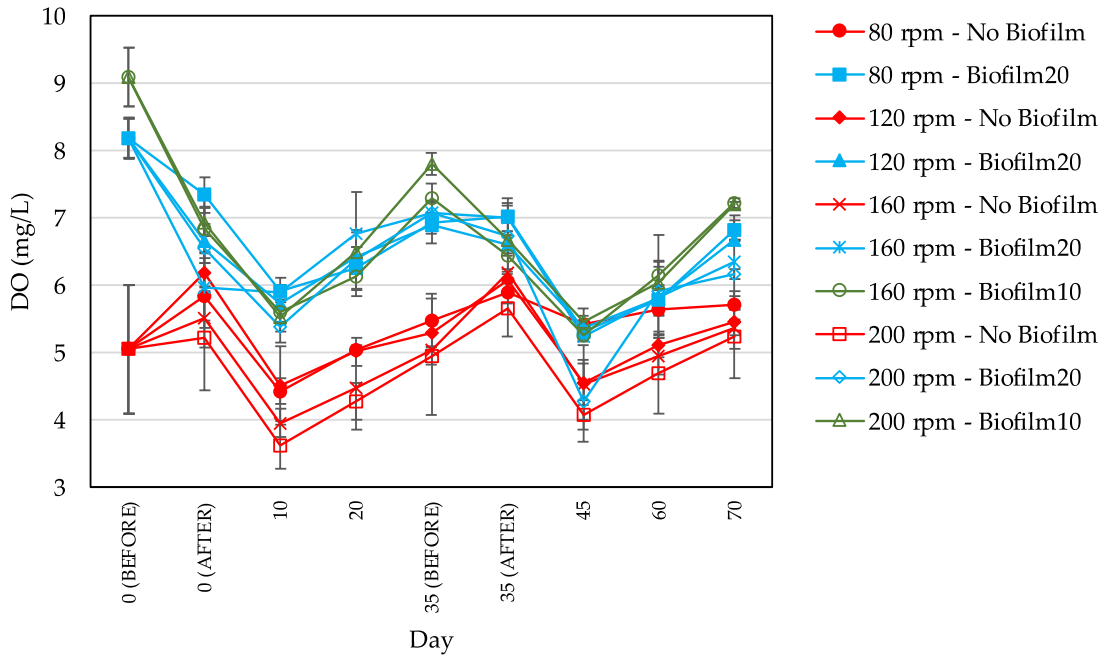

Figure A-5. Dissolved oxygen (DO) concentrations in No Biofilm, Biofilm10, and Biofilm20 jars during the first and second mixing tests. Before and After labels in the x-axis indicate measurements taken immediately before or after the first or second 1 hr mixing period, which occurred on Days 1 and 35. Biofilm10 corresponds to 10-week-old biofilms; Biofilm20 corresponds to 20-week-old biofilms.

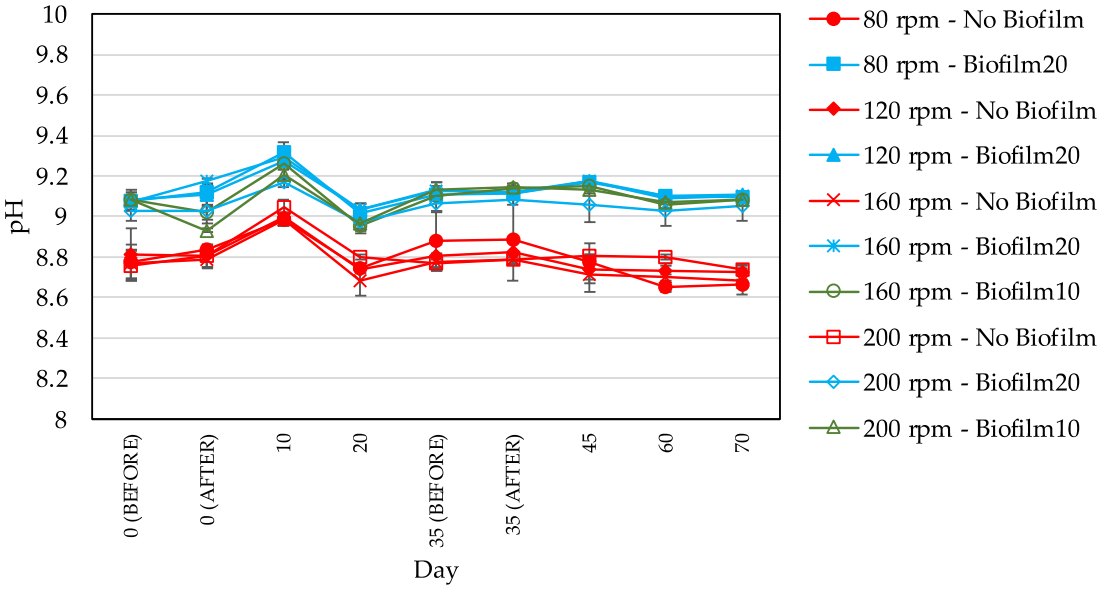

Figure A-6. pH in No Biofilm, Biofilm10, and Biofilm20 jars during the first and second mixing tests. Before and After labels in the x-axis indicate measurements taken immediately before or after the first or second 1 hr mixing period, which occurred on Days 1 and 35. Biofilm10 corresponds to 10-week-old biofilms; Biofilm20 corresponds to 20-week-old biofilms.

APPENDIX B:

SUPPLEMENTARY INFORMATION FOR CHAPTER 4

Appendix B1: Statistical Analysis Data

Table B-1 presents results of ANOVA tests conducted to determine the statistical significance of five factors (column size, tailings treatment, temperature, hydrocarbon amendments, and CO_2 addition) on various geotechnical and biogeochemical parameters measured over the course of the experiment. Only statistically significant factors and interactions are provided, as well as their corresponding F and p values (based on Type III Sum of Squares).

Table B-1. Statistical analysis of column size, tailings treatment, temperature, hydrocarbon amendments (HC), and CO_2 addition on various geotechnical and biogeochemical parameters. Statistical significance of column size, tailings treatment, temperature, and hydrocarbon amendments are based on analysis of 40 columns (excluding 24 columns with CO_2 addition). Statistical significance of CO_2 factor is based on analysis of 48 1 L columns only. Most influential factor (highest F-value) in bold.

Parameters	Statistically Significant (at $\alpha = 0.05$) Factors & Interactions, with F and p values
NWR (%)	HC (F=86.7, p<0.0001), Temperature (F=187.2, p<0.0001), Treatment (F=415.2, p<0.0001), **Size (F=466.1, p<0.0001),** HC*Temperature (43.9, p<0.0001), HC*Size (F=5.5, p=0.027), Temperature*Treatment (F=10.8, p=0.003), Temperature*Size (F=12.2, p=0.002), Treatment*Size (F=101.7, p<0.0001), HC*Treatment*Size (F=17.8, p=0.000), CO_2 (F=58.5, p<0.0001), HC*CO_2 (F=22.7, p<0.0001), Treatment*CO_2 (F=49.6, p<0.0001), HC*Treatment*CO_2 (F=21.6, p<0.0001)
Solids content (wt%)	HC (F=13.9, p=0.001), Treatment (F=15.1, p=0.001), **Size (F=218.6, p<0.0001),** HC*Temperature (F=6.6, p=0.017), HC*Treatment (F=6.2, p=0.020), CO_2 (F=8.6, p=0.006), HC*CO_2 (F=5.7, p=0.023), Treatment*CO_2 (F=4.4, p=0.043), HC*Treatment*CO_2 (F=11.8, p=0.002)
Bitumen content (wt%, 19 L columns only)	**HC (F=6.5, p=0.031),** Treatment (F=6.5, p=0.031)
Pore water sulfate (mg/L)	**HC (F=3238.8, p <0.0001),** Treatment (F=2099.2, p<0.0001), HC*Temperature (F=4.9, p=0.036), HC*Treatment (F=127.8, p<0.0001), Treatment*Size (F=10.1, p=0.004), HC*Treatment*Size (F=8.8, p=0.007)

Water cap sulfate (mg/L)	**HC (F=1807.6, p<0.0001),** Temperature (F=25.2, p<0.0001), Treatment (F=486.1, p<0.0001), Size (F=81.8, p<0.0001), HC*Treatment (F=78.7, p<0.0001), HC*Size (F=380.1, p<0.0001), Temperature*Size (F=24.3, p<0.0001), HC*Temperature*Size (F=6.7, p=0.016), HC*Treatment*Size (F=9.7, p=0.005), Treatment*CO_2 (F=5.1, p<0.029)
Pore water sulfide species (mg/L)	HC (F=49.2, p<0.0001), Temperature (F=14.8, p=0.001), Treatment (F=32.8, p<0.0001), Size (F=21.5, p=0.000), HC*Temperature (F=12.7, p=0.002), **HC*Treatment (F=54.7, p<0.0001),** Temperature*Treatment (F=10.3, p=0.004), Temperature*Size (F=9.1, p=0.006), HC*Temperature*Treatment (F=11.3, p=0.003), HC*Temperature*Size (F=7.4, p=0.013), Temperature*Treatment*Size (F=10.3, p=0.004)
Solid phase sulfur content (%)	*No statistical significance*
Pore water alkalinity (mg/L)	**HC (F=352.2, p<0.0001),** Treatment (F=33.4, p<0.0001), Size (F=66.5, p<0.0001), HC*Temperature (F=4.6, p=0.044), HC*Treatment (F=9.7, p=0.005), Temperature*Size (F=4.8, p=0.040)
Water cap alkalinity (mg/L)	**HC (F=121.0, p<0.0001),** Treatment (F=6.2, p=0.020), Size (F=76.4, p<0.0001), HC*Temperature (F=7.8, p=0.010), HC*Treatment (F=10.7, p=0.003), HC*Size (F=25.6, p<0.0001), Treatment*Size (F=13.5, p=0.001), Temperature*Treatment*Size (F=5.6, p=0.026), CO_2 (F=6.8, p=0.014), HC*Temperature*CO_2 (F=4.1, p=0.050)
Pore water calcium (mg/L)	**HC (F=747.8, p<0.0001),** Treatment (F=475.7, p<0.0001), Size (F=285.3, p<0.0001), HC*Treatment (F=51.5, p<0.0001), Temperature*Size (F=9.7, p=0.005), Treatment*Size (F=12.9, p=0.001), HC*Temperature*Treatment (F=4.4, p=0.046), CO_2 (F=14.1, p=0.001), HC*CO_2 (F=4.6, p=0.039)
Water cap calcium (mg/L)	**HC (F=961.1, p<0.0001),** Temperature (F=127.1, p<0.0001), Treatment (F=540.7, p<0.0001), Size (F=289.5, p<0.0001), HC*Treatment (F=45.4, p<0.0001), HC*Size (F=296.8, p<0.0001), Temperature*Treatment (F=11.1, p=0.003), Temperature*Size (F=18.5, p=0.000), HC*Temperature*Treatment (F=13.5, p=0.001), HC*Temperature*Size (F=7.2, p=0.013), HC*Treatment*Size (F=4.8, p=0.038), Temperature*Treatment*Size (F=8.3, p=0.008), CO_2 (F=16.8, p=0.000), Temperature*CO_2 (F=4.6, p=0.040), HC*Treatment*CO_2 (F=15.5, p=0.000)

Pore water magnesium (mg/L)	HC (F=917.6, p<0.0001), Temperature (F=6.3, p=0.020), **Treatment (F=991.3, p<0.0001),** Size (F=633.9, p<0.0001), HC*Treatment (F=69.6, p<0.0001), Temperature*Size (F=12.8, p=0.002), Treatment*Size (F=38.7, p<0.0001), HC*Treatment*Size (F=4.7, p=0.040), CO_2 (F=17.3, p=0.000), HC*CO_2 (F=12.5, p=0.001), Temperature*CO_2 (F=4.6, p=0.040)
Water cap magnesium (mg/L)	**HC (F=978.7, p<0.0001),** Temperature (F=168.4, p<0.0001), Treatment (F=297.2, p<0.0001), Size (F=381.5, p<0.0001), HC*Treatment (F=25.6, p<0.0001), HC*Size (F=277.1, p<0.0001), Temperature*Treatment (F=22.2, p<0.0001), Temperature*Size (F=28.5, p<0.0001), Treatment*Size (F=20.8, p=0.000), HC*Temperature*Treatment (F=10.2, p=0.004), HC*Temperature*Size (F=6.3, p=0.019), Temperature*Treatment*Size (F=20.4, p=0.000), CO_2 (F=24.2, p<0.0001), HC*CO_2 (F=4.2, p=0.048), Temperature*CO_2 (F=6.8, p=0.014), HC*Treatment*CO_2 (F=19.8, p<0.0001)
Pore water sodium (mg/L)	HC (F=50.9, p<0.0001), Temperature (F=18.1, p=0.000), Treatment (F=9.2, p=0.006), **Size (F=718.8, p<0.0001),** HC*Treatment (F=14.8, p=0.001), Temperature*Size (F=19.1, p=0.000), Treatment*Size (F=16.2, p=0.000), CO_2 (F=7.5, p=0.010), HC*CO_2 (F=17.7, p=0.000)
Water cap sodium (mg/L)	HC (F=8.7, p=0.007), Temperature (F=8.2, p=0.008), Treatment (F=203.6, p<0.0001), **Size (F=526.5, p<0.0001),** Temperature*Treatment (F=20.1, p=0.000), Temperature*Size (F=27.1, p<0.0001), Treatment*Size (F=12.0, p=0.002), HC*Treatment*CO_2 (F=10.7, p=0.003), Temperature*Treatment*CO_2 (F=7.8, p=0.009)
Pore water potassium (mg/L)	**HC (F=410.7, p<0.0001)**, Temperature (F=6.6, p=0.017), Treatment (F=138.5, p<0.0001), Size (F=351.4, p<0.0001), HC*Temperature (F=8.9, p=0.006), HC*Treatment (F=14.5, p=0.001), HC*Size (F=14.6, p=0.001), Temperature*Treatment (F=5.0, p=0.036), Temperature*Size (F=45.5, p<0.0001), Treatment*Size (F=28.5, p<0.0001), HC*Temperature*Treatment (F=5.0, p=0.034), HC*Treatment*Size (F=25.3, p<0.0001), Amendment*CO_2 (F=8.3, p=0.007), Amendment*Treatment*CO_2 (F=5.8, p=0.022)

Water cap potassium (mg/L)	HC (F=962.7, p<0.0001), Temperature (F=105.3, p<0.0001), Treatment (F=67.9, p<0.0001), **Size (F=1327.3, p<0.0001),** HC*Size (F=313.2, p<0.0001), Temperature*Treatment (F=61.2, p<0.0001), Temperature*Size (F=105.0, p<0.0001), Treatment*Size (F=46.3, p<0.0001), HC*Temperature*Treatment (F=7.4, p=0.012), HC*Treatment*Size (F=6.1, p=0.021), Temperature*Treatment*Size (F=52.8, p<0.0001), Amendment*CO_2 (F=6.6, p=0.015), Treatment*CO_2 (F=6.2, p=0.018), Amendment*Treatment*CO_2 (F=16.7, p=0.000)
Pore water chloride (mg/L)	HC (F=24.6, p <0.0001), Temperature (F=32.6, p<0.0001), **Treatment (F=285.5, p<0.0001),** Size (F=20.8, p=0.000), HC*Treatment (F=24.1, p<0.0001), Temperature*Size (F=29.5, p<0.0001), Treatment*Size (F=4.5, p=0.045), HC*Treatment*Size (F=4.4, p=0.047), CO_2 (F=6.3, p=0.017)
Water cap chloride (mg/L)	**Treatment (F=3967.6, p<0.0001),** Size (F=935.7, p<0.0001), HC*Size (F=8.6, p<0.007), Temperature*Size (F=13.4, p<0.001), Treatment*Size (F=21.3, p<0.000), CO_2 (F=5.6, p=0.023)
Pore water DOC (mg/L)	**HC (F=695.6, p<0.0001),** Treatment (F=27.1, p<0.0001), Size (F=131.4, p<0.0001), Treatment*Size (F=9.2, p=0.006), HC*Treatment*Size (F=4.7, p=0.039)
Water cap DOC (mg/L)	**HC (F=540.2, p<0.0001),** Temperature (F=38.2, p<0.0001), Size (F=519.9, p<0.0001), HC*Treatment (F=47.4, p<0.0001), HC*Size (F=99.4, p<0.0001), Temperature*Treatment (F=35.2, p<0.0001), Treatment*Size (F=89.7, p<0.0001), Temperature*Treatment*Size (F=29.9, p<0.0001), CO_2 (F=15.7, p=0.000)
Pore water pH	HC (F=21.8, p=0.000), Treatment (F=22.7, p=0.000), **Size (F=30.4, p<0.0001),** HC*Temperature (F=4.9, p=0.038), HC*Treatment (F=18.7, p=0.000), HC*Temperature*Size (F=5.9, p=0.024)
Water cap pH	Temperature (F=4.8, p=0.038), Treatment (F=12.7, p=0.002), Size (F=12.6, p=0.002), **HC*Temperature (F=13.4, p=0.001),** HC*Treatment (F=5.7, p=0.025), HC*Temperature*Size (F=4.7, p=0.040), Temperature*Treatment*Size (F=7.6, p=0.011), CO_2 (F=6.7, p=0.014), Treatment*CO_2 (F=10.4, p=0.003), HC*Temperature*CO_2 (F=19.4, p=0.000), HC*Treatment*CO_2 (F=15.0, p=0.000)
Headspace CO_2 (mL CO_2/L tailings)	**HC (F=23.4, p<0.0001),** Temperature (F=9.5, p=0.005), HC*Temperature (F=7.5, p=0.001), Temperature*Size (F=4.5, p=0.045), HC*Treatment*CO_2 (F=5.9, p=0.021), Temperature*Treatment*CO_2 (F=5.4, p=0.026)

Headspace CH_4 (mL CH_4/L tailings)	HC (F=45.2, p<0.0001), Temperature (F=33.2, p<0.001), Treatment (F=20.1, p=0.000), **Size (F=51.0, p<0.0001),** HC*Temperature (F=30.3, p<0.0001), HC*Treatment (F=17.8, p=0.000), HC*Size (F=41.9, p<0.0001), Temperature*Treatment (F=10.2, p=0.004), Temperature*Size (F=31.2, p<0.0001), Treatment*Size (F=20.6, p=0.000), HC*Temperature*Treatment (F=6.6, p=0.017), HC*Temperature*Size (F=28.1, p<0.0001), HC*Treatment*Size (F=18.0, p=0.000), Temperature*Treatment*Size (F=10.0, p=0.004), HC*CO_2 (F=7.5, p=0.010), Temperature*CO_2 (F=6.8, p=0.014), Treatment*CO_2 (F=6.7, p=0.014), HC*Temperature*CO_2 (F=8.3, p=0.007), HC*Treatment*CO_2 (F=12.9, p=0.001)

Appendix B2: FSConsol Model Input and Output Data

FSConsol (GWP Software Inc. 2007) was used to evaluate the self-weight consolidation of untreated FFT in the two sizes of columns over 540 d. Input data was as follows: the initial solids content was 33.5 wt% (as in Table 4-2) and the specific gravity was 2.45 (determined experimentally by performing triplicate pycnometer tests). The initial FFT deposit height was 1.22 m and 0.255 m in the 19 L and 1 L columns, respectively, with a constant head at 1.71 m and 0.358 m for 19 L and 1 L columns, respectively. Hydraulic conductivity power law parameters and compressibility data for the FSConsol model were taken from Jeeravipoolvarn et al. (2009) (Standpipe 1). Jeeravipoolvarn et al. (2009) conducted 10 m standpipe tests on oil sands tailings at roughly 20°C and the geotechnical properties (solids content, fines content, bulk density, void ratio, specific gravity, and SFR) of the initial untreated FFT in Standpipe 1 were similar to that of the untreated FFT (on Day 0) used in this study.

Figure B-1 shows FSConsol output for FFT deposit height versus time for 19 L columns (A) and 1 L columns (B) over 540 d. Figures B-2 and B-3 show FSConsol output for excess pore water pressure dissipation and effective stress generation, respectively, over 540 d as a function of FFT deposit height. Figure B-4 shows FSConsol output for solids content versus FFT deposit height at various time intervals between 0 and 540 d. The purpose of consolidation modeling was to compare the self-weight consolidation of FFT in 19 L versus 1 L columns. Self-weight consolidation was quickly achieved in the 1 L columns, as seen by the plateau in column height after roughly 60 d (Figure B-1B), the relatively quick excess pore water pressure dissipation (Figure B-2B), and the small increase in solids content after Day 60 (Figure B-4B). Conversely, the 19 L columns did not achieve self-weight consolidation within 540 d (Figure B-1A), but the tailings in these columns achieved a higher effective stress (Figure B-3A) and solids content (Figure B-4A) overall because of the higher total stress in the 19 L columns.

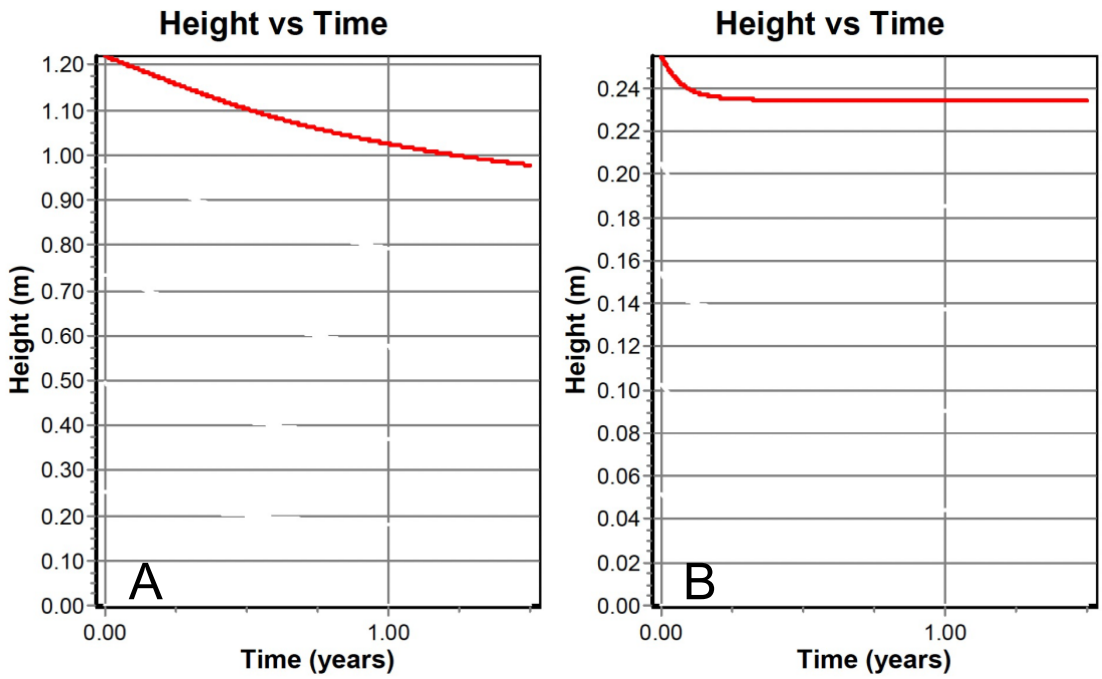

Figure B-1. Height of untreated FFT deposit versus time in (A) 19 L columns and (B) 1 L columns, predicted using FSConsol.

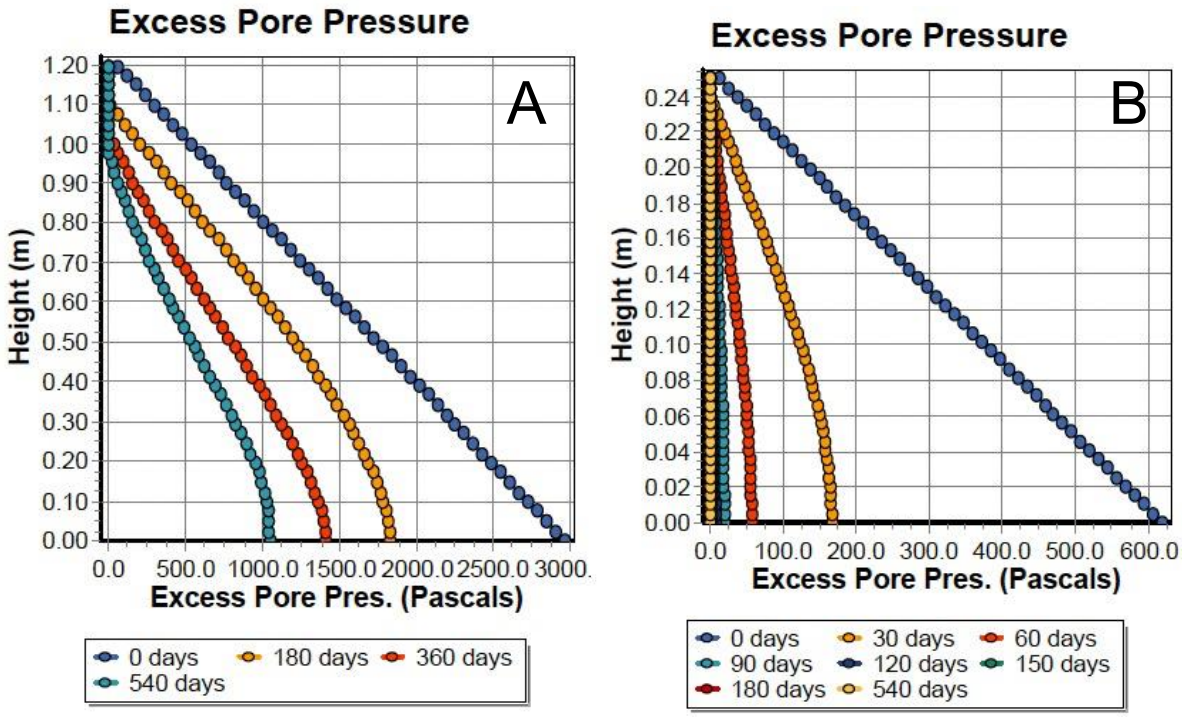

Figure B-2. Excess pore water pressure dissipation over 540 d in (A) 19 L columns and (B) 1 L columns, predicted using FSConsol. Excess pore water pressure shown at various time intervals between 0 and 540 d.

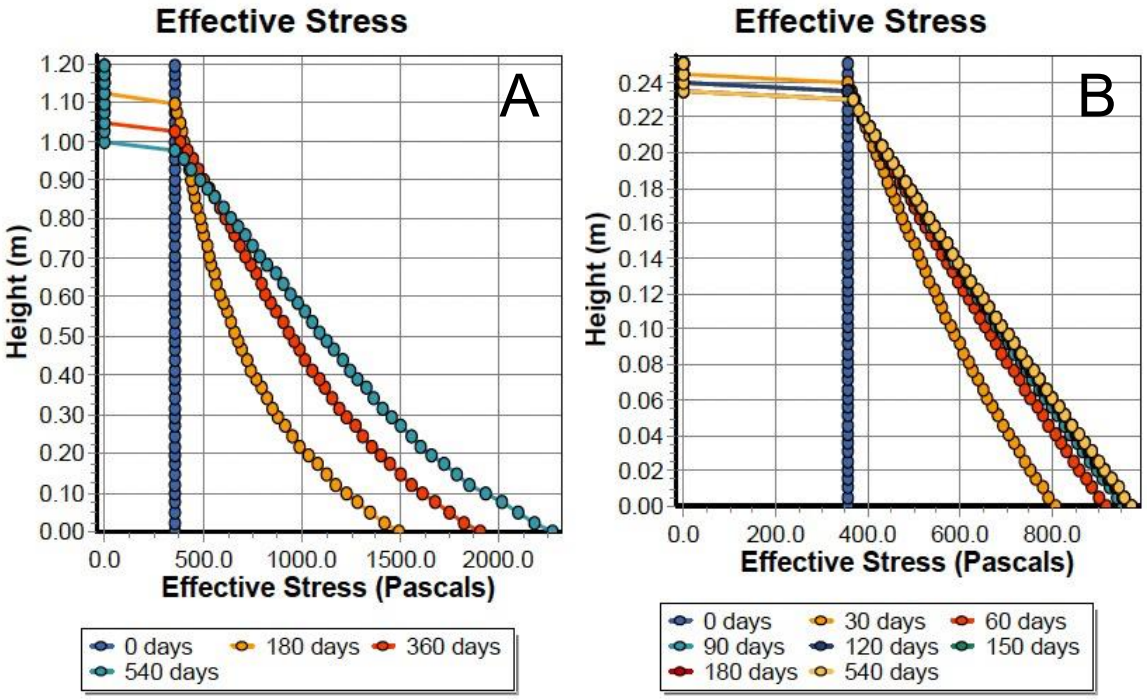

Figure B-3. Effective stress generation over 540 d in (A) 19 L columns and (B) 1 L columns, predicted using FSConsol. Effective stress shown at various time intervals between 0 and 540 d.

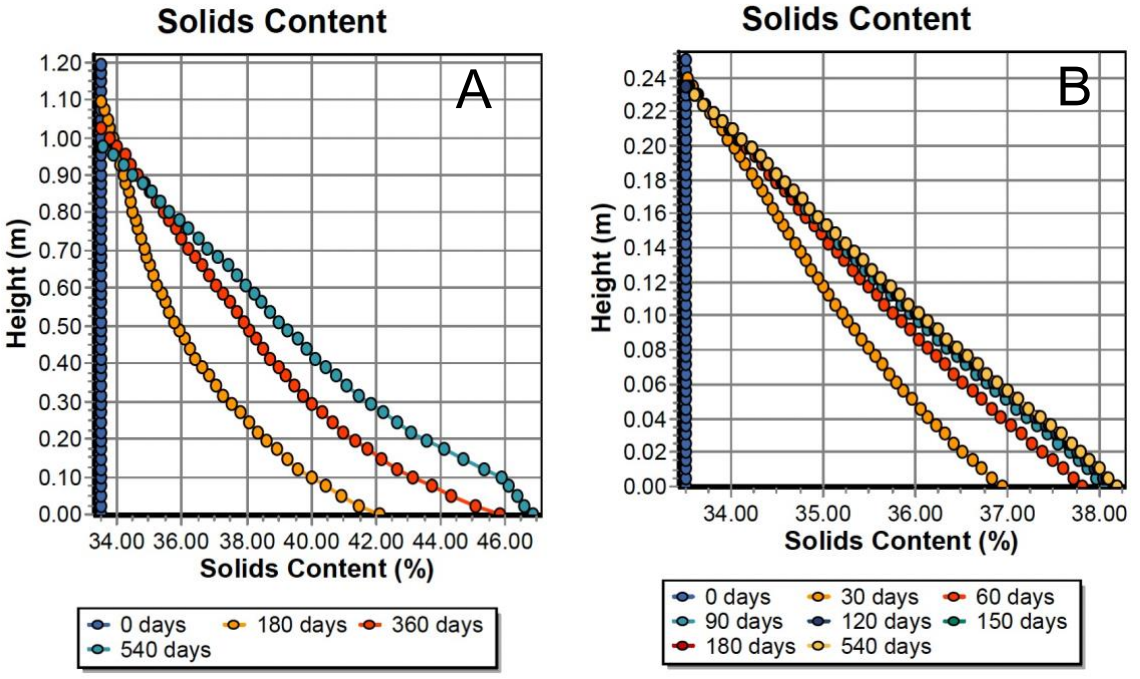

Figure B-4. Solids content versus FFT deposit height in (A) 19 L columns and (B) 1 L columns, predicted using FSConsol. Solids content shown at various time intervals between 0 and 540 d.

Appendix B2 References

GWP Software Inc. FSCONSOL Slurry Consolidation Software User Manual. GWP Software Inc.: Edmonton, CA, 2007.

Jeeravipoolvarn, S.; Scott, J.D.; Chalaturnyk, R.J. 10 m standpipe tests on oil sands tailings: Long-term experimental results and prediction. *Can. Geotech. J.* **2009**, *46*, 875–888.

Appendix B3: Supplementary Geotechnical and Biogeochemical Figures

Figure B-5 presents bitumen content in the 19 L column tailings on Day 540. Bitumen content was positively influenced by hydrocarbon amendments (p=0.031) in almost all cases. This is assumed to be the result of decreased bitumen viscosity and enhanced bitumen mixing in hydrocarbon amended tailings. Hydrocarbon amendments seemingly increased the bitumen content of the tailings (relative to Day 0 values), which further supports the theory of enhanced bitumen mixing and mobility in hydrocarbon amended tailings.

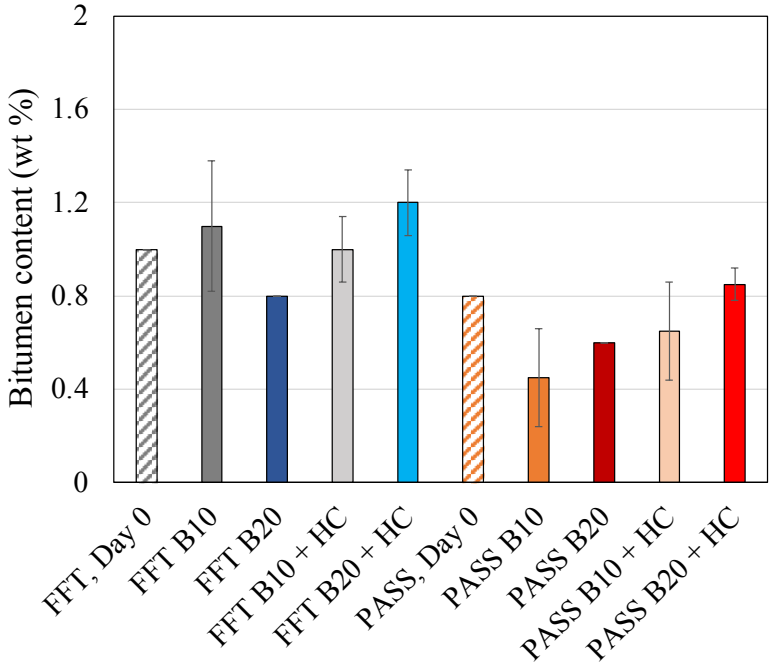

Figure B-5. Bitumen content in 19 L columns on Day 540. The bitumen contents of untreated and PASS-treated FFT on Day 0 are provided for comparison. Day 0 (untreated FFT) and Day 540 results are averages of duplicate columns and error bars represent one standard deviation of duplicates. The Day 0 PASS-treated FFT value is based on a single measurement. Label B refers to Big (19 L) columns; 10 or 20 refer to 10°C or 20°C storage temperature; HC refers to hydrocarbon amended tailings.

Figure B-6 presents total sulfide species concentrations in the 19 L and 1 L column water caps. Total sulfide species were measured every 60 d in the 19 L column water caps and on Day 540 in the 1 L water caps (because of the large sample volume required for this measurement). Water cap

concentrations of total sulfide species in all 1 L columns were ≤ 0.05 mg/L on Day 540, though most of the 1 L columns had concentrations of 0 mg/L.

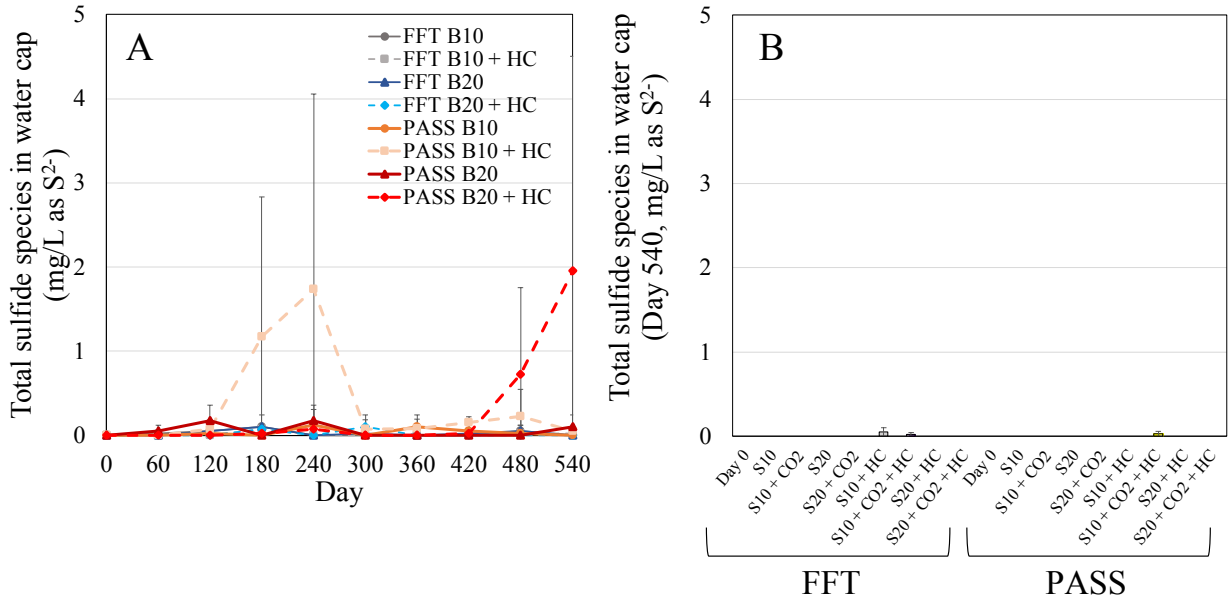

Figure B-6. Water cap total sulfide species (S^{2-}, HS^-, H_2S) concentrations in (A) 19 L columns (Day 0 to 540) and (B) 1 L columns (Day 0 and Day 540 only). Results are averages of duplicate (A) and triplicate (B) columns and error bars represent one standard deviation of replicates. Labels B or S refer to Big (19 L) or Small (1 L) columns; 10 or 20 refer to 10°C or 20°C storage temperature; CO2 and HC refer to CO_2 and hydrocarbon amended tailings.

Figures B-7 and B-8 present pH measurements in the tailings (Figures B-7) and water caps (Figure B-8). pH changes throughout the experiment were relatively minor and bitumen frequently coated the pH probes which impacted the accuracy of the pH readings. Pore water potassium concentrations are presented in Figure B-9 and are similar to that of pore water sodium. Figure B-10 shows pore water chloride concentrations. Pore water chloride concentrations decreased slightly, particularly in the PASS-treated columns, and this may be due to diffusion (columns with PASS-treated FFT would have a higher concentration gradient) and/or measurement error. Table B-2 presents concentrations of ammonia/ammonium measured in the pore water (Days 360 and 540) and water cap (Days 540) of the 19 L columns. Average ammonia/ammonium concentrations were ≤ 1.2 mg/L (as NH_3) in all cases. Figures B-11, B-12, and B-13 display water cap concentrations of calcium, magnesium, and potassium, respectively. Water cap concentrations of

these cations were impacted by numerous factors including advection, diffusion, and the biogeochemistry of the tailings.

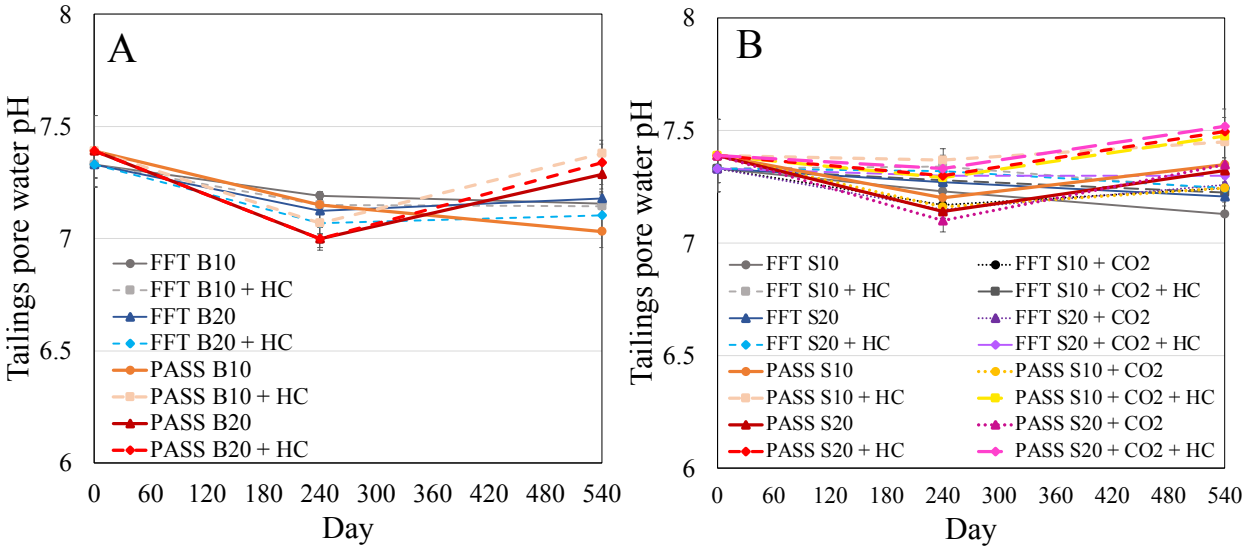

Figure B-7. Pore water pH measurements in (A) 19 L columns and (B) 1 L columns. Results are averages of duplicate (A) and triplicate (B) columns and error bars represent one standard deviation of replicates. Labels B or S refer to Big (19 L) or Small (1 L) columns; 10 or 20 refer to 10°C or 20°C storage temperature; CO2 and HC refer to CO_2 and hydrocarbon amended tailings.

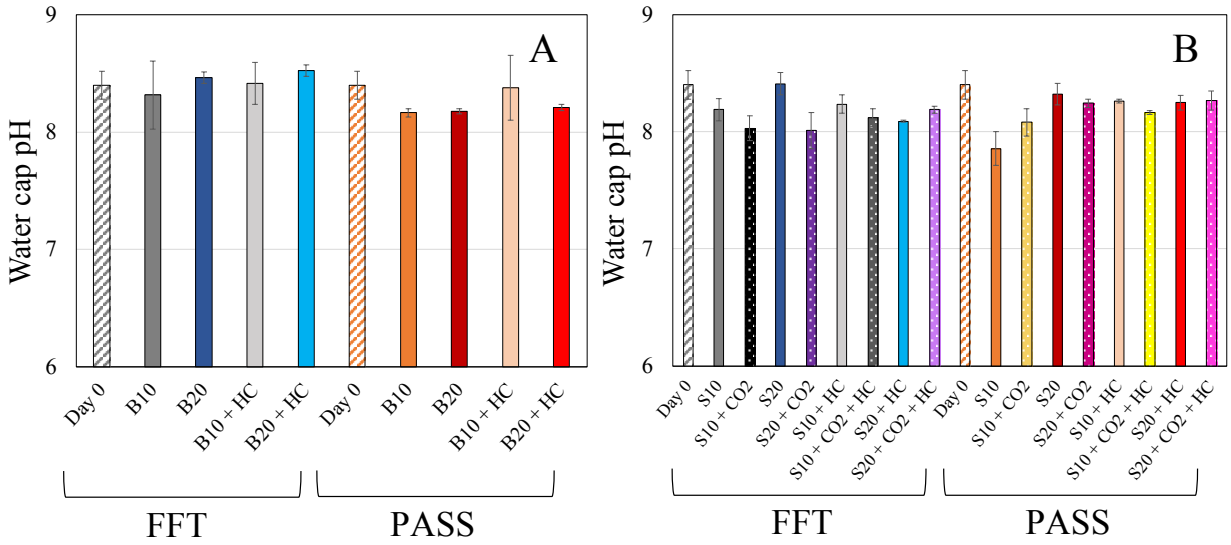

Figure B-8. Water cap pH measurements in (A) 19 L columns and (B) 1 L columns on Day 540. The Day 0 water cap pH is provided for comparison. Results are averages of duplicate (A) and triplicate (B) columns and error bars represent one standard deviation of replicates. Labels B or S refer to Big (19 L) or Small (1 L) columns; 10 or 20 refer to 10°C or 20°C storage temperature; CO2 and HC refer to CO_2 and hydrocarbon amended tailings.

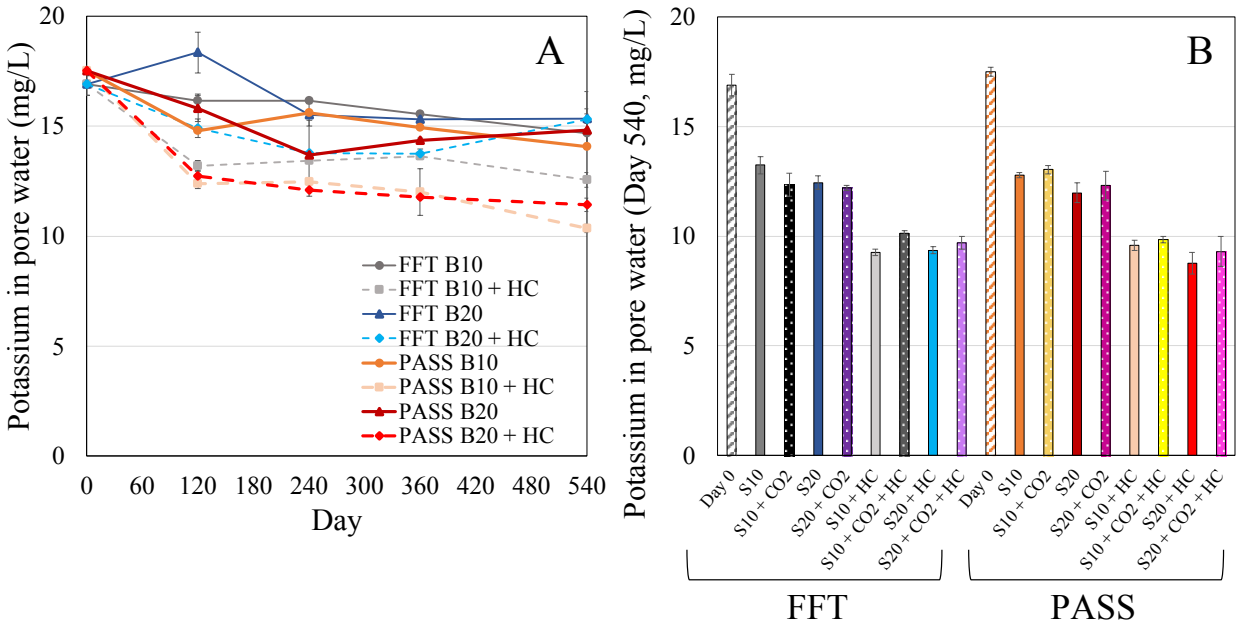

Figure B-9. Pore water potassium concentrations in (A) 19 L columns (Day 0 to 540) and (B) 1 L columns (Day 0 and Day 540 only). Results are averages of duplicate (A) and triplicate (B) columns and error bars represent one standard deviation of replicates. Labels B or S refer to Big (19 L) or Small (1 L) columns; 10 or 20 refer to 10°C or 20°C storage temperature; CO2 and HC refer to CO_2 and hydrocarbon amended tailings.

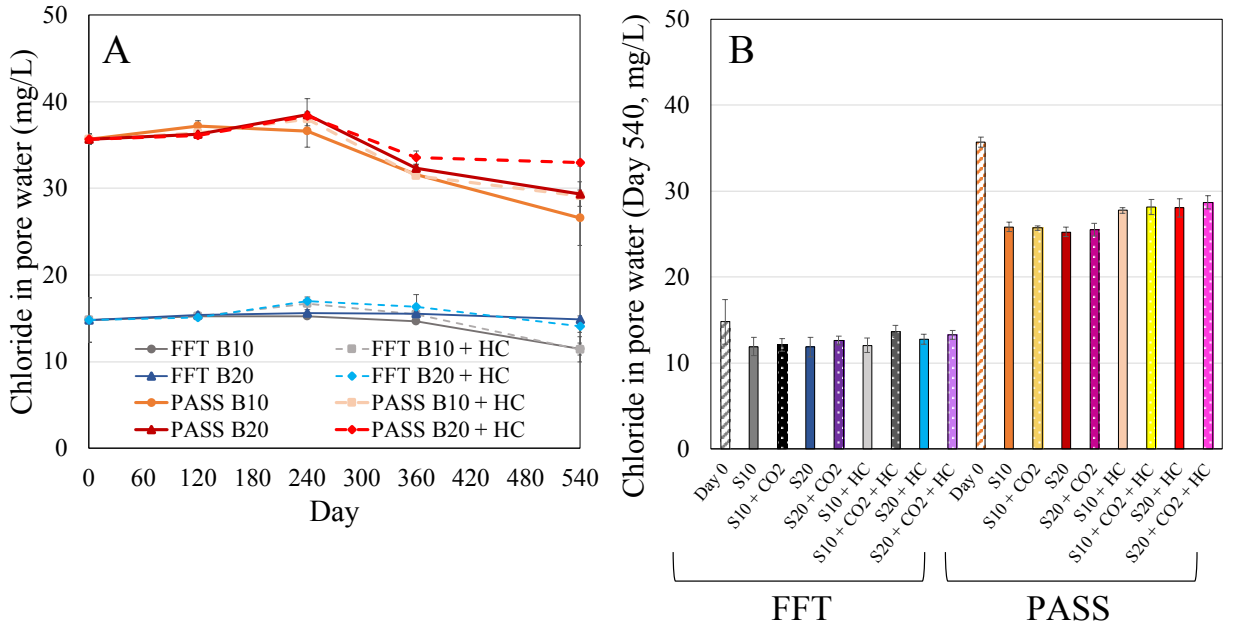

Figure B-10. Pore water chloride concentrations in (A) 19 L columns (Day 0 to 540) and (B) 1 L columns (Day 0 and Day 540 only). Results are averages of duplicate (A) and triplicate (B) columns and error bars represent one standard deviation of replicates. Labels B or S refer to Big (19 L) or Small (1 L) columns; 10 or 20 refer to 10°C or 20°C storage temperature; CO2 and HC refer to CO_2 and hydrocarbon amended tailings.

Table B-2. Concentrations of ammonia/ammonium measured in the 19 L columns on Days 360 and 540. Results are average of duplicate columns and error bars represent one standard deviation of duplicates. Day 0 ammonia/ammonium concentrations were 0.0 ± 0.0 in both the untreated and PASS-treated FFT pore waters and BCR water cap. Label B refers to Big (19 L) or Small (1 L) columns; 10 or 20 refer to 10°C or 20°C storage temperature; HC refers to hydrocarbon amended tailings.

	Ammonia/Ammonium (as NH_3, mg/L)		
	Pore Water		Water Cap
Day	**360**	**540**	**540**
FFT B10	0.0 ± 0.0	0.0 ± 0.0	0.0 ± 0.0
FFT B10 + HC	0.0 ± 0.0	0.0 ± 0.0	0.0 ± 0.0
FFT B20	1.2 ± 1.7	0.0 ± 0.0	0.0 ± 0.0
FFT B20 + HC	1.2 ± 0.0	0.6 ± 0.9	0.6 ± 0.9
PASS B10	0.6 ± 0.9	0.0 ± 0.0	0.0 ± 0.0
PASS B10 + HC	0.0 ± 0.0	0.0 ± 0.0	0.0 ± 0.0
PASS B20	0.0 ± 0.0	0.0 ± 0.0	0.0 ± 0.0
PASS B20 + HC	0.0 ± 0.0	0.0 ± 0.0	0.0 ± 0.0

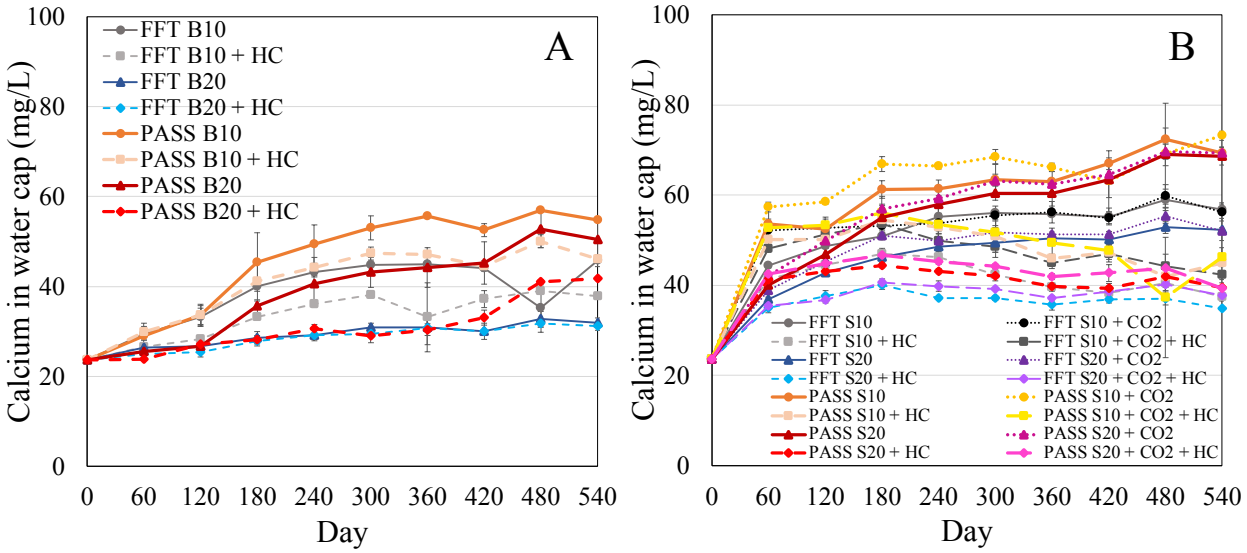

Figure B-11. Water cap calcium concentrations in (A) 19 L columns and (B) 1 L columns. Results are averages of duplicate (A) and triplicate (B) columns and error bars represent one standard deviation of replicates. Labels B or S refer to Big (19 L) or Small (1 L) columns; 10 or 20 refer to 10°C or 20°C storage temperature; CO2 and HC refer to CO_2 and hydrocarbon amended tailings.

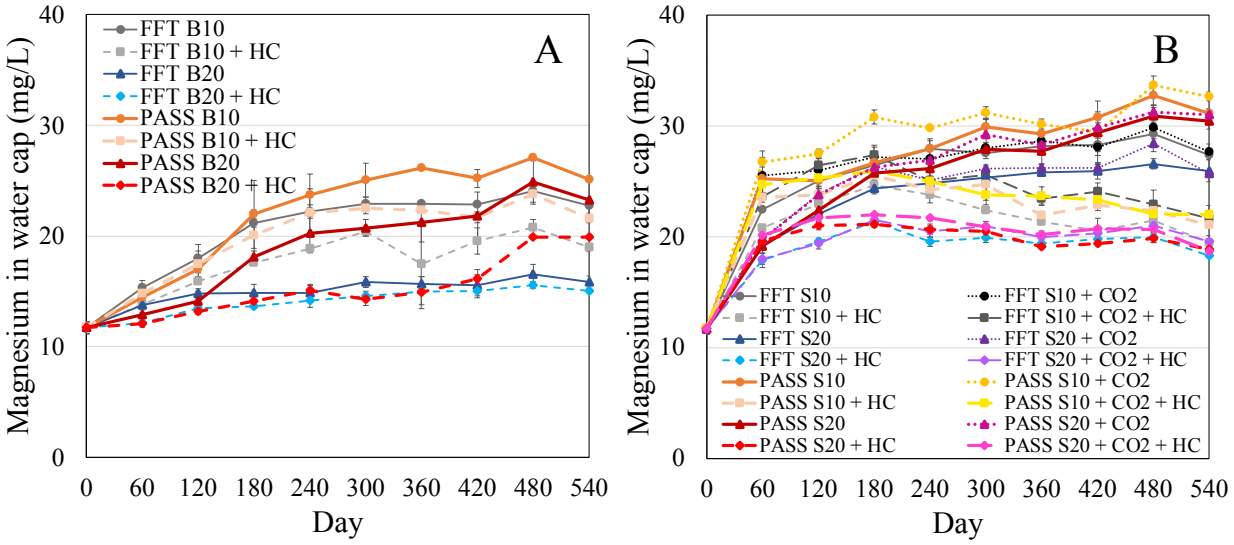

Figure B-12. Water cap magnesium concentrations in (A) 19 L columns and (B) 1 L columns. Results are averages of duplicate (A) and triplicate (B) columns and error bars represent one standard deviation of replicates. Labels B or S refer to Big (19 L) or Small (1 L) columns; 10 or 20 refer to 10°C or 20°C storage temperature; CO2 and HC refer to CO_2 and hydrocarbon amended tailings.

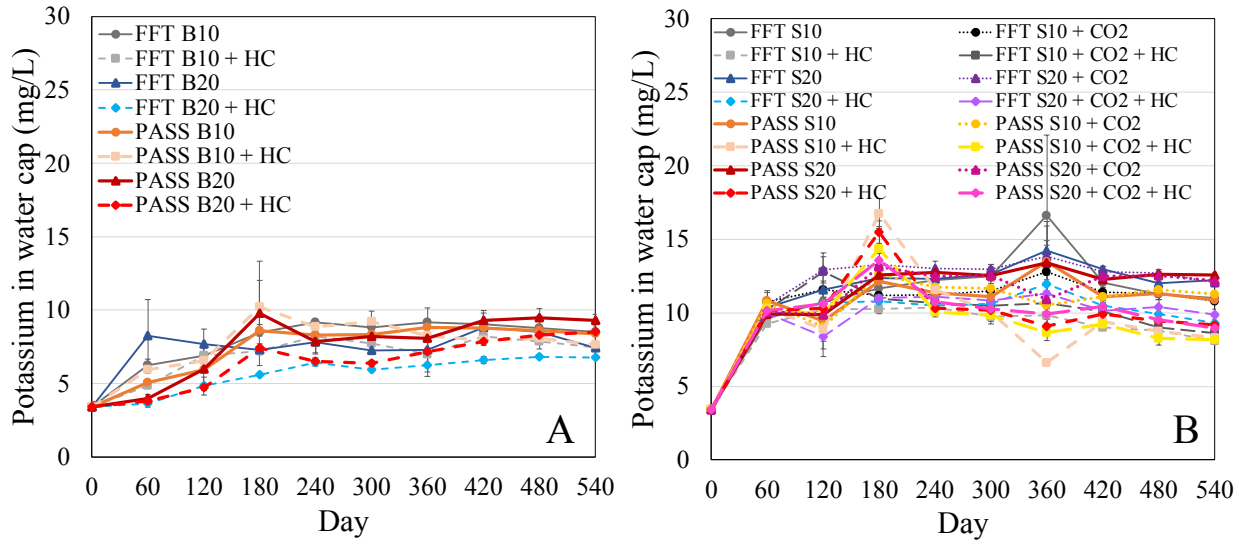

Figure B-13. Water cap potassium concentrations in (A) 19 L columns and (B) 1 L columns. Results are averages of duplicate (A) and triplicate (B) columns and error bars represent one standard deviation of replicates. Labels B or S refer to Big (19 L) or Small (1 L) columns; 10 or 20 refer to 10°C or 20°C storage temperature; CO2 and HC refer to CO_2 and hydrocarbon amended tailings.

Figure B-14 presents the volume of CO_2 emitted per L of tailings in 19 L columns (Figure B-14A) and 1 L columns (Figure B-14B) on Day 540. Column size was not a significant factor in the volume of CO_2 generated per L of tailings. While the 1 L FFT S20 + HC and PASS S20 + CO_2 + HC columns produced the highest volumes of CO_2 per L of tailings (on average), these measurements were influenced by outliers in the triplicate data. Further, the CO_2 concentrations measured on the GC-TCD were relatively low for all 1 L columns which likely contributed to the high standard deviations seen in Figure B-14B. As such, the volume of CO_2 generated per L of tailings is comparable for the 19 L and 1 L columns.

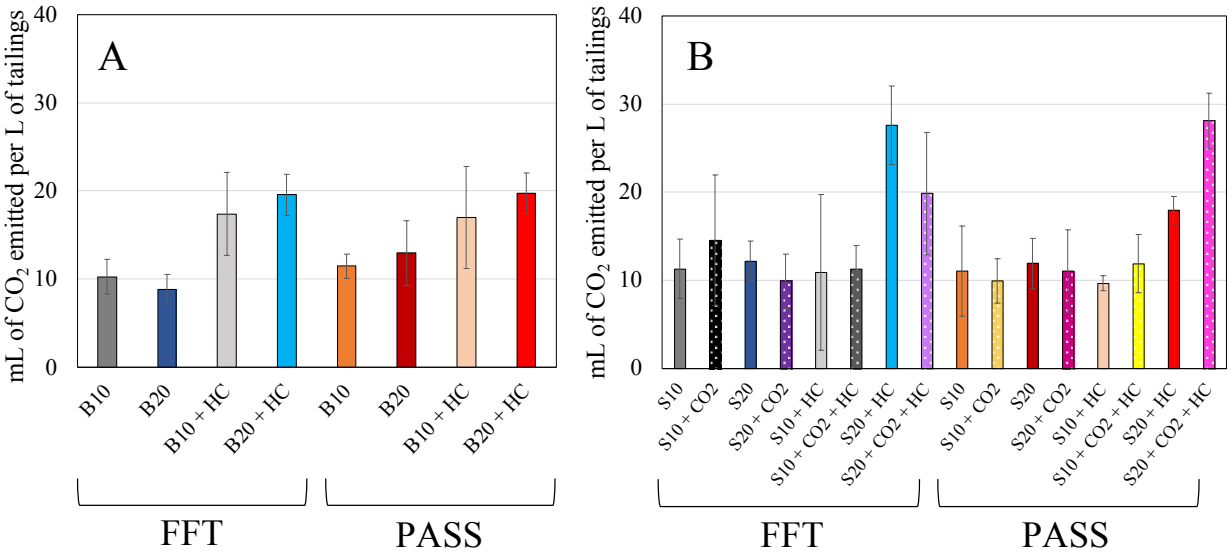

Figure B-14. Volume of carbon dioxide emitted per L of tailings in (A) 19 L columns and (B) 1 L columns on Day 540. Results are averages of duplicate (A) and triplicate (B) columns and error bars represent one standard deviation of replicates. Labels B or S refer to Big (19 L) or Small (1 L) columns; 10 or 20 refer to 10°C or 20°C storage temperature; CO2 and HC refer to CO_2 and hydrocarbon amended tailings.

Appendix B4: Relative Abundance of Microorganisms and Degradation of Hydrocarbon Amendments

Figure B-15 present the relative abundance of microbial communities (at the class level) on Day 120 in 19 L columns with untreated and PASS-treated FFT. Microbial communities in the untreated and PASS-treated FFT on Day 0 are provided for comparison. The most notable differences in Day 120 microbial communities, relative to Days 0 and 540 (see Figure 4-21), are changes in the relative abundances of classes containing known SRB (*Desulfitobacteriia*, *Desulfobacteria*, and *Desulfobulbia*). In addition, the relative abundance of *Gammaproteobacteria* increased substantially in FFT B10 + HC and FFT B20 + HC columns on Day 120, though this may be due to an error in sequencing or poor-quality DNA, as this high proportion of *Gammaproteobacteria* (roughly 76%) was only present on Day 120.

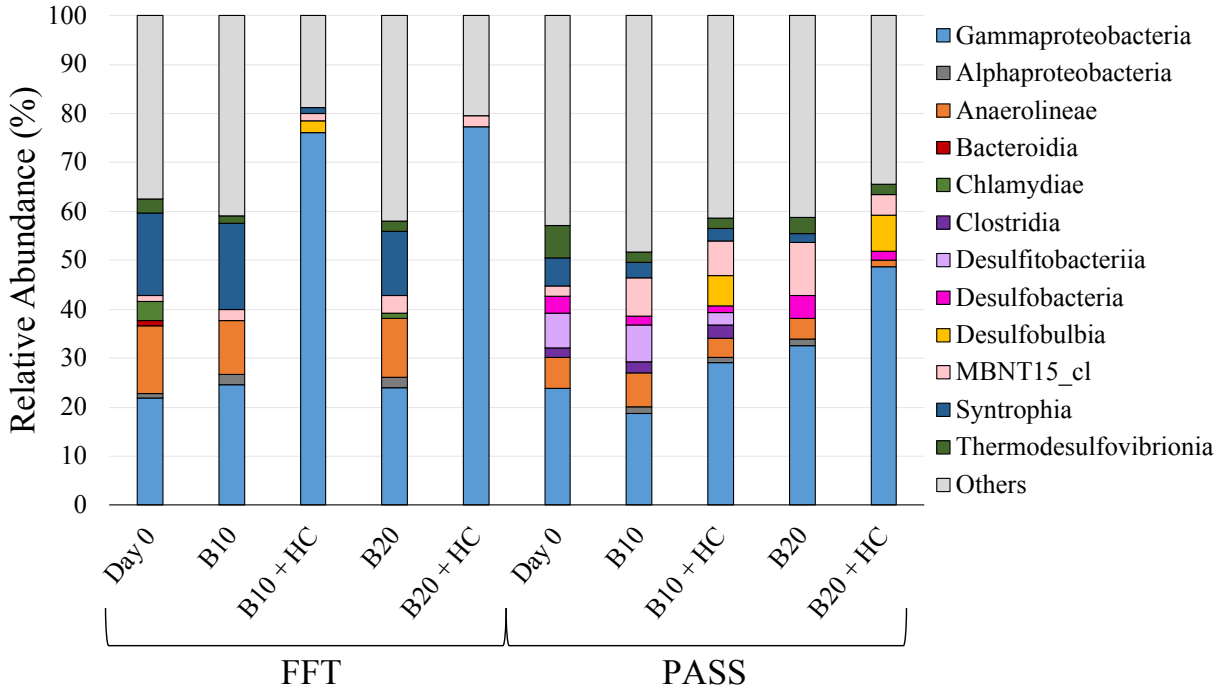

Figure B-15. Stacked bars illustrating the relative abundances of microorganisms at the class level in FFT and PASS, represented by the percentage of the 16S rRNA read counts within each group. A relative abundance of less than 1% is assigned to 'Others'. All bars (except for FFT, Day 0 and PASS, Day 0) represent tailings samples collected from 19 L columns on Day 120. FFT, Day 0 and PASS, Day 0 are provided for comparison. Label B refers to Big (19 L) columns; 10 or 20 refer to 10°C or 20°C storage temperature; HC refers to hydrocarbon amended tailings.

Table B-3 presents concentrations of hydrocarbons (toluene, o-xylene, m-xylene, p-xylene, n-octane, n-decane, 2-methylpentane, and 3-methylhexane) measured in tailings in the 19 L columns on Day 540. Concentrations of hydrocarbon amendments were measured to confirm that the hydrocarbons added were degraded by microbial communities in the tailings. Table B-3 does not include the Day 540 hydrocarbon concentrations that were measured in the unamended columns as all hydrocarbon concentrations in these columns were 0.0 ± 0.0 ppm. Similarly, hydrocarbon concentrations (toluene, o-xylene, m-xylene, p-xylene, n-octane, n-decane, 2-methylpentane, and 3-methylhexane) in untreated FFT and PASS-treated FFT on Day 0 were 0.0 ± 0.0 ppm. It was not possible to separate the peaks for m- and p-xylenes and as such, these hydrocarbons are shown together in Table B-3.

Table B-3. Concentrations of hydrocarbons in amended 19 L columns on Day 540. Results are average of duplicate columns and error bars represent one standard deviation of duplicates. Day 0 hydrocarbon amendment concentrations are included for reference. Label B refers to Big (19 L) columns; 10 or 20 refer to 10°C or 20°C storage temperature; HC refers hydrocarbon amended tailings.

Hydrocarbon (ppm)	**Day 0 Amendments**	**Day 540**			
		FFT B10 + HC	**FFT B20 + HC**	**PASS B10 + HC**	**PASS B20 + HC**
Toluene	150	0.0 ± 0.0	0.2 ± 0.0	0.0 ± 0.0	0.0 ± 0.0
o-Xylene	50	0.6 ± 0.2	1.0 ± 0.1	0.6 ± 0.1	0.7 ± 0.1
m- & p-Xylene	100	1.2 ± 0.3	2.1 ± 0.1	1.6 ± 0.1	1.6 ± 0.3
Octane	500	4.9 ± 1.1	8.4 ± 1.3	5.1 ± 0.3	6.9 ± 0.6
Decane	500	2.4 ± 0.9	4.1 ± 0.5	2.9 ± 0.2	3.4 ± 0.3
2-Methylpentane	500	7.8 ± 0.5	11.8 ± 2.5	5.2 ± 0.7	5.4 ± 1.2
3-Methylhexane	500	8.3 ± 0.8	12.7 ± 2.9	6.6 ± 0.8	8.2 ± 0.8

APPENDIX C:

SUPPLEMENTARY INFORMATION FOR CHAPTER 5

Appendix C1: Statistical Analysis Data

Table C-1 presents results of ANOVA tests conducted to determine the statistical significance of two factors (pressure and hydrocarbon amendments) on various geotechnical and biogeochemical parameters measured over 360 d. Only statistically significant factors and interactions are provided, as well as their corresponding F and p values (based on Type III Sum of Squares). Statistical significance was analyzed on the Day 360 measurements of all parameters. Select parameters were also analyzed for statistical significance on Day 60, 120, 180, 240, and/or 300 as appropriate.

Table C-1. Statistical analysis of pressure and hydrocarbon amendments on various geotechnical and biogeochemical parameters. Most influential factor (highest F-value) in bold. Blank cells indicate statistical significance was not analyzed.

Parameters	**Statistically Significant (at α = 0.05) Factors & Interactions on Day 360, with F and p values**	**Statistically Significant (at α = 0.05) Factors & Interactions on Day 60, 120, 180, 240, or 360, with F and p values**
NWR (%)	**Pressure (F=621.8, p<0.0001)**	
Solids content (wt%)	**Pressure (F=876.6, p<0.0001)**	
Bitumen content (wt%)	**Hydrocarbon Amendment (F=35.8, p=0.000)**	
Pore water sulfate (mg/L)	*No statistical significance on Day 360*	*Day 60:* **Hydrocarbon Amendment (F=719.0, p<0.0001)**; *Day 120:* Pressure (F=7.1, p=0.029), **Hydrocarbon Amendment (F=8.5, p=0.020)**
Water cap sulfate (mg/L)	Pressure (F=16.8, p=0.003), **Hydrocarbon Amendment (F=54.7, p<0.0001)**	
Pore water sulfide species (mg/L)	**Pressure (F=6.7, p=0.036)**	
Water cap sulfide species (mg/L)	*No statistical significance on Day 360*	*Day 60:* **Hydrocarbon Amendment (F=5.8, p=0.042)**
Solid phase sulfur content (%)	*No statistical significance on Day 360*	

Pore water alkalinity (mg/L)	**Hydrocarbon Amendment (F=25.7, p=0.001)**	
Water cap alkalinity (mg/L)	**Pressure (F=56.5, p<0.0001),** Hydrocarbon Amendment (F=55.0, p<0.0001)	
Pore water pH	**Hydrocarbon Amendment (F=7.4, p=0.026)**	
Water cap pH	**Hydrocarbon Amendment (F=13.4, p=0.006)**	
Headspace CO_2 (mL CO_2/L tailings)	**Pressure (F=227.3, p<0.0001),** Hydrocarbon Amendment (F=14.0, p=0.006)	
Headspace CH_4 (mL CH_4/L tailings)	Pressure (F=170.5, p<0.0001), **Hydrocarbon Amendment (F=310.9, p<0.0001)**, Pressure*Hydrocarbon Amendment F=25.9, (p=0.001)	*Day 120:* **Pressure (F=42.7, p=0.000)***; Day 180:* **Pressure (F=41.6, p=0.000)***; Day 240:* **Pressure (F=71.8, p<0.0001)***; Day 300:* **Pressure (F=252.1, p<0.0001),** Hydrocarbon Amendment (F=39.2, p=0.000)
Pore water DOC (mg/L)	*No statistical significance on Day 360*	*Day 240:* **Pressure (F=913.0, p<0.0001),** Hydrocarbon Amendment (F=7.1, p=0.032)*; Day 300:* **Pressure (F=414.0, p<0.0001)**
Water cap DOC (mg/L)	**Pressure (F=152.2, p<0.0001)**	
Pore water COD (mg/L)	**Pressure (F=6.6, p=0.037)**	
Water cap COD (mg/L)	**Pressure (F=611.3, p<0.0001)**	
Pore water ammonium (mg/L)	**Hydrocarbon Amendment (F=6.9, p=0.030)**	*Day 180:* **Pressure (F=102.1, p<0.0001)***; Day 240:* **Pressure (F=41.1, p=0.000)***; Day 300:* **Pressure (F=102.1, p<0.0001)**
Water cap ammonium (mg/L)	**Pressure (F=37.7, p=0.000)**	
Pore water sodium (mg/L)	**Pressure (F=6.4, p=0.035),** Hydrocarbon Amendment (F=5.5, p=0.047)	
Water cap sodium (mg/L)	**Pressure (F=12.8, p=0.007),** Hydrocarbon Amendment (F=9.2, p=0.016)	

Pore water calcium (mg/L)	Pressure (F=11.9, p=0.009), **Hydrocarbon Amendment (F=43.4, p=0.000)**	
Water cap calcium (mg/L)	**Hydrocarbon Amendment (F=146.4, p<0.0001)**	
Pore water magnesium (mg/L)	Pressure (F=17.5, p=0.003), **Hydrocarbon Amendment (F=47.9, p=0.000)**	*Day 240:* **Pressure (F=22.7, p=0.001)***; Day 300:* **Pressure (F=8.2, p=0.021)**
Water cap magnesium (mg/L)	**Pressure (F=225.3, p<0.0001),** Hydrocarbon Amendment (F=128.3, p<0.0001)	
Pore water potassium (mg/L)	**Pressure (F=22.4, p=0.001)**	
Water cap potassium (mg/L)	**Pressure (F=32.4, p=0.000),** Hydrocarbon Amendment (F=11.9, p=0.009)	
Pore water chloride (mg/L)	**Pressure (F=16.7, p=0.004)**	
Water cap chloride (mg/L)	**Pressure (F=164.9, p<0.0001)**	

Appendix C2: Supplementary Geotechnical and Biogeochemical Data

Figure C-1 presents a photo showing unsaturated pockets of gas in one of the PASS, HC + P columns. Figure C-2 presents the average pore pressure measurements in the columns over 360 d. Pore pressure measurements for four of the columns were excluded because the readings were unrealistic and beyond the range of the transducers. The scan number roughly corresponds to a 30 min time interval, though the frequency of the scans was increased to every 2 min during a dead load application. The arrows indicate the application of a new dead load, which occurred roughly every 60 d. Some of the spikes in pore pressure were caused by a spike in headspace pressure during nitrogen flushing or pressure testing rather than by the application of a dead load. The pore pressure values and trends are not consistent with the expected values and trends and this may be a result of both i) the accuracy of the pore pressure transducers, which is similar to the pore pressure fluctuations expected given the volume of tailings in the columns and the dead loads applied and ii) unsaturated zones throughout the tailings. For these reasons, the pore pressure measurements were deemed unreliable and as such, could not be used to determine the end of a consolidation phase.

Figure C-1. Photo of unsaturated pockets of biogenic gas in a PASS, HC + P column. Photo taken on Day 90 (approximately).

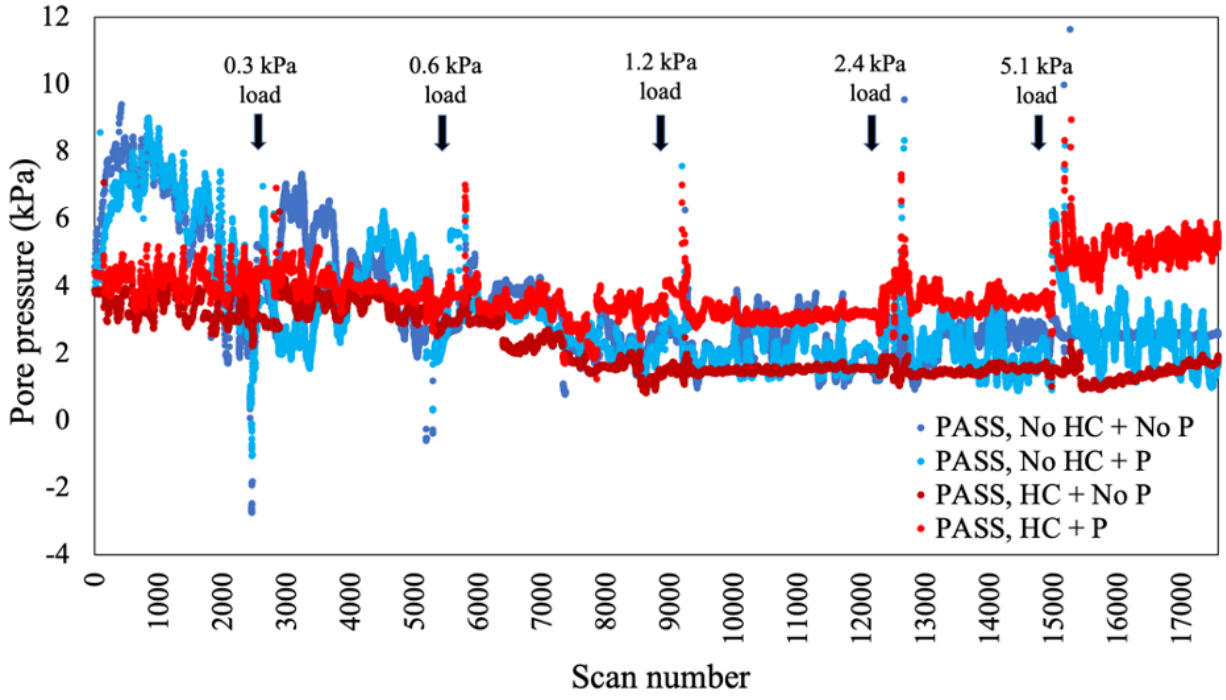

Figure C-2. Average pore pressure measurements at base of 5.5 L columns over 360 d. Dead load (pressure) applications are indicated by arrows and occurred roughly every 60 d. Scan number roughly corresponds to a 30 minute time interval. Label HC refers to hydrocarbon amended tailings; P refers to tailings under pressure.

Bitumen content in the tailings on Day 360 is presented in Figure C-3. The bitumen content on Day 0 was only measured in one PASS-treated FFT sample, and this measurement was higher than that of the triplicate untreated FFT samples. Thus, it is assumed that the bitumen content of the Day 0 PASS-treated FFT is overestimated. Regardless of the uncertainty surrounding the Day 0 measurement, hydrocarbon amendments had a significant impact on bitumen content on Day 360. This is presumably due to the decreased viscosity and therefore increased mixing and mobility of bitumen in hydrocarbon amended tailings, rather than bitumen biodegradation in unamended tailings. Further, prior to collecting the Day 0 sample for Dean-Stark analysis, the tailings were thoroughly mixed and homogenized, while tailings in the columns were not homogenized prior to sample collection on Day 360. This lack of mixing may have influenced the Day 360 bitumen measurements, particularly in the unamended tailings.

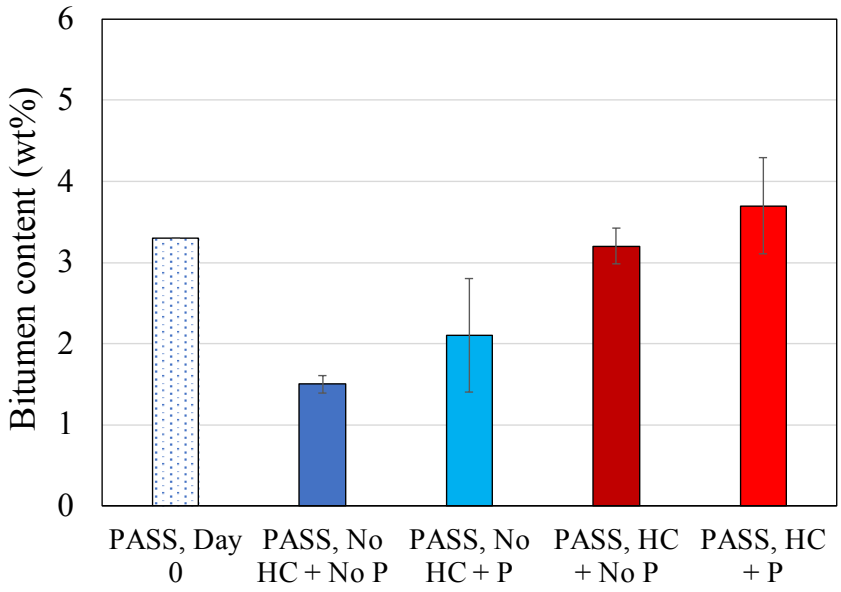

Figure C-3. Bitumen content of PASS-treated FFT in 5.5 L columns on 360 d. The bitumen content of PASS-treated FFT on Day 0 is provided for comparison. Day 360 results are averaged from triplicate columns and error bars represent one standard deviation of triplicates. The Day 0 result is based on a single measurement. Label HC refers to hydrocarbon amended tailings; P refers to tailings under pressure.

Table C-2 presents average gaseous H_2S measurements in the headspace of all columns over 360 d. Gaseous H_2S measurements were highest on Day 60, which is consistent with the extensive sulfate reduction that occurred during this period. Headspace H_2S measurements are not cumulative as column headspaces were flushed with nitrogen every 60 d.

Table C-2. Gaseous H_2S measurements in column headspace. Presented as average ± standard deviation of triplicates. Results are not cumulative as headspace was purged after each reading. H_2S was not measured on Day 240. BDL indicates below detection limit of 0.1 ppmv. Label HC refers to hydrocarbon amended tailings; P refers to tailings under pressure.

	H_2S (ppmv)				
Day	**60**	**120**	**180**	**300**	**360**
PASS, No HC + No P	23.6 ± 42.7	BDL	BDL	1.7 ± 3.0	BDL
PASS, No HC + P	1.2 ± 1.5	BDL	BDL	BDL	BDL
PASS, HC + No P	32.2 ± 17.9	BDL	BDL	BDL	BDL
PASS, HC + P	16.7 ± 10.1	0.8 ± 1.3	BDL	BDL	BDL

Figure C-4 presents pH measurements of the tailings (A) and water cap (B) in all columns over 360 d. pH changes in the tailings are presumably the result of biogeochemical changes while pH changes in the water cap are likely the result of both biogeochemical changes and NWR from the tailings. The spike in the tailings pH on Day 300 is assumed to be an error, as it occurred in all columns and only on Day 300. Further, the accuracy of the pH readings in the tailings was impacted by bitumen which frequently coated the pH probes.

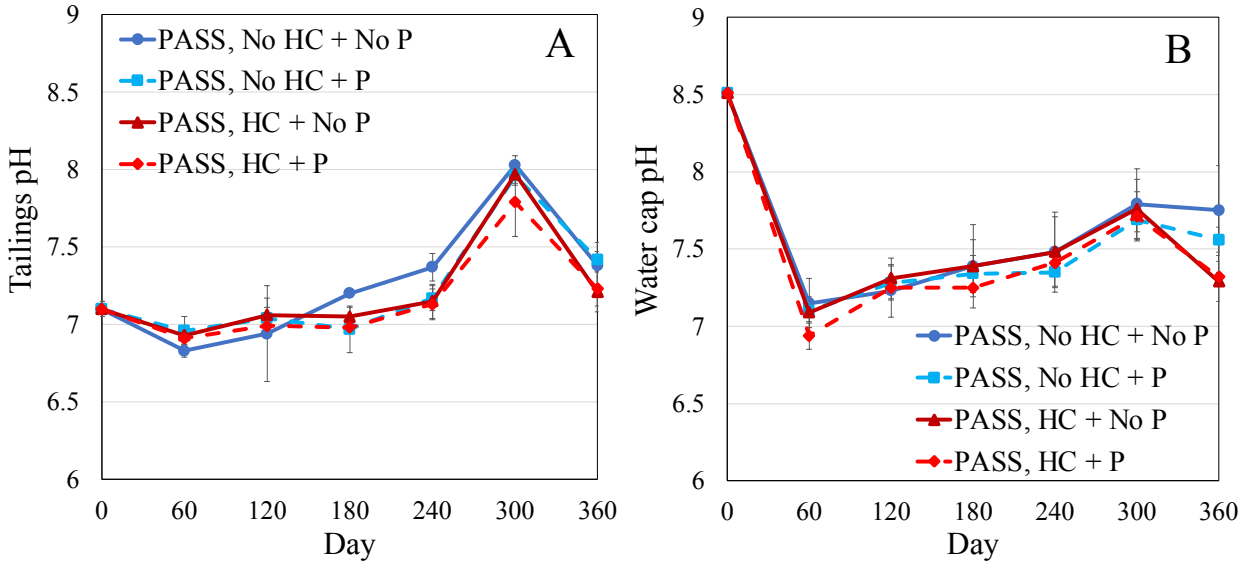

Figure C-4. pH in tailings (A) and water cap (B) in PASS-treated FFT columns over 360 d. Results are averaged from triplicate columns and error bars represent one standard deviation of triplicates. Label HC refers to hydrocarbon amended tailings; P refers to tailings under pressure.

Concentrations of major cations and chloride in the pore water and water caps in all columns are provided in the figures below (Figure C-5: Na^+, Figure C-6: Ca^{2+}, Figure C-7: Mg^{2+}, Figure C-8: K^+, Figure C-9: Cl^-). The trends in the water cap figures (B) are generally consistent with NWR. There is an initial drop in the pore water cation concentrations, especially for divalent cations, and this can be attributed to carbonate mineral precipitation as a result of sulfate reduction as well as diffusive fluxes into the water cap. Interestingly, on Day 180 pore water and water cap concentrations of magnesium, potassium, and chloride started to increase in columns with pressure. These increasing trends continued to Day 360. This behavior could be due to ion exchange, though none of the other ion measurements showed a simultaneous decrease. Other possible explanations for this behavior could include pressure impacting the solubility of salts

(Sawamura et al. 2007), though this is unlikely to have occurred at the relatively low pressures used in this work, or that the higher ionic strengths in the columns with pressure enhanced mineral solubility (the 'salting in effect'). Charge balance calculations performed on all the cation and anion measurements were within ± 5%, except for three which were ± 6% . The charge balances that were outside acceptable limits were: Day 120 PASS, No HC + P pore water, Day 360 PASS, No HC + P water cap, and Day 360 PASS, HC + P water cap. The larger charge balances are presumably due to cation or anion measurement errors, which is consistent with the higher standard deviations seen in some of the Day 120 or Day 360 ion measurements in these columns.

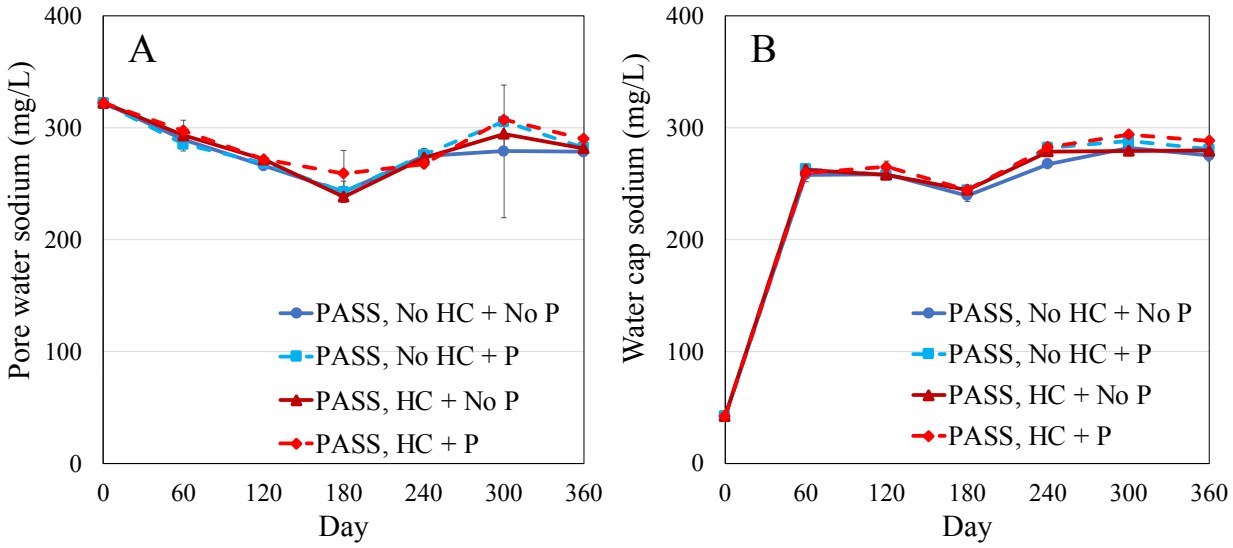

Figure C-5. Sodium concentrations in the pore water (A) and water cap (B) in PASS-treated FFT columns over 360 d. Results are averaged from triplicate columns and error bars represent one standard deviation of triplicates. Label HC refers to hydrocarbon amended tailings; P refers to tailings under pressure.

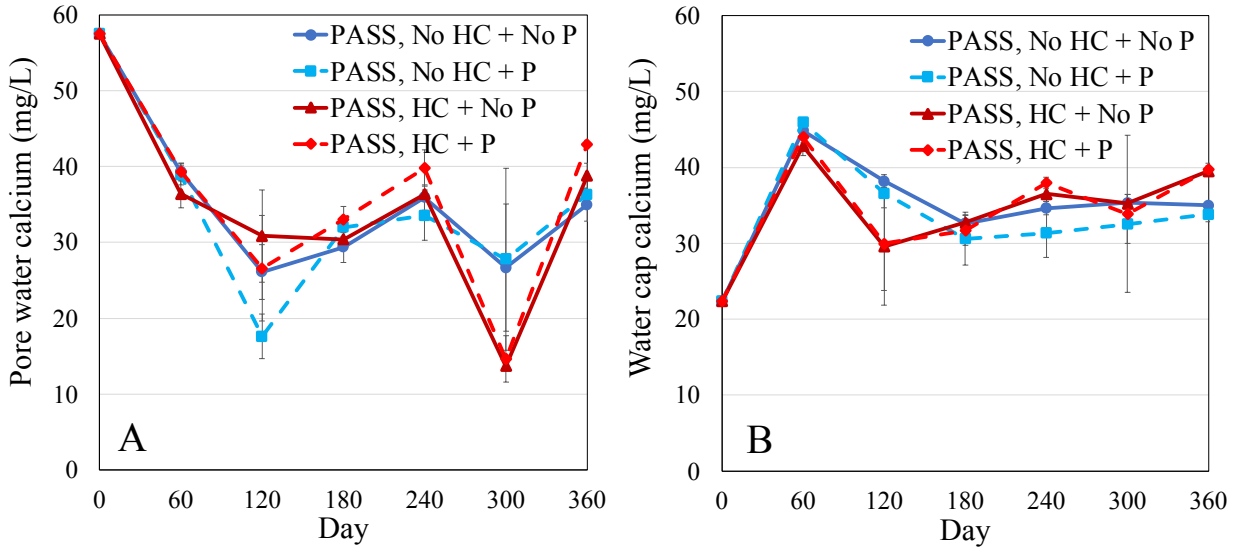

Figure C-6. Calcium concentrations in the pore water (A) and water cap (B) in PASS-treated FFT columns over 360 d. Results are averaged from triplicate columns and error bars represent one standard deviation of triplicates. Label HC refers to hydrocarbon amended tailings; P refers to tailings under pressure.

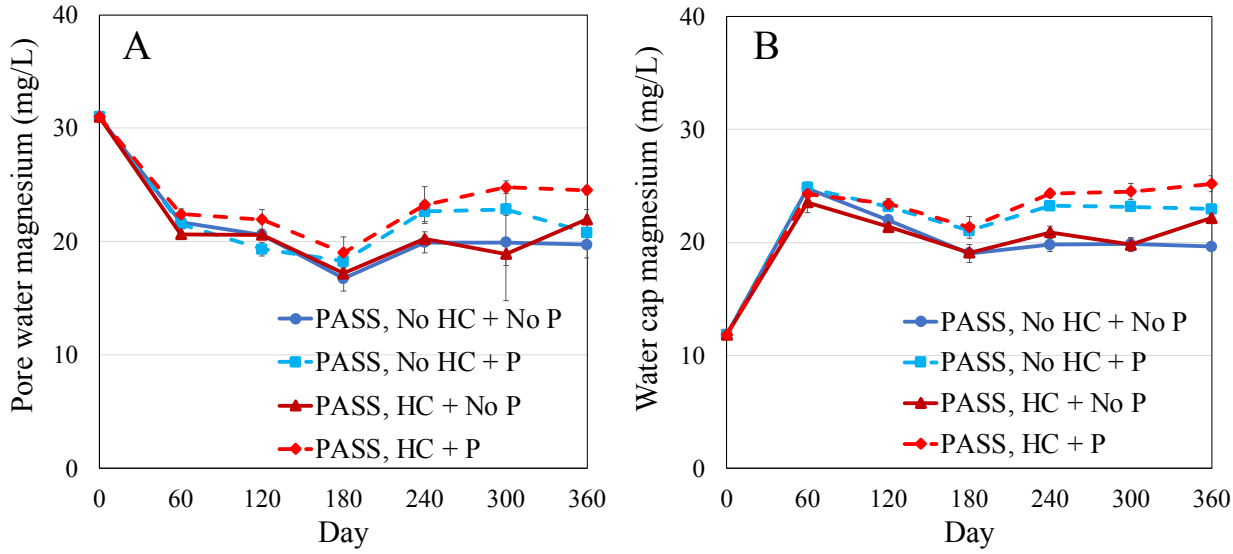

Figure C-7. Magnesium concentrations in the pore water (A) and water cap (B) in PASS-treated FFT columns over 360 d. Results are averaged from triplicate columns and error bars represent one standard deviation of triplicates. Label HC refers to hydrocarbon amended tailings; P refers to tailings under pressure.

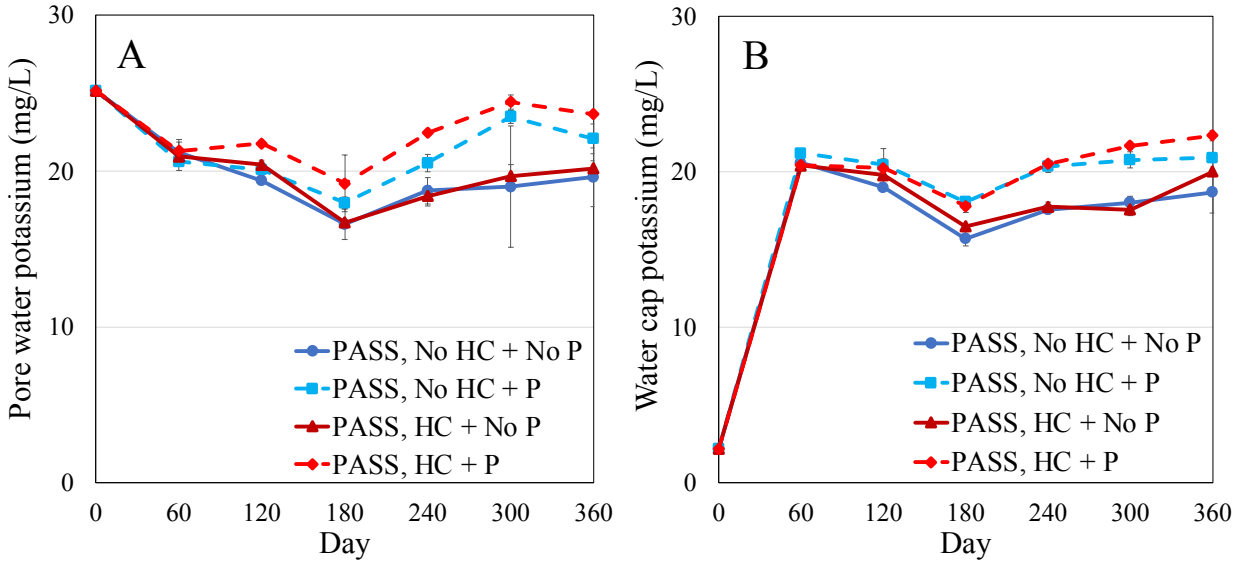

Figure C-8. Potassium concentrations in the pore water (A) and water cap (B) in PASS-treated FFT columns over 360 d. Results are averaged from triplicate columns and error bars represent one standard deviation of triplicates. Label HC refers to hydrocarbon amended tailings; P refers to tailings under pressure.

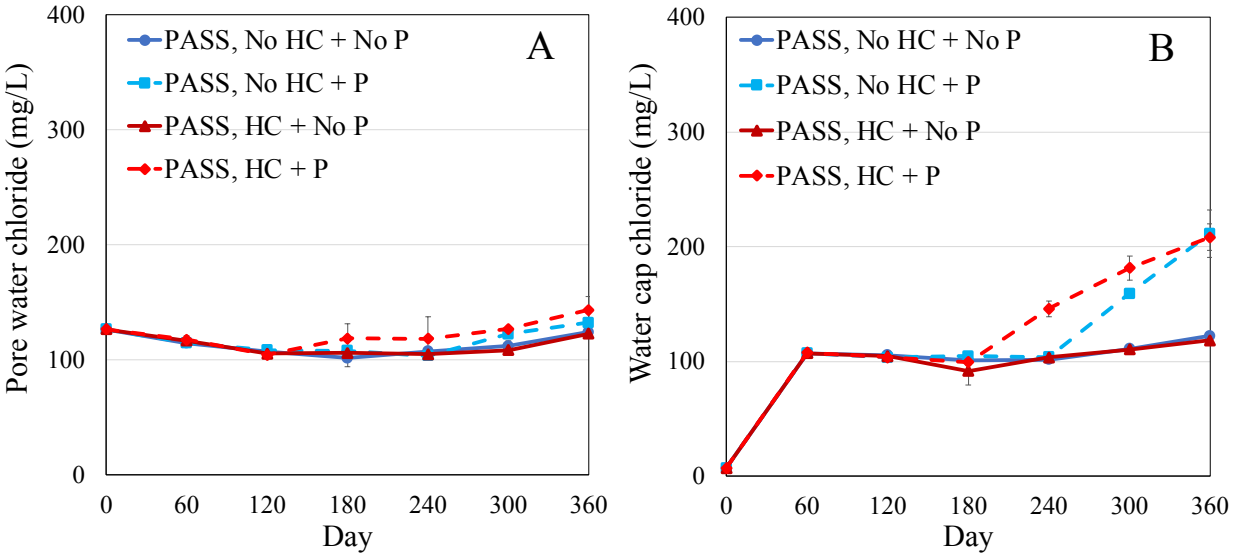

Figure C-9. Chloride concentrations in the pore water (A) and water cap (B) in PASS-treated FFT columns over 360 d. Results are averaged from triplicate columns and error bars represent one standard deviation of triplicates. Label HC refers to hydrocarbon amended tailings; P refers to tailings under pressure.

COD is presented in Figure C-10 for both the pore water and water caps in the columns. Note that COD pore water measurements started on Day 240 and COD water cap measurements were not

taken on Day 60 or Day 180. The trends in COD are similar to that of DOC and provide an indication of the oxidizable organic matter in the columns. The columns with pressure had higher COD in the water cap ($p < 0.0001$) and pore water ($p = 0.037$), which provides further evidence of the enhanced microbial activity in these columns.

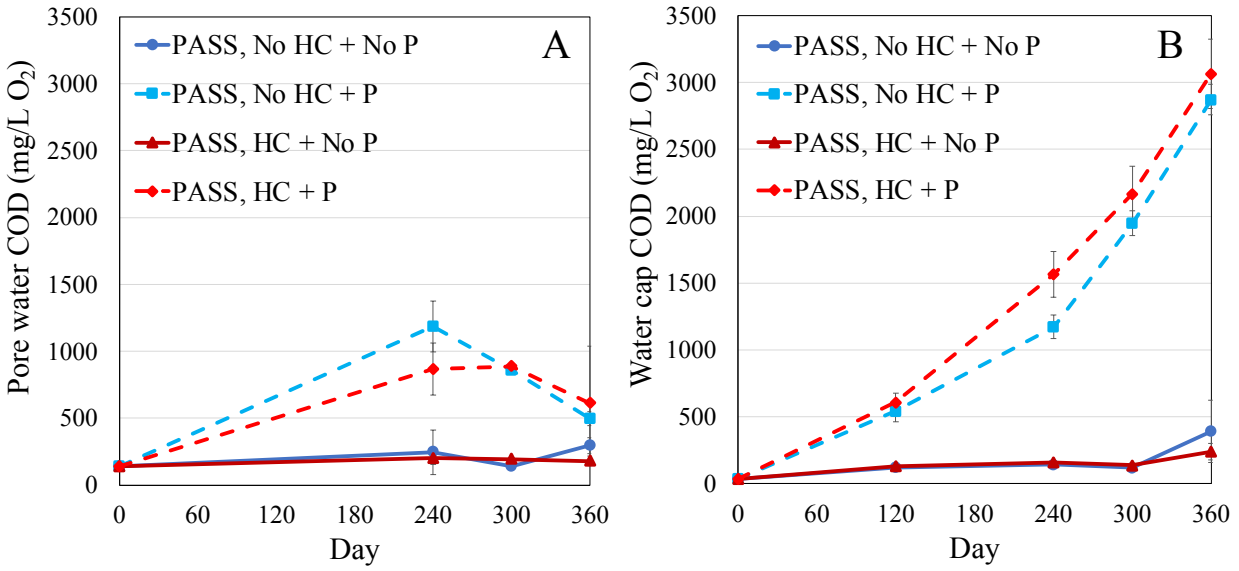

Figure C-10. Chemical oxygen demand in the pore water (A) and water cap (B) in PASS-treated FFT columns over 360 d. Results are averaged from triplicate columns and error bars represent one standard deviation of triplicates. Label HC refers to hydrocarbon amended tailings; P refers to tailings under pressure.

Appendix C2 References

Sawamura, A.; Egoshi, N.; Setoguchi, Y.; Matsuo, H. Solubility of sodium chloride in water under high pressure. *Fluid Phase Equilib.* **2007**, *254*, 158.162.

Appendix C3: Degradation of Hydrocarbon Amendments

Table C-3 presents concentrations of hydrocarbons (toluene, o-xylene, m-xylene, p-xylene, n-octane, n-decane, 2-methylpentane, and 3-methylhexane) measured in the columns on Day 360. Note that m- and p-xylenes are combined in Table C-3 as it was not possible to separate the peaks of these two hydrocarbons. Hydrocarbon concentrations were measured to confirm that the hydrocarbons added to tailings in six of the columns on Day 0 were degraded by microbial communities over the course of the experiment. Trace amounts of m- and p-xylenes and 2-methylpentane were present in the unamended tailings on Day 0 and were detected in all columns on Day 360, though the Day 360 concentrations of m- and p-xylenes and 2-methylpentane were higher in hydrocarbon amended columns.

Table C-3. Concentrations of hydrocarbons in the tailings on Day 360. Results are average of triplicate columns and error bars represent one standard deviation of triplicates. Day 0 hydrocarbon amendment concentrations are included for reference, as well as Day 0 hydrocarbon concentrations in the unamended tailings. Label HC refers to hydrocarbon amended tailings; P refers to tailings under pressure.

Hydrocarbon (ppm)	Day 0 Amendments	Day 0	Day 360			
		PASS, No HC	PASS, No HC + No P	PASS, No HC + P	PASS, HC + No P	PASS, HC + P
Toluene	150	0.0 ± 0.0	0.0 ± 0.0	0.0 ± 0.0	1.0 ± 1.0	0.1 ± 0.0
o-Xylene	50	0.0 ± 0.0	0.0 ± 0.0	0.0 ± 0.0	1.3 ± 1.0	1.1 ± 0.4
m- & p-Xylene	100	0.1 ± 0.0	0.2 ± 0.0	0.2 ± 0.0	3.2 ± 2.6	4.8 ± 1.4
Octane	500	0.0 ± 0.0	0.0 ± 0.0	0.0 ± 0.0	0.8 ± 0.8	0.1 ± 0.6
Decane	500	0.0 ± 0.0	0.1 ± 0.0	0.0 ± 0.0	0.6 ± 0.4	0.8 ± 0.3
2-Methylpentane	500	1.6 ± 0.7	2.5 ± 0.3	1.9 ± 0.3	3.4 ± 2.9	6.7 ± 2.7
3-Methylhexane	500	0.0 ± 0.0	0.0 ± 0.0	0.0 ± 0.0	8.9 ± 7.5	13.8 ± 5.0